La collana della Scuola di Alta Formazione Dottorale accoglie le migliori tesi di dottorato dell'Università degli Studi di Bergamo, insignite della dignità di stampa e sottoposte a procedura di *blind peer review*.

This work falls within the research field of Structural Health Monitoring (SHM), with specific reference to the civil engineering context. Nowadays, SHM-based approaches may constitute fundamental tools to pursue the goal of structural safety, preventing possible structural failures. In particular, this research work proposes complementary post-processing approaches to address the issue of noise cleaning on dynamic structural response signals encountered in structural engineering applications. Two approaches are presented: Heterogeneous Data Fusion (HDF) procedures, which involve a Kalman Filter (KF), and a denoising approach. These techniques are then combined within an integrated strategy, for assessing the health conditions of bridges. Synthetic and real response signals are processed, and then employed toward modal identification purposes, for extracting the modal properties of the monitored structure.

GABRIELE RAVIZZA holds a PhD degree in Engineering and Applied Sciences (33rd cycle) in 2021 at University of Bergamo (Italy), under the guidance of Prof. Egidio Rizzi. His research interests include structural health monitoring, signal processing, "output-only" modal dynamic identification techniques, numerical approaches for structural identification, heterogeneous data fusion techniques and signal denoising.

ISBN: 978-88-97413-64-6
DOI: 10.13122/978-88-97413-64-6

Gabriele Ravizza
Heterogeneous Data Fusion Approaches

44

Collana della Scuola di Alta Formazione Dottorale
- 44 -

Gabriele Ravizza

Heterogeneous Data Fusion Approaches and Modal Dynamic Identification of Civil Structures

UNIVERSITÀ DEGLI STUDI DI BERGAMO

2022

Collana della Scuola di Alta Formazione Dottorale

Diretta da Paolo Cesaretti

Ogni volume è sottoposto a *blind peer review*.

ISSN: 2611-9927

Sito web: https://aisberg.unibg.it/handle/10446/130100

Gabriele Ravizza

Modal dynamic identification of civil structures via inverse analysis based on Heterogeneous Data Fusion and post-processing

Università degli Studi di Bergamo

2022

Modal dynamic identification of civil structures via inverse analysis based on Heterogeneous Data Fusion and post-processing
/ Gabriele Ravizza. – Bergamo :
Università degli Studi di Bergamo, 2022.
(Collana della Scuola di Alta Formazione Dottorale; 44)

ISBN: 978-88-97413-64-6
DOI: 10.13122/978-88-97413-64-6

Progetto grafico: Servizi Editoriali – Università degli Studi di Bergamo
© 2018 Università degli Studi di Bergamo
via Salvecchio, 19
24129 Bergamo
Cod. Fiscale 80004350163
P. IVA 01612800167

https://aisberg.unibg.it/handle/10446/227490

Acknowledgements

I would like to thank Prof. Rizzi for the fundamental contribution given to this research work, through the countless teachings, combined with the constant presence and, more generally, I would like to express to him my gratitude for the key role he has played for me in these years of studies. A heartfelt thanks also to Dr. Ferrari, for the important support and the precious advices she was able to give me.

Table of contents

Introduction **1**

Chapter 1. Main state of the art **7**

1.1 Structural Health Monitoring **7**

1.1.1 The role of displacement and acceleration data in SHM **7**

1.2 Data Fusion **11**

1.2.1 Heterogeneous Data Fusion **11**

1.2.2 Definitions and kay concepts **12**

1.2.3 Classification of DF-related issues **13**

1.2.4 Data Fusion treatment **16**

1.2.5 Emerging Data Fusion trends **23**

1.3 Kalman Filter **29**

1.3.1 KF generalities **29**

1.3.2 Filtering **30**

1.3.3 On Kalman Filter **37**

1.4 Final remarks **45**

Chapter 2. Effective HDF-based procedure via KF for clarifying synthetic ambient vibration response signals **47**

2.1 Introduction and contextualization **48**

2.1.1 Achievements of the investigation **50**

2.2 Theory **50**

2.2.1 Description of the benchmark structural system **50**

2.2.2 Analysis procedure **52**

2.2.3 Numerical KF implementation **53**

2.3 Analysis results **56**

2.3.1 Noise-free acceleration case **56**

2.3.2 Noise-affected acceleration case **60**

2.4 Final remarks **64**

Chapter 3. HDF approach via KF for modal identification of seismic-excited structural systems 67

3.1 Introduction 67

3.1.1 Goals of the research scenario 68

3.2 Seismic-excited benchmark structure 69

3.1.2 Examined earthquake excitations 69

3.3 Analysis results 70

3.3.1 Results in the Time Domain 71

3.3.2 Results in the Frequency Domain 74

3.4 Final remarks 78

Chapter 4. Critical assessment of two denoising techniques for purifying synthetic structural vibration response signals 81

4.1 Introduction and contextualization 81

4.1.1 Goals of the research scenario 85

4.2 Theoretical framework 85

4.2.1 Problem statement 85

4.2.2 Discrete Wavelet Transform-based denoising 87

4.2.3 Singular Value Decomposition-based denoising 92

4.3 Analysis procedure 95

4.3.1 Presentation of a selected benchmark structure 95

4.3.2 Synthetic generation of noise-corrupted response signals 96

4.3.3 Denoising application and results 99

4.3.3.1 DWT-based denoising application 99

4.3.3.2 SVD-based denoising application 104

4.3.4 Denoising technique comparison 106

4.4 Final remarks 119

Chapter 5. Denoising technique assessment for purifying real structural vibration response signals 121

5.1 Case study with real response signals **121**

5.1.1 SU Unterwalden railway bridge generalities **122**

5.2 Denoising technique application **123**

5.3 Analysis results **126**

5.3.1 Results in the Time Domain **126**

5.3.2 Results in the Frequency Domain **132**

5.4 Final remarks **138**

Chapter 6. An integrated monitoring strategy fur current condition assessment of historic bridges **141**

6.1 Introduction and contextualization **141**

6.1.1 Research goals **143**

6.2 Presentation of the monitored structure **143**

6.3 Monitoring methodology description **145**

6.4 Analysis results **148**

6.4.1 Time-Domain analysis **148**

6.4.2 Frequency-Domain analysis **151**

6.5 Final remarks **154**

Conclusions **157**

Appendices **163**

Appendix A **165**

Appendix B **171**

Appendix C **175**

Appendix D **179**

List of figures **183**

List of tables **189**

Bibliography **193**

Introduction

This Doctoral Thesis condenses the main outcomes of a three-year research work (October 2017 – September 2020) performed at the University of Bergamo, within the Doctoral Programme in Engineering and Applied Sciences (Department of Engineering and Applied Sciences). Belonging to the Scientific-Disciplinary Sector of Mechanics of Solids and Structures (ICAR/08 – Scienza delle Costruzioni), it falls within the Structural Health Monitoring (SHM) research field, spanning along two interrelated main directions, namely Heterogeneous Data Fusion (HDF) and Structural Identification (SI), with a main target also on the post-processing of signals, with specific reference to the Denoising of dynamic response signals.

The motivations behind this work may be found in the deep bond existing among these disciplines: HDF, SI and signal denoising represent strictly related topics, which constitute a continuously evolving research field, increasingly attracting the interest of researchers, engineers, property stakeholders and infrastructure managers around the world. Among other reasons, this may be attributed to the high technological level that the developed methodologies have nowadays reached, together with the increasing requirements for smart monitoring and assessment of existing infrastructures, a significant portion of which is now reaching its design life-cycle capacity, especially within the Italian country. Consequently, the need for an effective simulation and monitoring of the dynamic behavior of structural systems under different loading conditions, may constitute a crucial target, toward ensuring the safety of existing structures and infrastructures, especially if dated but still subjected to enduring loading conditions, and possibly endowed with historical and heritage value.

The present research work develops its presentation along eight chapters. After a brief introduction, provided in the present section, a main state of the art on the covered topics is further reported in Chapter 1. It introduces SHM, as the process of assessing the state of health of an examined structure, and the main goals that SHM aims at achieving, namely the improvement of safety and reliability of structural systems, by detecting potential damage, before it may reach a critical state, allowing for a rapid post-event assessment. SHM may be considered as a multidisciplinary approach, which involves the integration of sensors, data transmission, computational processing capabilities, allowing to reconsider the design and the full management of a structure, as a single system or as a part of a group of systems. A critical literature review on existing Data Fusion methodologies, as well as on the principles underlying the functioning of the so-called Kalman Filter (KF) toward SHM applications, are also presented. Furthermore, this chapter introduces the typologies of signals to which this work is addressed to, i.e. acceleration and displacement dynamic response signals,

explaining the motivations of this choice and the importance that such signals shall assume within monitoring procedures, aiming at providing a reliable evaluation of the health conditions of a specific structure. In particular, in this work, both synthetic response signals (Chapters 2–4), artificially generated through a numerical computational procedure, and real response signals (Chapters 5–6), directly detected on a real structure by setting up an appropriate sensor network, are successfully considered and effectively processed.

Chapter 2 outlines a computational procedure for the effective merging of diverse sensor measurements, in order to conveniently monitor and simulate the current health condition of civil structures under dynamic loadings. In particular, it investigates a Kalman Filter implementation toward the Heterogeneous Data Fusion of displacement and acceleration synthetic response signals of a numerical structural system, for dynamic identification purposes. A white-noise input force is assumed to be applied at the top floor of a 3-DOF shear-type frame, and its structural dynamic response is inspected, in terms of displacements and accelerations. The presented procedure is perspectively aimed at enhancing extensive remote displacement measurements (commonly affected by high levels of noise), by possibly integrating them with a few standard acceleration measurements (considered instead as noise-free or corrupted only by a slight amount noise). Within the Data Fusion analysis, a Kalman Filter algorithm is implemented and its effectiveness in improving noise-corrupted displacement measurements is investigated. The performance of the filter is assessed, based on the RMS error between the original (noise-free, numerically determined) displacement signal and the Kalman Filter displacement estimate, and on the structural modal parameters (natural frequencies) that can be extracted from displacement signals, refined through the combined use of displacement and acceleration recordings, through inverse analysis algorithms for output-only modal dynamic identification.

Chapter 3 aims at generalizing the KF-based implementation presented in the previous chapter, by extending it to the successful monitoring of the current health condition of seismic-excited structural systems. In order to do this, a data-set of ten seismic input signals, which differ for magnitude, location, duration and Peak Ground Acceleration (PGA), are considered, during the computational analyses. The earthquake input is assumed to be applied at the base of the same 3-DOF dynamic system considered in Chapter 2, taken as a benchmark structure for the numerical validation of the proposed HDF implementation. A multi-rate Kalman Filter is employed for fusing together the noise-added non-stationary displacement data with the acceleration data, synthetically generated from the benchmark numerical system. The analysis is conducted for several Noise-to- Signal (N/S) ratios, aiming at simulating errors that may arise during experimental campaigns (e.g. due to the intrinsic limits of the employed instrumentation), within the phase of signal acquisition. The filtered

displacement response signals, complemented by a few acceleration recordings, are then employed for extracting the modal natural frequencies of the examined structural system, and a good agreement between the resulting estimates obtained through the modal identification performed on displacements and those deriving from accelerations, is achieved.

In Chapter 4, a denoising-based approach, aiming at clarifying dynamic response signals, is introduced. In fact, within the civil engineering context, vibration-based monitoring is receiving an increasing attention, due to the high technological level that the developed methodologies are nowadays reaching, together with the increasing quest for the implementation of an effective, but ideally low-cost, monitoring instrumentation. The latter is relatively easy to be deployed, and allows for the recording of the structural vibration response at multiple locations, which, for large strategical infrastructures, such as high-rise buildings, bridges, wind farms, etc. may be of a critical importance. On the other hand, a low-cost instrumentation may typically be accompanied by high N/S ratios, contaminating the structural response, increasing the induced uncertainties and rendering more difficult the implementation of SHM methods. Thus, the availability of appropriate and effective denoising techniques may play a key role in these circumstances. In tackling such an associated denoising problem, several methods have been proposed and are currently under further development. Among specific variants, the utilization of multi-rate filter banks, especially the one based on Discrete Wavelet Transform (DWT), as well as the application of Singular Value Decomposition (SVD), have revealed to be rather effective. Yet, they have mostly been applied to problems where structural vibration response signals originate from specific behavioral classes, as, e.g., in monitoring applications of rotating machinery. In this chapter, the aforementioned methods are reconsidered and reimplemented; then, assessed on noise-corrupted vibration response signals related to civil engineering applications. Different noise levels and excitation types are considered, acting on a 10-DOF structural dynamic system, i.e. earthquake and ambient vibration excitations, since they may be assumed as representative of more general non-stationary and stationary signal typologies, respectively. Advantages and limitations of both denoising approaches are presented and discussed, and a detailed critical analysis in both the Time and Frequency Domains, comparing results obtained from non-stationary and stationary response signals, is presented.

It is worth noting that all signals considered within the chapters presented so far will be synthetic signals, since their preliminary employment is considered to be necessary in the phase of validation of the developed SHM procedures. The further target, to which Chapters 5 and 6 are dedicated, is represented by the employment of real signals, directly acquired “in situ", by means of appropriate accelerometers and displacement sensors.

In particular, in Chapter 5, a real case study is analyzed, where both the two previously considered denoising approaches are adapted and employed for clarifying real non-stationary acceleration response signals, detected on a modern short-span railway RC bridge, by predisposing appropriate accelerometer sensors at a certain number of locations. Through an analysis conducted within both the Time Domain and the Frequency Domain, it has been proven that the application of the DWT- and SVD-based denoising techniques may result quite effective in the clarification of the considered real response signals, suggesting a possible adoption of these techniques for the treatment of similar noise-corrupted vibration signals that may be encountered within civil engineering applications.

Chapter 6 presents an effective integrated SHM strategy, specifically addressed to the preservation of the integrity and safety of strategic and historic infrastructures, like bridges. In fact, given the critical conditions that characterize many of these structures (e.g. due to their age, or the considerable dynamic loads that they may have endured), the availability of efficient monitoring strategies is becoming increasingly urgent. Thus, within SHM, several vibration-based methodologies have already been developed, including the previously mentioned HDF-based approaches, as well as the denoising techniques for the treatment of noise-corrupted vibration response signals. In this chapter, these two approaches are reconsidered and rejoined, toward developing an innovative signal processing methodology for current condition assessment, specifically referring to historic bridges. In particular, a HDF-based procedure, i.e. the process of combining information from multiple sources (acceleration and displacement response signals), in an effort to enhance the reliability of the monitoring process, and a denoising approach, devoted to the cleaning of spurious noise from the acquired signals, are combined all together, in an integrated strategy. The effectiveness of the proposed platform is tested on data acquired from a real infrastructure, i.e. the historic Reinforced Concrete (RC) Brivio bridge (1917), subjected to operational loading conditions. Both dynamic acceleration and displacement response signals, directly detected on the bridge, are processed within the proposed methodology, and subsequently employed toward modal dynamic identification purposes (for the identification of the modal natural frequencies and vibration modes of the bridge), and possible model updating of the structure at hand.

Finally, conclusions and final remarks are outlined in last chapter, where the main achievements of the present work are summarized, and a few possible future perspectives are also disclosed.

This research work aims at providing an original, methodological research contribution to the thriving research field of Structural Health Monitoring. In particular, it aspires at proposing new perspectives for the treatment of spurious noise that may appear on recorded structural response signals, due to multiple and different reasons, explored within the research. Thus, the present research work specifically focuses on the post-processing phase of the acquired signals, by presenting post-

processing approaches such as Heterogeneous Data Fusion procedures and denoising-based techniques, as well as hybrid approaches, which integrately involve both the aforementioned processes. Through several implementations based on artificially generated response signals, firstly, and on real response signals, directly detected on real structures, subsequently, the analysis aims at making the monitoring process more consistent, and its outcomes much reliable, resulting in a further precise and comprehensive description of the current health condition of a determined monitored structure. The results prove the effectiveness of the proposed implementations, also highlighting the possible limitations which may characterize each studied technique, for instance depending on the typology of the data to be processed, by also motivating further specific research in this latter scenario.

Chapter 1. Main state of the art

This chapter provides a main critical literature review on the research topics explored within the present research work. In particular, starting from the "on field" purposes of Structural Health Monitoring (SHM), below discussed in Section 1.1, Data Fusion (DF) methodologies are then examined and reported in Section 1.2, and a comprehensive overview of the main available theories is provided. Focus is finally placed on Kalman Filter (KF), to which Section 1.3 is dedicated, as a powerful tool to be employed within a DF-based analysis, for fusing together heterogeneous data acquired from different typologies of sensors.

Although these research topics cover a wide range of applications, which belong to different disciplinary areas, given the specific purposes of this research work, these themes will here always be treated in the main perspective of the civil engineering field.

1.1 Structural Health Monitoring

In recent years, Structural Health Monitoring has become more and more important to ensure reliability and efficient management of strategical or historical civil infrastructures such as, for instance, long-span bridges, concrete dams and high-rise buildings. The main reason lies in the fact that structural damage resulting from extensive service loading conditions, or even structural failure, may induce significant risks for human life. SHM represents a constantly evolving research field, addressed to the evaluation of the health condition of a monitored structure, based on its current structural performance. It is generally articulated into multiple phases, each of which characterized by different levels of detail, i.e. detection of damage, localization of damage, its identification, and prognosis. By using information deriving from a certain number of sensors, suitably arranged along the structure, SHM procedures aim at estimating the dynamic behaviour of the monitored structure at all its locations. For this purpose, the acquisition stage of signals, which describe the current structural condition, constitutes a fundamental phase for the success of the whole monitoring analysis.

1.1.1 The role of displacement and acceleration data in SHM

Generally, SHM is relying on measurements of accelerations and/or displacements detected on a structural system; in fact, these typologies of data represent two significant physical quantities which may effectively be related to fatigue and damage estimation. The most common techniques lately adopted for acquiring acceleration and displacement structural response signals, within the field of

civil engineering, are below presented and discussed, and a brief overview on the typologies of sensors that may be employed to collect such kind of data is also provided.

1.1.1.1 Displacement data

The knowledge of the displacement response constitutes one of the most important features for determining the current health condition of a structure. Indeed, if a structure response lies within the elastic range, the occurred deformations are proportional to the internal stresses and, consequently, they can directly be exploited to determine the presence and the level of possible damage.

Measuring static or dynamic displacements of in-service structures represents an important issue for the purposes of design validation, performance monitoring, or safety assessment. Currently, available techniques for such a purpose can roughly be classified into two categories: direct measurement and indirect measurement techniques.

Among the instrumentation that rely on direct measurement techniques, noteworthy are the Global Positioning System (GPS) and the Laser Doppler Vibrometer (LDV). Indeed, whereas GPS can provide real-time displacement measurements with an accuracy level of about 5-10 mm (Roberts and Dodson [170]), at a frequency up to 20 Hz, LDV can provide accurate displacement measurements at multiple locations within a considerable range of distance (the laser intensity may become dangerously strong for distances greater than 75-100 m, Nassif et al. [142]). These instrumentations, however, are quite expensive, in particular when displacements at a large number of locations are desired. So, alternative measurement techniques have been developed in recent years.

For example, one of the most recent developed techniques for displacement acquisition relies on photogrammetry. This technique exploits the geometrical relationship between a three-dimensional object and its twodimensional photographic images. When sequences of images are used to capture a spatial-coordinate time history of an object, the technique can also be referred to as videogrammetric technique.

As compared to the above mentioned measurement techniques, the videogrammetric technique is a non-contact one, able to provide direct displacement measurements in both time and space. Methods that incorporate photogrammetric techniques with computer-vision strategies have also been developed, to investigate the dynamic characteristics of structures (Olaszek [145]). For instance, in Chang and Xiao [23], results from various tests conducted on a pedestrian bridge turned out to show that this method is characterized by an accuracy of 0.1-1 mm for a camera-target distance ranging between 10 m and 100 m, respectively, with a vibration frequency under 5 Hz. In Patsias and Staszewski [149], a videogrammetric technique is employed, to obtain the mode shapes of a cantilever beam and a high-speed professional camera system is used to capture the beam vibration. The system,

however, is limited to 2D planar vibration measurements, since only one camera is employed. Indeed, in order to capture the 3D dynamic behavior, avoiding that some geometrical information might be lost, more cameras become necessary. In fact, the transformation between an object in a 3D space and its 2D images is a degenerating process during which some geometrical information of the object may be lost. Hence, unless the object moves on a 2D plane, the reconstruction of its 3D motion normally requires at least two image sequences acquired from different cameras. Only few examples of such multi-camera approach are found in the literature: whereas Yoshida et al. [215] used a three-camera system, to capture the 3D dynamic behavior of a membrane, Chang and Ji [22] developed a dual-camera videogrammetric system to measure the 3D structural vibration response.

The use of multiple image sequences, however, demands for a precise synchronization among the cameras, which might be difficult to be achieved, especially for experimental "on field" tests. Point correspondence among multiple image sequences also requires significant computational efforts and may lead to larger reconstruction errors.

Alternatively, displacements can be measured by using traditional structural displacement sensors, such as Linear Variable Differential Transformers (LVDTs) and dial gauges, which are able to record infinitesimal displacements, as well as other similar direct displacement measuring devices. All these kinds of devices, however, require a fixed reference, to work properly (usually a stationary platform near the measurement point). This is one of the main issues related to the employment of such systems, which often limits their application for structures like bridges (Lee and Shinozuka [124]).

Finally, the use of optical transducers, to measure displacements, might represent an interesting alternative but, because of their high price, their employment is not so common yet in the current practice. Indirect measurement techniques, instead, require a double time integration of the recorded acceleration time histories. The accuracy of indirect

measurement techniques, however, has always been a concern. In fact, the double integration of acceleration is not readily automated and it requires selection of filters and baseline corrections, as well as the use of personal judgment when anomalies come to arise in the records.

1.1.1.2 Acceleration data

Regarding the direct acquisition of acceleration recordings, the most common solution is represented by the employment of accelerometers. Accelerometers are inertial sensors, to be located directly on the structure, and able to acquire accelerations in a vast range of sensing. Furthermore, they may detect accelerations along one, two, or three orthogonal axes. These sensors are widely employed for monitoring tests and they are becoming increasingly affordable. Differently from displacement measurement techniques, accelerometers can provide real-time acceleration measurements, with a

high accuracy level also at frequency rates with the order of size of kHz. There are several different principles based on which an accelerometer may be built: the two more common types are based on the capacity sensing and on the piezoelectric effect, to take the acceleration of a proof mass located within the sensors. It is worth noting that the accelerometer output value is always a scalar, corresponding to the magnitude of the acceleration vector.

Accelerometers display multiple applications within the engineering field, turning out to be fundamental for SHM purposes, as for instance in the reconstruction of the modal dynamic properties of the examined structure.

In fact, as previously mentioned, recording abnormal dynamic behavior, evaluating serviceability, detecting diffused and localized damage, as well as estimating the residual performance capacity of structures, constitute crucial aspects of SHM. These ambitious goals may be pursued through the application of modal dynamic identification techniques, which aim at determining the modal dynamic parameters of a structure, i.e. natural frequencies, mode shapes and damping ratios. Indeed, variations of these quantities during the life-cycle of a structure may reveal a change in its performance characteristics. According to the literature, mainly acceleration but also displacement measurements may be employed within inverse analysis algorithms, for structural identification purposes. Furthermore, also Finite Element Method (FEM) models, with related model updating, represent consistent tools for the condition assessment of existing civil constructions.

From the above, it clearly emerges how displacements and accelerations constitute strictly connected quantities. Indeed, after measuring an acceleration signal, which may relatively be convenient to be captured, it is possible to obtain the corresponding displacements through a double time integration of the acceleration data. This approach is quite common because accelerations are obtained without requiring the knowledge of initial velocity and displacement information. So, in this case, the transformed response is only affected by the initial conditions in terms of acceleration. As above mentioned, however, the main weakness of this procedure lies in the fact that the double integration of acceleration data may cause a low-frequency noise amplification of the acquired signal and this may lead to wrong estimates. Moreover, the so-called displacement drift issue can be observed as a consequence of the integration process. Thus, within the civil and mechanical structural modeling, for which accelerometers are most often used, also displacement sensors, such as non-contact optical techniques, as well as GPS-based methods for civil structures, are becoming increasingly widespread.

1.1.1.3 Frequency resolution of sensors

A common feature of displacement-based sensing is that the high-frequency resolution is limited, and often relatively low sampling rates are used. In contrast, accelerometers are often more accurate for

higher frequencies and higher sampling rates are often available. For civil infrastructures, the most damaging resonant modes of structures such as buildings or bridges are typically excited at less than 10 Hz. Within such a range, it is possible to assert that accelerations should always be preferred to be measured.

In light of what it has been stated, fusion processes between displacement and acceleration signals may offer the possibility to obtain a merge of the benefits deriving from each of the two types of measurements. This aspect, with some related issues, is inspected in the next section.

1.2 Data Fusion

This section deals with Data Fusion (DF) processes, and the modalities concerning the relative data treatment, since they depend on the typology of imperfection that may affect the data involved in the process. In fact, data may be affected by a great variety of factors that, in many cases, could lead to wrong estimates of the observed phenomenon. DF may be considered as a multi-disciplinary research field, with a wide range of potential applications, within diversified areas, such as defense (in the military field), robotics, automation and intelligent system design, pattern recognition, etc. This has been and will continue to act as the driving force behind the ever-increasing interest of the research community in developing more advanced Data Fusion methodologies and architectures. In the civil engineering field, however, the DF process is still far from being extensively investigated, despite the fact that researchers have increased their focus on this kind of topic, in recent years. In particular, within the civil engineering field, multi-sensor DF procedures may be employed for structural purposes to evaluate the health conditions of strategical constructions like bridges, dams or skyscrapers, configuring itself as an important tool for achieving an effective SHM.

Here, a summarizing review of the DF literature, which aims at exploring its conceptualizations, benefits, and challenging aspects, is provided. An overview of existing methodologies is also presented, and several future research perspectives on DF-based approaches are eventually outlined.

1.2.1 Heterogeneous Data Fusion

Data Fusion is a technique conceived to allow combining information from several objective sources, in order to form a unified framework. About data modality, sensor networks may collect qualitatively similar (homogeneous) or different (heterogeneous) data, such as for instance displacement and acceleration measurements. The present research focuses especially on this latter kind of subject, exploring Heterogeneous Data Fusion (HDF) procedures between different dynamic response signals. HDF is defined as a technique which allows the merging of information from multiple sensor typologies, in order to increase the accuracy of the measurements themselves, aiming at achieving a

more reliable description of dynamic behaviour of an examined structural system. The motivation behind the study of such procedures lies in the possibility to link these techniques to the monitoring of the health condition of a structure, through the acquisition of displacement and acceleration response signals, which may be related to damage and structural fatigue estimation. In this sense, the DF concept means bringing together information deriving from measurements acquired from displacement and acceleration sensors, for providing a more accurate estimation of the current structural condition, as well as the improved identification of the associated modal parameters.

1.2.2 Definitions and key concepts

This section provides main definitions about DF procedures, drawn from the literature, as well as the most common existing and popular conceptualizations of fusion systems.

Multiple definitions of DF may be found in the literature. Joint Directors of Laboratories (JDL) [221] defines DF as a "multilevel, multifaceted process handling the automatic detection, association, correlation, estimation, and combination of data and information from several sources". Klein [115] generalizes this definition, stating that data can be provided either by a single source or by multiple sources.

Both definitions appear to be quite general, and they can be applied within different research fields, including remote sensing. Even in Bostrom et al. [15], a review and discussion about many DF definitions may be found. In particular, in such a paper, an interesting definition of information fusion is proposed, as follows: *"The study of efficient methods for automatically or semi-automatically transforming information from different sources and different points in time into a representation that provides effective support for human or automated decision making".*

It is worth noting that DF constitutes a multidisciplinary research area, borrowing ideas from many different fields, such as signal processing, information theory, statistical estimation and inference, and artificial intelligence. Generally, performing DF displays several advantages that mainly involve enhancements in data authenticity or availability. Examples of the former are improved detection, confidence and reliability, as well as reduction in data ambiguity. Instead, extending spatial and temporal coverage belongs to the latter category of benefits.

Various conceptualizations of the fusion process exist in the literature. The most common and popular conceptualization of fusion systems is the JDL model [221]. The JDL classification is based on the input data and on the produced output. The JDL formalization, which originates from the military domain, focuses on (input/output) data rather than on data processing. The original JDL model considers the fusion process at four increasing levels of "abstraction", namely: object, situation, impact, and process refinement. Despite its popularity, the JDL model has many shortcomings, such

as being too restrictive and especially tuned for military applications. For this reason, it has been the subject of several extension proposals, attempting to alleviate its drawbacks (Steinberg et al. [196], Llinas et al. [132]).

An alternative conceptualization of DF is provided by the so-called Dasarathy's framework [40]. It considers the fusion system from a software engineering perspective, as a data flow characterized by input/output, as well as functionalities.

Another general conceptualization of fusion is given by the work of Goodman et al. [80], which is based on the notion of random sets. The distinctive aspect of this framework lies in its ability to combine decision uncertainties with decisions themselves, as well as presenting a fully generic scheme of uncertainty representation.

Finally, it is worth mentioning also the fusion frameworks proposed by Kokar et al. [116]. This formalization is based on category theory and it is claimed to be sufficiently general to capture all kinds of fusion, including data fusion, feature fusion, decision fusion, and fusion of relational information. It may be considered as the first step towards the development of a formal theory of fusion. The major novelty of that work lies in expressing all the aspects of the multi-source information processing, namely both data and processing. Furthermore, it allows for a consistent combination of the processing elements, with measurable and provable performance. Such formalization of fusion is important for the application of formal methods, for a standardization and virtuous development of fusion systems.

1.2.3 Classification of DF-related issues

Most of the issues that make the Data Fusion process a challenging task arise from the data to be merged, the imperfection and diversity of the sensor technologies, as well as the "nature" of the application environment.

This section provides an overview of data-related crucial aspects that may characterize the DF procedures. All this kind of issues may be represented according to a very convenient classification, provided by Khaleghi et al. [111], and reproposed in following Fig. 1.1. Despite many of these problems have been identified and heavily investigated, no single DF algorithm is capable of addressing all the involved challenges. The variety of methods available in the literature focus on a subset of these issues to be solved, which would be determined based on the application at hand.

The input data to the fusion system may be imperfect, correlated, inconsistent and appearing in disparate forms or modalities. Two out of four main categories of challenging problems can further be sub categorized into more specific problems, as shown in Fig. 1.1. The following sections introduce such main categories.

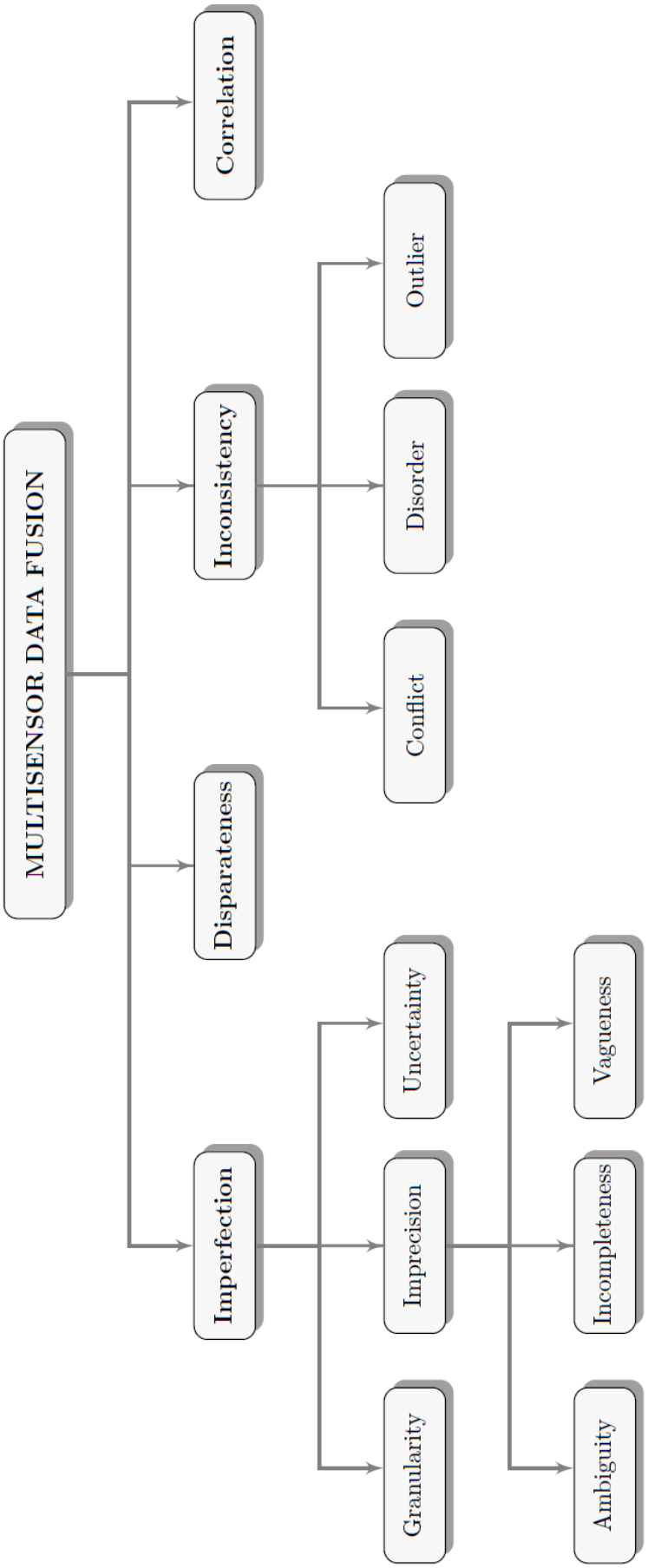

Figure 1.1: Taxonomy of the main challenging issues of input data (adapted from Khaleghi et al. [111]).

1.2.3.1 Data imperfection

Data provided by sensors are always affected by some level of impreciseness, as well as uncertainty in the measurements. DF-based algorithms should be able to effectively express such imperfections, and to exploit the data redundancy, in order to reduce their effects.

Three aspects of data imperfection are considered in the classification: granularity, imprecision, and uncertainty. Data granularity refers to the ability to distinguish among objects, which are described by data, being dependent on the provided set of attributes. Data is uncertain when the associated confidence degree is low, whereas imprecise data is that data which refers to several objects, rather than only one.

Moreover, imprecision possesses a sub-categorization. Indeed, it can manifest itself as: ambiguity, incompleteness or vagueness of data.

Ambiguous data refers to those data where the attributes are exact and well-defined, yet imprecise. Instead, imprecise data characterized by some missing information is called incomplete data. Finally, vague data is characterized by having ill-defined attributes: this means that the attribute is more than one and not a well-defined set or interval. For example, it may be subjectively interpreted and it may display a different meaning from one observer to the other.

1.2.3.2 Data disparateness

The input data to a fusion system may be generated by a wide variety of sensors, human, or even archived sensory data. Fusion of such disparate data, in order to build a coherent and accurate global view or the observed phenomena, constitutes a very difficult task.

1.2.3.3 Data inconsistency

Inconsistency in input data due to conflicting, spurious (outlier), or disordered data, is now considered. In fact, uncertainties in sensors arise not only from the impreciseness and noisiness in the measurements. They are also caused by ambiguities and inconsistencies present in the environment, and from the inability to distinguish between them. So, when it is not possible to exclude outliers and spurious data, DF-based algorithms should be able to exploit redundant data, to alleviate such effects.

About conflicting data, fusion of such data may be problematic, especially when the fusion system is based on evident belief reasoning. To avoid producing counter-intuitive results, any DF-based algorithm should treat highly conflicting data with special care.

1.2.3.4 Data correlation

Correlated (dependent) data is also a challenge for data fusion systems and it should be properly treated. This issue is particularly important and common in distributed fusion settings, for example in wireless sensor networks. In fact, some sensor nodes are likely to be exposed to the same external noise, biasing their measurements. If such data dependencies are not accounted for, the fusion algorithm may suffer from over- or under-confidence in the results.

1.2.3.5 Data alignment

Another important feature in DF systems that is not taken into account in the proposed classification (see Fig. 1.1), because it is not strictly connected to the data collection stage, is the necessity of alignment or registration of such measurements after their acquisition.

Sensor data, in fact, must be transformed from each sensor's local frame into a common frame, before fusion occurs. Such an alignment issue is often referred to as sensor registration and deals with the calibration error induced by individual sensor nodes. Data registration is of a critical importance for the successful deployment of fusion systems in practice.

1.2.4 Data Fusion treatment

The inherent imperfection of data is the most fundamental challenging problem of DF systems, and thus a main bulk of the work in the research community devoted to the DF treatment has been focused on tackling this issue. There appear a large number of mathematical theories available to deal with data imperfection (Sheridan [188]). These theories refer in particular to Probability Theory (Durrant-Whyte and Henderson [55]), Fuzzy Set Theory (Zadeh [226]), Possibility Theory (Zadeh [227]), Rough Set Theory (Pawlak [150]), Dempster-Shafer Evidence Theory (DSET) (Shafer [186]) and its "hybridization" with Fuzzy Set Theory, namely Fuzzy DSET Theory (Yen [213]), and Random Finite Set Theory (Kendall [110]). Each of these theories is targeted to a specific kind of imperfection, as represented in Fig. 1.2.

On the x axis, various aspects of data imperfection, already introduced in Fig. 1.1, are depicted. The box around each mathematical theory designates the range of imperfection aspects mainly targeted by that theory. Most of these approaches are capable of representing a specific aspect (or aspects) of imperfect data. For example, a probabilistic distribution (Probability Theory) may efficiently express data uncertainty; Fuzzy Set Theory may represent vagueness of data; Evidential Belief Theory may represent uncertain, as well as ambiguous data. Historically, Probability Theory was used for a long time to deal with almost all kinds of imperfect information, because it originally was the only existing theory. Then, alternative techniques such as Fuzzy Set Theory and Dempster-Shafer Theory have

been proposed to deal with perceived limitations in probabilistic methods, such as complexity, inconsistency, imprecision of models, and uncertainty about uncertainty.

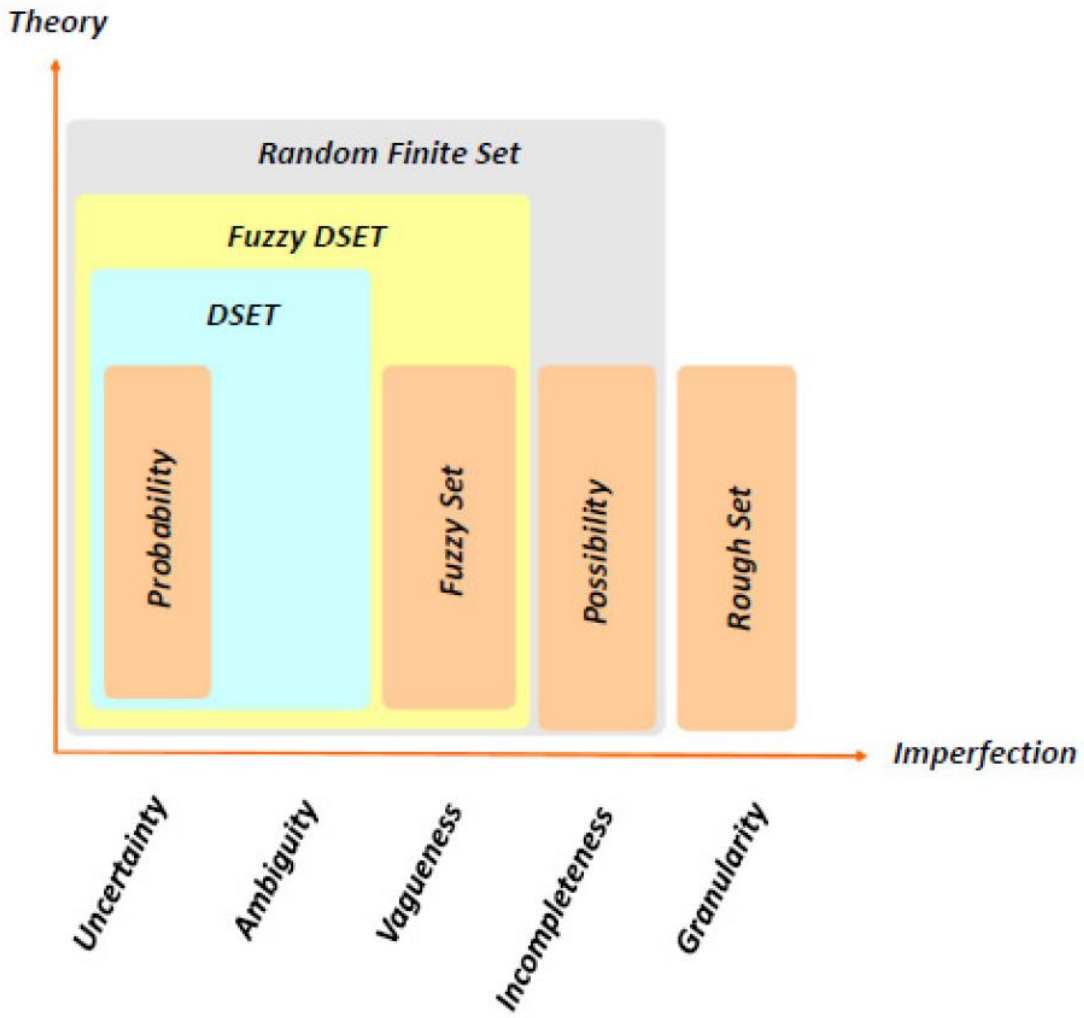

Figure 1.2: Main mathematical theories available to deal with data imperfection (adapted from Khaleghi et al. [111]).

1.2.4.1.1 Probability Theory

Probabilistic methods rely on a Probability Density Function (PDF), to express data uncertainty. At the core of these methods lies the so-called Bayes estimator, which enables fusion of pieces of data, hence the name Bayesian fusion.

It is generally possible to apply the Bayes estimator for updating the probability density (or distribution) of a system state, by recursively fusing a new piece of data, in order to obtain a better solution estimation. However, the Bayes estimator usually contains integrals that cannot be analytically evaluated, and an analytic solution of the Bayes estimator is thus only occasionally available.

This is the case of KF. In fact, it may be interpreted as a particular case of a Bayes filter with an exact analytical solution of the integrals that characterize the latter, allowed by enforcing simplifying constraints on the system dynamic to be linear-Gaussian. This means that observed measurements and considered models are assumed to display a linear form and to be contaminated with a zero-mean Gaussian noise (Mahler [136]). Nonetheless, KF is one of the most popular DF methods, mainly due to its immediacy, ease of implementation, and optimality in a mean-squared error sense. It constitutes a well-established method, whose properties are deeply studied and examined both theoretically and practically. Similar to other least-square estimators, KF however displays some drawbacks. Indeed, it is very sensitive to data corrupted with outliers. Furthermore, KF turns out to be inappropriate for applications whose characteristic errors are not readily parametrized.

When dealing with non-linear system dynamic, it may often be necessary to resort to approximation techniques, and the application of the Extended Kalman Filter (EKF) (Hoshiya and Sato [94]) or the Unscented Kalman Filter (UKF) (Julier and Uhlmann [102]) may reveal to be useful. In fact, these are extensions of KF that are applicable to non-linear systems, which are based on a first-order and on a second-order Taylor series approximation, respectively. However, both these methods can handle nonlinearities only to a limited extent.

Among probability theories, grid-based methods (Stone et al. [197]) provide an alternative approach for approximating non-linear PDFs, although they may require higher computational costs.

1.2.4.1.2 Dempster-Shafer Theory

The theory of belief functions was initiated by Dempster [42] in 1968 and then mathematically formalized by Shafer [186] in 1976, toward achieving a general theory of reasoning, based on evidence. Belief functions theory constitutes a popular method to deal with uncertainty and imprecision, within a theoretically attractive framework.

Dempster-Shafer (D-S) theory introduces the concept of assigning beliefs and plausibilities to possible measurement hypotheses, along with a required combination rule to merge them. It may be considered as a generalization of Bayesian Theory, that deals with the so-called probability function (Khaleghi et al. [111]).

The employment of Dempster-Shafer theory for the DF problem was first presented by Garvey et al. [75] in 1981. Unlike Bayesian inference, D-S theory allows each source to contribute information at different levels of detail. For example, one sensor may provide information to distinguish individual entities, while other sensors may provide information to distinguish classes of entities. D-S theory has established itself as a promising and popular approach to DF, especially in the latest years. Nonetheless, there appear issues such as the exponential complexity of the computations (in general

the worst case scenario), as well as the possibility of producing counterintuitive results, when fusing conflicting data by using Dempster's rule of combination. Both these issues have been heavily studied within the literature and numerous strategies have been proposed to solve or alleviate them (Barnett [12], Gordon and Shortliffe [81]).

1.2.4.1.3 Fuzzy Set Theory

Fuzzy Set Theory is an alternative theoretical scheme for dealing with imperfect data. In particular, fuzzy DF represents an efficient solution when vague or partial sensory data is "fuzzified" using a gradual membership function. Fuzzy data may then be combined using fuzzy rules to produce fuzzy fusion output. According to Zadeh [226], fuzzy fusion rules can be divided into conjunctive and disjunctive categories. Conjunctive fuzzy fusion rules are considered to be appropriate when fusing data provided by equally reliable and homogeneous sources. On the other hand, disjunctive rules are deployed when (at least) one of the sources is deemed as reliable, or when highly conflictual data have to be merged (Zadeh [226]). Accordingly, some adaptive fuzzy fusion rules have been developed, as a compromise between the two categories, which may be applied in both cases (Dubois and Prade [53]).

In contrast to Probability and Evidence theories, which are well suited to modeling the uncertainty of the membership of a target in a well-defined class of objects, Fuzzy Set Theory is well suited to modeling the fuzzy membership of a target in an ill-defined class. Yet, similar to Probability Theory, which requires a prior knowledge of the probability distributions, Fuzzy Set Theory requires prior membership functions for different fuzzy sets. Being a powerful theory to represent vague data, Fuzzy Set Theory is particularly useful to represent and fuse vague data produced by human experts in a linguistic fashion (Zadeh [226]). Furthermore, it may often be integrated with probabilistic (Sasiadek and Hartana [182]) and D-S evidential (Zhu and Basir [234]) fusion algorithms, in a complementary manner.

1.2.4.1.4 Possibility Theory

Possibility Theory was founded in 1978 by Zadeh [227] and later extended in 1988 by Dubois and Prade [51]. It is based on Fuzzy Set Theory, despite it was mainly designed to represent incomplete rather than vague data. In fact, the data combination rules used for a "possibilistic" fusion, are similar to those deployed for a fuzzy fusion. The main difference is that possibilistic rules are always normalized. Moreover, while the previously mentioned basic symmetric conjunctive and disjunctive fusion rules of Fuzzy Set Theory are sufficient only for restricted cases, possibilistic fusion methods offer a number of enhancements that allow for handling a quite vast range of fusion scenarios (Dubois

and Prade [51]). Also, possibilistic fusion is argued to be most appropriate in poorly informed environments (no available statistical data) as well as in the fusion of heterogeneous data sources.

1.2.4.1.5 Rough Set Theory

Rough Set is a theory developed by Pawlak [150] in 1992, for dealing with imperfect data and especially to represent imprecise data, ignoring uncertainty at different granularity levels. Indeed, Rough Set Theory would allow the approximation of possible states of the system based on the granularity of the input data.

Granularity indicates the level of detail used to describe a specific feature, with reference to the size of the elements of which it is composed. Within the computational field, granularity means the level of detail of the data stored in the data warehouse, and the elements from which it is composed are called data "granules". The higher is the level of detail, the lower the granularity, and viceversa. Granularity represents a very important design aspect to be taken into account, because it is directly linked to the volume of saved data and, consequently, to the performance of the system and the need for hardware resources. To choose the right level of granularity, in order to avoid storing details that will never be considered, constitutes not an easy task.

In order to successfully perform fusion, in fact, data granules must neither be too fine nor too rough. In the case of data granules being too fine, Rough Set Theory reduces to Classical Set Theory. On the other hand, for very rough data granules, the lower approximation of data is likely to be empty, resulting in a total ignorance. Once approximated as rough sets, data granules can be fused together using a Classical Set Theory, with conjunctive or disjunctive fusion operators (i.e. intersection or union).

The major advantage of Rough Set Theory, if compared to its alternatives, is that it does not require any preliminary or additional information, such as data distribution or membership function. Rough Set Theory allows for fusion of imprecise data approximated merely based on its internal structure (granularity).

Due the fact that such theory has not been well understood within the fusion community, Rough Set Theory has been rarely applied to data fusion problems.

1.2.4.1.6 Hybrid fusion approaches

The main idea behind the development of hybrid fusion algorithms is that different fusion methods such as Fuzzy Set Theory, D-S Evidence Theory, and Probability Theory should not be competing, as they approach DF from different (but possibly complementary) perspectives. Examples of hybrid frameworks are Fuzzy Rough Set Theory (FRST) (Dubois and Prade [52]) (omitted from the

representation of Fig. 1.2, in order to avoid confusion) and Fuzzy Dempster-Shafer Theory (Fuzzy DSET) (Yen [213]). At the theoretical level, hybridization of Fuzzy Set Theory with D-S Evidence Theory has been deeply studied (Yager [212], Yen [213]), aiming at providing a framework for a more comprehensive treatment of data imperfection.

Among many proposals, the work by Yen [213] is perhaps the most popular approach that extends the D-S Evidence Theory into the fuzzy realm, while maintaining its major theoretical principles. Yen's theory of Fuzzy D-S Evidence Theory frequently appears in the reference literature (Basir et al. [13], Zhu and Basir [234]).

Combination of Fuzzy Set Theory with Rough Set Theory (FRST), proposed by Dubois and Prade [52] constitutes another important theoretical hybridization existing in the literature. In spite of constituting a powerful representation tool for vague as well as ambiguous data, the original FRST displays some limitations, such as relying on special fuzzy relations. This issue has been subsequently addressed by Yeung et al. [214], in an attempt to generalize FRST to arbitrary fuzzy relations. However, the application of FRST to DF remains poorly investigated within the DF literature, as Rough Set Theory itself is still not an established DF approach.

1.2.4.1.7 Random Finite Set Theory

The principles of Random Set Theory were first proposed in the 1970s by Kendall [110], to study integral

geometry. The unifying capability of Random Set Theory has been shown by some researchers (Goodman et al. [80], Kreinovich [121], Mori [140]). Among them, the work of Goodman et al. [80] has been most successful in gaining a visible attention.

This theory is based on random subsets of measurement, to represent many aspects of imperfect data, and it may potentially provide a unifying framework for fusion of such a data. The main limit of Random Set Theory is that it is relatively new and not yet very well appreciated within the fusion community.

1.2.4.2 Fusion of correlated data

Many DF-based approaches, including the KF algorithm, require either the independence or the prior knowledge of the cross covariance of data, for producing consistent results. Unfortunately, in many applications, DF is correlated with potentially unknown cross covariance. This may occur due to the presence of noise in the observed phenomena (Julier and Uhlmann [102]) in centralized fusion settings, or due to the rumor propagation issue (also known as data incest or double counting problem,

Makarenko et al. [137]), where measurements are inadvertently used several times in distributed fusion settings.

Most of the proposed solutions for correlated DF attempt to solve it by either eliminating the cause of correlation or tackling the impact of correlation in the fusion process. Data correlation is especially problematic in distributed fusion systems, and it is commonly caused by data incest. The data incest situation itself happens when a same information takes several different paths from the source sensor to the fusion node. This issue may be eliminated (before fusion) either explicitly, by removal of data incest, or implicitly, through reconstruction of measurements.

Instead of removing data correlation, it is alternatively possible to design a fusion algorithm that accounts for the correlated data. Covariance Intersection (CI) (Julier and Uhlmann [102]) is the most common fusion method to deal with correlated data. CI was originally developed to avoid the problem of the covariance matrix underestimation due to data incest.

It solves this problem in a general form, for two data sources, by formulating an estimate of the covariance matrix as a combination of the means and covariances of the input data. As a drawback, CI requires a non-linear optimization process and therefore is computationally demanding.

1.2.4.3 Fusion of inconsistent data

The notion of data inconsistency may relate, in a generic sense, to spurious, as well as disordered or conflicting data, as already shown in Fig. 1.1. There exist various techniques available within the DF literature that have been developed to tackle each of these three aspects of data inconsistency.

Data provided by sensors to the fusion system may be spurious due to unexpected situations such as permanent failures, short duration spike faults, or slowly developing failure. If fused with correct data, such spurious data may lead to dangerously inaccurate estimates. For instance, as previously mentioned, KF would easily break down if exposed to outliers (Djurovic and Kovacevic [45]).

The majority of the research work in the field of DF on treating spurious data has been focused so far on the identification or prediction and subsequent elimination of the outliers from the fusion process. A common issue that may occur in using these techniques concerns the requirement of the prior information, often in the form of specific failure models. As a result, they would poorly perform in a general case, where a prior information is not available, or unmodeled failures occur.

1.2.4.4 Fusion of disparate data

Since the input data may be generated by a wide variety of sensors, humans, or even archived sensory data, fusion of such disparate data constitutes a very difficult task. In fact, the DF process should be able to build a coherent and accurate global view of the observed phenomena, despite this

disparateness. Nonetheless, in some fusion applications such as “Human Computer Interaction” (HCI) (Hall et al. [88]), such diversity of sensors is necessary to enable for a natural interaction with humans.

Within this context, the focus is placed on fusion of human generated data (so-called soft data) as well as fusion of soft and hard data (namely electronic data). In comparison to conventional fusion systems, in which input data is generated by calibrated electronic sensor systems with welldefined characteristics, research on soft DF considers combining humanbased data, preferably expressed in an unconstrained natural language. Research in this direction has attracted a considerable attention in recent years (Hall et al. [88]). This is motivated by the inherent limitations of electronic (hard) sensors and the recent availability of communication infrastructures that allow humans to act as soft sensors (Hall et al. [88]). Furthermore, while a great amount of research has been developed on DF using conventional sensors, very limited work has devoted to study fusion of data produced by human and non-human sensors.

An example of preliminary research in this area includes the work on generating a dataset for hard/soft DF, intended to serve as a foundation resource for future research (Pravia et al. [160, 161]). In Hall et al. [88], the authors provide a brief review on ongoing work on dynamic fusion of soft/hard data, identifying motivations and advantages, challenges and requirements of such an objective.

Frontier research focuses on the so-called “human-centered” data fusion paradigm, which emphasises the human role within the fusion process (Hall et al. [89]). This new paradigm allows humans to participate in the DF process, not merely as soft sensors, but also as hybrid computers and ad hoc teams. It relies on emerging technologies such as virtual world and social network software, to support humans in their new fusion role. Recent developments in the literature, having as their object the “human-centered” DF paradigm (Hall et al. [89]), as well as preliminary work on soft/hard fusion (Ferrin et al. [70], Pravia et al. [161], Premaratne et al. [162]) are an indicator of this new trend towards a more general DF framework, where both human and non-human sensory data may be efficiently processed. In spite of all these developments, research on hard/soft data fusion, as well as “human-centered” fusion still lies in its infancy, and it is believed that it will soon provide rich opportunities for further theoretical advancements and practical demonstrations.

1.2.5 Emerging Data Fusion trends

In this section, the discussion attempts to shed light on some of the emerging trends and frameworks within the sensor DF field. In addition, it explores many of the fusion aspects that are the subject of active ongoing research, from which it emerges how, despite research on DF is fairly well established, it is still rather poorly understood or employed. Finally, the theoretical effectiveness of a DF process

is inspected, especially with regard to the quality evaluation of the input data, as well as to the performance evaluation of the fusion system.

1.2.5.1 Alternative Data Fusion models

Two further alternative modalities of DF, which differ from the (traditional) procedures discussed so far, are here disclosed. Such DF-based approaches are known as “opportunistic DF” and “adaptive DF”.

1.2.5.1.1 Opportunistic DF

Concerning the limitations of traditional DF systems, which are mostly designed to use dedicated sensors and information resources, as well as the availability of new communication technologies, the “opportunistic” DF paradigm considers the possibility of treating sensors as shared resources and performing fusion in an opportunistic manner (Challa et al. [21]).

Nonetheless, some preliminary research works concerning this kind of DF are reported in the literature. For instance, in Wu and Aghajan [224] an opportunistic fusion of data across time, space, and feature level is performed within a visual sensor network for achieving human gesture analysis. In Al-Hmouz and Challa [5], the authors study the issue of optimal camera placement in a visual sensor network designed to serve multiple applications (each to be operated in an opportunistic manner). The problem is formulated as a multi-objective optimization problem and efficiently solved using a multi-objective genetic algorithm.

A variant of the opportunistic DF methodology is known as Opportunistic Information Fusion Model (OIFM). Among the peculiar features of such a procedure, compared to the conventional approach, there are the need of ad hoc computational load and of dynamic (not pre-defined) fusion rules. The key enabling component required to make an OIFM is a new approach towards a middleware development, called Opportunistic Middleware Model (OMM) (Challa et al. [21]). Unfortunately, current specifications for the OMM do not address many issues related to its implementation and thus future research is still needed to make OIFM viable.

1.2.5.1.2 Adaptive DF

Adaptation enables DF in situations where required environment parameters are not a-priori known or they dynamically change, and thus they must be re-estimated every time. Early work on adaptive DF dates back to the early 1990s (Hong [93]). Nonetheless, this problem has been rarely explored within the DF literature so far.

Some of the existing works are focused on the incorporation of "adaptivity" into Kalman Filtering. In Loy et al. [133], an adaptive fusion system capable of intelligent allocation of limited resources, which enables efficient tracking of moving targets in 3D, is presented. An "adaptive" variant of KF, called Fuzzy Logic Adaptive Kalman Filter (FLAKF), is proposed in Escamilla-Ambrosio and Mort [60]. It relies on fuzzy inference based on covariance matching, to adaptively estimate the covariance matrix of the measurement noise. Through a similar approach, Tafti and Sadati [201] present a Novel Adaptive Kalman Filter (NAKF) that achieves adaptation using a mathematical function called degree of matching, which is based on covariance matching. Finally, recently a further adaptive filter algorithm has been proposed and applied to the "pico satellite attitude" estimation problem, as presented in Soken and Hajiyev [193].

1.2.5.2 Theoretical effectiveness of DF processes

Most of the DF literature is based on an optimistic assumption about the reliability of models, producing the beliefs associated with data. For instance, sensory data are commonly considered as equally reliable and play a symmetrical role within the fusion process (Rogova and Nimier [171]). Nonetheless, different models usually display different reliabilities and they are valid just for a specific range. A recent trend in DF has addressed this issue, mostly by attempting to account for the reliability of beliefs. This has been accomplished through the introduction of the notion of a second level of uncertainty, that is "uncertainty about uncertainty", represented as reliability coefficients. The main challenges are first to estimate these coefficients, and then to incorporate them into the fusion process. Within the literature, a number of approaches for estimating such reliability coefficients is proposed. They rely on domain knowledge and contextual information (Nimier [143]), learning through training (Yu and Sycara [216]), Possibility Theory (Delmotte et al. [41]), and expert judgment (Sandri et al. [179]). Furthermore, the issue of reliability incorporation has been studied within several fusion frameworks such as Dempster- Shafer Theory (Haenni and Hartmann [87]), Fuzzy and Possibility Theory (Dubois and Prade [54]), Transferable Belief Model (Elouedi et al. [58]), and Probability Theory (Wright and Laskey [223]).

The issue of reliability in DF is still not well established, and several open questions such as interrelationship between reliabilities, reliability of heterogeneous data, and comprehensive architecture to manage DF algorithm and reliability of data sources remains parts of future research (Rogova and Nimier [171], Haenni and Hartmann [87]).

In light of this, the evaluation of the fusion procedure effectiveness seems to represent a very ambitious task. Performance evaluation aims at studying the behavior of a DF system operated by various algorithms and comparing their advantages and disadvantages based on a set of measures or

metrics. The outcome is typically a mapping of different algorithms into different real values or partial orders for ranking (Chen et al. [31]).

Generally speaking, the obtained performance of a DF system seems to be particularly dependent on two components: the quality of the input data and the efficiency of the fusion algorithm. As a result, the literature work on fusion evaluation may be categorized into two macro-groups, discussed in the two following sections.

1.2.5.2.1 Evaluating the quality of input data

The former category concerns the quality of input data evaluation. The aim here is to develop approaches that enable for the quality assessment of the data, which are fed to the fusion system, and the calculation of the degree of confidence in the data, in terms of attributes such as reliability and credibility (Cholvy [36]). The most notable works in this group are by far the NATO standardization agreements STANAG 2022 [195].

STANAG adopts an alphanumeric system of rating, which combines a measurement of the reliability of the source information with a measurement of the credibility of such an information, both evaluated using the existing knowledge. STANAG recommendations are expressed using natural language statements, which in many cases makes them quite imprecise and ambiguous.

Some researchers attempted to analyze these recommendations and provide a formal mathematical system of information evaluation, in compliance with NATO recommendations (Cholvy [36], Nimier [144]). The proposed formalism relies on the observation that three notions underline an information evaluation system: the number of independent sources supporting an information, their reliability, and that the information may conflict with some prior information. Accordingly, a model of evaluation is defined and its fusion method, which accounts for the three aforementioned notions, is formulated.

Subsequently, the same authors have extended their work to enable dealing with the notion of degree of conflict, in contrast with merely conflicting or non-conflicting information (Cholvy [37]). Nonetheless, the current formalism is still uncomplete as there are some foreseen notions of the STANAG recommendations, such as the total lack of knowledge about the reliability of the information source, which are not being considered.

Another important aspect related to input information quality, which is largely ignored, is the rate at which it is provided to the fusion system. The information rate is a function of many factors, including the revisit rate of the sensors, the rate at which data sets are communicated, and also the quality of the communication link (Gelfand et al. [77]). The effect of information rate is particularly important in decentralized fusion settings, where imperfect communication is common.

1.2.5.2.2 Evaluating the performance of the fusion system

The latter category concerning the effectiveness assessment of a DF procedure is based on the evaluation of the fusion system. The performance of the fusion system itself is computed and compared using a specific set of measures referred to as Measures Of Performance (MOP). The literature work on MOP is rather extensive and includes a wide variety of measures.

The choice of the specific MOP of interest depends on the characteristics of the fusion system. For instance, there is more to evaluate in a multiple sensor system than in a single sensor system. Furthermore, in the case of multi-target problems, the data association part of the system also needs to be evaluated along with the estimation part.

Commonly used measures for evaluating the system performance may be categorized into two main categories: metrics computed for each target and metrics computed over an ensemble of targets. Some of the MOPs belonging to the former category are: data accuracy, data covariance consistency, data purity, and data continuity. Instead, examples of measures in the latter category are: average number of missed targets, average number of extra targets, average data initiation time and data history (Drummond [50], Rothrock and Drummond [172]).

There are also other less popular measures related to the discrimination and classification capability of the fusion system that may be useful to be collected in some applications. Aside from the conventional approaches for performance measurement, the notable works of Zajic et al. [229] and Schumacher et al. [184] are worth mentioning on the development of MOPs for multi-target fusion systems within the Finite Set Theory framework.

Finally, some of the fusion evaluation tools that have recently become available are mentioned. For instance, the Fusion Performance Analysis (FPA) tool is a software that enables for the computation of technical performance measures virtually for any fusion system (Jackson and Musiak [97]). Another interesting development is the Multi-Sensory Tracking Testbed (Akselrod et al. [1]). Recently introduced, it represents the first step towards the realization of a state of the art testbed for the evaluation of large-scale distributed fusion systems.

1.2.5.3 Concluding remarks

To the best of the present knowledge, there is no standard and well-established evaluation framework to assess the performance of DF algorithms. Most of the work is being done on simulation and based on some idealized assumptions, which makes it difficult to predict how the algorithm would perform in real-life applications. A literature review on DF performance evaluation is presented in van Laere [205], where challenging aspects of DF performance evaluation, with reference to the practice, are discussed. In this work (van Laere [205]), it is shown that only very few articles (less then 5%) of the

analyzed research work, treat the fusion evaluation problem from a practical perspective. Indeed, it is demonstrated that most of the existing works are focused on performing evaluation in simulation or unrealistic test environments, which is substantially different from what experienced in practical cases.

One of the major challenging problems of the fusion evaluation in practice, which is usually ignored in the literature, is the fact that performance displays different, possibly conflicting, dimensions that are difficult to be captured in one comprehensive and unified measure (van Laere [205]). Then, in order to constitute a fair indicator of the fusion performance, the performance measures might need to be adapted over time or according to the given context or situation. This issue represents the importance of taking into consideration the specific situation or context under which the fusion system is being evaluated. This is the most difficult evaluation scenario, because of the difficulty for the fusion system to maintain the desired performance level. Based on this observation, some researchers have proposed metrics to enable a quantification of the complexity of the evaluation scenario, which is typically referred to as context metrics (Chong [38]).

A similar alternative approach is the so-called Goal Dependent Performance (GDP) metrics, which is capable of adjusting itself to the circumstances defined by the context at a certain moment in time (van Laere [205], Schumacher et al. [185]).

From what it has been presented, it emerges that research on DF systems is becoming more and more a common but rather non-trivial task. There appear a number of areas within the Data Fusion community that most likely will be highly active in the near future. For instance, the everincreasing demand for DF on extremely large scales, such as sensor networks and the Web, will drive intense research on highly scalable DF algorithms. In addition, the availability and abundance of non-conventional data, for example in the form of human-generated reports, will lead to the development of new and powerful fusion frameworks capable of processing a wide variety of data forms. Such fusion frameworks might potentially be realized by exploiting strong mathematical tools for modeling imperfect data, such as Random Set Theory (Khaleghi et al. [111]). With DF algorithms extending their application from the military domain to many other fields, such as robotics, sensor networks, image processing and structural monitoring, the need for standard fusion evaluation protocols that are applicable, independently from the given application domain, will grow more and more. As a result, the fusion community will be driven towards the adoption of such protocols in the future. So, there appears to be a serious need for further research on development and standardizing measures of performance applicable to the practical evaluation of DF systems.

1.3 Kalman Filter

This section is devoted to an introductory description on the Kalman Filter (Kalman [105]), as an algorithm that may be exploited for estimating the health condition of linear dynamic systems perturbed by a zero-mean Gaussian white-noise, through the fusion of data that may also be affected by measurement errors. In this sense, KF shall constitute a fundamental tool that may be involved within HDF procedures, aiming at pursuing an effective SHM. In addition to applications related to the civil engineering context, the mathematical model behind the KF constitutes a reasonable representation for many other problems of a practical interest, including control problems, as well as estimation problems.

Here, the KF is introduced, and some of the most important bibliographic references on this topic are discussed. Then, after a general brief historical perspective on signal filtering, the discussion attempts to shed light on the probabilistic origin of the filter, and examples of applications in which KF has been successfully employed within the civil engineering field are also reported. Finally, some possible future perspectives for KF employment and development are also presented.

1.3.1 KF generalities

Kalman Filter (Kalman [105]) (and its variants, such as Extended Kalman Filter (EKF) (Hoshiya and Sato [94]) and Unscented Kalman Filter (UKF) (Julier and Uhlmann [104])), represents one of the most celebrated and popular DF algorithms in the field of information processing. It was introduced by Hungarian electrical engineer Rudolf Emil Kalman (1930-2016), in his famous 1960's publication (Kalman [105]). For the greatness of the invention, he was later awarded with the National Medal of Science by former USA President Barack Obama, on October 7, 2009.

In spite of being over 50 years old, KF is still widely used. The great success of KF is due to its small computational requirement and elegant recursive properties, which confer to the filter the status of the optimal estimator for one-dimensional linear systems with Gaussian error statistics. From a theoretical standpoint, in fact, KF is an algorithm that allows for an exact inference in a linear dynamical system, which may be considered a Bayesian model where all latent and observed variables display a Gaussian distribution (often a multivariate Gaussian distribution). Typical uses of KF include smoothing noisy data and providing estimates of parameters of interest. Applications also include GPS receivers, phaselocked loops in radio equipment, smoothing the output from laptop trackpads, and many others. The most famous employment of KF was probably in the Apollo navigation computer, that took Neil Armstrong's crew to the moon in 1969. Today, Kalman Filters are at work in every satellite navigation device, every smartphone, and many computer games. However, its adoption in structural engineering is still far from being exhaustive.

1.3.2 Filtering

This section aims at providing some general rudiments about the concept of filtering. It is developed through a brief historical introduction and, further, by an excursus on the fundamental characteristics of a basic filter. A description of a considered standard system, with a presentation of its initial conditions, and a description of the noise process, are also provided.

1.3.2.1 Brief history of signal filtering

Filtering in one form or another has been around since long time. For many centuries, man has attempted to remove the more visible of the impurities in his water by filtering, and the dictionary gives a first meaning for the noun filter as *"a contrivance for freeing liquids from suspended impurities, especially by passing them through strata of sand, charcoal, etc."* (Anderson [6]). Modern usage of word filter often involves more abstract entities than fluids with suspended impurities. However, there is usually the notion of something passing a barrier: there is talk of news filtering out of the war zone, or sunlight filtering through the trees, etc. Sometimes the barrier is interposed by man for the purpose of sorting out something that is desired from something else with which is contaminated. One example is provided by water purification; the use of an ultraviolet filter on a camera provides another example. When the entities involved are signals, the barrier - in the form of an electric network - becomes a filter in the sense of signal processing. It is easy to think of engineering situations in which filtering of signals might be desired. Communication systems always display unwanted signals, or noise, entering into them. The user of the system naturally tries to minimize the inaccuracies caused by the presence of this noise, by filtering. Again, in many control systems, the control is derived by feedback, which involves processing measurements derived from the system. Frequently, these measurements contain random inaccuracies or may be contaminated by unwanted signals, and filtering becomes necessary, in order to make the control close to what is desired.

Filters were originally seen as circuits or systems with a frequency selective behavior. The series or parallel tuned circuit represents one of the most fundamental circuits in electrical engineering. Something more sophisticated than collections of tuned circuits is necessary for many applications and, as a result, an extensive research field has grown up in filter design theory. Some of the most known linear filters are: *constant k* and *m-derived filters* (Skilling [190]), *Butterworth filters*, *Chebyshev filters* and *elliptical filters* (Storer [198]).

In more recent years, there has been an extensive development of numerical algorithms for filter design. Usually, specifications on amplitude and phase response characteristics are given, and often, with the support of sophisticated computer-aided design packages, which allow for interactive

operation, a filter is designed to meet such specifications. Normally, there also appear constraints imposed on the filter structure which need to be met. These constraints may involve, for example, impedance levels, types and number of components.

Non-linear filters have also been used for many years, and results are reported in the literature. The simplest is the AM envelope detector (Termanù [202]), which is a combination of a diode and a low-pass filter. In a similar vein, an Automatic Gain Control (AGC) circuit uses a low-pass filter and a non-linear element (Terman [202]). The phase-locked loop used for FM reception is another example of a non-linear filter (Viterbi [210]).

A common classification is to distinguish between analog filters and digital filters. Made possible by innovations in integrated circuit technology, the digital approach has brought many advantages to filtering procedures (Gold and Rader [79], Rabiner and Gold [164]). Probably, the most important one is the fact that the filter parameters may be set and maintained to a high order of precision, thereby achieving filter characteristics in terms of reliability that normally could not be obtained with analog filtering. Another advantage is that parameters may easily be reset or made adaptive with a little extra cost.

As well as by the digitalization process, the notion of filter has been influenced by a second significant development, namely the application of statistical ideas to filtering problems (Wiener [222], Wainstein and Zubakov [219]).

The statistical approaches for the filtering treatment postulate that certain statistical properties are possessed both by the useful signal and the unwanted noise. Measurements are available as the sum of these latter quantities, and the task is still to eliminate by some means as much of the noise as possible. Concerning the statistical approach, the earliest contributions by Kolmogorov [117] and Wiener [222] proposed filtering processes with statistical properties which do not change with time, like stationary processes. In this way, they proved possible to relate the statistical properties of the useful signal and the unwanted noise with their frequency domain properties.

A significant aspect of statistical approaches is the definition of a measure of the suitability or the performance of a filter. Roughly, the best filter might be declared as the one which presents an output closest to the correct (or useful) signal.

As noted above, the assumption that the underlying signal and noise processes be stationary is crucial to the Wiener-Kolmogorov Theory. It was not until the late 1950s and early 1960s that a new theory was developed that did not require such a stationarity assumption (Kalman and Bucy [106]). Such theory arises from the inadequacy of Wiener-Kolmogorov Theory for coping with certain applications in which the “non stationarity” of the signal and of the noise is intrinsic to the problem. The new theory soon acquired the name of Kalman Filter Theory.

Because the stationary theory, and therefore also the Wiener-Kolmogorov Theory, were normally developed and thought of in Frequency Domain terms, while the non stationary theory, such as the KF Theory, was naturally developed and thought of in time domain terms, the contact between the two theories initially seemed slight. Nevertheless, there appears a substantial contact, if for no other reason than that a stationary process is a particular type of a non stationary process. In this sense, a rapprochement of Wiener Theory and KF Theory is achieved. It is pertinent to note that the issues in implementing Kalman Filters and Wiener Filters were both consistent with the technology at the time of their conceptualization. In particular, while Wiener filters were implementable with amplifiers and time invariant network elements, such as resistors and capacitors, Kalman Filters were implementable with digital integrated circuit modules.

The point of contact between the two streams of development discussed in this section, i.e. the digital approach and the statistical approach to filtering problems, arises with the need of implementing a discrete-time KF using digital hardware (Anderson and Moore [6]). Looking at the future, it would be clearly desirable to incorporate the practical constraints associated with digital filter realization into the mathematical statement of the statistical filtering problem, in order to achieve a better design of the filters for estimation purposes. At present time, however, this has not been done yet and, as a consequence, there is little contact between the two mainstreams.

1.3.2.2 Fundamental characteristics of a filter

According to Anderson and Moore [6], four main characteristics describe a basic filter, namely:

- Operation in discrete time;
- Optimality;
- Linearity;
- Finite dimensionality.

Each of these characteristics is discussed in the following. It is worth noting that filters derived by KF inherit most, but not all, of these characteristics.

1.3.2.2.1 Operation in discrete time

Signal processing is becoming increasingly digital and therefore, basic filters may today be considered as characterized of this sort. For this reason, it is important to understand continuous-time signal processing as well as to understand discrete-time signal processing.

In fact, signals are mathematically described as functions of an independent variable, commonly and conventionally represented by time (although in some cases, it may even not correspond to time), that can be either continuous or discrete. In particular, continuous-time signals are defined along a

continuum of time and they are thus represented by a continuous independent variable. These signals are often referred to as analog signals. Instead, discrete-time signals are defined at discrete time instances, and thus, the independent variable assumes discrete values, which means that these signals are represented by sequences of numbers (samples).

Signals such as speech or images may have either a continuous- or a discrete-variable representation, and if certain conditions hold, these representations may also be totally equivalent. Besides the independent variables being either continuous or discrete, the signal amplitude may be either continuous or discrete. Signals for which both time and amplitude are discrete are known as digital signals. The assumption of operating in discrete time should be facilitated, due to the fact that discrete-time statistical filtering theory is much easier to be learned than continuous-time statistical filtering theory.

1.3.2.2.2 Optimality

Filters may express optimality in different ways. Certain classes of optimal filters tend to be robust in their maintenance of performance standards when the quantities assumed for design purposes are not the same as the quantities encountered in the operation. In other words, such kind of optimal filters are normally free from stability issues.

In general, optimal filters are characterized by a high degree of complexity. This is the reason because, frequently, it is preferable to use a much less complex filter, with a little sacrifice of performance. One approach for such an end consists in approximating the model by one that is simpler than the original one; then, obtaining the optimal filter for this latter model, and finally using it for the original one. In this way, the filter becomes suboptimal and thus it is expected to become less complex. This approach may fail on several grounds: the resulting filter may still be to complex, or the amount of sub-optimality may unacceptably be great. In this case, it may be very difficult to obtain a satisfactory filter of a much lower complexity than that of the optimal filter, even because theories for suboptimal design are in some ways much less developed than theories for optimal design.

1.3.2.2.3 Linearity

The term linearity refers to a property of a system (in this case, a filter) that indicates how its output may get in linear relationship with its input. So, it may be possible to study the behavior of a linear filter through the Principle of Superposition of Causes and Effects (PSCE). This makes it possible to calculate the final output as a linear sum of the individual responses to various input, taken one at a time. This allows to greatly simplify the study of linear filters than the of non-linear ones, in which, instead, the output depends on the non-linear combination of the input, which therefore must all

concurrently be studied. In fact, the existence of correlation terms that depend simultaneously from a multiple input of the system, prevents to decompose the initial problem into similar but simpler sub-problems. In such cases, the PSCE cannot be applicable.

Many electronic applications involve linear systems with associated Gaussian random processes, from which it transpires that the optimal filter, in a minimum mean-square-error sense, is the linear one. Of course, many other applications involve non-linear systems with associated non Gaussian random processes and, for these situations, non-linear filters seem to be necessarily involved. The matter is that optimal non-linear filter design and implementation are very hard, if not impossible, in many instances. However, for this reason, suboptimal linear filters may sometimes be used as a substitute for optimal non-linear filters, or some form of non-linear filter may be derived, usually through a modification of a linear filter or, sometimes, using a collection of linear filters.

1.3.2.2.4 Finite dimensionality

It is straightforward that finite-dimensional filters should be used when the processes to be filtered are associated with finite-dimensional systems. Now, most physical systems are not finite dimensional. However, almost all infinite-dimensional systems may be approximated by finite-dimensional systems, and this is generally what happens in modeling processes. Thus, the finite-dimensional modeling of the physical system leads to an associated finite-dimensional filter. Of course, this finite-dimensional filter will be suboptimal to the extent that the model of the physical system is in some measure an approximation of physical reality.

It may be legitimate to wonder why a suboptimal finite-dimensional filter should be used. The reason lies in the fact that, through its adoption, it is possible to treat infinite-dimensional filtering problems in discrete time fairly easily. In particular, finite-dimensional filters are to be preferred due to the fact that they are easier to be designed and far easier to be implemented, than infinite-dimensional filters.

1.3.2.3 System, noise and filtering

This section aims at providing some fundamental definitions useful for the comprehension of the concepts of system, noise and filtering, distinguishing between smoothing and prediction.

To deal with any sort of filtering problem, in the first place there must be a system, generally dynamic, of which measurements should be available. The system behavior may normally be described by equations. It operates in real time, so that the independent variable in the equations is time, and it is assumed to be causal, so that an output at some time $t = t_0$ is always independent on an input applied at times subsequent to t_0. Further, the system may operate in continuous or discrete time, depending

on the nature of the source signal to be processed. Consequently, the output may change at discrete time instants or on a continuous basis.

In this research, the attention is to focus on discrete-time systems. In particular, the class of discrete-time systems presented in this section takes as a prototype the linear, finite-dimensional system, represented in following Fig. 1.3.

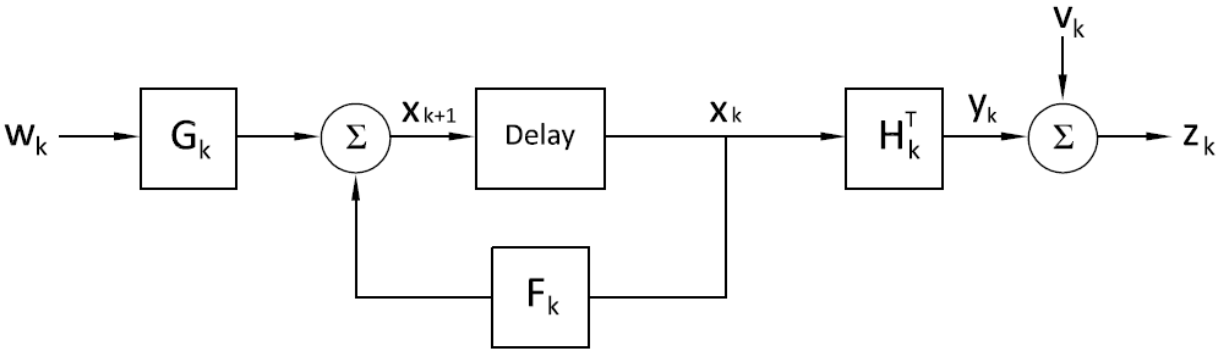

Figure 1.3: Finite-dimensional linear system serving as a signal-model (adapted from Anderson and Moore [6]).

The system depicted in Fig. 1.3 may be described by the so-called state-space equations, as follows:

$$\mathbf{x}_{k+1} = \mathbf{F}_k \mathbf{x}_k + \mathbf{G}_k \mathbf{w}_k \tag{1.1}$$

$$\mathbf{z}_k = \mathbf{y}_k + \mathbf{v}_k = \mathbf{H}_k^T \mathbf{x}_k + \mathbf{v}_k \tag{1.2}$$

Subscript k is a time argument. It is assumed that the initial time of the system is finite. Then, by a shift of the time origin, it is possible to assume that Eq. (1.1) and Eq. (1.2) hold for $k > 0$.

In Eq. (1.1) and Eq. (1.2), $\mathbf{x}_k$ represents the system state at time k. Under normal circumstances, $\mathbf{H}^T_k$ $\mathbf{x}_k$ (or equivalently $\mathbf{y}_k$) would be the corresponding system output but, in this case, noise process $\mathbf{v}_k$ is added to $\mathbf{y}_k$, which results in measurement process $\mathbf{z}_k$. The input process to the system is $\mathbf{w}_k$ and, like $\mathbf{v}_k$, is a noisy process. Adding details about $\mathbf{w}_k$ and $\mathbf{v}_k$ are later given within the discussion, in general terms, and in Chapters 2–3, where a filtering problem for a specific linear dynamic structural system is solved. So far, none initial condition for Eq. (1.1) has been specified. Under normal circumstances, it may be expected that, at initial step k = 0, state $\mathbf{x}$, namely $\mathbf{x}_0$, is some prescribed vector. From the practical point of view, since it is impossible to exactly know $\mathbf{x}_0$, this leads to the adoption of a random initial condition for the system.

In particular, it is common to assume that $\mathbf{x}0$ is a Gaussian random variable of known mean $\mathbf{x}_0$ and known covariance $\mathbf{P}_0$:

$$\mathbf{E}[\mathbf{x}_0] = \bar{\mathbf{x}}_0 \tag{1.3}$$

$$\mathbf{E}\left\{[\mathbf{x}_0 - \overline{\mathbf{x}}_0][\mathbf{x}_0 - \overline{\mathbf{x}}_0]^T\right\} = \mathbf{P}_0 \tag{1.4}$$

where **E** represents the expected value.

The Gaussian assumption is adopted for three main reasons. The first is linked with experiments. In fact, experimental reality establishes that many naturally-occurring processes are Gaussian. Secondly, by modeling certain natural processes as resulting from the sum of a number of individual, possibly non Gaussian processes, the central limit theorem of Probability Theory (Tucker [204]) suggests a Gaussian distribution for their sum. Finally, the filtering problem is generally easier to be solved with the Gaussian assumption. That is essentially why the Gaussian assumption is commonly adopted for filter processing.

As it has been observed, in discussing filtering and related issues, it is implicit that the systems under consideration are assumed to be noisy. Noise may arise in many ways. For example, input to the system may be unknown and unpredictable, except for its statistical properties, and this lack of information may be considered as a kind of noise. Moreover, or output from the system may be acquired through noisy sensors or, again, output may only be observed via a sensor after transmission over a noisy channel, etc.

As a general rule, almost nothing may be done for filtering processing until a sort of probabilistic structure is placed in defining input noise process $\mathbf{w}_k$ and output noise process $\mathbf{v}_k$.

For the aims being pursued, the following assumptions are hereinafter considered:

1. $\mathbf{v}_k$ e $\mathbf{w}_k$ are individual white-noise processes. This means that, for any k and l, with k≠l, $\mathbf{v}_k$ and $\mathbf{v}_l$, and $\mathbf{w}_k$ and $\mathbf{w}_l$ are independent random variables;
2. $\mathbf{v}_k$ and $\mathbf{w}_k$ are individual zero-mean Gaussian processes with known covariances;
3. $\mathbf{v}_k$ and $\mathbf{w}_k$ are independent processes.

Assumption 2 would mean that the Probability Density Function (PDF) of $\mathbf{v}_k$ for arbitrary *k*, is Gaussian. In view of the whiteness of $\mathbf{v}_k$, declared by Assumption 1, PDF $X_{v,w}$ corresponds to the product of the two individual densities yv and yw. Therefore, $X_{v,w}$ is Gaussian if the PDFs of $\mathbf{v}_k$ and $\mathbf{w}_k$, for each *k*, are Gaussian.

Now, the focus is on what is meant for filtering. Suppose that there is some quantity (possibly a vector quantity) associated with a system, whose value would be liked to be known at each time instant. For the sake of argument, assume the system in question to be a continuous time system, and the quantity in question to be denoted by **x**. It may be that this quantity is not a directly measurable one, or that it can only be measured with an error. Thus, suppose that noisy measurements **z** are available, with **z**≠**x**.

Now, the term filtering may be used in two different ways. First, it may be used as a generic term: filtering is the recovery of **x** through **z**, or an approximation to **x**, or even some information about **x**.

In other words, noisy measurements of a system are used to obtain information about some quantity that is essentially internal to the system. Secondly, the term filtering may be used to distinguish a certain kind of information processing from two other related kinds of information, i.e. smoothing and prediction. Smoothing differs from filtering since the information about **x**(t) needs not to become available at time t, and measurements derived later than time t may be used for obtaining information about **x**(t). This means that there must be a delay in producing the information about **x**(t), as compared with the filtering case, but the penalty of having a delay may be weighed by the ability to use more measurement data than in the filtering case, in producing the information about **x**(t). Indeed, it is possible to use measurements not only up to time t, but also after time t. For this reason, the smoothing process may be expected to be more accurate than the filtering process.

Prediction is the forecasting side of information processing. The aim is to obtain at time t information about $\mathbf{x}(t + l)$ for some $l > 0$. In other words, the aim is to achieve information about how **x** will be in the future. In obtaining such a kind of information, measurements up to time t have to be used. Generally, any prediction task becomes more difficult as the environment becomes noisier.

Finally, filtering means the recovery at time t of some information about **x**(t), using measurements up to time t. In other words, through filtering procedures, it may be possible to obtain information about **x** at time t (hence **x**(t)), so that the information becomes available only at time t, and not at some later time.

An example of the application of filtering in everyday life is represented by radio reception, where the signal of interest, constituted by the voice signal, is used to modulate a high frequency carrier that is transmitted to a radio receiver. The received signal is inevitably corrupted by noise and, consequently, when demodulated, for recovering the original signal as better as possible it needs to be opportunely filtered.

1.3.3 On Kalman Filter

After the presented general overview on filtering, here, a specific filter, i.e. Kalman Filter (KF), is inspected through a dedicated historical introduction, by providing its definition, exploring its applications in the engineering field, and analyzing the main issues related to this kind of filter.

1.3.3.1 Origin of KF

A historical survey on the development of Kalman filtering can be found in Sorenson [194]. The origins of KF may be dated back to the late eighteenth century, at the time of the study of planetary orbits by Gauss. Later theories in which KF is rooted, are those of maximum likelihood estimation by Fisher [71], and the previously mentioned stationary filtering theory by Wiener [222] and

Kolmogorov [117], which focus on linear minimum variance estimation. It is furthermore a commonly known view that, whereas the use of a recursive approach in estimating constant parameters to cop with new measurements essentially dates back to Gauss, the idea of recursion in the presence of a dynamic evolution of the quantity being estimated as more measurements become available, is much more recent. Despite the fact of using a state-variable rather than an impulse response or a transfer function for describing linear systems is closely associated with the name of Kalman, many people consider that the concepts contained in the famous Kalman's publication of 1960 [105] were already stated by Swerling a year earlier (Swerling [200]). However, there is no doubt that subsequent contributions by Kalman regarding matters such as stationary filters and stability (e.g. Kalman [107]), went far beyond what stated in Swerling [200].

1.3.3.2 KF definition

Theoretically, KF is defined as a Linear Quadratic Gaussian (LQG) problem, which corresponds to the problem of estimating the instantaneous state (i.e. the dynamic behaviour) of a linear dynamic system perturbed by Gaussian white-noise, by using measurements linearly related to the state, but corrupted by Gaussian white-noise. It is proven that the resulting estimator is statistically optimal with respect to any quadratic function of the estimation error.

KF is certainly one of the greatest discoveries in the history of statistical estimation theory, and likely also one of the greatest discoveries in the twentieth century. KF's most immediate applications have been channeled to the control of complex dynamic systems, such as continuous manufacturing processes, ships and aircrafts, spacecrafts, and satellites.

In order to control a dynamic system, it is necessary to know what the system is doing. However, it is not always possible to measure all the variables that rule such a system; namely, only a partial knowledge of it is achievable. In a similar scenario, KF provides a means for inferring the missing information from indirect (and noisy) measurements. In particular, KF is employed for estimating the complete state vector of a system from partial state measurements. Moreover, KF may also be used for prediction, as in the case of estimations of the flow of rivers during flood conditions, trajectories of celestial bodies, or prices of traded commodities.

From a practical point of view, the following definitions of KF may be provided (Mohinder and Angus [139]):

- *KF is a tool.* In fact, it makes easier to solve a problem, but it does not solve all the problem by itself. In particular, it is not a physical tool, but a mathematical tool, since it is made by mathematical models.

- *KF is a recursive algorithm.* It uses a finite representation of an estimation problem by a finite number of variables (Gelb et al. [76]). However, it does assume that these variables are real numbers with an infinite precision. Some of the problems encountered on its use arise from the distinction between finite dimension and finite information, and the distinction between finite and manageable problem sizes. These are all issues on the practical side of KF that have to be considered along with the theory.
- *KF is a complete statistical characterization of an estimation problem.* It is much more than an estimator, because it propagates the entire probability distribution of the variables it is tasked to estimate. This is a complete characterization of the current state of knowledge of the dynamic system, including the influence of all past measurements. These probability distributions are also useful for statistical analysis and predictive design of sensor systems.
- *KF is a learning process.* It uses a model of the estimation problem that distinguishes between phenomena (what is possible to be observed), noumena (what is really going on), and the state of knowledge about noumena that is possible to be deduced from phenomena. That state of knowledge is represented by probability distributions.

1.3.3.3 How it came to be called a filter

It might seem strange that the term filter has been applied to an estimator. More commonly, a filter is a *"physical device for removing unwanted fractions of mixtures"* (Mohinder and Angus [139]). The word *"filt"* comes from the same medieval Latin term, for the material that was used as a filter for liquids.

Originally, a filter solved the problem of separating unwanted components of gas-liquid-solid mixtures; later, in the era of crystal radio receivers, the term was applied to analog circuits that "filter" electronic signals. These signals are a mixture of different frequency components, and these physical devices preferentially attenuate unwanted frequencies. This concept was extended in the 1930s and 1940s to the separation of signal from noise, both of which characterized by their power spectral densities. Wiener [222] and Kolmogorov [117] used this statistical characterization of their probability distribution in forming an optimal estimate of the signal, given the sum of signal and noise.

With Kalman filtering, the term assumed a meaning that goes well beyond the original idea of separation of the components of a mixture. It has also come to include the solution of an inverse problem, in which it is known how to represent the measurable variables as a function of the variables of principal interest. In essence, it inverts this functional relationship and estimates the independent

variables as inverted functions of the dependent (measurable) variables. These variables of interest are also allowed to be dynamic, with dynamic processes that are only partially predictable.

Fig. 1.4 depicts the essential subjects forming the mathematical foundations of Kalman Filtering theory. Although this shows KF as the apex of a pyramid, it is itself part of the foundations of another discipline, i.e. Modern Control Theory, and a proper subset of Statistical Decision Theory (Mohinder and Angus [139]).

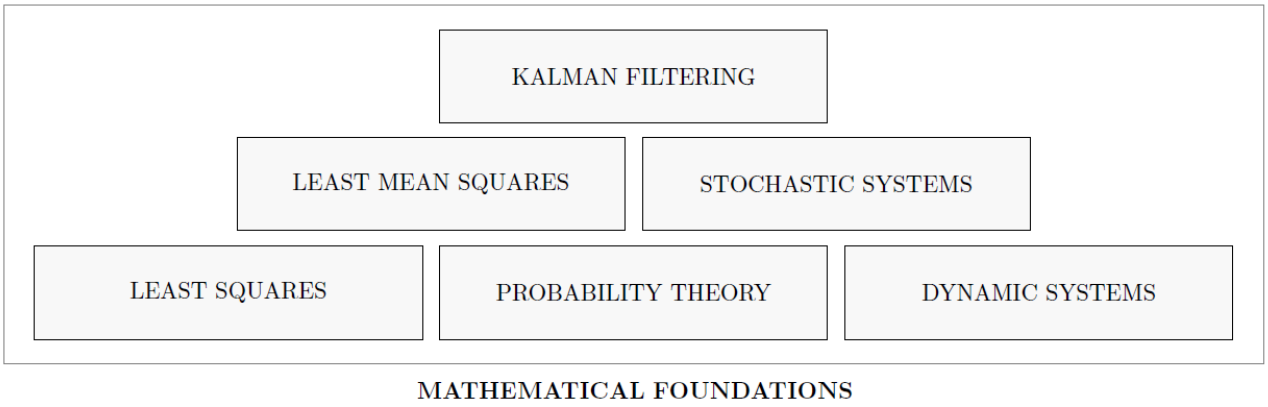

Figure 1.4: Founding concepts in Kalman filtering theory (adapted from Mohinder and Angus [139]).

1.3.3.4 KF applications

Here, some applications which exploit KF are provided. The formulation of KF involves a blend of a model with measurements. The improvements in the predictions of the response, in comparison to the "open loop" (i.e. a system that does not contain any feedback terms from the output), result from incorporating the measured data into the estimation process. An "open loop" system is opposed to a "closed loop" one, i.e. a system in which part of the excitation instead depends on the feedback from the response.

KF theory has received serious attention in many fields such as electrical engineering, robotics, navigation and economics since the 1960's. The problems and applications that originated the development of KF theory, as it stands today, are not issues related to structural engineering. However, the employment of KF theory may become more prominent because the types of problems that exploit it are more common than before, and there appears to be a significant potential in incorporating KF theory into a variety of issues concerning existing structural systems. As new challenges arise, regarding critical infrastructures, blending FEM models with measured data, may represent an increasingly important approach to modern structural engineering problems.

As already stated, applications which involve KF encompass many fields, but its employment as a tool is essentially adopted for two main purposes, namely the state estimation of dynamic systems and the analysis of estimator performance. These two perspectives are individually discussed in the following paragraphs.

1.3.3.4.1 State estimation of dynamic systems

First, it is important to establish what is meant for a dynamic system. Except for a few fundamental physical constants, in fact, there is hardly anything in the universe that may be considered to be truly constant. The orbital parameters of the asteroids, for instance, are not constant, and even the "fixed" stars and continents are moving. Nearly all physical systems are dynamic, to a some degree. So, if the aim is to obtain a very precise estimate of their characteristics over time (i.e. their state), then it is necessary to take their dynamic into consideration.

The problem is that it is not always possible to know very precisely their dynamic. So, given this state of partial ignorance, the best that is possible to do is to express this ignorance more precisely, using probabilities. KF allows to estimate the state of dynamic systems with certain types of random behavior, by using such statistical information. A few examples of these systems are listed in the second column of Table 1.1.

Application	Dynamic System	Sensor Types
Process control	Chemical plant	Pressure Temperature Flow rate Gas analyzer Weather radar
Tracking	Spacecraft	Radar Imaging system Rain gauge
Navigation	Ship	Gyroscope Log GPS receiver Accelerometer

Table 1.1: Examples of estimation problems (adapted from Mohinder and Angus [139]).

1.3.3.4.2 Analysis of estimation systems

The third column of Table 1.1 lists some possible sensor types that might be used in estimating the state of the corresponding dynamic systems. The aim of design analysis is to determine how best to

use these sensor types for a given set of design criteria. These criteria are typically related to estimation accuracy and system cost.

KF exploits a complete description of the probability distribution of its estimation errors in determining the optimal filtering gains, and this probability distribution may be used in assessing its performance as a function of the design parameters of an estimation system, such as:

- types of sensors to be used;
- locations and orientations of the various sensor types with respect to the system to be estimated;
- permissible noise characteristics of the sensors;
- pre-filtering methods for smoothing sensor noise;
- data sampling rates for the various sensor types;
- level of model simplification to reduce implementation requirements.

The analytical capability of KF formalism also allows a system designer to assign an "error budget" to subsystems of an estimation system and to trade off the budget allocations, for optimizing costs or other measures of performance, while achieving a required level of estimation accuracy. Furthermore, it acts as an observer through which all the states not measured by sensors, may be reconstructed and used in control system applications.

1.3.3.5 KF in structural engineering

Over the past twenty years there has been a significant progress in the development of new methods for the analysis of structural deformation measurements, in order to guarantee construction's safety. According to Gulal [85], stability and operational safety of a structure consist of three main components, namely emergency concept, surveillance and constructional safety.

The emergency concept includes normative aspects such as material integrity and structural damage assessment, intensified surveillance and diagnostic technologies, lifetime and utilization evaluation, maintenance and repair, out-of-service and replacement decisions.

Aim and purpose of any surveillance is the earliest possible detection of damage, failure or injury to the safe operation of a construction, in order to be able to appropriately and timely react.

Referring to structural safety, it may be seen as a part of the surveillance concept. Determination of stability and operational safety of a structure requires an interdisciplinary approach among Engineering Geodesy, System Theory and Structural Mechanics. This is depicted in the Venn diagram of Fig. 1.5.

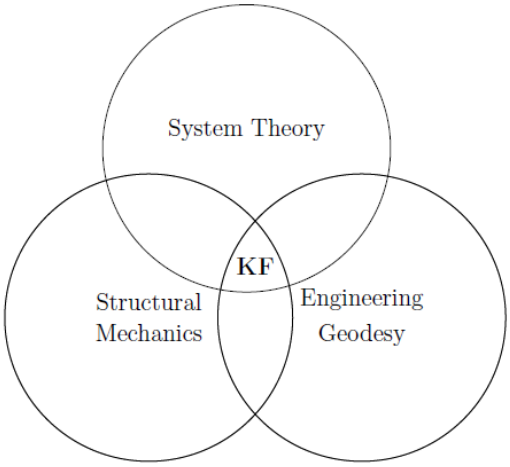

Figure 1.5: Venn diagram detailing the role of KF in the interdisciplinary approach of stability and operational safety of structures (adapted from Gulal [85]).

Brunner [16] defines Engineering Geodesy as "the production of geodetic information necessary for the planning of technical projects, setting out of the project design, control of the correct construction, and monitoring of deformations". This definition is comprehensive and consistent with the stability and safety of a structure. However, a more pertinent definition of Engineering Geodesy for the context of this work is that provided by Kuhlmann at al. [122], according to which "Engineering geodesy is the discipline of reality capture, setting-out and monitoring of local and regional geometry-related phenomena paying particular attention to quality assessment, sensor systems and reference frames".
Instead, Structural Mechanics is referred to as the determination of deformations, deflections and internal forces or stresses within structures, either for design purposes of new structures or for performance evaluation of existing structures. A powerful technique originally developed for the numerical solution of complex problems in structural mechanics, is the well-known Finite Element Method (FEM). Today, it surely represents the preferred analysis method to deal with complex structural systems.
Finally, System Theory is a method for constituting and analyzing complex structural systems. In System Theory, the setup of an appropriate mathematical-physical representation of the Transfer Function (TF) of a dynamic system is called System Identification (SI). Setting up a model for the transfer function is fundamental for the choice of a parametric or a non-parametric identification (Heunecke and Welsch [92]).
The issue of structural system identification lies at the heart of condition assessment of existing structures and in developing SHM strategies. This class of problems concerns inverse problems, in which properties of the structure need to be estimated based on noisy data for the applied forces and a limited set of response measurements, detected by predisposing an appropriate sensors network.

These problems are closely related with problems of FEM updating and structural damage detection using response data, and such issues have received wide attention in the broader context of engineering dynamical systems (Ljung [131], Ewins [61], Pintelon and Schoukens [151]). Within this scenario, KF may represent an important mathematical tool constituting the basis of the development of structural system identification methods. In fact, KF and its variants (EKF and UKF) have been widely used within the development of structural system identification strategies, for both linear and non-linear dynamical systems (Yun and Shinozuka [217], Hoshiya and Sato [94], Imai et al. [96], Shinozuka and Ghanem [189]).

It is worth reiterating that KF is able to provide the exact solution to the problem of System Identification when process and measurement equations are linear and the noise is additive and Gaussian. When these conditions are not met, suboptimal strategies should be developed, based on linearization or transformation methods, or, alternatively, Monte Carlo simulation strategies should be employed to solve the problem (Chen et al. [32], Ching et al. [34]).

Within the literature, cases where KF was successfully exploited in the civil engineering field, in combination with FEM models, are widespread. For instance, Heunecke andWelsch [92] have determined the diurnal variation due to solarization of a suspension bridge, Hesse [91] analyzed a shell structure under varying loads, Eichhorn [56] calculated the thermal deformations of bar-shaped machine elements, whereas Teskey [203] and Gulal [84] used this technique for the monitoring of a dam.

Another important issue for which KF has been successfully employed is the reconstruction of the dynamic response of a structure subjected to partially unknown external loads. Specifically, a more appropriate tool for this specific purpose is considered to be the Unscented KF (Julier and Uhlmann [104]), a particular variant of KF.

In fact, in many modern structural engineering applications, such as SHM, control, model validation and damage detection, reconstructing the response of an existing structure subjected to partially (or totally) unknown excitations is often required. If the structure is not instrumented, the best that it may be done is to estimate the unknown loads and applying these together with the known loading to a model of the structure, and obtaining its response. In this approach, the accuracy of the estimations entirely depends on how accurately the physical system is represented by the model and the predicted loading. Nevertheless, if the structure is instrumented and measurements of the response at some locations are available, the accuracy of the estimation may be improved by combining measurements and model in some consistent way. The idea of response reconstruction for partially instrumented systems has been studied in the area of control and state estimation since the 1950s, and new contributions continue to appear.

1.3.3.6 KF issues

Three main problems may arise in employing KF within the structural field.

The first issue consists in estimating the steady state KF gain from the measurements. In the classical formulation of KF, it is possible to calculate the filter gain, given the information of a model and the covariance of unknown disturbances and measurement noise. If the noise covariance matrices are not available, it has been shown that the KF gain may be extracted from the data. Several methods have been proposed; however, ultimately, all exploit the fact that the discrepancy between measured and predicted output signal, which is called innovation, is white when the filter gain is optimal. Examination of the literature shows that the problem is an ill-conditioned one.

The second problem concerns the state estimation using a nominal model that displays uncertainty. In classical KF theory, one of the key assumptions is that an a-priori knowledge of the system model, which represents the actual system, is known without error. In this work, the goal is to examine the feasibility of an approach that takes into account the effects of the uncertain parameters of the nominal model, in the state estimation using KF, without estimating the uncertain parameters themselves. In this approach, the model errors are approximated by fictitious noise and the covariance of the fictitious noise is calculated on the premise that the norm of discrepancy between the covariance functions of measurements and their estimates from the nominal model is minimum.

The third problem is related to the use of KF as a fault detector. It is known that the innovation process of the KF is a white one. When the system changes due to damage, the innovations are no longer white and correlations of the innovations may be used to detect damage. A difficulty arises, however, when the statistics of unknown excitations and/or measurement noise fluctuate, because the filter also detects these changes, and it becomes necessary to differentiate what comes from damage and what does not.

1.4 Final remarks

In this chapter, a brief state of the art on data-related issues, existing DF methodologies, as well as on KF generalities and their applications within the civil engineering research field, has been presented. Such a general overview appeared to be crucial, since it shall represent the foundations for a subsequent phase of implementation and analysis, to which the next chapters are going to be dedicated. Indeed, acceleration and displacement structural response signals will be processed, within HDF-based procedures involving a KF, and many issues here discussed in theoretical terms, as for instance the presence of spurious noise on measurements, will then be reconsidered and also addressed from a practical point of view, also toward denoising. Another important assumption that holds true for the whole research work is the Gaussian assumption, to which Section 1.3.2.3 has been

dedicated. In fact, here, the aforementioned spurious noise affecting the response signals will always be modeled as a Gaussian process displaying a mean equal to zero, since such an assumption allows to well characterize real cases, besides the fact that it is easy-to-handle within a numerical environment.

Furthermore, numerous other concepts and definitions that have been given in this chapter, will be useful and often resumed in the analyses that follow. For instance, the concept of a discrete signal, here presented, constitutes a fundamental notion for all the work. Indeed, all signals involved within the subsequent analyses will be discrete signals, i.e. signals whose independent variable takes discrete values and, consequently, this implies that they may simply be represented as sequences of numbers. Specifically, within the research, the mathematical variable used to describe the signals will conventionally be a time variable, configuring such signals as discrete-time signals.

Both numerically generated synthetic response signals, firstly, and real structural response signals, subsequently, will be included and processed within the present dissertation. Dealing with real signals, i.e. recordings directly acquired on real structures by predisposing an appropriate sensor network, the concept of sampling takes on a particular importance, which is worth recalling. In fact, sampling means the reduction of a continuous-time signal to a discrete-time signal, namely to a sequence of samples, where by sample one means a value or set of values at a point in time and/or space. Here, different sampling rates will be considered, according to the typology of the signal to be analyzed (for instance, acceleration or displacement response signals), also bearing in mind the possible limitations of the sensor instrumentation that may be employed during the acquisition stage.

Finally, it is worth reiterating that, although the literature review proposed in this chapter was deliberately general in nature, since the present work specifically focuses on the civil engineering context, all the notions here presented will be declined in the next chapters towards the specific research field of civil engineering.

Chapter 2. Effective HDF-based procedure via KF for clarifying synthetic ambient vibration response signals

In this chapter, a KF-based implementation is proposed, for clarifying noise- affected displacement response signals of a linear dynamic system subject to an ambient vibration excitation. In particular, the instance in which KF is employed within a HDF procedure between acceleration and displacement response signals of a structural system is investigated. The procedure is specifically aimed at enhancing the displacement measurements, supposedly affected by higher noise, using acceleration measurements (considered instead as noise-free or corrupted only by a slight noise). In the the Data Fusion procedure, the crucial influence of the initial parameters characterizing KF is inspected, in its effectiveness for improving displacement signals affected by an increasing zero-mean Gaussian noise level. It is worth mentioning that all signals considered within the present analysis are synthetic response signals, namely artificially generated response signals obtained by numerical computation on a given structural model.

The chapter is organized as follows. Section 2.1 aims at introducing and contextualizing the present investigation, placing it within the pertinent scientific literature, and setting out its main goals and achievements. Section 2.2 provides a brief description of the benchmark dynamical system taken into consideration for the entire analysis, i.e. a 3-DOF shear-type frame. The main points followed during the analysis are outlined, and a multi-rate KF scheme involved within the HDF procedure, as originally derived by Smyth and Wu [192], is here further elaborated, through a dedicated home-made numerical implementation. Section 2.3 presents various scenarios of numerical analysis, involving the KF algorithm, aiming at improving the displacement response of a linear dynamic system by complementary acceleration data. Different artificial Gaussian white-noise signals are added to the observed (numerically determined) synthetic response displacements of a 3-DOF frame under ambient vibration force top-floor loading, simulating the error that may occur in the displacement sensor during an “on field” measurement acquisition stage. Also, the cases of noise-free accelerations and (slight) noise-affected accelerations are investigated, through several numerical analyses, at increasing displacement noise levels, and for different inherent modal damping ratios of the underlying structural system. Limits of applicability of such a technique are explored and KF effectiveness is evaluated in terms of RMS error between originally (uncorrupted) displacements and filtered displacements, and on the basis of the modal parameters (natural frequencies) that may be extracted from the KF response estimation through appropriate inverse analysis algorithms. The

results related to the analyzed cases are presented and commented. Conclusions and global remarks are finally outlined in Section 2.4, and a few future perspectives are disclosed.

2.1 Introduction and contextualization

In the wide field of civil engineering, SHM and the associated development of consistent simulation tools, such as model updating (see for instance Lee et al. [123], Wu and Wang [225], Ferrari et al. [66, 67], and references quoted therein), represent usual but non-trivial tasks. In the recent years, supported by the broad development of novel measurement technologies for structural identification purposes, HDF-based approaches are increasingly adopted for supporting such activities (e.g. Xiao et al. [211], Jiang et al. [99, 100], Su et al. [199], Zhao et al. [231], Cho et al. [35], Ferrari et al. [65, 67], and cited references). Several pertinent contexts also concern the possible limitation and control of structural vibration, within different excitation regimes, by the insertion of appropriate damping devices (Salvi and Rizzi [175,177,178], Salvi et al. [176], and references quoted therein), which may need a fine tuning, as coupled to the same identification process (Wang and Lin [220]).

DF procedures consist in integrating measurements acquired from different types of sensors, so that the resulting information may be characterized by a lower degree of uncertainty (Chapter 1). In addition, if the measured data display a heterogeneous nature (for example, displacements and accelerations), an appropriate fusion is required for rendering a comprehensive description of the structure of interest (and this may also alleviate errors of displacements computed on the basis of double numerical time integration from accelerometer records). In fact, while acceleration-based monitoring may detect variations on the structural condition, displacement records may alert for the presence of excessive service loads, as well as to enable for fatigue estimation. Also, they may be remotely acquired, in a convenient way. As discussed in previous Chapter 1, although DF represents a usual procedure in many research areas where signal analysis is commonly involved, its application to the civil engineering domain has not been deeply explored yet (first contributions in this field may be found in Smyth and Wu [192], Chatzi and Smyth [25], Chatzi and Fuggini [26, 27], Park et al. [147], Ferrari et al. [67]). A crucial aspect is that, within this scenario, known difficulties commonly related to structural identification are augmented by issues connected to the necessary calibration of the filters employed within the Data Fusion procedure itself.

Here, a KF-based implementation is developed for merging simulated noise-added displacements and accelerations of a numerical structural system, for several types and levels of added noise. This aims at simulating measurements that may extensively be acquired “on field”, through displacement sensors, and at exploring the perspective of their use for SHM and modal identification purposes, possibly complemented by the information coming from a few acceleration measurements.

DF approaches between displacement and acceleration data involving KF are available within the recent literature (see e.g. Kim et al. [112], Lei et al. [128], Lin and Luo [129], Liu et al. [130]), through which KF should assist in estimating the condition of structures that undergo ambient vibrations, allowing for predicting potential damage and evaluating the residual performance capacity of a structure (Lei et al. [127], Yuqing [218]). Appropriate damage detection may also require an optimal design of the adopted sensor network, in terms of number, type and spatial deployment of sensors (Capellari et al. [19]).

In this study, these goals may be pursued through modal dynamic identification techniques, which aim at determining the modal dynamic characteristics of a structure, primarily the natural frequencies. In fact, it is well known that the variation of these quantities during the life-cycle of a structure may reveal potential changes in its performance characteristics. In the present identification perspective, main remote displacement signals are taken for the modal frequency extraction, possibly corroborated by a few acceleration response signals, in order to clear the frequency targeting, through effective DF based on KF.

Papadimitriou et al. [148] first suggested the possibility to adopt the structural dynamic response for fatigue damage identification purposes. In the last years, many other scientists have dealt with the topic of the dynamic response estimation of a structural system within a stochastic framework, and several algorithms have been developed to treat both linear models, e.g. KF [105], and non-linear models, e.g. Particle Filter (Gordon et al. [82]) and Unscented Kalman Filter (Julier and Uhlmann [103]). The state of the system is represented in terms of displacements and velocities of the response at specific locations along the structure. In practice, however, not always it is possible to measure displacements and velocities of the considered structural system (Lee et al. [123]); thus, when the knowledge of such quantities may be required, KF represents an important tool for accurately reconstructing the whole dynamic response, starting from incomplete measurements (Lee and Yun [125], Azam et al. [10], Ding and Guo [44], Eichstadt [57], Kim and Sohn [113]).

In the following, a KF is implemented into a HDF process in order to combine numerically determined data from heterogeneous sensors, i.e. displacement and accelerometer sensors, aiming at deriving accurate displacement estimates of a studied dynamical system, adopted then for modal dynamic identification purposes, based on displacement data. Both displacement and, to a lesser extent, acceleration measurements are considered to be affected by errors, represented by noise added to the signals, here computed in terms of Noise-to-Signal (N/S) ratios, in order to simulate the errors that may occur in the “on field” detection of such a kind of data. Then, thanks to the use of the enhanced KF estimated displacements, through the adoption of appropriate inverse analysis algorithms for output-only modal dynamic identification (e.g. Zghal et al. [228], Pioldi et al. [152–

154], Chatzis et al. [29], and wide reference frameworks discussed therein) it becomes possible to extract the natural frequencies of the benchmark structure. Finally, from a comparison between these frequencies and the numerically determined natural frequencies, it is possible to cross-evaluate the accuracy of the achieved KF estimates.

2.1.1 Achievements of the investigation

The main achievements of the research work may be resumed as follows:

- the adoption of remote displacement signals, possibly enriched by reliable acceleration recordings, through an original KF-based implementation included within the DF procedure, is shown to become effectively useful for structural monitoring purposes, as leading to a truthful reconstruction of the original structural response, despite for possible disturbances of various kinds;
- the maximum level of noise that may be tolerated on displacement and acceleration measurements is determined, to allow for a successful HDF and to achieve reliable estimates of the current structural dynamic response; within this process, filtered displacements (taking benefit from DF processing) reveal to be more sensitive to noise-affected accelerations than to noise-affected displacements (as raw displacement data);
- since displacements and accelerations are supposed to be detected at different rates, the KF is implemented in its multi-rate configuration, as in Smyth and Wu [192]. This multi-rate KF feature allowing for a relatively low sampling rate for the displacement measurements, fundamental to overcoming low-frequency integration errors, and for higher sampling rates for the accelerations (i.e. within the frequency range where accelerometers result more accurate), is revealed, enabling each sensor type to play on its inherent strengths.

2.2 Theory

2.2.1 Description of the benchmark structural system

The dynamical structural system taken into consideration for the present numerical simulation analyses is a 3-DOF shear-type building, as represented in Fig. 2.1.

This choice is motivated by the simplicity of the geometrical and structural properties that characterize such a kind of mechanical system, thus allowing for easy analytical and numerical treatments. Furthermore, this structural modelization may be good enough to represent real benchmark structures, within the realm of dynamic response here inspected.

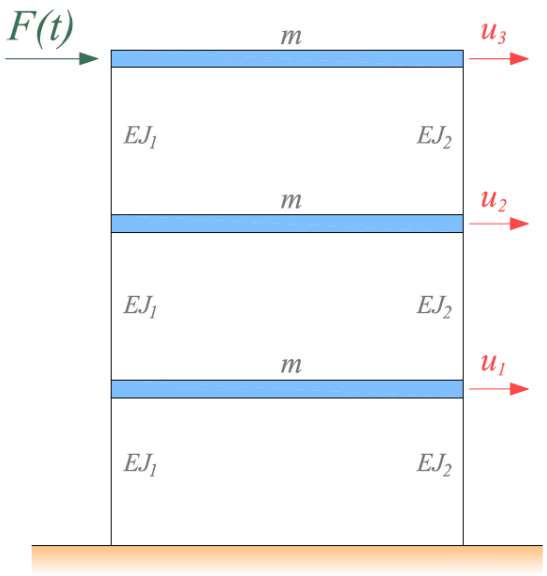

Figure 2.1: Schematic view of the analyzed 3-DOF shear-type building under top-floor input force.

In order to make the analyses the more reliable as possible, plausible values of mass, stiffness, damping and geometrical structural characteristics are assumed. Mass m of each floor is taken equal to 144 tons, and the stiffness of the columns is set as follows: $EJ_1 = 3.75 \cdot 10^7$ kN/m for the left columns and $EJ_2 = 1.56 \cdot 10^8$ kN/m for the right ones. Columns display a height h of 3 m. Additionally, modal damping ratios z_i are assumed to be equal to 1%, 3% or 5% for all the modes, according to each analyzed case, spanning the whole dynamic response at increasing sub-critical realistic inherent structural damping.

Concerning input load F(t) to be applied to the dynamical system, a common trend for KF estimation purposes (Kitanidis [114], Hsieh [95], Gillijns and DeMoor [78]) is to avoid using any a-priori knowledge of such an input force. In fact, structural systems are inherently characterized by uncertainty, relating to measurement errors, sensor noise, inefficacy of the numerical models, and lack of a-priori knowledge on both the system and the loading conditions. Here, a zero-mean random ambient vibration load F(t) at around $1 \cdot 10^5$ kN is considered, as applied to the top floor of the building (Fig. 2.1), to compute the floor responses.

Numerically determined undamped modal natural frequencies $f_{n,i}$ of the benchmark structure are obtained as: $f_{n,1} = 2.658$ Hz, $f_{n,2} = 7.448$ Hz and $f_{n,3} = 10.763$ Hz. Damped modal frequencies $f_{d,i}$ have also been calculated for the damped cases with z_i=1%, 3% and 5%, for all the modes. Results are reported in Table 2.1.

Damped natural frequencies $f_{d,i}$ will later be used as comparison terms for evaluating the accuracy of the KF estimations.

		$f_{d,1}$ [Hz]	$f_{d,2}$ [Hz]	$f_{d,3}$ [Hz]
	1%	2.658	7.448	10.762
ζ_i	**3%**	2.657	7.445	10.758
	5%	2.655	7.439	10.749

Table 2.1: Frequencies $f_{d,i}$ of the damped system (z_i=1%, 3% and 5%).

2.2.2 Analysis procedure

The procedure of analysis is summarized as follows:

i. The dynamic response of the system is first determined in terms of displacements and accelerations, through the implementation of the Newmark's method, consisting of a step-by-step direct time integration of the equations of motion. It is worth mentioning that only the third floor's kinematic response is going to be monitored, as this may resume the whole structural response and be suitable enough for first SHM purposes based on a single-channel recording.

ii. To simulate the measurement error that may occur in sensors during the data acquisition stage, a simulated noise signal is selectively added to the original measurements. It is well-known that, for estimation purposes, KF provides the exact PDF of the state of linear dynamical systems with a linear measurement model, with additive zero-mean Gaussian noise processes (Chapter 1, Section 1.3.2.3). Thus, a zero-mean Gaussian white-noise is employed to contaminate the response data. During the analyses, both displacements (mainly) and accelerations are contaminated with increasing N/S ratios.

iii. Moreover, within the numerical analyses, displacement and acceleration measurements are considered to be sampled at different rates, in accordance with the common capability of the employable instrumentation. In particular, displacements are sampled at lower frequencies than accelerations. From the literature, a usual frequency range of acquisition has been observed as varying between 12.5 Hz and 100 Hz for displacements, from 100 Hz up to 300 Hz for accelerations. Consequently, for the purposes of the fusion procedure, a multi-rate KF scheme is adopted, as originally developed by Smyth and Wu [192].

iv. KF effectiveness is measured in two different ways. The first one is based on the calculation of the Root Mean Square (RMS) error between the estimated displacements after KF application and the original (noise-free, numerically determined) displacements; the second one is based on the comparison between the modal frequencies that can be extracted via appropriate inverse analysis algorithms from the original (noise-free, numerically determined)

displacement recordings, and those that can be extracted from the filtered displacement estimations, possibly enriched by means of an appropriate HDF procedure with a few reliable acceleration data.

2.2.3 Numerical KF implementation

KF is an algorithm that may be used to estimate the health conditions of linear dynamical systems perturbed by a zero-mean Gaussian white-noise, through the merge of data that may also be affected by measurement errors. As presented in previous Chapter 1, the mathematical model exploited in the derivation of such a filter constitutes a reasonable representation for many issues of a practical interest, including control problems as well as estimation problems.

This section provides a schematic description of the linear multi-rate KF employed within the present analyses for improving the estimation of measured displacements $x_m(t)$ (related here to SDOF top-floor displacement signal $u_3(t)$, see Fig. 2.1) by using measured accelerations $\ddot{x}_m(t)$, supposed to be acquired from acceleration sensors (here on the same SDOF, namely related to $a_3(t) = \ddot{u}_3(t)$).

According to Smyth and Wu [192], in the case in which the acceleration and displacement are available to be measured, the measurement process may be modeled in state-space form as follows:

$$\begin{bmatrix} \dot{x}(t) \\ \ddot{x}(t) \end{bmatrix} = \begin{bmatrix} 0 & 1 \\ 0 & 0 \end{bmatrix} \begin{bmatrix} x(t) \\ \dot{x}(t) \end{bmatrix} + \begin{bmatrix} 0 \\ 1 \end{bmatrix} \ddot{x}_m(t) + \begin{bmatrix} 0 \\ 1 \end{bmatrix} w(t) \tag{2.1}$$

$$x_m(t) = \begin{bmatrix} 1 & 0 \end{bmatrix} \begin{bmatrix} x(t) \\ \dot{x}(t) \end{bmatrix} + v(t) \tag{2.2}$$

where $\ddot{x}_m(t)$ denotes the exogenous input to the state transition function, which effectively coincides with the measured accelerations; $x_m(t)$ denotes the measured displacements; w(t) and v(t) are the process noise sources associated to accelerations and displacements, respectively (assumed to be Gaussian). By setting vector $\mathbf{x}(t) = [x(t); \dot{x}(t)]$, representing the system state vector (i.e. the unknown output from the filter), formulated via aggregation of filtered displacement x(t) and velocity $\dot{x}(t)$ signals, Eqs. (2.1) and (2.2) may compactly be rewritten in matrix form as:

$$\dot{\mathbf{x}}(t) = \mathbf{A}\mathbf{x}(t) + \mathbf{B}u(t) + \mathbf{w}(t) \tag{2.3}$$

$$y(t) = \mathbf{C}\mathbf{x}(t) + v(t) \tag{2.4}$$

where $u(t) = \ddot{x}_m(t)$, $y(t) = x_m(t)$, $\mathbf{w}(t) = [0;w(t)]$, and state matrix **A**, input matrix **B** and output matrix **C** are defined as follows:

$$\mathbf{A} = \begin{bmatrix} 0 & 1 \\ 0 & 0 \end{bmatrix}, \qquad \mathbf{B} = \begin{bmatrix} 0 \\ 1 \end{bmatrix}, \qquad \mathbf{C} = \begin{bmatrix} 1 & 0 \end{bmatrix} \tag{2.5}$$

Since these matrices are assumed to be known within the filtering analysis, this shall lead to a linear model-based (vs. model-free; Hamilton et al. [90]) KF, relying on minimizing the error between measured and filtered data, based on the availability of the above-mentioned matrices, governing corresponding state-space Eqs. (2.3) and (2.4), which represent the linear relationships between the states, the measurements and the associated measurement noises (Crawley and O'Donnell [39]).
To implement the DF procedure, Eqs. (2.3) and (2.4) are then transformed into discrete form (zero-order hold assumption), as further indicated in the resuming flowchart of Fig. 2.2 (adapted from Ferrari et al. [67]).

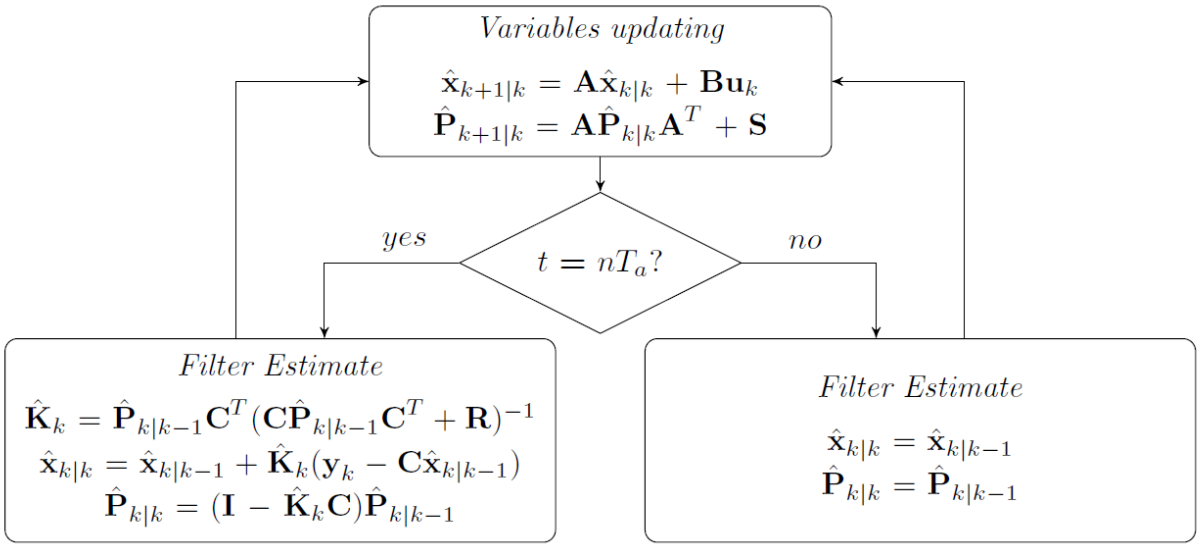

Figure 2.2: Multi-rate KF flowchart (adapted from Ferrari et al. [67]).

In Fig. 2.2, $\mathbf{x}_{j|i} = \mathbf{E}(\mathbf{x}_{j|i})$ represents the estimated expected value (mean) of state vector $\mathbf{x}_{j|i}$ at time instant *j*, using measurements up to (and including) time instant *i* (conditional expectation); similarly, $\mathbf{P}_{j|i} = \mathrm{Var}(\mathbf{x}_{j|i})$ is the estimated variance of state vector $\mathbf{x}_{j|i}$; **S** and **R** represent the covariance of associated process noise sources **w**(t) and v(t); **K** is the so-called Kalman gain. Given matrices **A**, **B**, **C**, **S**, **R**, and supposing to know state mean **x** and variance **P** at time *k*, the recursive procedure summarized in the flowchart of Fig. 2.2 is based on the calculation of Kalman gain **K** at same time step *k*, through

which the knowledge about the state is updated, predicting quantities **x** and **P** at time $k + 1$, using measurements up to time $k + 1$.

The selection of assumed process noise (p-noise) covariance matrix **S**, usually mainly based on intuition, and of observation noise (o-noise) covariance matrix **R** displays a significant effect on the estimation performance of the KF. A basic way to think of matrices **S** and **R** is that they constitute weighting factors between the prediction (state) equations and the measurement (output) equations, and this ratio is expressed within the Kalman gain equation. Considering a larger **S** corresponds to accounting for a larger uncertainty in the state equations, which is equivalent to less trusting the result of these equations, effectively meaning that the filter should more correct, by the measurement update. Similarly, considering a larger **R** corresponds to accounting for a larger uncertainty in the measurements, which is equivalent to less trusting the measurements, effectively meaning that the filter should less correct, by the measurement update. On the basis of this, p-noise has been intuitively set equal to 10^{-12} for the whole analysis, since the model is considered to be very robust (the lower this is, the more accurate the model is considered to be). Instead, o-noise, which reveals the confidence given to the acquired measurements, has been set at around 10^{-3}, so that the increasing level of noise on the displacements provides the filter with much of a freedom to adjust itself with the smaller mean square error for the estimated acceleration signals (the lower the observation noise, the more severely the KF estimator is forced to fit the recorded accelerations). Such values of process noise and observation noise are then kept constant during the performed analyses, regardless of the noise level affecting the displacement data. From the assumed values of o-noise and p noise, matrices **S** and **R** are build up as follows (Smyth and Wu [192]): matrix **S** is a 2x2 matrix with zero entries, excepted for the o-noise level set in position S_{22}; matrix **R** reduces to a scalar, which is indeed set to the selected p-noise value.

As previously mentioned, since accelerations and displacements are sampled at different time intervals, respectively named T_a and T_d, where $T_d/T_a = n \in \aleph$ (Chatzi and Fuggini [26]), the filter has been implemented in a multi-rate configuration (Smyth and Wu [192]). This means that, at times $t = nT_a$, both the time and measurement update steps of the KF are performed, whereas when $nT_a < t < (n + 1)T_a$ only the time update step (ignoring the observation innovation) is carried out. Despite that the outcomes of the filter represent the "updated" estimates of both the displacements and the velocities (derived from the acceleration input) of the benchmark structure, the present work plan focuses only on the displacement output.

2.3 Analysis results

In this section, a selection of the results from the numerical analyses performed by involving the multi-rate KF algorithm are reported. Two main scenarios are presented. Initially, only the displacement response signal is considered to be affected by noise, while the acceleration response signal is taken as noise-free. This might represent a quite realistic scenario, since accelerometers are able to capture signals with a higher level of accuracy than for displacement sensors (Smyth and Wu [192]). Secondly, also the acceleration signal is "noisified" with a slight zero-mean Gaussian white-noise. Indeed, also data acquired via accelerometers may be subjected to measurement errors, albeit smaller than errors affecting displacements. Additional simulation results, concerning the present research scenario, are available in Ravizza [165]. All the analyses have been developed within an autonomous MATLAB implementation environment.

A general resuming conceptual scheme of the treated HDF cases, with and without noise affecting the accelerations, also including the possible subsequent modal identification analysis performed on the filtered displacements, is synoptically depicted in Fig. 2.3.

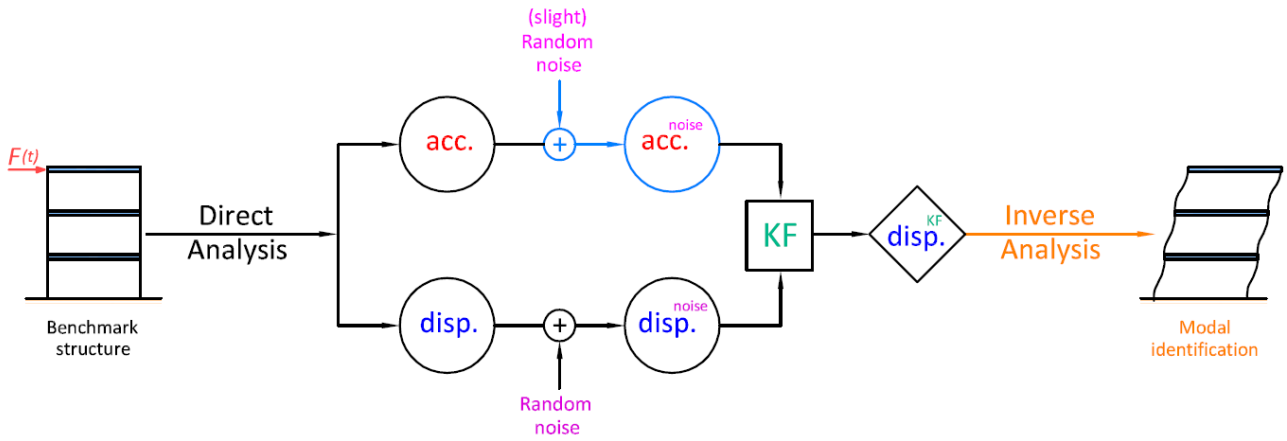

Figure 2.3: Schematic conception of the treated HDF cases: noise-free acceleration case (excluding the part in blue colour) and noise-affected acceleration case (considering the whole scheme). Determination of filtered displacements and possible subsequent phase of modal identification, based on displacements.

2.3.1 Noise-free acceleration case

Acceleration data are here assumed as noise-free. In practice, it means to consider accelerometer measurements without errors, as illustrated in the synoptic scheme in Fig. 2.3 (i.e. without considering the part in blue colour).

In particular, 5%, 10%, 25%, 50%, 150% and 300% N/S ratios are considered, as applied to the displacements, for the different considered underlying modal damping ratios, namely z_i=1%, 3% and 5%. From the analyses it emerges that, by involving KF within the HDF procedure, it is possible to obtain refined displacement estimations, namely displacements endowed of an improved accuracy.

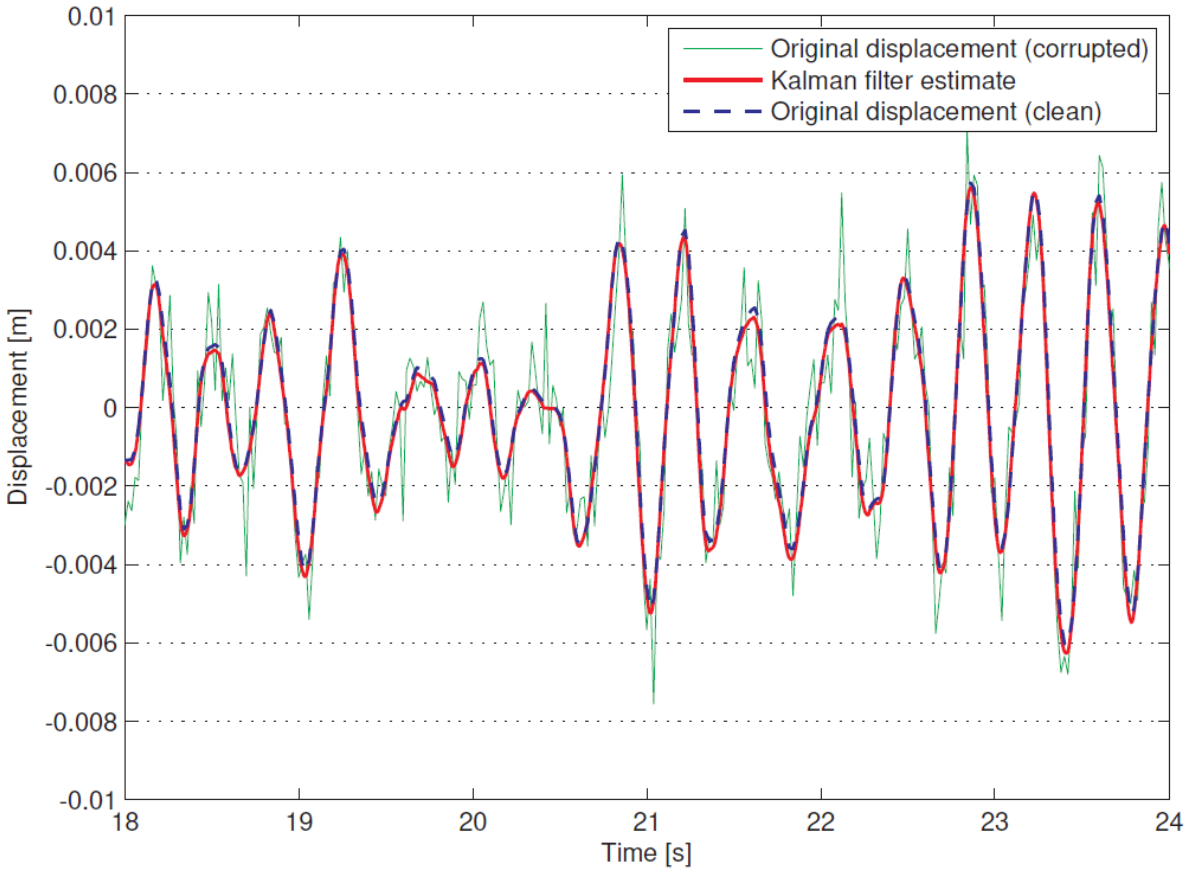

Figure 2.4: KF displacement response estimation (25% N/S ratio, z_i = 1%).

In particular, from Fig. 2.4, which shows displacements before and after the HDF-based procedure, it is possible to appreciated how the curves, representing the original displacements (blue curve) and the KF estimated displacements (red curve), show a similar trend for a N/S ratio on displacement equal to 25%. Further, in Table 2.2, the RMS errors between the original displacement signal and the KF estimated displacement signal are reported, for each examined scenario.

RMS error [%]							
		N/S ratio					
		5%	10%	25%	50%	150%	300%
ζ_i	1%	0.15	0.16	0.19	0.24	3.28	9.71
	3%	0.16	0.18	0.20	0.25	3.21	9.22
	5%	0.13	0.17	0.18	0.37	3.75	9.91

Table 2.2: RMS error of KF displacement response estimation for increasing imposed N/S ratios and damping ratios z_i (noise-free acceleration case).

From Table 2.2, it is possible to observe that the proposed HDF-based approach appears to be very robust if accelerations are set as noise-free, despite for the very high noise levels on displacements. In fact, the RMS error turns out to be much less than 1%, for N/S ratios on displacements up to 50%, regardless of the considered value of damping ratio z_i. Notice that N/S ratios greater then 25% are considered to be quite unrealistic for civil engineering applications (Smyth and Wu [192]). RMS errors of about 3% and 9% refer, instead, to the cases characterized by N/S ratios on the analyzed displacement signal equal to 150% and 300%, respectively.

Fig. 2.5 shows the qualitative behavior of the RMS error for increasing noise levels and damping ratios. From the graph, it clearly emerges how, up to a 50% of noise level, the RMS error lies well below 1%. It is interesting to note that the three depicted curves seem to present the same trend, with a very light influence of the inherent damping ratios, especially for noise levels below 50%. Consequently, it is possible to affirm that the KF algorithm provides very consistent estimates for all the cases so far considered. This also demonstrates the effectiveness of the filter in case of smaller values of displacements, as derived from the adoption of greater damping ratios.

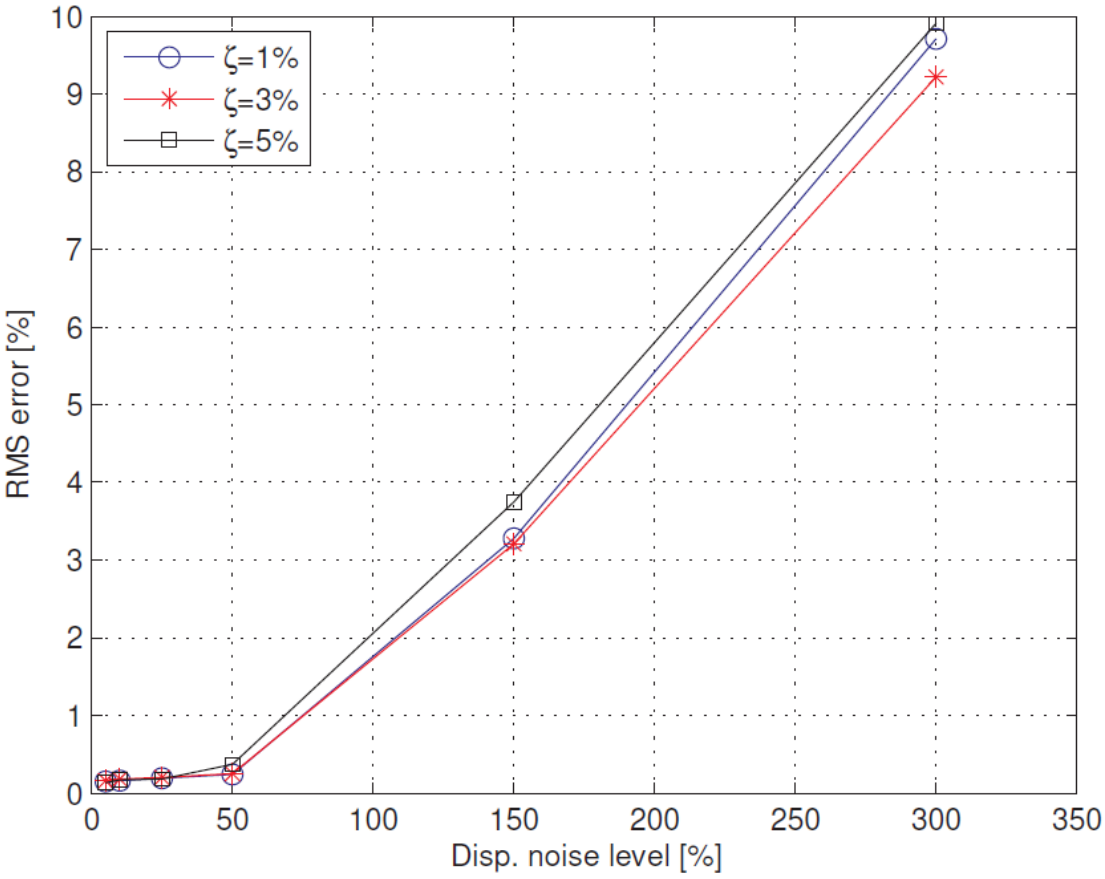

Figure 2.5: RMS error trend of KF estimation at increasing displacement noise levels (noise-free acceleration case). A visible kink is recorded at 50% noise level.

Effectiveness of the KF is also tested based on an inverse analysis conducted for modal identification purposes by means of a standard Welch's approach, based on displacement signals. In particular, the modal identification procedure has been applied to the displacement signal before (thus unprocessed by DF) and after (thus taking benefit from DF with accelerations) KF application, and results have been reported for each of the analyzed cases.

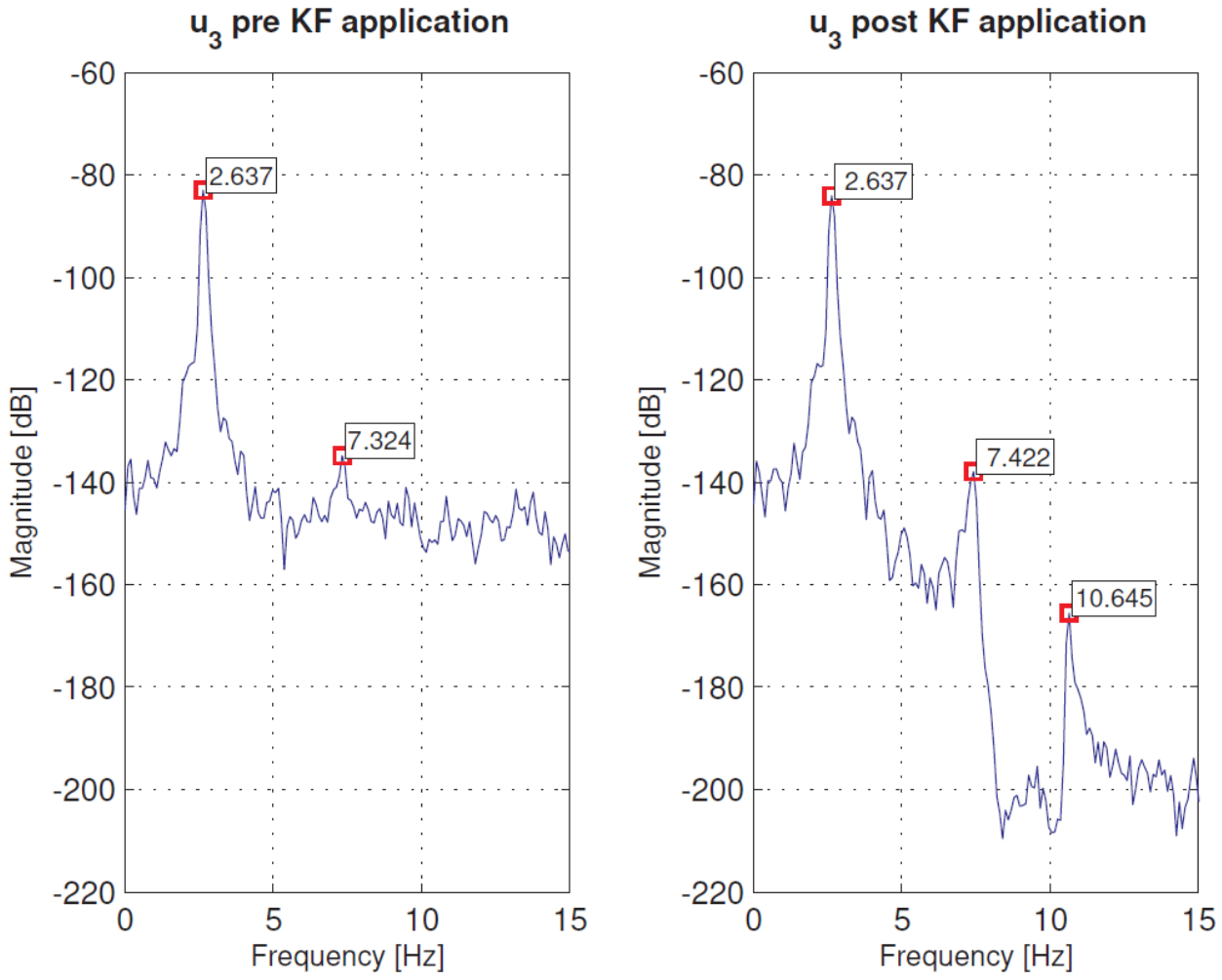

Figure 2.6: Welch-based modal frequency identification on displacements for a 25% N/S ratio (z_i = 1%).

From the comparison represented in Fig. 2.6 (target natural frequencies in the first line of Table 2.1), it is immediate to note how the peaks identified by automatic peak-picking procedure on the Welch's periodogram, after the filtering procedure, look much clearer than the same peaks identified from the unfiltered displacement data, especially when the noise level becomes considerable. This is primarily due to the beneficial effect induced by reliable acceleration data involved within the HDF procedure, which indeed display relatively better information in the high-frequency regions, to enrich displacements. The matching, in terms of frequency estimations (Table 2.1), looks anyway reasonable, for an identification based on displacements.

From the analyzed noise-free acceleration case, it may be asserted that the KF algorithm is only slightly influenced by the amount of sub-critical structural damping, with a modal damping ratio in the order of a few percents, since in each case the RMS error remains at around 1%, for N/S ratios on displacements up to 50% (see Fig. 2.5). It is worth noting that this may be considered as rather reliable for damping ratios typical of civil engineering structures; for higher damping ratios, further analyses may become necessary.

2.3.2 Noise-affected acceleration case

The noise-affected acceleration case (slight noise) is now considered. This represents a further common scenario in practical cases, because in reality not only displacement sensors but also acceleration sensors may present measurement errors, of a slight amount for the latter sensors. To take this into account, a slight Gaussian noise level has been added to the acceleration data too. Damping ratios z_i, instead, have been maintained as constant and all equal here to 1%, as representative of a slight sub-critical damping, in the whole analysis.

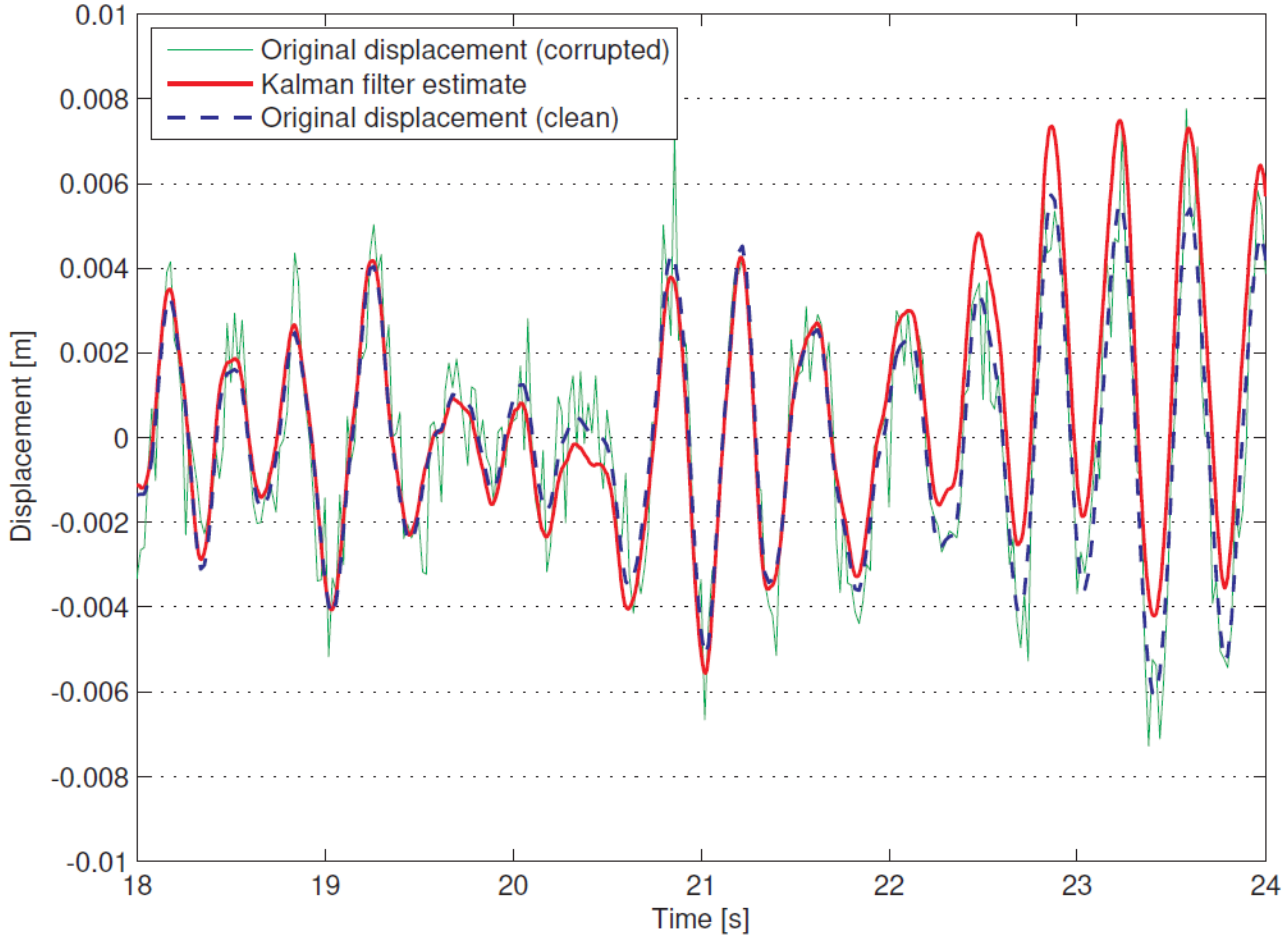

Figure 2.7: KF displacement response estimation for 25% N/S ratio on displacements and 1% N/S ratio on accelerations.

The analysis follows again the scheme of Fig. 2.3, now also including the part highlighted in blue colour. As previously stated, here, the focus is placed on the HDF scenario involving noise-affected acceleration measurements, even though here very low N/S ratios are applied. In particular, 0%, 5%, 10%, 25% and 50% N/S ratios are considered as applied to the displacement response signal, for simultaneous slight N/S ratios of 1%, 2% and 3% affecting the acceleration response signal. From the results of the noise-affected acceleration case, it emerges that KF seems to be significantly affected by the level of slight noise added to the accelerations.

In fact, from Fig. 2.7, which shows the displacement histories before and after the HDF procedure with acceleration data, it is possible to appreciate how the two curves, representing the original displacement signal (blue curve) and the KF estimated displacement signal (red curve), take different trends, already for low noise levels on accelerations.

In Table 2.3, the RMS errors are reported for each examined scenario. It is worth noting that only the 1% noise acceleration scenario may be considered to be acceptable for SHM purposes. In fact, the estimate errors related to the other two cases become too high, and this could lead to an unreliable prediction of the dynamic response of the structural system.

RMS error [%]						
		displacement noise				
		0%	**5%**	**10%**	**25%**	**50%**
acc. noise	**1%**	1.17	1.97	2.72	4.01	6.67
	2%	8.72	11.03	12.41	13.08	16.98
	3%	19.67	25.93	27.51	32.77	35.24

Table 2.3: RMS error of KF response estimation (z_i = 1%) at increasing displacement noise level (noise-affected acceleration case).

From Table 2.3, it is possible to observe how the RMS error rapidly increases with the increase of noise level on the acceleration signal, up to values over 30%, for a N/S ratio of 3%. However, in practice, considering the sensitivity of sensors, the most common scenario is to inherit a 1% N/S ratio on accelerations and a N/S ratio between 5% and 10% on displacements. Within such a range, RMS errors below 3% have been recorded. This may also be graphically observed in Fig. 2.8, in which the three trends are depicted.

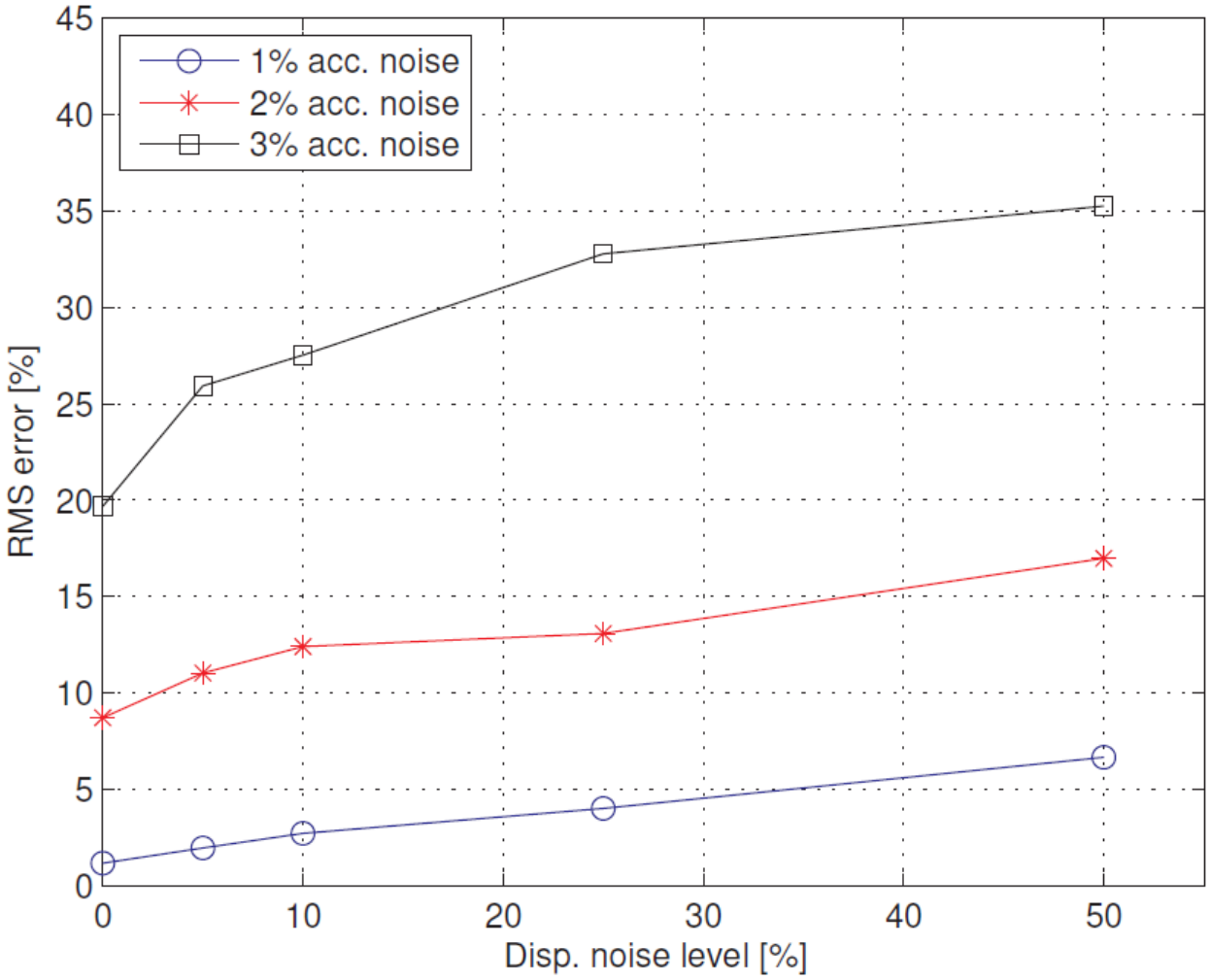

Figure 2.8: RMS error of KF displacement response estimation at increasing N/S ratios on displacements (for 1%, 2% and 3% N/S ratios on accelerations).

About the identification method, from the Welch analyses based on displacements, it emerges that the modal frequency identification process has been anyway successful after KF employment, as it may be appreciated from Fig. 2.9 (target natural frequencies in the first line of Table 2.1), in which a comparison between the frequencies identified from displacement signals before (DF unprocessed) and after (DF processed) KF application, through merging with acceleration signals, is provided. This is likely due to the frequency content, which still remains good, despite for the high levels of added noise. The frequency estimation based on displacements keeps anyway quite reliable (compare boxed values to targets in Table 2.1). A further important assertion that may be derived from the analysis presented in this chapter is that KF, differently from the modal identification procedure, appears to be strongly affected by the level of noise added to the acceleration data. The reason why filtered displacements seem to be very sensitive to noise-affected accelerations and, at the same time, rather insensitive to noise-affected displacements, has to be located in the adopted preliminary calibration

of the implemented KF-based approach. In fact, within the developed HDF procedure, a crucial step is constituted by the a priori definition of the degree of confidence to be given to the initial conditions of the model, stated in a probabilistic way. Such a degree of confidence has to be set within the state-space model in terms of process noise and observation noise, as previously stated in Section 2.2.3.

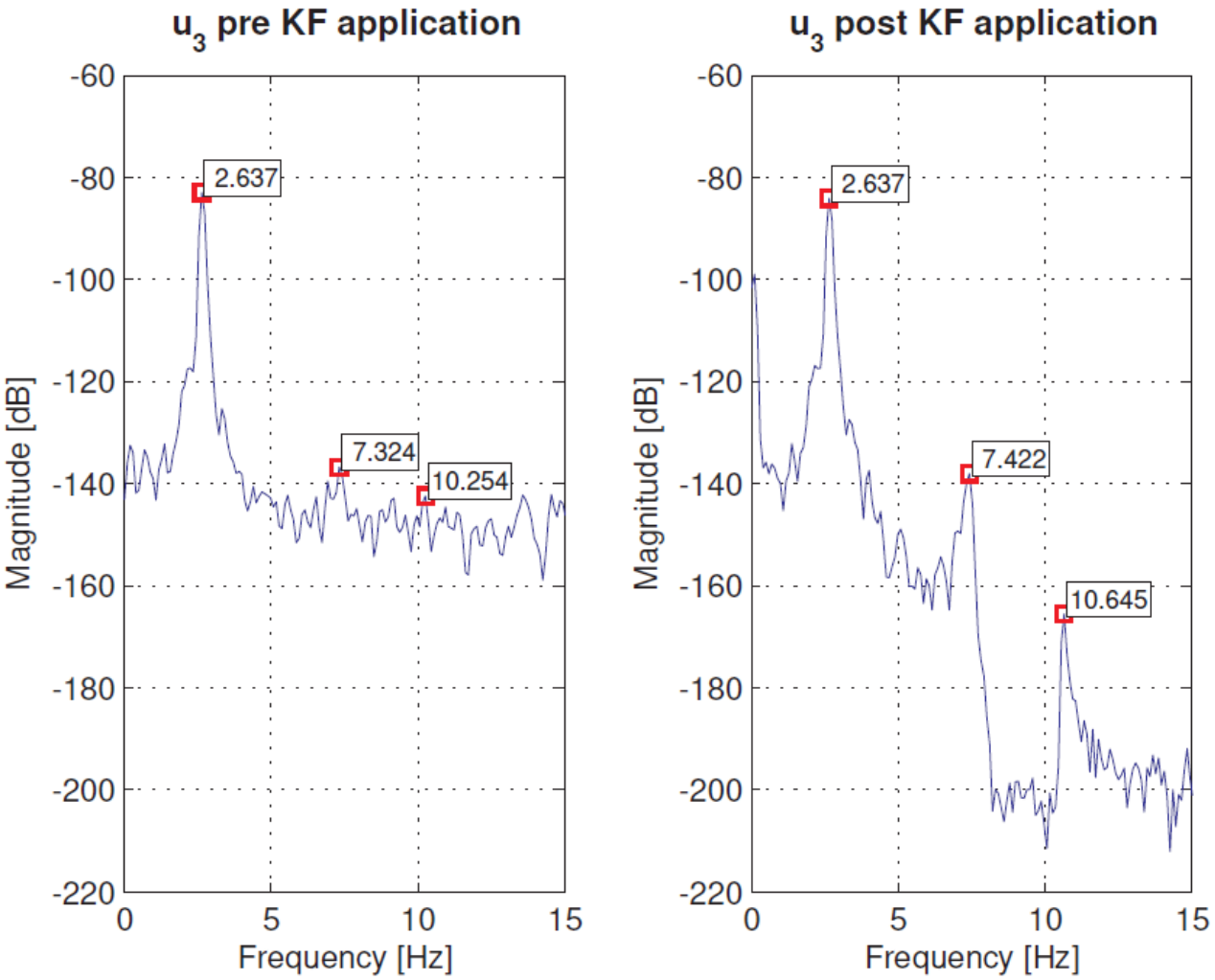

Figure 2.9: Welch-based modal frequency identification on displacements for a 25% N/S ratio on displacements and a 1% N/S ratio on accelerations.

In practice, from the acquired understanding of the present DF analysis, acceleration measurements bring in a more powerful information than displacement records; thus, noise affecting acceleration data more visibly affects the filtered displacements and then the identification outcomes that can be extracted from them. So, adopting this configuration of the filter, it is advisable to maintain a N/S ratio on acceleration signals approximately below 1%, so that reliable response estimations may be reached. Consequently, in practical cases, a great attention must be given to the acquisition stage of such a data; in this sense, also the preliminary study of the appropriate collocation of the acceleration sensors shall play a key role for the success of the whole HDF process.

2.4 Final remarks

By means of the performed numerical analyses, the proposed investigation sheds light onto several critical aspects inherent to the adoption of KF in civil engineering implementations, including for HDF and modal identification purposes. In particular, this holds true with reference to the maximum level of noise, in terms of N/S ratios, that may be tolerated, on displacement and acceleration measurements, respectively, in order to allow for a successful HDF and thereby to achieve reliable estimates of the current structural dynamic response, perspectively based on extensive remote displacement response signals, corroborated by a few reliable acceleration response data.

The following salient considerations from the performed analysis apply:

i. *Noise-free acceleration case.* From the performed analysis, it has been proven that KF turns out able to provide reliable estimates of the structural dynamic response, for N/S ratios on displacement measurements up to 50%. Indeed, in these cases, RMS errors well below 1% between the estimated displacements after KF application and the original (noise-free, numerically determined) displacements are recorded. This was made possible also by tuning the assumed noises of the filter, which usually constitutes a complex procedure to be made automatic.

ii. Noise-affected acceleration case. Numerical results have shown that only a 1% N/S ratio on accelerations may lead to reliable estimates of the dynamic response after DF by KF adoption. This could be improved, e.g. by providing an adequate procedure for the fine tuning of the filter (in terms of process and observation noise levels) and may constitute the subject of future investigations. Consequently, in the present scenario, the positioning and setting of the accelerometers shall play a key role for a true success in the KF estimates. In the current analysis, if the intrinsic error characterizing accelerometer recordings becomes greater than 1%, RMS errors greater than 8% between the estimated displacements after KF application and the original (noise-free, numerically determined) displacements, are observed. This constitutes at present a requirement of quality for the acceleration recordings, to be adopted within the current implementation settings, in the explored configuration.

In addition to the comparison between numerically determined displacements and displacements obtained through KF application, integrating information from acceleration response signals, defined in terms of RMS error, an output-only procedure of modal frequency identification within the Frequency Domain, has been used to evaluate the KF effectiveness in terms of modal dynamic identification. It has been proven that the KF adoption has been useful also towards the modal identification purposes, considering the cases of noise-free and noise-affected accelerations.

The present chapter brought forth some interesting aspects inherent to the employment of a model-based KF in a HDF procedure toward SHM purposes. The filter's effectiveness has been successfully demonstrated, leading to the conclusion that KF shall constitute a strong tool for DF within the field of structural monitoring. Thanks to its robustness, a proper KF implementation might also allow users to relax the acquisition rate of signals, shifting then the effort to the posterior stage of data processing. In this sense, KF could allow for handling practical situations in which, for different reasons, an optimal positioning of the sensors may not be feasible.

Another consideration that may be drawn from the present investigation is the perspective of cross-using extensive remote displacement measurements for the purposes of structural identification, through the support of selected reliable acceleration data, apt to enrich the available information. Thanks to the inspected HDF-based implementation, it has been shown that not only accelerations but also estimated displacements, embedding partial information from accelerations, may then be successfully employed within a modal identification procedure based on displacements. This may point out to the perspective of adopting wide displacement acquisitions for SHM and identification purposes, possibly corroborated by a few reliable acceleration recordings, through appropriate and effective HDF, as here outlined.

Chapter 3. HDF approach via KF for modal identification of seismic-excited structural systems

This chapter aims at extending the HDF-based implementation presented in the previous chapter to the additional, new treatment of seismic-excited dynamic structural systems. In particular, a numerical analysis exploring the effectiveness of a multi-rate KF in the clarification of non-stationary noisy displacement seismic response signals, is inspected. Some reliable (noise-free) standard acceleration measurements may also be involved within the HDF procedure, and a subsequent output-only modal identification analysis is performed, on the so-enhanced displacements, aiming at assessing the success of the whole procedure and monitoring process, within a seismic engineering scenario.

The chapter is organized as follows. After a brief introduction provided in Section 3.1, which states the goals of the present research endeavour, Section 3.2 recalls the same benchmark dynamic system taken into consideration in previous Chapter 2, i.e. a 3-DOF shear-type frame, and the different seismic input excitation here assumed as acting at the base of such a structure is also shown. Various scenarios of numerical analysis, which take advantage of the previously discussed HDF-based implementation via KF, are then presented in Section 3.3, with the aim of purifying the non-stationary noisy displacement response signal of the monitored dynamic system under seismic excitation. In the same section, the ambitious goal to perform the modal identification process from such enhanced nonstationary displacements is also inspected, and related results are deeply discussed and commented. Final considerations are eventually reported within last Section 3.4.

It is worth mentioning that all the assertions provided within this chapter hold true for non-stationary synthetic signals that are numerically generated from a direct time integration prior to the filter and identification analysis. This refers to a necessary-condition validation of the procedures that are here developed, before then moving to a subsequent processing analysis with real structural response signals.

3.1 Introduction

The research scenario presented in this chapter aims at pursuing the ambitious goal of exploiting the displacement data usefulness for structural identification purposes. Such a kind of approach, already addressed in previous Chapter 2 for stationary, white-noise signals, as well as prodromally in Ravizza et al. [166], is here further developed and extended to the case of structural systems excited by non-stationary signals, specifically under seismic excitation.

In KF-based approaches, the measured dynamic response at some locations of the structure and the numerical model of the structure itself are aligned, to identify real-time variations of the structural parameters. One of the major strengths of this method concerns its suitability for online implementations, because of its recursive formulation. Indeed, it only needs the knowledge of the previous condition of the structure to be monitored at a determined time step t_{i-1} and measurements at current time t_i, to estimate the unknown variables.

In previous chapter, KF has been specifically employed to combine numerically determined data from heterogeneous response signals (i.e. accelerations and displacements), in order to derive more accurate displacement estimates, for a 3-DOF shear-type building under white Gaussian top-floor input force. Here, instead, a similar approach still involving a multi-rate KF (Smyth and Wu [192]) scheme, based on a non parametric model with properties updated at each time step, is developed for fusing together simulated non-stationary (noise-affected) seismic response displacements and noise-free accelerations of the same numerical dynamic system, excited at the base by single instances of a data set of ten earthquake records, which differ for magnitude, duration, location of the epicenter and PGA.

In particular, the present implementation aims at clarifying the nonstationary displacement response signals, such that they might then be useful for modal identification purposes. In fact, a subsequent fundamental aspect of vibration-based health monitoring of civil structures concerns the identification of dynamic structural modal properties, i.e. natural frequencies, mode shapes and damping ratios, since it is well known that variations of these quantities during the life-cycle of a certain structure may reveal potential changes in its performance characteristics. Thus, structural identification via inverse analysis techniques is of a primary importance for damage monitoring and, consequently, it is essential for pursuing a contemporary and effective SHM. In the present identification perspective, the enhanced non-stationary displacement response signals are then considered for the modal frequency extraction procedure, possibly corroborated by a few reliable acceleration response signals, in order to successfully clarify even the signal frequency content.

3.1.1 Goals of the research scenario

Ultimately, the aim of the present research scenario is twofold, one relating to the Time Domain and the other related to the Frequency Domain, namely:

- primarily, it aims at inspecting the effectiveness of KF in the presence of non-stationary (seismic) signals, by assuming increasing N/S ratios, solely affecting the displacement measurements, and computing the percentage peak variation between the real numerical displacement at each floor of the benchmark structure and the KF displacement estimates;

- secondly, it aims at demonstrating the efficiency of output-only modal identification techniques performed on non-stationary displacement response signals, through a comparison between the numerically determined natural frequencies and the identified frequencies, extracted from the benchmark structure's displacements after KF application by means of Welch's method.

Such research topics are investigated in the next sections, aiming at providing an innovative approach which might reveal to be useful in SHM applications within the civil engineering context.

3.2 Seismic-excited benchmark structure

As above mentioned, the dynamic structural system taken into consideration for the present numerical simulation analyses is the same 3-DOF shear-type building monitored in Chapter 2 (see previous Fig. 2.1). This structural system is here re-proposed in following Fig. 3.1, here aiming at highlighting the presence of input excitation now acting at the base of such a structure. Characteristics of benchmark building, in terms of mass, stiffness, damping and geometry, may be found in Section 2.2.1.

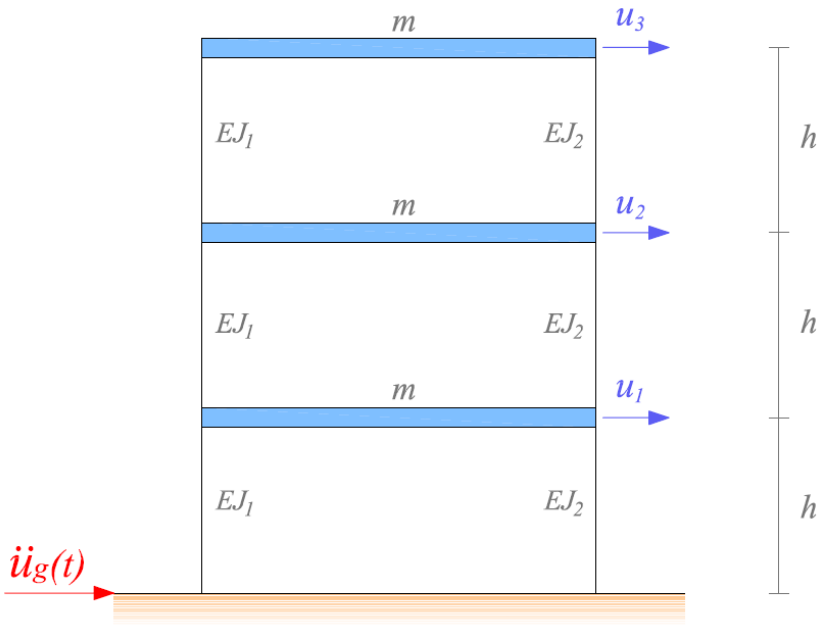

Figure 3.1: Schematic view of the monitored 3-DOF shear-type building under seismic ground excitation $\ddot{u}_g(t)$.

3.1.2 Examined earthquake excitations

Concerning the input load (seismic excitation), a set of ten seismic ground motions (Table 3.1), different for location of the epicenter, magnitude, duration and PGA, are assumed as acting at the base of the structure of interest (see Fig. 3.1). The seismic accelerograms of the considered earthquake

motions are reported in Appendix A. Further information on time-frequency spectra is available in Pioldi and Rizzi [157, 158] and in Pioldi et al. [152– 154], where the records have been selected and adopted for extensive modal identification analyses.

Earthquake	Station	Comp.	M	Dur. [s]	PGA [g]
Imperial Valley 1940	El Centro	S00E	6.9	40	0.359
Tabas 1978	70, Boshrooyeh	WE	7.3	43	0.929
Imperial Valley 1979	01260	NS	6.4	58	0.331
Loma Prieta 1989	Corralitos	0	7.0	25	0.801
Northridge 1994	24436	WE	6.7	60	1.778
L'Aquila 2009	Valle Aterno	WE	5.8	50	0.676
Chile 2010	Angle	WE	8.8	180	0.697
New Zealand 2010	163541	NS	7.1	82	0.752
Tohoku 2011	Sendai	NS	9.0	180	1.402
Katmandu 2015	Kanti Path	NS	7.8	100	0.164

Table 3.1: Seismic input data-set generalities (see also Appendix A).

In order to perform the direct analysis, and to obtain the numerically determined displacement and acceleration response signals of the dynamic system at each floor, seismic input at the base $\ddot{u}_g(t)$ has been considered as the effect of inertial forces $Fi = -m\ddot{u}_g$ acting at each floor *i*.

Numerically determined undamped modal natural frequencies $f_{n,i}$ of the benchmark structure, have already been calculated in the previous chapter, as well as damped modal frequencies $f_{d,i}$, considering the cases of z_i=1%, 3% and 5%, for all the modes (recall Table 2.1, reported in Section 2.2.1).

3.3 Analysis results

Various numerical-analysis scenarios, which involve the processing of the dynamic response of a 3-DOF shear-type building model, subjected to instances of a set of ten seismic input signals (see Table 3.1), have been performed, by exploiting the proposed multi-rate KF-based approach. In this section, a selection of the obtained results is reported and commented on.

In particular, two related research scenarios are presented: one belonging to the Time Domain, the other to the Frequency Domain. Primarily, the KF algorithm is implemented to clarify the displacement response signals, initially affected by different levels of noise, with the contribution of a few reliable (noise-free) acceleration data, involved in the HDF procedure. Secondly, the so-clarified displacements, whose quality has been improved by means of the KF application, are

employed for extracting the current modal natural frequencies of the 3-DOF benchmark structure, through appropriate inverse analysis approaches.

A general conceptual scheme summarizing the HDF case dealt with under seismic input, also including the subsequent modal identification analysis performed on the filtered displacements, is depicted in following Fig. 3.2.

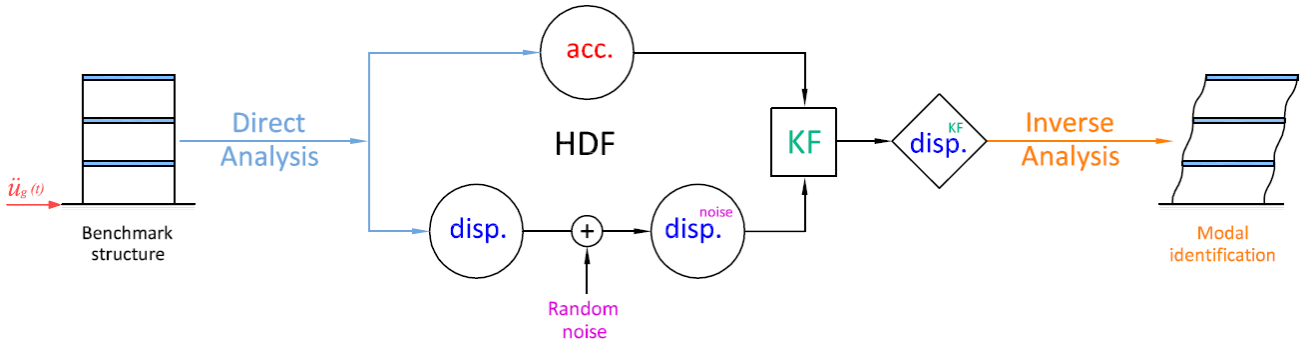

Figure 3.2: Schematic conception of the illustrated HDF procedure via KF between noise-affected displacements and noise-free accelerations at seismic excitation. Determination of filtered displacements and subsequent phase of modal identification, based on displacements.

In such a figure, different colors have been used to better appreciate the three interconnected steps constituting the accomplished procedure, i.e. direct analysis, HDF implementation via KF, and inverse analysis, as detailed in the following sections.

The KF effectiveness is assessed in both the Time Domain and the Frequency Domain, through the monitoring of the system dynamic response at each floor, namely u_1, u_2, and u_3.

All the analyses, which solely involve synthetic signals, have been developed within an autonomous MATLAB implementation environment.

3.3.1 Results in the Time Domain

In this section, original (numerically determined) seismic response displacements u_i are contaminated with increasing levels of zero-mean Gaussian white-noise, to obtain noisy displacements $u_{i,noisy}$, which have to be merged with accelerations ai, taken instead as noise-free. This reflects what might often happen in reality, since accelerometers shall be able to detect signals with a higher level of accuracy than displacement sensors (Smyth and Wu [192]). Here, since the analysis solely focuses on synthetic signals, being available the (noise-free) numerical response signals, the level of noise affecting the displacement data may easily be expressed in terms of N/S ratio, as the ratio between the RMS of the noisy corrupting signal with respect to the maximum measured displacement, in percentage.

N/S ratios of 0%, 5%, 10%, 15%, 20% and 25% are considered within the present analyses to contaminate the original displacements. Although, in practice, a good instrumentation for signals detection may typically be accompanied by intrinsic errors smaller than a 10% N/S, for academic purposes, also higher N/S ratios are here explored. This also aims at demonstrating the robustness of the presented HDF implementation. Modal damping ratios z_i, instead, have been maintained constant and equal to 1% for all the modes, as representative of a slight sub-critical damping, for the whole investigation.

Here, just the results obtained from the analyses preformed on the shear- type building of Fig. 3.1 subjected to L'Aquila seismic input, 2009, acting at the base, are presented, in both graphic and tabular form. Results deriving from the other analyzed seismic ground motions are instead subsequently reported only in tabular form. In fact, from the emerged outcomes, the L'Aquila earthquake scenario appears to be well representative also for general cases and, consequently, considerations deriving from it may be extended to structures that undergo generic earthquake shakings, as those summarized in previous Table 3.1.

Fig. 3.3 shows the third-floor displacement response signal pre- and post-application of the HDF-based procedure via KF, for two specific noise levels contaminating numerically determined displacements u_3, i.e. the cases of 10% and 25% N/S ratios. Further results, showing the KF estimates obtained considering all the analyzed N/S ratio cases (i.e. 0%, 5%, 10%, 15%, 20% and 25%), are available in Appendix B (Figs B.1–B.6).

It may be appreciated how the two curves, representing the numerically determined displacements u_3 (dotted blue line) and KF estimated displacements $u_{3,KF}$ (red line), show a similar trend, despite for the increasing noise level assumed on the measurements.

The effectiveness of such a technique is inspected in terms of percentage variation between original displacements u_i and KF estimated displacements $u_{i,KF}$. In Table 3.2, signal peak values and percentage variations Δu_i between these two quantities are reported, considering each degree of freedom of the analyzed dynamic system, and assuming an increasing level of noise on the measurements. In fact, it is worth noting that, as previously mentioned, for a more thorough understanding of the dynamic behavior of the structure of interest, not only displacement response signal u_3, but also displacement response signals of the lower floors, u_1 and u_2 (see Fig. 3.1), are monitored within the analysis.

From Table 3.2, it emerges how the filter is able to significantly enhance the noisy measurements that may derive from displacement sensors, overcoming the intrinsic limitations which characterize such a kind of instrumentation. For instance, in the possible case of a N/S ratio equal to 10% (see Fig. 3.3a), the sensor would have measured a maximum displacement $u_{3,noisy}$ of 11.25 cm, against a

numerically determined value u_3 of 9.38 cm, in the absence of noise. Thanks to the KF support, instead, a more reliable estimate of maximum displacement $u_{3,KF}$ equal to 9.32 cm is obtained, leading to a percentage variation well below 1%.

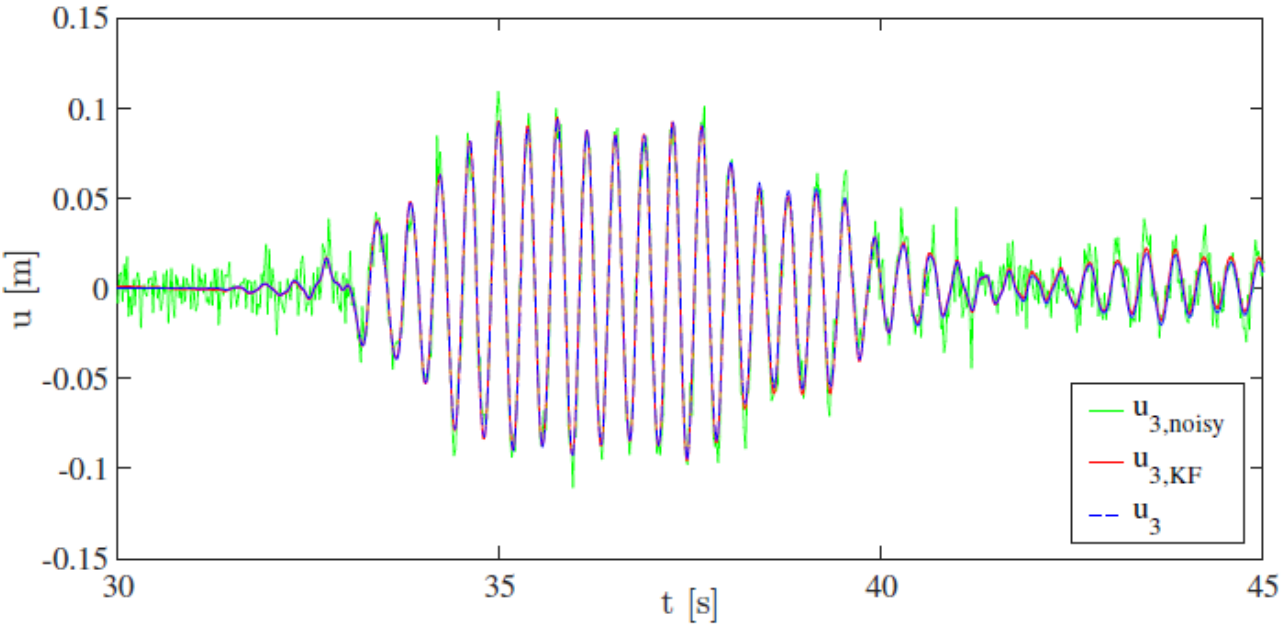

a) 10% *N/S ratio.*

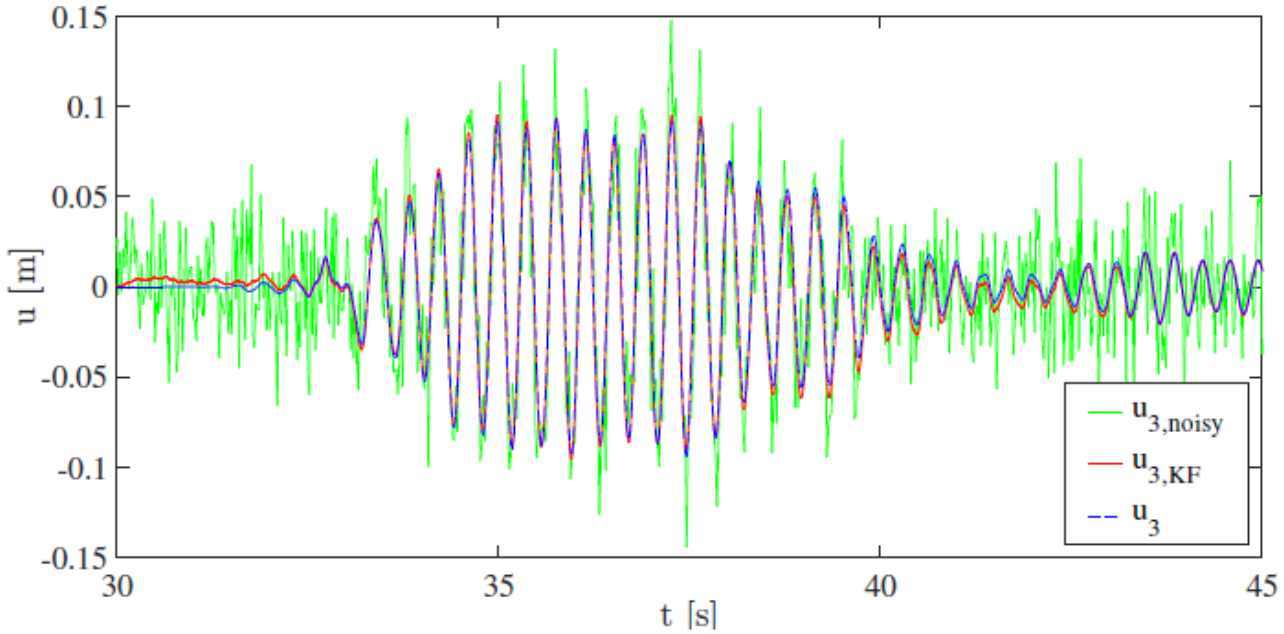

b) 25% *N/S ratio.*

Figure 3.3: KF application on top-floor displacement response signal of a 3-DOF shear-type frame subjected to L'Aquila 2009 earthquake input, for different N/S ratios on displacements (top-floor displacements are depicted).

N/S ratio [%]	$u_{1,noisy}$ [cm]	$u_{1,KF}$ [cm]	Δ_{u_1} [%]	$u_{2,noisy}$ [cm]	$u_{2,KF}$ [cm]	Δ_{u_2} [%]	$u_{3,noisy}$ [cm]	$u_{3,KF}$ [cm]	Δ_{u_3} [%]
0	*4.15*	*4.15*	*0*	*7.48*	*7.48*	*0*	*9.38*	*9.38*	*0*
5	4.58	4.18	0.72	8.29	7.50	0.27	10.13	9.41	0.32
10	4.48	4.20	1.20	8.87	7.53	0.67	11.25	9.32	0.64
15	5.48	4.22	1.69	10.82	7.68	2.67	10.60	9.50	1.28
20	5.65	4.34	4.57	12.15	7.76	3.74	12.71	9.12	2.77
25	6.59	4.41	6.27	12.46	8.08	8.02	14.60	9.85	5.01

Table 3.2: L'Aquila 2009 earthquake: maximum values of numerically determined displacements u_1, u_2, u_3 and KF estimates $u_{1,KF}$, $u_{2,KF}$, $u_{3,KF}$, and their percentage variation Δu_i , for different N/S ratios.

To emphasize the effectiveness of the performed HDF procedure, and to further prove the quality of the displacement estimates that may be obtained through the proposed KF-based implementation, an analogous analysis on the same structure subjected to the other seismic input signals listed in Table 3.1, is conducted. Results are reported in tabular form in Appendix C (Tables C.1–C.10), for each considered seismic ground motion.

Similar positive conclusions about the effectiveness of the inspected HDF-based procedure involving KF may also be drawn in these cases, comparing noisy maximum displacement $u_{i,noisy}$ with corresponding filtered maximum displacement $u_{i,KF}$, regardless of the applied seismic input. In fact, from percentage variations Δu_i , summarized in Tables C.1–C.9, it may be observed how the proposed HDF technique appears to be very robust, if accelerations are set as noise-free, as in this case, despite for the significant noise levels considered on displacements. Such an approach reveals to be quite useful for more clearly bringing out the characteristics of the signal in the Time Domain, configuring itself as an approach that might play a key role within practical monitoring applications.

3.3.2 Results in the Frequency Domain

Aiming at identifying the modal features (natural frequencies) of the monitored structure, before and after the application of the proposed HDF-based procedure, a further analysis within the Frequency Domain is also performed. In this section, previously clarified top-floor displacement response signal u_3 is employed toward identification purposes, by means of appropriate inverse analysis algorithms. In particular, Welch's method (Otis [146]) is first applied on the unprocessed (noise-corrupted) displacements, and, through an automatic peak-picking procedure performed on Welch's PSD, it may be possible to obtain the fundamental modal frequencies of the benchmark shear-type building. As it can be appreciated from the graph in Fig. 3.4a, considering a source signal affected by a realistic 5% N/S ratio, only the first modal frequency emerges, while the other two appear to be indistinguishable,

due to the presence of the spurious noise. The benefits which the proposed HDF-based implementation brings in to the identification process clearly emerge in Fig. 3.4b, where a similar Frequency-Domain analysis performed on the filtered displacements leads to the identification of all the three natural frequencies of the structure, represented in the graph by the three frequency peaks.

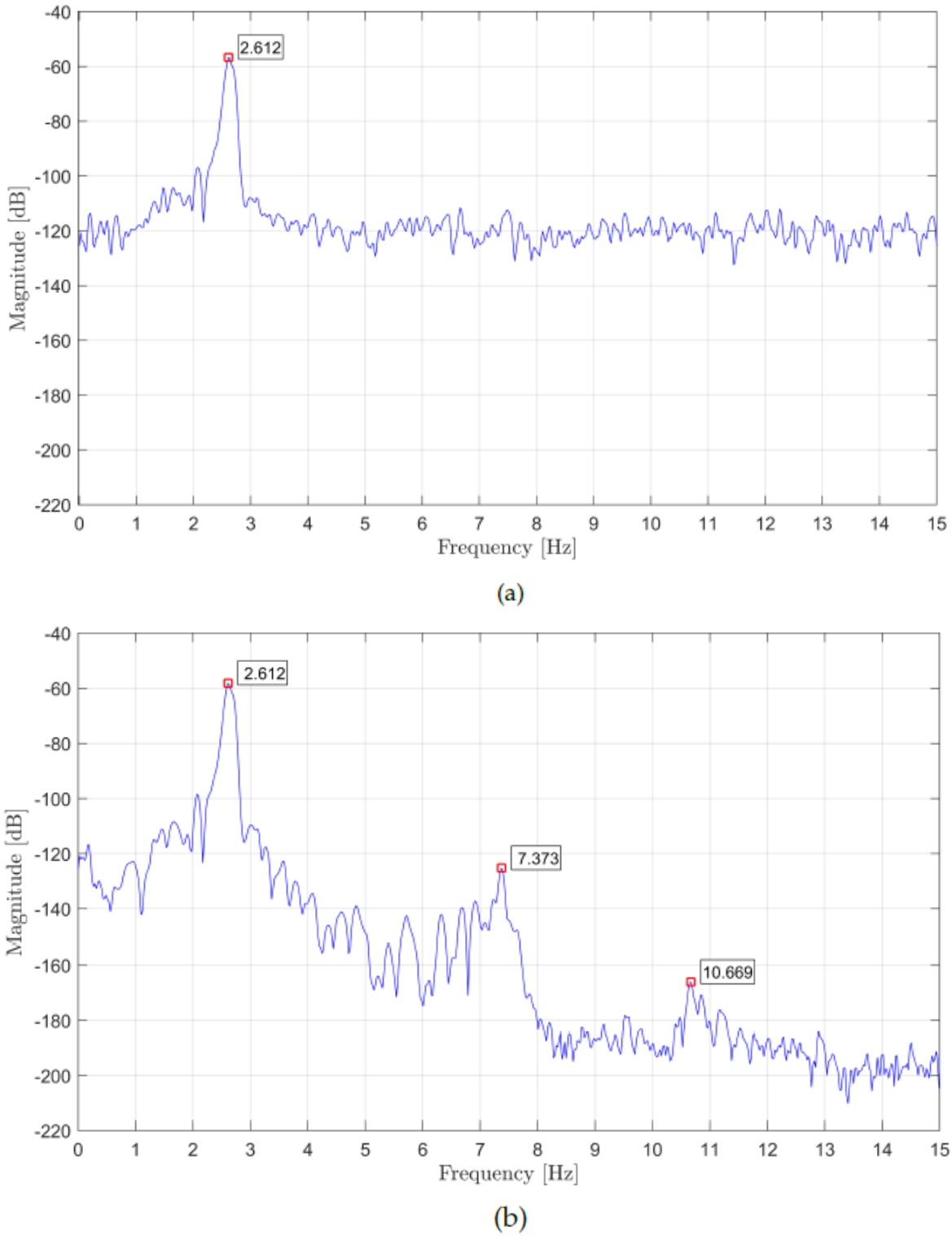

Figure 3.4: Identified natural frequencies by an automatic peak-picking procedure on displacements (Welch's method): (a) pre-KF application; (b) post-KF application.

To inspect the reliability of the estimates obtained through the modal identification procedure made on the displacement seismic response signal, a more classic identification approach based on the top-floor acceleration response signal, is also proposed.

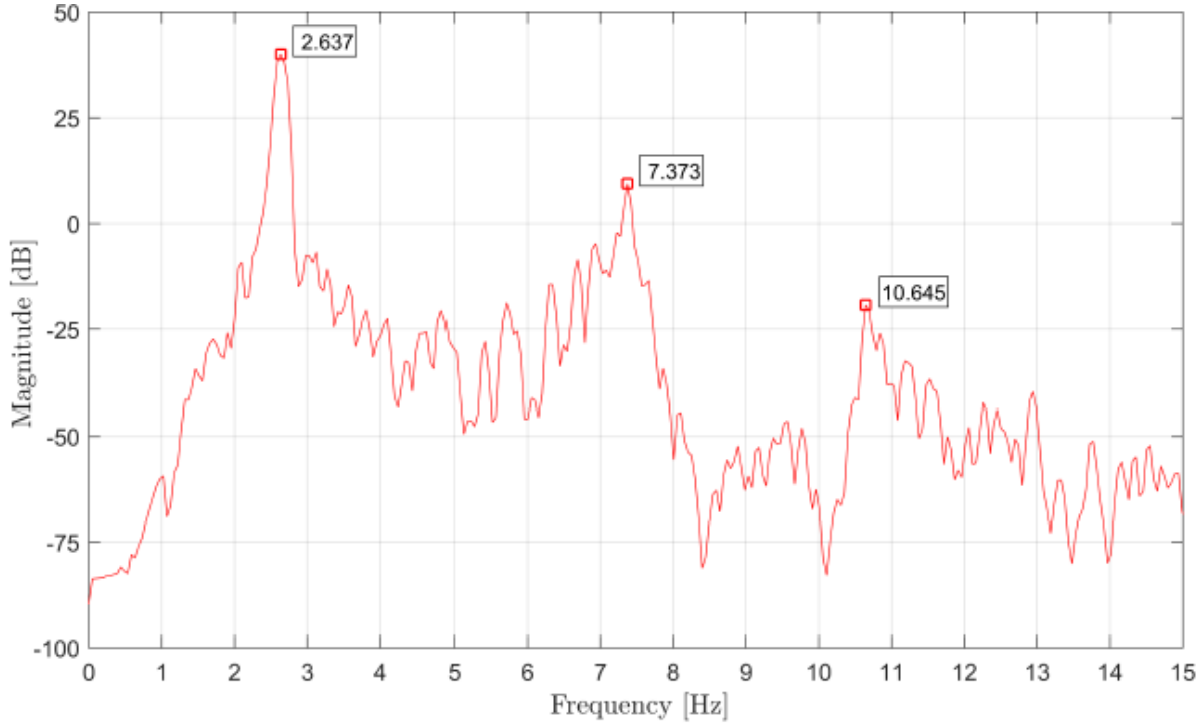

(a)

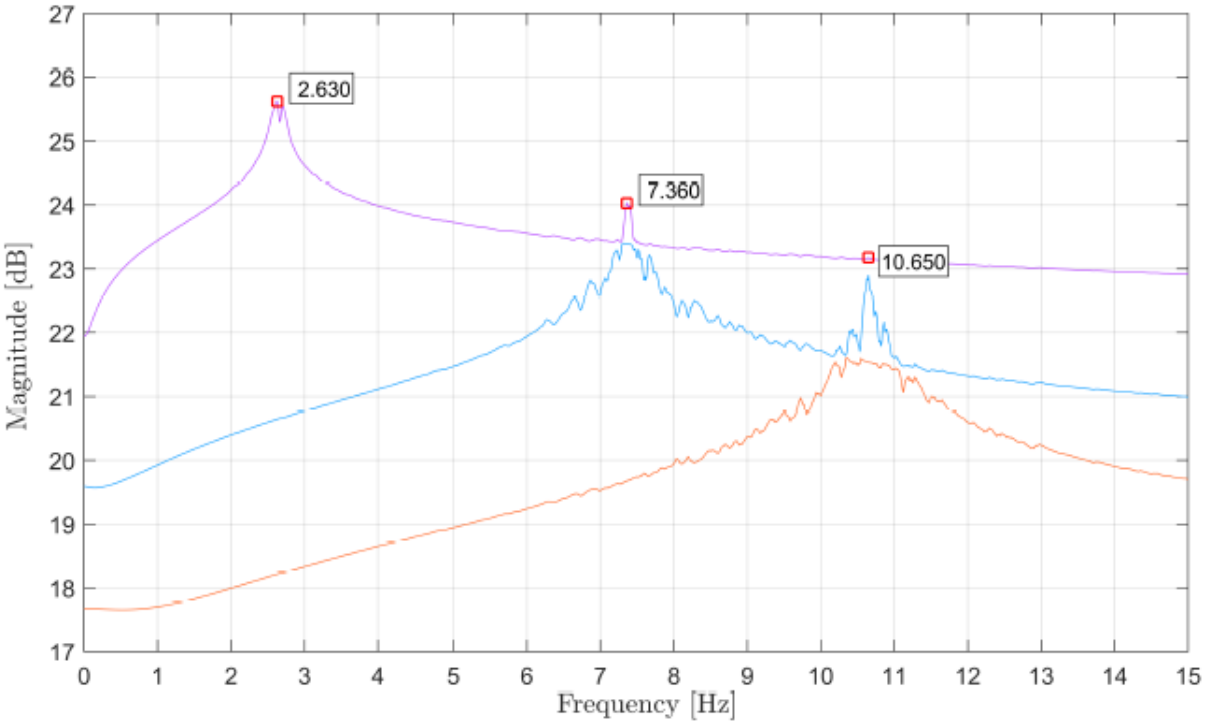

(b)

Figure 3.5: Identified natural frequencies by an automatic peak-picking procedure on accelerations: (a) Welch's method; (b) standard FDD method.

For this purpose, two different methods are employed. Firstly, a Welch's method, analogous to that previously exploited for the displacement-based identification, is performed on acceleration response signal a_3, leading to the results shown in the graph in Fig. 3.5a. Comparing the so-obtained three natural frequencies with those extracted from the displacements, represented in Fig. 3.4b, a good agreement may be observed. Secondly, a further modal identification approach based on accelerations, namely a standard FDD method, is performed on same top-floor acceleration response signal a_3, and represented in Fig. 3.5b. Again, the three main frequency peaks, corresponding to the natural frequencies of the monitored structure, appear to be clearly visible, and their estimated values are very close to those previously exposed. Better estimates of the structural modal properties may even be obtained by applying a more sophisticated variant of the FDD method, known as refined FDD method, as deeply explored in Pioldi et al. [152–154] as well as in Pioldi and Rizzi [155–158], and references cited therein.

Furthermore, numerically determined damped natural frequencies $f_{d,I}$ are employed as a comparison term for evaluating the accuracy of the resulting estimates, and the percentage variation between each identified frequency and the corresponding numerical value is also calculated and reported in Table 3.3, for the three structural vibration modes. It is worth noting that such a table solely refers to L'Aquila 2009 earthquake, whereas the results obtained on the other analyzed seismic ground motions may be found in Tables D.1–D.10, as reported in Appendix D.

The very low percentage variations obtained between the identified modal frequencies and the numerical ones, in every case around 1%, prove the effectiveness of the proposed implementation involving a KF in determining the modal features of a monitored structure, at least concerning L'Aquila 2009 seismic input.

Modes	**I**	**II**	**III**
$f_{d,i}$ [Hz]	*2.658*	*7.448*	*10.762*
$f_{dspl,Welch}$ [Hz]	2.612	7.373	10.669
Δ [%]	−1.73	−1.01	−0.86
$f_{acc,Welch}$ [Hz]	2.637	7.373	10.645
Δ [%]	−0.79	−1.01	−1.09
$f_{acc,FDD}$ [Hz]	2.630	7.360	10.650
Δ [%]	−1.05	−1.18	−1.05

Table 3.3: L'Aquila 2009 earthquake: natural frequencies identified from top-floor displacements $f_{dspl,Welch}$ vs. natural frequencies identified from accelerations $f_{acc,Welch}$ and $f_{acc,FDD}$: comparison and their variation with respect to target numerically determined damped frequencies $f_{d,i}$.

Moreover, looking at the results available in Appendix D, this consideration may be generalized, and extended even to the other considered ground motions. In fact, similar trends may be highlighted for all cases, since the frequencies identified from the processed displacements prove to be competitive with the same frequencies identified from the accelerations. Such estimates also reflect the targeted numerical values, proving the fact that the identification based on displacements may be considered as a valid alternative to the more standard identification based on accelerations.

3.4 Final remarks

In this chapter, a KF has been involved within a HDF-based procedure, aiming at enhancing the non-stationary (seismic) displacement response of a numerical structural system subjected to single instances of a set of ten different seismic ground motions. Different noise levels, in terms of N/S ratios, have been selectively added to the displacement response signals, and the effectiveness of the proposed implementation within the Time Domain has been evaluated by comparing the filtered displacements with the numerically determined displacements. Instead, about the Frequency Domain, the KF effectiveness has been assessed by extracting the natural frequencies from the processed displacements and, subsequently, by comparing such estimates with the modal frequencies identified from the accelerations, as well as with the targeted numerically determined frequencies.

The main achievements that the presented research scenario has brought to light may be summarized in the following three salient points:

- within the Time Domain, the effectiveness of the KF may be considered to be fully proven, for all the analyzed seismic ground motions, at least for N/S ratios commonly involved in civil engineering applications (say, in the order of less than 10%);
- within the Frequency Domain, the adoption of the presented procedure has brought great benefits to the modal identification process, in terms of number of natural frequencies which may be extracted from the filtered displacement response signal. In fact, all the three natural frequencies of the monitored structure have been clearly identified, differently from what it had happened by considering the unprocessed displacement signal into the identification process;
- the obtained results show that the ambitious goal to successfully perform an output-only identification by using non-stationary response displacement measurements, opportunely processed, instead of the more common acceleration-based approach, may be considered to be achieved.

In conclusion, it may be asserted that, although it is well known that modal dynamic identification made exclusively on accelerations is often enough to obtain reliable estimates of modal parameters

of a certain structure, the possibility to exploit displacement records (possibly corroborated by a few acceleration data) for the same identification purposes, moreover with reference to non-stationary input excitations, might represent an important alternative scenario in the structural identification field. In fact, it might open up new perspectives, especially during the signal acquisition stage, since it would make it possible to monitor a specific structure (and to deduce its current modal properties) without directly acting on it (or only partially involving the structure through the placement of a few accelerometers), for instance by simply using a total station.

Chapter 4. Critical assessment of two denoising techniques for purifying synthetic structural vibration response signals

This chapter introduces the denoising problem, as the procedure through which it may be possible to purify a signal from undesired noise, which commonly affects recorded data, by altering its content. In this sense, it can be considered as an alternative approach to the HDF-based procedure, discussed in the previous chapters, aiming at achieving a better understanding of the detected data. In particular, two specific denoising techniques, i.e. a Discrete Wavelet Transform (DWT)-based denoising, as well as a Singular Value Decomposition (SVD)-based denoising, are explored. Exclusively, synthetic response signals of a different nature (non-stationary and stationary) are involved within the analysis, for assessing the effectiveness of the two studied denoising techniques.

The chapter is organized as follows. After a general contextualization of the denoising problem, given in introductory Section 4.1, which aims at providing some of the most important bibliographical references on this topic, a brief theoretical framework concerning the adoption of the DWT and SVD techniques for denoising purposes is presented in Section 4.2, together with the needed strategies for their adaptation in the handling of the present civil engineering scenario. Section 4.3 presents the analysis procedure, through the description of the benchmark dynamical system, the process of generation of the simulated noise-affected signals and the obtained results. Here, a particular importance is placed on the preliminary calibration of the denoising technique based on DWT, through the search for the optimal configuration of its characteristic parameters; additionally, the criterion through which a SVD approach may effectively be exploited toward denoising purposes is also explored. Within the same section, a performance assessment of the two studied approaches is presented, and a critical comparison is provided. Conclusions and global remarks are finally outlined in Section 4.4, as well as some possible further research perspectives.

4.1 Introduction and contextualization

SHM refers to the process of a continuous assessment of the current health condition of a structural system, aiming at improving its safety and integrity by detecting potential manifestations of damage, before this may reach a critical state and become detrimental for structural safety. Dealing with the structural engineering context in general terms, in addition to the literary references already provided in Chapter 1, further very recent virtuous examples in which SHM procedures have been successfully implemented, on different typologies of structures, may be found in the literature, e.g. by Capellari et al. [20], Chatzi and Smyth [28], Ferrari et al. [65–68], Koo et al. [120], Lee et al. [123], Roberts and

Dodson [170], and therein cited references. It is clear that the acquisition stage of signals, from which the current structural conditions may be detected, constitutes a crucial phase for the global success of such an analysis.

Referring to the civil engineering field, in particular, the most common typologies of sensors employed for the detection of response signals may be considered as accelerometers and displacement sensors, as the kind of response data that can be recorded from them may be good enough to effectively describe the current health conditions of a structure. However, the widespread need to adopt a low-cost and easy-to-use monitoring instrumentation, toward recording the dynamic behavior of structures subjected to live external loads, may often lead to measurements affected by even sensible amounts of noise. This spurious signal contamination, superposed upon the useful structural response signal, may lead to modify its monitoring information content. Such a process might substantially alter the prediction of the structural response and induce significant discrepancies in estimating the structural dynamic behavior, increasing the induced uncertainties and leading to unreliable SHM implementations. Consequently, noise reduction from acquired response signals constitutes a crucial issue in the whole process of efficient health monitoring of civil structures, in particular, concerning the subsequent phase of signal processing after the data acquisition stage.

The procedure through which it becomes possible to reconstruct a certain source signal, starting from a recorded, noise-affected one, removing its noisy part, without losing the useful information contained in it, may be referred to as denoising (Buades and Coll [17], Chen and Bui [30], Portilla and Strela [159]). Two main issues have to be taken into account in dealing with a denoising procedure, namely: (a) how the initial data may be affected by the added noise; (b) how the reconstructed signal, out of the denoising procedure, shall be able to correctly reproduce the original (truthful) signal, preserving all its fundamental characteristics. Thus, the crucial matter of each denoising process lies in removing most of the unwanted noise, without losing the useful part of the signal, namely the one containing the true monitoring information.

Several computational techniques have been proposed to address the denoising of signals, some of which are currently in continuous development. The most basic and traditional way to remove the noise affecting the signals is represented by the employment of band-pass filters with cut-off frequencies, i.e. high-pass or low-pass filters, which allow to remove all the frequency contents greater or lower than a certain frequency value, respectively. Moving average filters, as well as Gaussian filters, can be considered as typical examples belonging to such a category. However, although the application of such filters may be useful when the noise is located within a precise frequency band, which is different from the frequency band in which the signal shall lay, in most cases, when the noise displays a similar frequency content as that of the signal to be analyzed, they

cannot be effective, since even much of the useful signal may be lost. This also constitutes a main drawback in the use of the Fourier Transform toward denoising purposes (Ergen [59]). In other words, such methods act in a global sense, since they process the signal regardless of whether the noise displays a uniform frequency distribution or not. However, in real cases, the noise distribution may be far from being uniform and it may be desirable to apply a "localized" form of denoising. In the past decades, this has led to searching for different methodological approaches and alternative filtering techniques toward achieving an effective denoising.

Kam et al. [108] and Arezki and Berkani [8] proposed the application of adaptive filters to remove Gaussian white-noise and impulse noise from signals. Within their works, an iterative procedure was set up for minimizing in real time the error between the original signal and the denoised signal (Madisetti and Williams [135]). In order to suppress impulse noise, Veerakumar et al. [207] introduced a new algorithmic approach based on the combination of fuzzy logic and on an asymmetric trimmed median filter, whereas in Premchaiswadi et al. [163] a kFill algorithm was combined with a median filter for reducing the impulse noise that could occur on images (denoising methods can also be successfully applied on images, since an image may be interpreted as a two-dimensional signal, Ergen [59]).

A further powerful methodology for separating noise out of corrupted data involves the application of a Discrete Wavelet Transform (DWT). In particular, in Dohono [48], a first DWT-based approach for denoising one-dimensional signals was provided. Afterwards, Chang et al. [24] introduced an innovative adaptive Wavelet thresholding for image denoising and compression, called BaeyShrink method.

Furthermore, the use of Singular Value Decomposition (SVD) for denoising purposes has also attracted considerable interest, as demonstrated e.g. in Konstantinides et al. [118] and Konstantinides and Yao [119], where the authors introduced a new filtering and noise estimation technique, known as Block-based Singular Value Decomposition (BSVD) filtering.

Finally, a possible alternative approach that may be adopted in enhancing the quality of noise-affected signals may concern the application of a KF (Chatzi and Fuggini [26, 27], Ravizza et al. [166], and works cited

therein). For instance, in previous Chapter 1 and 2, a KF has been successfully employed within a HDF-based procedure, in order to correct noisy displacement measurements, by enhancing them through a few reliable acceleration response signals, toward cleaning structural acquisition extraction and modal dynamic identification.

Here, two of the above-mentioned approaches are systematically reconsidered and developed, in first tackling a controlled denoising problem set on reference structural response signals. In particular, the

development of a DWT procedure as a multi-rate filter bank, as well as the implementation of a SVD technique are extensively inspected, in their employment toward denoising structural response signals. Here, the two approaches are implemented and assessed on noise-corrupted structural vibration response signals that may be typical of practical applications belonging to the civil engineering context. In signal processing, DWT is actually commonly applied for many other purposes, in addition to signal denoising. For instance, its employment shall be rather useful in detecting trends, breakdown points, discontinuities in higher derivatives and self-similarity of signals (Sifuzzaman et al. [191]). Moreover, as a denoising technique, it has been already performed on signals presenting a different nature, i.e. gravity and magnetic signals (Fedi et al. [63]), biological signals (Alyasseri et al. [4], Aqil et al. [9]), such as electroencephalograms (EEG) or electrocardiograms (ECG), but also on acoustic (Feng et al. [64]) and pressure signals (Shanxue and Chao [187]). However, its application in denoising structural signals typical of the civil engineering field does not seem to have been deeply inspected yet. Similarly, also SVD has found applications in digital signal processing as a technique for noise reduction. In particular, its effectiveness has been already proven dealing with audio signals (e.g. in Baravdish et al. [11], where it is combined with a non-linear PDE method), or biomedical signals (Schanze [183]), or even for radar target recognition of electromagnetic signals (Lee et al. [126]), but also for improving the quality of images (Guo et al. [86]). Moreover, in the civil engineering domain, it has been exploited for many purposes, including those of modal dynamic identification (e.g. in Pioldi et al. [152–154]) and of damage detection in structures at an early stage of development (Ruotolo and Surace [173]).

Within the present investigation, the performances of the DWT- and SVD-based denoising techniques is first assessed on earthquake and ambient vibration synthetic response signals, and a critical comparison based on the effectiveness of such methods is provided, at variable values of added noise. The selection of these two types of response signals is also motivated by the fact that they can be considered as being well representative of two great families of signals, since they display a very different nature. In particular, the earthquake excitation input is known as a typical nonstationary signal, whereas the ambient vibration signal is instead considered as a common stationary signal, since it may almost be constant in time and frequency. To inspect advantages and possible limitations of the mentioned denoising techniques, in relation to the typology of the processed signal, shall constitute an important goal of this chapter.

In order to synthetically generate numerical response signals, the seismic input as well as the ambient vibration input are separately examined and applied on a reference structure, namely a one-bay ten-story shear-type frame building, used as a benchmark mockup for the whole study. In particular, the first- and last-floor acceleration responses are monitored, in the cleaning of the response signals

(accelerations). Furthermore, to simulate the effect of the errors that may occur on the measurements during a real signal acquisition stage, within the analysis, several N/S ratios are considered for a superimposed noise signal affecting the data. As previously stated, the present investigation solely targets synthetic response signals, i.e. numerically generated signals, since their employment has been preliminarily considered for a crucial, necessary condition validation of the denoising procedures. Further preliminary simulations of the present research efforts confined only to synthetic signals, were presented in Ravizza et al. [167].

4.1.1 Goals of the research scenario

The main goals that this study aims to pursue are the following:

- to explore which is the optimal calibration of a DWT-based denoising technique, for dealing with both seismic and ambient vibration response signals;
- to examine the possibility to successfully exploit a SVD-based implementation, toward the clarification of the above-mentioned response signal typologies;
- to provide a critical comparison of the strengths and weaknesses of each denoising method, aiming at exploring their effectiveness, at a controlled, increasing level of noise inserted on the source signals;
- to recover the original signal in the Time Domain, with also the target of preserving its spectrum in the Frequency Domain, in order to achieve a comprehensive and more reliable reconstruction of the response signal, to be considered as rather truthful toward real monitoring purposes.

All these topics will be addressed and deeply discussed throughout the chapter, by a dedicated numerical analysis performed within a MATLAB environment.

4.2 Theoretical framework

This section presents the denoising problem, as well as the mathematical theory behind the DWT- and the SVD-based denoising approaches. The Percentage Root Mean Square Difference (PrmsD) index, namely the parameter employed within the analysis for evaluating the effectiveness of the explored denoising techniques, is also defined.

4.2.1 Problem statement

A classical way of dealing with a typical denoising problem is to decompose noise-corrupted signal $\mathbf{y} = \{y_1, ..., y_i, ..., y_N\}$ into the sum of two different contributions: clean (noise-free) signal $\mathbf{x} = \{x_1, ...,$

$x_i..., x_N\}$, which contains the useful information that has to be preserved out of the denoising process and additive noise $\mathbf{n} = \sigma\{\tilde{n}_1, ..., \tilde{n}_i, ..., \tilde{n}_N\}$, of an intensity given by standard deviation σ, which instead represents the portion of the signal that shall be removed. Thus, such a relation may be expressed as $\mathbf{y} = \mathbf{x} + \mathbf{n}$, for each *i-th* component of the signals at recording time t_i, i = 1, ..., N, where N is the length of the signal:

$$y_i = x_i + \sigma\tilde{n}_i \tag{4.1}$$

Here, the additive noise contaminating the data may be modeled as a stationary independent zero-mean Gaussian term (Alfaouri and Daqrouq [2], Moulin and Liu [141]) and both noise-free and noise-corrupted signals are taken as artificially generated synthetic signals. The assumption of these hypotheses constitutes a necessary requirement in this preliminary phase of denoising technique assessment, as it allows for working within a controlled environment, where potentialities and critical issues of such techniques may be brought to light in a convenient way, than for real signals. The aim of each denoising process is to obtain a best approximation $\hat{\mathbf{x}} = \{\hat{x}_1, ..., \hat{x}_i, ..., \hat{x}_N\}$ of the original (noise-free) signal, starting from the noise-affected one, removing the undesired noisy part, without losing appreciable and useful information contained in the processed data.

A few indexes have been proposed in the literature toward evaluating the performance of denoising techniques (Sadooghi and Khadem [174]). In this study, in which a Gaussian white-noise is added to a synthetic signal and the denoising procedure is performed on such an artificial noisy signal, the PrmsD index (Karthikeyan et al. [109]) is used as an effectiveness denoising evaluation parameter. In fact, since both the original (noise-free) signal and the denoised signal are entirely available, the percentage error between them may readily be expressed by the following relation:

$$\mathrm{PrmsD} = 100 \cdot \sqrt{\frac{\sum_{i=1}^{N} (x_i - \hat{x}_i)^2}{\sum_{i=1}^{N} x_i^2}} \tag{4.2}$$

To obtain a most truthful reconstruction of the original signal, a smallest value of PrmsD is desired. The same index will also be used as a comparison term to confront the performances of the two different denoising techniques that are taken into account, namely the ones based on DWT and SVD. Other possible evaluation indexes that may be found in the literature as an alternative to the PrmsD index are, for instance, the Cross-Correlation value (Al-Qazzaz et al. [3]), which expresses the similarity between two discrete-time sequences, the Mean Square Error (MSE) (Sadooghi and Khadem [174]) and the Signal-to-Noise ratio (SNR) (Gradolewski and Redlarski [83]).

In real applications, however, the source benchmark signal, which expresses the true (noise-free) response of a structure, is of course unavailable. Consequently, in these cases, the PrmsD index cannot be used for the direct evaluation of the denoising effectiveness, and alternative ways to handle with that should be considered.

In the next two sections, a fundamental theoretical framework on DWT and SVD-based denoising approaches is provided, especially regarding their specific employment toward denoising both non stationary and stationary structural vibration response signals, targeted on civil engineering applications.

4.2.2 Discrete Wavelet Transform-based denoising

Wavelet Transform (WT) may be seen as the process through which a certain signal can be decomposed into its low and high frequency components, via the introduction of a set of orthonormal wavelet functions, constituting a wavelet basis, which originate from the mother wavelet by scaling and shifting operations through two parameters known as *scale parameter j* and *shift parameter k*. In particular, when *scale parameter j* is chosen as a power of two, a dyadic orthonormal wavelet transform is obtained (Vetterli and Herley [209]).

The measure of frequency content similarity between the signal that has to be denoised and the selected wavelet function is expressed by the so-called wavelet coefficients, determined as a convolution of the signal and the scaled wavelet function, which may be considered as an expanded band-pass filter (Rioul and Vetterli [169]). In particular, approximation coefficients are associated with low frequency components, whereas detail coefficients refer to high frequency components. In this way, WT is implemented with a reconstruction filter bank using an orthogonal wavelet family. Such an employment of WT as a filter bank for signal denoising purposes is also known as DiscreteWavelet Transform (DWT) (Ergen [59]).

A DWT denoising procedure may be summarized according to the following three main conceptual steps:

1. *Decomposition of the original signal into the wavelet domain.*

In general terms, a discrete recorded signal $\mathbf{y} = \{y_1, ..., y_i..., y_N\}$, with i = 1, ..., N, and length N taken as a power of two, may be turned into the wavelet domain using an orthonormal wavelet basis (Mallat [138]), as follows:

$$Y_{j,k} = \sum_{i=1}^{N} y_i W_{i,(j,k)} \tag{4.3}$$

where forward transform operator $W_{i,(j,k)}$ is defined as:

$$W_{i,(j,k)} = 2^{-j/2}\psi(2^{-j}i - k) \tag{4.4}$$

so that the orthonormal basis functions are all obtained through translations and dilations of a certain mother wavelet Ψ by means of shift (or translation) parameter $k \in \aleph$ and scale (or dilation) parameter $j \in \aleph$, sampled along the dyadic sequence (Blue [14], Zou and Tewlik [236]). About the choice of function Ψ, it is an oscillating function that may be selected among a set of pre-defined functions, namely *Symlet, Coiflet, Daubechies, Biorthogonal, Reverse Biorthogonal* and *Discrete Meyer* mother wavelets.

Thus, referring to the denoising problem here presented, and exploiting the linearity of DWT, Eq. (4.1) may be rewritten in the wavelet domain by operating $W_{i,(j,k)}$ on each signal components, according to the following relation:

$$Y_{j,k} = X_{j,k} + N_{j,k} \tag{4.5}$$

where a usual notation here denotes with a capital letter a quantity in the transformed wavelet domain, i.e. the wavelet coefficients, at fixed j and k.

It is worth noting that the representation into the wavelet domain allows to preserve the linear structure of the model, so that transformed noise $N_{j,k}$ is still distributed as a Gaussian white-noise, with standard deviation σ, as it can be seen comparing Eq. (4.1) and (4.5). Through the introduction of transfer function D, i.e. the *denoising operator*, original (noise-free) signal $X_{j,k}$ may be estimated starting from noisy signal $Y_{j,k}$, such that:

$$\widehat{X}_{j,k} = DY_{j,k} \tag{4.6}$$

where D, which has to be designed to minimized the error between $X_{j,k}$ and $\hat{X}_{j,k}$, depends on the considered denoising method. To this evaluation end, so-called *estimation risk r*, i.e. the Mean Squared Error (MSE), is mainly adopted in measuring such an error:

$$r = E[(X_{j,k} - DY_{j,k})^2] = \frac{\sum_{i=1}^{N}(X_{j,k} - DY_{j,k})^2}{N} \tag{4.7}$$

where E labels the expected value. Consequently, the main issue consists in optimizing D for the current signal typologies, i.e., here, earthquake excitation and ambient vibration.

2. Thresholding of the DWT coefficients.

Introducing a certain non-dimensional threshold value λ, which may be a function of DWT decomposition level l (level-dependent threshold) or not (level-independent threshold), according to Donoho and Johnston [47], the noise affecting the signals may considerably be reduced by scaling the wavelet coefficients smaller than λ, so that only the coefficients greater than λ are considered to be associated to reliable data, whereas the ones below λ are then set equal to zero.

The basic idea is that the noise in the transformed domain tends to disperse over all the wavelet coefficients, so that a strategy in which values below a proper threshold are set to zero removes most of the noise, preserving the source information. In fact, switching into the wavelet domain, transformed signal $Y_{j,k}$ will have many more non-zero coefficients than transformed signal $X_{j,k}$, due to the noise contribution. Thus, by selecting an appropriate threshold λ, which allows to switch from wavelet coefficients $Y_{j,k}$ to thresholded coefficients $Y_{j,k}(D, \lambda)$, it may be possible to alleviate the noise effect.

Two different types of thresholding may be performed, namely hard thresholding and soft thresholding (Dohono and Johnston [46]). Hard thresholding zeros out all the wavelet coefficients (in absolute value) smaller than λ, by preserving the others as unaltered, as described by the following relation:

$$Y_{j,k}(D,\lambda) = \begin{cases} Y_{j,k} & if \quad |Y_{j,k}| \geq \lambda \\ 0 & if \quad |Y_{j,k}| < \lambda \end{cases} \tag{4.8}$$

In soft thresholding, instead, wavelet coefficients (in absolute value) greater than λ are reduced by a quantity equal to the threshold itself, as follows:

$$Y_{j,k}(D,\lambda) = \begin{cases} |Y_{j,k}| - \lambda & if \quad |Y_{j,k}| \geq \lambda \\ 0 & if \quad |Y_{j,k}| < \lambda \end{cases} \tag{4.9}$$

Since typically the noise mainly affects the high frequency components, it is common to apply the thresholding to the so-called *detail coefficients*, i.e. to the low-frequency band that usually contains the most important components of the signal.

However, both thresholding types display some drawbacks. In fact, soft thresholding, also known as *wavelet shrinkage*, although it tends not to produce discontinuities in the resulting signal, it may lead to unwanted bias, when the preserved coefficients are large. Hard thresholding, instead, might be very sensitive even to small changes in the signal, resulting unstable.

To overcame these issues, some new hybrid solutions have been provided (Gao and Andrew [73], Gao [74]). From Eqs. (4.8) and (4.9), it clearly emerges how the most critical and delicate point in

the DWT-based approach is represented by the choice of an appropriate threshold λ, since the accuracy of the denoised signal mainly depends on it. In particular, the setting of a too small threshold λ might lead to a reconstructed signal that will still considerably be affected by noise and the denoising process would not be effective. Otherwise, a too large λ might lead to the suppression of too many coefficients, losing also the useful part of the signal, containing the information to be preserved. The importance of this choice is also demonstrated by the large variety of methods available in the literature in that respect (Dohono and Johnston [46,47], Karthikeyan et al. [109]). In fact, although for a generic signal of length N a *Universal Threshold* λ has been proposed, many other level-dependent or block dependent approaches exist.

Within this study, the following thresholding rules belonging to the Donoho-Johnson thresholding method family, are considered:

- *Visu shrink (Sqtwolog)* (Dohono and Johnston [46]). According to this thresholding rule, λ may be estimated starting from the Universal method, regardless of the DWT decomposition level, through the following relation:

$$\lambda = \sigma\sqrt{2lnN} \tag{4.10}$$

  where σ is the standard deviation of the zero-mean Gaussian white-noise added to the clean signal.

- *SURE shrink (Rigorous SURE)* (Dohono and Johnston [47]). In this case, a threshold level is assigned to each decomposition level of the WT. The setting of threshold λ is based on the principle of minimizing the Stein Unbiased Estimate of Risk (SURE), as follows:

$$SURE(\lambda, \mathbf{y}) = d + \sum_{i=1}^{d} [\min(|Y_{j,k}|, \lambda)]^2 - 2(i : |Y_{j,k}| < \lambda) \tag{4.11}$$

  where d is the size of noisy vector data $\mathbf{y}$ and $Y_{j,k}$ are the wavelet coefficients. This procedure is very versatile and suitable for denoising a wide range of functions: from those that present lots of discontinuities to those that are essentially smooth.

- *Heuresure (Heuristic SURE)* (Karthikeyan et al. [109]). The method combines features from the two previous thresholding rules. In particular, being λ_1 and λ_2 the threshold values obtained from Universal and Rigorous SURE methods, respectively, according to the Heuristic SURE rule, threshold λ may be computed as follows:

$$\lambda = \begin{cases} \lambda_1 & if \quad A < B \\ \min(\lambda_1, \lambda_2) & if \quad A \geq B \end{cases} \tag{4.12}$$

  where:

$$A = \frac{s - N}{N}, \qquad B = \sqrt{N(log_2 N)^3} \tag{4.13}$$

being *s* the sum of the squared wavelet coefficients (Verma et al. [208]).

- *Minimax* (Dohono and Johnston [49], Karthikeyan et al. [109]). This is a level-independent method based on a Minimax statistical principle. According to a Minimax criterion, the denoised signal may be assimilated to the estimator of the unknown regression function, so that Minimax realizes the minimum of the maximum MSE obtained for a given set of functions and, consequently, optimal threshold λ may be determined as follows:

$$\lambda = \begin{cases} 0.3936 + 0.1829 \cdot log_2 N & if \quad N > 32 \\ 0 & if \quad N \leq 32 \end{cases} \tag{4.14}$$

Here, all these thresholding rules have been applied, combined with different mother wavelets, i.e. *Symlet, Coiflet, Daubechies, Biorthogonal, Reverse Biorthogonal* and *Discrete Meyer* wavelets (Sadooghi and Khadem [174]), for evaluating the effectiveness of a DWT denoisingbased approach on seismic and ambient vibration signal typologies.

3. Signal reconstruction.

Finally, decomposed signal $\hat{x}_i$ can be reconstructed, returning to the original Time Domain, by applying the inverse WT to the thresholded signal:

$$\widehat{x_i} = \sum_{j=1}^{J} \sum_{k=1}^{K} \widehat{X}_{j,k} W^*_{i,(j,k)} = \sum_{j=1}^{J} \sum_{k=1}^{K} DY_{j,k} W^*_{i,(j,k)} \tag{4.15}$$

by means of inverse wavelet transform operator $W^*_{i,(j,k)}$, defined as follows:

$$W^*_{i,(j,k)} = 2^{j/2} \psi(2^j i - k) \tag{4.16}$$

In next Section 4.3.3, a signal denoising analysis based on DWT is performed for different N/S ratios of the added noise signal, in both Time and Frequency Domains. In fact, not only the PrmsD index between the original (noise-free) signal and the denoised one, but also the post-denoising signal frequency content is inspected.

4.2.3 Singular Value Decomposition-based denoising

Differently from the denoising technique based on DWT, the one based on Singular Value Decomposition (SVD) constitutes a non-parametric signal analysis tool that may be implemented without pre-defined basis functions. In particular, it is common to refer to SVD as a numerical method through which a m x n matrix **A** of rank L, containing the data points describing noise-corrupted signal **y**, may be decomposed into the product of three matrices, as follows (Zhao and Ye [230]):

$$\mathbf{A} = \mathbf{U}\mathbf{S}\mathbf{V}^T \tag{4.17}$$

where $\mathbf{U} \in R^{mxm}$ and $\mathbf{V} \in R^{nxn}$ are orthogonal matrices, so that $\mathbf{U}^T\mathbf{U} = \mathbf{I}_m$ and $\mathbf{V}^T\mathbf{V} = \mathbf{I}_n$ (**I** identity matrices), while $\mathbf{S} \in R^{mxn}$ is a "diagonal" matrix storing the square roots of non-zero eigenvalues s_i of positive semi-definite matrix $\mathbf{A}^T\mathbf{A}$ (i.e. the singular values of **A**) in decreasing order, namely $\mathbf{S} = \text{diag}(s_1, s_2, ..., s_L)$, with L = min(m, n). The SVD is adopted in several, different statistical and engineering contexts. For instance, in the realm of modal dynamic identification, SVD is much used in Frequency Domain Decomposition (FDD) methods toward output-only identification (see, for instance, Pioldi et al. [152–154], Pioldi and Rizzi [155–158], and references quoted therein).

The SVD method is able to provide an optimal approximation of the original signal data points, using a matrix of lower rank *l* with respect to that of **A**. In other words, it exists a *m x n* matrix $\hat{\mathbf{A}}$ of rank $l \leq L$ which minimizes the sum of the squared errors between the elements of matrix **A** and the corresponding elements of reconstructed matrix $\hat{\mathbf{A}}$, so that:

$$\hat{\mathbf{A}} = \mathbf{U}_l\mathbf{S}_l\mathbf{V}_l^T \tag{4.18}$$

where subscript $l \leq L$ denotes the reduced rank of each matrix. In particular, matrix $\hat{\mathbf{A}}$ is obtained by considering only the largest (significant) *l* singular values, whereas the remaining ones are replaced by zeros, so that:

$$s_i > \varepsilon,\ i = 1, ..., l; \qquad s_i \leq \varepsilon,\ i = l+1, ..., L \tag{4.19}$$

choosing an appropriate threshold value ε, for instance in the order of 10^{1}. This procedure resembles the way of proceeding of the mentioned DWT-based denoising approach, in the sense that, there, wavelet coefficients below a certain *l* threshold are removed. Such a property may successfully be exploited for signal data reduction also in a SVD-based denoising, allowing to alleviate a conspicuous amount of noise from noisy signals.

Considering now a typical denoising problem, as the one described by Eq. (4.1), according to Antoni and Randall [7], it may be expressed in vector notation as follows:

$$\mathbf{y} = \mathbf{x} + \mathbf{n} \tag{4.20}$$

where **y** denotes the generic noisy vibration signal, which it can be interpreted as the sum of a noise-free signal **x** and of a noise effect **n**. Consequently, also matrix **A** related to **y** may be seen as the sum of two contributions: aforementioned matrix $\hat{\mathbf{A}}$, containing noise-free data, i.e. the useful information embedded within the signal, and matrix **N**, representing the noise contribution, which has to be removed. From Eqs. (4.17) and (4.18) it follows that:

$$\mathbf{A} = \hat{\mathbf{A}} + \mathbf{N} = \begin{bmatrix} \mathbf{U}_l & \mathbf{U}_0 \end{bmatrix} \begin{bmatrix} \mathbf{S}_l & \mathbf{0} \\ \mathbf{0} & \mathbf{S}_0 \end{bmatrix} \begin{bmatrix} \mathbf{V}_l^T \\ \mathbf{V}_0^T \end{bmatrix} \tag{4.21}$$

where $\hat{\mathbf{A}}$ and **N** are related to **x** and **n**, respectively, $\mathbf{S}_l$ contains only significant singular values s_i (i = 1, ..., l), which are employed in the reconstruction of the uncontaminated signal, while $\mathbf{S}_0$ includes the remaining smaller singular values s_i ($i = l + 1, ..., L$), which have to be set at zero. Thus, concerning the application of the SVD method, the main issue now shifts in estimating optimal threshold ε for successfully separating the contaminated part of the signal from the good one. In this regard, many different approaches dealing with this point appear in the literature (e.g. Chen and Zhang [33], Jing et al. [101]), mainly based on the construction of matrix **A** using measured data. Among them, the one based on the Hankel matrix is the most widely employed, essentially thanks to its zero phase-shift property and wavelet-like characteristics (Zhao and Ye [230]).

Similarly to the denoising method based on DWT, also the SVD-based approach may be summarized according to the following three main conceptual steps (Zhao and Jia [233]):

1. Construction of the Hankel matrix.

Since in the common practice detected signals are expressed as time series, they have to be first reshaped into a matrix form in order to be suitable for denoising purposes based on a SVD implementation. Considering a generic discrete noise-corrupted vibration signal $\mathbf{y} = [y_1, ..., y_i, ..., y_N]$, this may be done by assembling its Hankel matrix as follows (Jensen et al. [98]):

$$\mathbf{A} = \begin{bmatrix} y_1 & y_2 & \cdots & y_n \\ y_2 & y_3 & \cdots & y_{n+1} \\ \vdots & \vdots & \ddots & \vdots \\ y_m & y_{m+1} & \cdots & y_N \end{bmatrix} \tag{4.22}$$

where parameter m=N−n+1 is usually adopted for determining the number of decomposed components in SVD in the way that m should be about three times greater than number of components N in the noise-affected signal (Di Monte and Arun [43]).

2. Signal decomposition and reconstruction.

Above-mentioned Hankel matrix **A** is then used within a SVD procedure, according to Eq. (4.17):

$$\mathbf{A} = \begin{bmatrix} \mathbf{u}_1 & \mathbf{u}_2 & \dots & \mathbf{u}_m \end{bmatrix} \begin{bmatrix} s_1 & 0 & \dots & 0 \\ 0 & s_2 & \dots & 0 \\ \vdots & \vdots & \ddots & \vdots \\ 0 & 0 & \dots & s_m \end{bmatrix} \begin{bmatrix} \mathbf{v}_1^T \\ \mathbf{v}_2^T \\ \vdots \\ \mathbf{v}_n^T \end{bmatrix} = \tag{4.23}$$

$$= \sum_{i=1}^{m} s_i \mathbf{u}_i \mathbf{v}_i^T = \sum_{i=1}^{m} \mathbf{A}_i$$

In this way, matrix **A** has been expressed as the superposition of m sub-matrices $\mathbf{A}_i = s_i \mathbf{u}_i \mathbf{v}_i^T$, each of them corresponding to a singular component y_i of the noise-corrupted signal. It is worth noting that, consequently, such a signal may be completely reconstructed by simply adding all decomposed singular components y_i (which may be obtained from sub-matrices $\mathbf{A}_i$ by applying the diagonal averaging method (Sanliturk and Cakar [180])), as displayed in the following relation:

$$\mathbf{y} = \sum_{i=1}^{m} y_i \tag{4.24}$$

3. Signal denoising.

The basic concept, according to the SVD approach, is based on the assumption that the core signal pattern is mainly embedded within singular components y_i with large singular values (Zhao and Ye [232], Zijian and Zhengrong [235]). Consequently, the main issue is now concerning how to appropriately select threshold ε in order to denoise the noise-corrupted signal, by preserving the singular components with the largest singular values s_1, ..., s_l , while lower components s_{l+1}, ..., s_L may be replaced by zeros, namely:

$$\widehat{\mathbf{A}} = \begin{bmatrix} \mathbf{u}_1 & \mathbf{u}_2 & \dots & \mathbf{u}_m \end{bmatrix} \begin{bmatrix} s_1 & 0 & \dots & 0 & \mathbf{0} \\ 0 & s_2 & \dots & 0 & \mathbf{0} \\ \vdots & \vdots & \ddots & \vdots & \vdots \\ 0 & 0 & \dots & s_l & \mathbf{0} \\ \mathbf{0} & \mathbf{0} & \dots & \mathbf{0} & \mathbf{0} \end{bmatrix} \begin{bmatrix} \mathbf{v}_1^T \\ \mathbf{v}_2^T \\ \vdots \\ \mathbf{v}_n^T \end{bmatrix} = \tag{4.25}$$

$$= \sum_{i=1}^{l} s_i \mathbf{u}_i \mathbf{v}_i^T = \sum_{i=1}^{l} \widehat{\mathbf{A}}_i$$

from which:

$$\widehat{\mathbf{x}} = \sum_{i=1}^{l} \widehat{x}_i \tag{4.26}$$

where $\hat{\mathbf{A}}$ and $\hat{\mathbf{x}}$ are the denoised matrix and signal, respectively.

4.3 Analysis procedure

4.3.1 Presentation of a selected benchmark structure

Within the current numerical investigation, a one-bay 10-DOF shear-type frame building, as sketched in Fig. 4.1, is considered as a benchmark dynamical system.

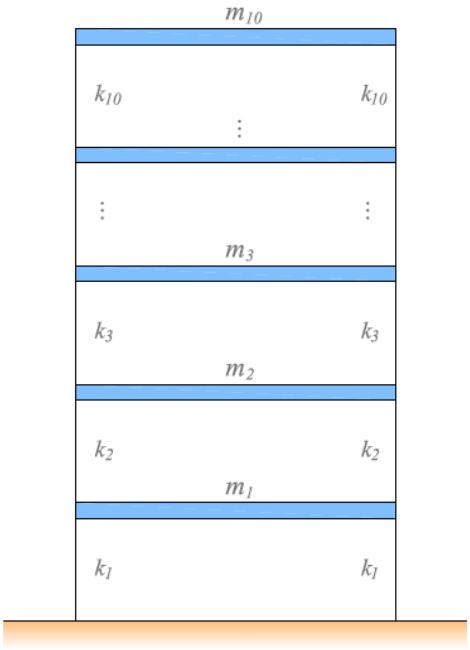

Figure 4.1: Schematic view of the analyzed one-bay 10-DOF shear-type frame building.

Such a selection appears rather reasonable because, although its characteristics may be well suitable for describing real civil engineering cases, even more complex ones, such a modelization may nevertheless allow for a rather easy analytical and numerical treatment of the present structural problem and for a convenient exploitation of the denoising techniques in this context.

To make the analysis as much realistic as possible, in the characterization of the structure, reasonable geometrical properties as well as reliable values of mass, stiffness and modal damping ratio (uncoupled modal damping is assumed), are considered. For the first floor, greater values of mass and stiffness are assumed, with respect to those of the upper floors. In particular, $m_1 = 100$ t and $k_1 = 2 \cdot 10^6$ kN/m for each bearing column (see Fig. 4.1), whereas $m_i = 80$ t and $k_i = 1.5 \cdot 10^6$ kN/m, with $i = 2, ..., 10$. Mass-normalized stiffness matrix $\mathbf{K}' = \mathbf{M}^{-1/2}\mathbf{K}\,\mathbf{M}^{-1/2}$ is used within the performed implementation in handling the solution of the structural eigenvalue problem. In addition, a modal damping ratio zi equal to 5%, namely a typical value concerning engineering structures, is considered, for all the modes. Through the proposed implementation, up to two dofs may simultaneously be monitored.

In particular, the present structural analysis context focuses on the monitoring of the first and last floor's dynamic acceleration responses of the benchmark structure represented in Fig. 4.1, as subjected to two different types of excitation input: an earthquake acceleration excitation, acting at the base of the building, and an ambient vibration force distribution, as a common white-noise time signal applied along the structure with a linear (triangular) variation (the signal magnitude increases from the bottom to the top of the building, from zero to a maximum value).

4.3.2 Synthetic generation of noise-corrupted response signals

Considering real signals of any nature and typology, it may be stated that signals without noise may not exist. In particular, during the phase of signal detection, extrinsic noise sources, i.e. cross-talk noise or environmental perturbations, and intrinsic noise sources, i.e. thermal noise, diffusion noise, white-noise or shot noise, constitute inevitable causes of disturbance, which tend to overlap onto the useful signal, altering its information content (Vasilescu [206]). Moreover, the impossibility to precisely identify the physical reason lying behind the noise appearance led to the conclusion that it cannot be considered as a deterministic process and, thus, it has to be modeled by means of statistical approaches. In particular, the noise process may be assimilated to a stationary stochastic process, whose characteristics do not change over time. Furthermore, it is characterized by a Gaussian distribution of amplitudes and mean value equal to zero, so that all its spectral components are uniformly distributed over the whole frequency spectrum. The fact that it indifferently affects every single frequency component over the whole length of the signal makes the Gaussian white-noise the most difficult kind of noise to be removed. Since the noise has its importance not in absolute terms but always in relation to the useful signal to which it overlaps, in order to express such an influence in percentage terms, the N/S ratio is again adopted. Solely for academic purposes, N/S ratios up to 50% will be investigated, in the forthcoming analysis, even though, in common sensor technology, N/S ratios greater than about 20% might already be considered as rather unrealistic.

In this section, the process of signal corruption is presented with reference to the two analyzed input types. The selected non-stationary input is the earthquake excitation that in 1986 struck Kalamata, the capital town of the Messinia prefecture of southern Peloponnese, Greece. The seismic record is shown in Fig. 4.2, in both Time and Frequency Domains.

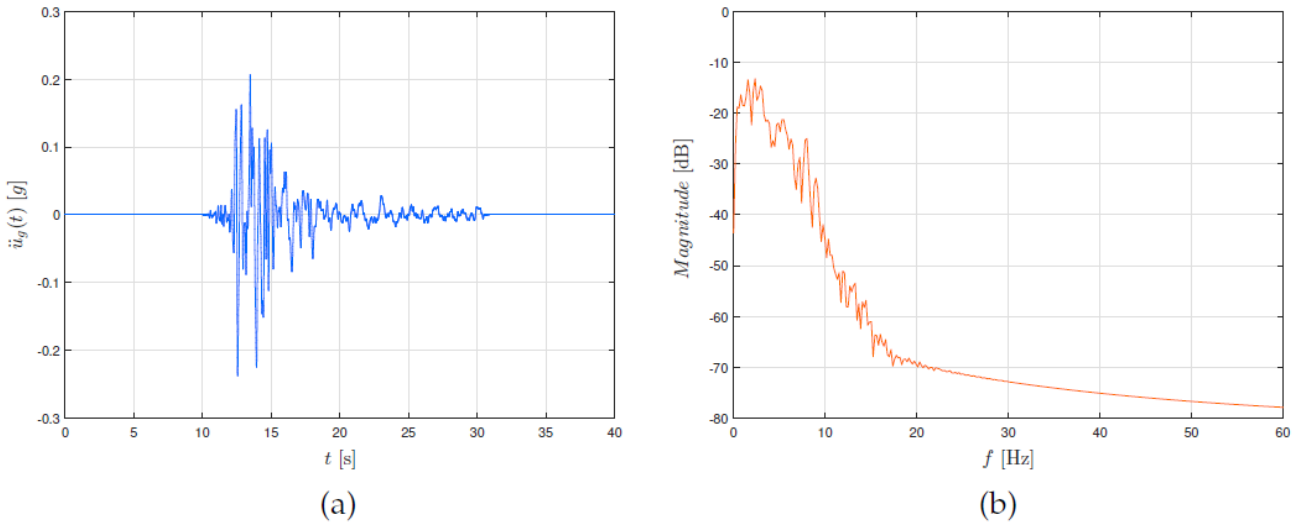

Figure 4.2: Kalamata (1986) seismic input acting at the base on the benchmark structure: (a) Time Domain; (b) Frequency Domain.

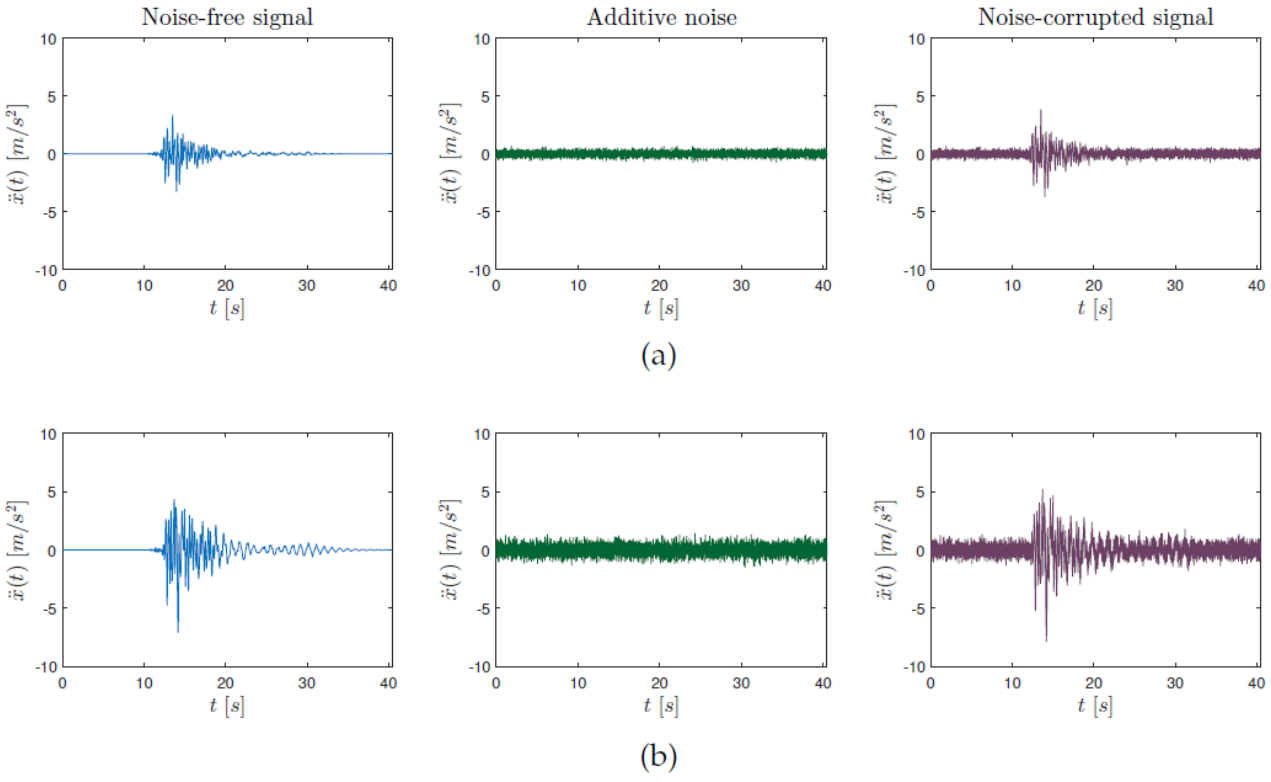

Figure 4.3: Dynamic acceleration response signals of the benchmark structure under Kalamata earthquake input and noise addition process (25% N/S ratio); (a) 1st floor; (b) 10th floor.

High spectral accelerations characterized the records, responsible for the partial or total collapse of several reinforced concrete buildings. Peak Ground Acceleration (PGA) of 0.24 g, magnitude of M = 5.9 and focal depth of 22 km were recorded. The main shock's epicenter (37.07° N, 22.18° E) was very near Kalamata, and many aftershocks followed, causing extensive damage in most parts of the ancient town, as well as in some nearby villages (Lyon-Caen et al. [134]).

Such a seismic excitation has been assumed acting at the base of the ten-story shear-type frame building represented in Fig. 4.1, and the structural response determined by a numerical integration through a dynamic direct analysis based on Newmark's integration method. In particular, numerically determined acceleration response signals related to the first and tenth floor have been recorded. Results are depicted in following Fig. 4.3, as well as with the process of generation of noisy data, obtained from the clean ones by adding different white Gaussian noise levels (in the figure, the case of 25% N/S ratio is reported).

Ambient vibration is then investigated. Also known as "microtremor", it represents the stationary excitation to which a structure is subjected to during its regular operational conditions (Farrar and James III [62]). It is associated to environmental loads, such as wind or, dealing with bridges, traffic load and wave motion. Ambient vibration may be considered as a random type of signal, which affects a broad frequency range and, despite being characterized by limited amplitudes, it is usually enough to excite several modes of structural vibration. Within the present analysis, a very light ambient vibration input force of around 3 kN is considered acting at the top-floor of the reference structure, whose characterization in Time and Frequency Domains may be appreciated in Fig. 4.4.

Similarly to the earthquake input case, also the dynamic response of the benchmark structural system subjected to ambient vibration input has been inspected in terms of acceleration for the first and last floors. The outcomes and the process of noise corruption of the response signals are shown in Fig. 4.5, where a 25% N/S ratio is still considered in affecting the source data.

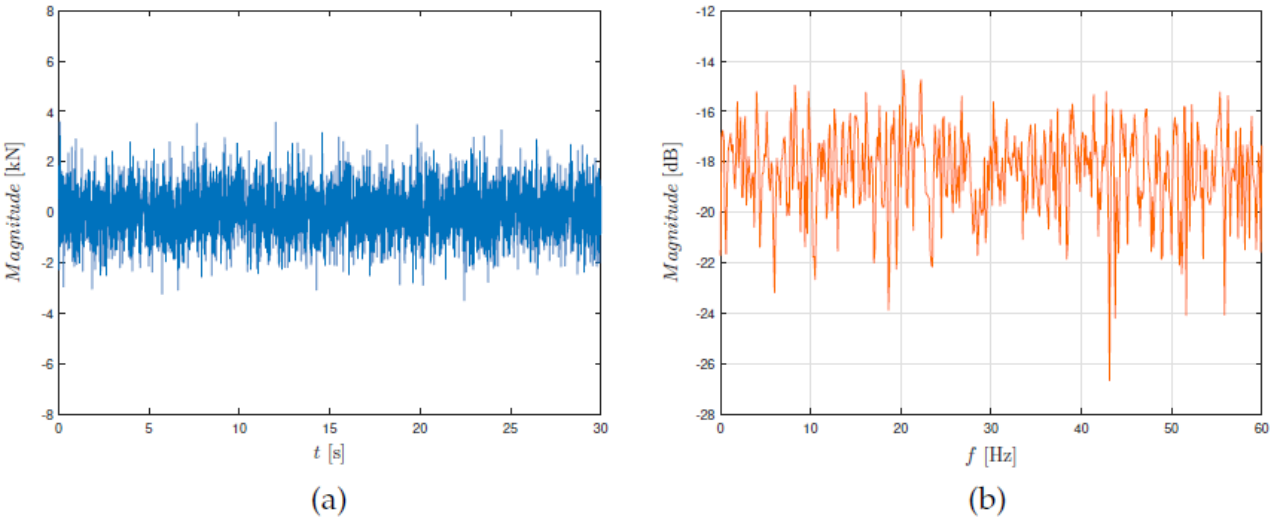

Figure 4.4: Ambient vibration input acting on the last floor of the benchmark structure: (a) Time Domain; (b) Frequency Domain.

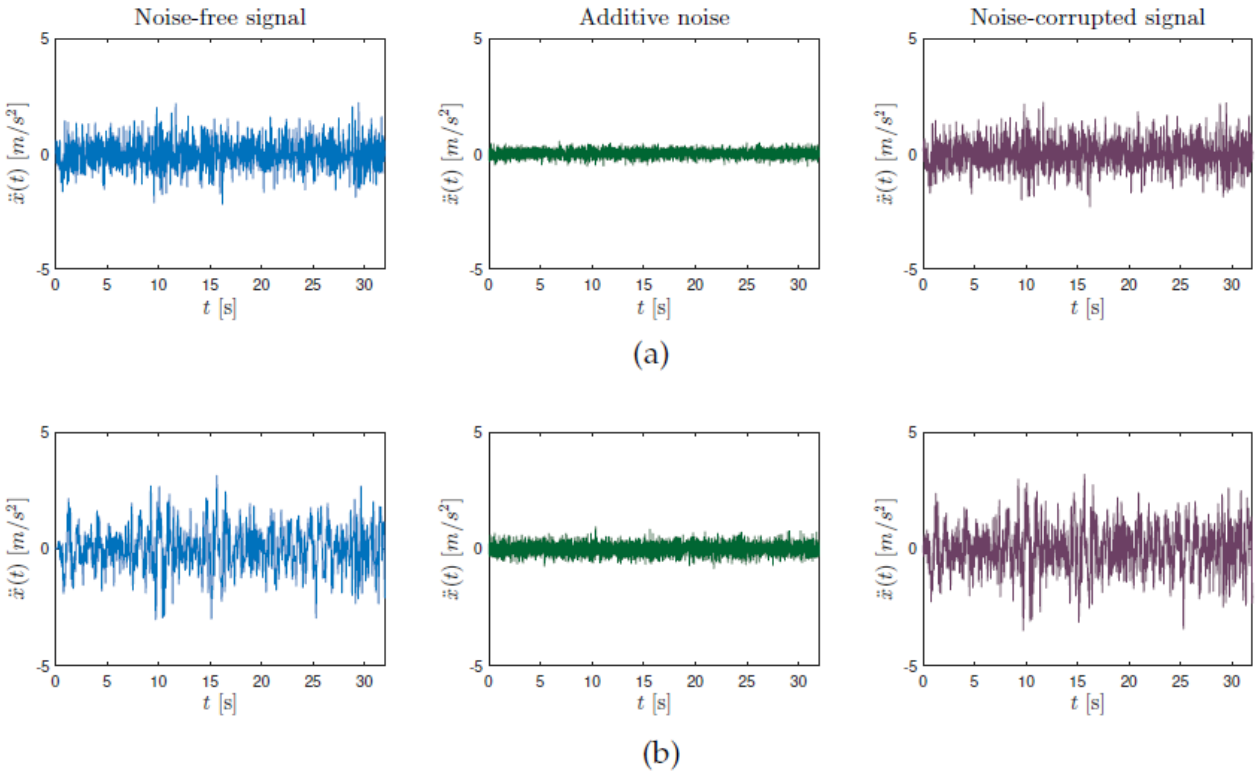

Figure 4.5: Dynamic acceleration response signals of the benchmark structure under ambient vibration input and noise addition process (25% N/S ratio); (a) 1st floor; (b) 10th floor.

4.3.3 Denoising application and results

Artificially generated noise-corrupted acceleration response signals ẍ(t), reported in previous Fig. 4.3 and Fig. 4.5, are now processed within a denoising-based implementation involving the DWT and SVD approaches, aiming at evaluating their performances in the clarification of noisy response signals, in both Time and Frequency Domains. All the analyses have been performed within a self-implemented numerical computing environment (MATLAB).

4.3.3.1 DWT-based denoising application

As previously stated, since the DWT-based denoising method constitutes a non-parametric signal analysis tool, it necessarily requires a preliminary phase of calibration of some pre-defined parameters, namely the mother wavelet typology, the thresholding rule, the type of thresholding and the wavelet decomposition level. In this section, in order to prove the effectiveness of such a denoising method, and to determine the optimal calibration to be set for the subsequent analysis, several tests in which the wavelet assessment is based on the PrmsD between the original (noise-free) signal and the denoised signal, have been performed. In particular, optimal wavelet parameters are selected according to a criterion of minimization of such a PrmsD index.

In order to select the most appropriate combination of mother wavelet and thresholding rule for the denoising of earthquake and ambient vibration response signals, at first, the N/S ratio is maintained constant and equal to 10%, as well as the wavelet decomposition level, set to 3.

The denoising performance is assessed for several mother wavelets of a diverse nature, i.e. *Symlet, Coiflet, Daubechies, Biorthogonal, Reverse Biorthogonal* and *Discrete Meyer*, combined with the previously treated four main thresholding rules, belonging to the Donoho-Johnston family, i.e. *Heuristic SURE, Sqtwolog, Minimax* and *Rigorous SURE*. Furthermore, for each mother wavelet, different numbers of oscillations have been considered (indicated with a number next to the wavelet mother name).

Since the performed analysis has not revealed substantial differences in the processing of the 1st- and 10th-floor acceleration responses, in the rest of the chapter, only results concerning the top-floor acceleration signal are reported, and commented on. The PrmsD index for the explored combinations of mother wavelets and thresholding rules are summarized in Table 4.1.

It is interesting to observe how, while for the seismic excitation the results do not seem to be significantly affected by the number of oscillations characterizing the considered mother wavelet, for the ambient excitation signal, instead, a considerable dispersion of the outcomes occurs.

Moreover, from the performed analysis it can be affirmed that, assuming seismic response signals, *Smylet* having two oscillations in its mother wavelet combined with a *Heursure* thresholding rule lead to the lowest value of PrmsD index (see Table 4.1), whereas, considering ambient vibration response signals, the best solution seems to be produced by the combination of *Coiflet,* having four oscillations in its mother wavelet, with a *Minimax* thresholding rule (see Table 4.1). These settings will then be kept constant throughout the whole forthcoming investigation.

Once the optimal combination of mother wavelet and thresholding rule are established, the decomposition level that minimizes the PrmsD index may be obtained, for both soft and hard thresholding. Analysis results are presented in Table 4.2.

From the outcomes, dealing with seismic response signals with a 10% N/S ratio, it is suggested to adopt a hard thresholding at level 2, whereas, for ambient vibration response signals affected by the same N/S ratio, the optimal setting is given by a hard thresholding at level 3. In light of the derived results, it clearly emerges how the choice of the mother wavelet type as well as the selection of the decomposition level, play a crucial role for the success of the DWT-based denoising approach. Such a mother wavelet should be chosen such that it shall be able to well characterize the processed signal, and this may be established according to the correlation between the wavelet and the signal itself.

Mother wavelet	Thresholding rule							
	Heursure		Sqtwolog		Minimax		Rigrsure	
	seismic	ambient	seismic	ambient	seismic	ambient	seismic	ambient
sym2	0.22	6.27	0.84	7.22	1.97	7.71	0.69	7.57
sym3	0.42	5.33	0.90	6.79	2.11	7.12	0.91	7.31
sym4	0.47	5.05	0.90	6.16	2.18	6.70	0.96	6.86
sym5	0.46	5.60	0.86	5.93	2.19	6.26	0.99	5.80
sym6	0.47	5.05	0.92	5.92	2.19	6.13	0.92	6.88
sym7	0.46	5.34	0.85	5.31	2.20	6.01	1.00	5.53
sym8	0.43	5.49	0.55	7.46	2.21	5.74	0.92	6.18
coif1	1.24	5.17	0.67	8.20	0.29	7.56	1.92	6.77
coif2	1.43	4.90	0.82	5.89	0.32	5.17	2.12	5.63
coif3	1.50	4.89	0.93	6.25	0.39	5.66	2.14	4.94
coif4	1.46	4.93	0.85	5.29	0.35	4.74	2.15	4.92
coif5	1.49	4.92	0.94	5.89	0.39	5.30	2.14	4.69
db1	0.87	9.66	1.45	9.35	0.58	9.82	0.52	9.97
db2	0.55	7.47	0.29	7.15	1.28	7.06	1.02	9.08
db3	0.84	7.22	0.52	7.65	1.41	6.75	1.21	7.59
db4	0.82	5.94	0.50	8.46	1.43	5.69	1.24	7.41
db5	0.93	6.55	0.56	7.07	1.49	6.08	1.27	7.97
db6	0.84	5.57	0.51	7.52	1.44	5.40	1.23	6.93
db7	0.94	6.21	0.59	7.11	1.51	5.73	1.27	7.71
db8	0.85	5.41	0.50	6.91	1.44	5.37	1.24	6.67
db9	0.94	5.94	0.58	7.28	1.51	5.42	1.28	7.45
db10	0.86	5.44	0.51	6.40	1.45	5.44	1.24	6.68
bior1.1	0.87	8.65	0.92	8.73	0.50	8.80	0.91	8.99
bior2.4	0.84	7.45	0.90	6.35	1.36	7.93	0.98	6.14
bior3.5	0.98	6.53	1.19	5.28	1.50	7.56	1.08	6.27
bior6.8	0.89	5.70	1.06	4.95	1.42	6.59	0.97	5.30
rbio1.1	0.87	9.66	0.32	9.80	0.45	9.82	0.28	9.41
rbio2.4	0.88	6.29	1.47	5.44	1.46	7.25	1.61	5.14
rbio3.5	1.18	4.97	1.74	5.12	1.75	4.87	1.86	4.91
rbio6.8	0.90	5.51	1.52	5.46	1.52	6.80	1.62	5.78
dmey	0.94	5.37	0.27	6.44	1.51	5.50	0.55	5.01

Table 4.1: PrmsD index [%] between original (noise-free) signal and denoised signal for different mother wavelets and thresholding rules (10% N/S ratio, decomposition level 3).

Moreover, also the setting of the decomposition level has to be carefully decided. In principle, if the noise is hardly noticeable, more levels of decomposition might be needed, in order to reconstruct even the finest details of the signal; consequently, in some cases, it may be useful to work with multiple decomposition levels. Since the optimal decomposition level of the wavelet may be different, depending on the level of noise affecting the data, within the present analysis, the optimal decomposition level will be each time re-adjusted, according to the considered N/S ratio, in order to achieve the best denoising estimates.

	Decomposition level	Thresholding			
		soft		hard	
		seismic	ambient	seismic	ambient
PrmsD [%]	1	0.33	6.43	0.33	6.43
	2	0.20	5.41	0.13	5.30
	3	0.22	4.74	0.21	4.58
	4	1.38	14.41	0.96	4.98
	5	4.48	28.20	1.06	7.03
	6	7.32	45.72	1.17	7.77
	7	7.95	51.21	1.17	8.75
	8	8.41	52.09	1.18	9.10
	9	8.72	52.62	1.23	9.20
	10	8.70	52.85	1.23	9.32

Table 4.2: PrmsD index [%] between original (noise-free) signal and denoised signal for different decomposition levels and thresholding types (10% N/S ratio).

Fig. 4.6 shows the denoised seismic response signal, in comparison with the noise-corrupted one, assuming now a 25% N/S ratio. The DWT-based denoised technique has been applied in its optimal configuration (i.e. Smylet2 + Heursure, adopting a hard thresholding at level 2) and the benefits of the denoising process are tangible, as it may be seen from the last graph in such a figure, in which the difference between the denoised signal and the clean (numerically determined) signal is represented. It may be stated that, at least in dealing with simulated seismic response signals, through the DWT-based denoisng approach, the noise is largely successfully removed and the original data set can almost completely be reconstructed.

The same considerations cannot be drawn for the processing of ambient vibration response signals, as represented in Fig. 4.7. In fact, although the optimal calibration has been set for dealing with this specific kind of signal (i.e. Coiflet4 + Minimax, adopting a hard thresholding at level 3), the error in terms of difference between the original clean signal and the denoised one is not negligible.

Already at this stage, the discrepancy in the displayed results shows how the effectiveness of the DWT-based denoising technique strongly depends on the nature of the source signal to be processed. In fact, if the denoising performed on non-stationary response signals can be very effective, viceversa, the use of DWT for denoising purposes on stationary response signals displays visible limitations.

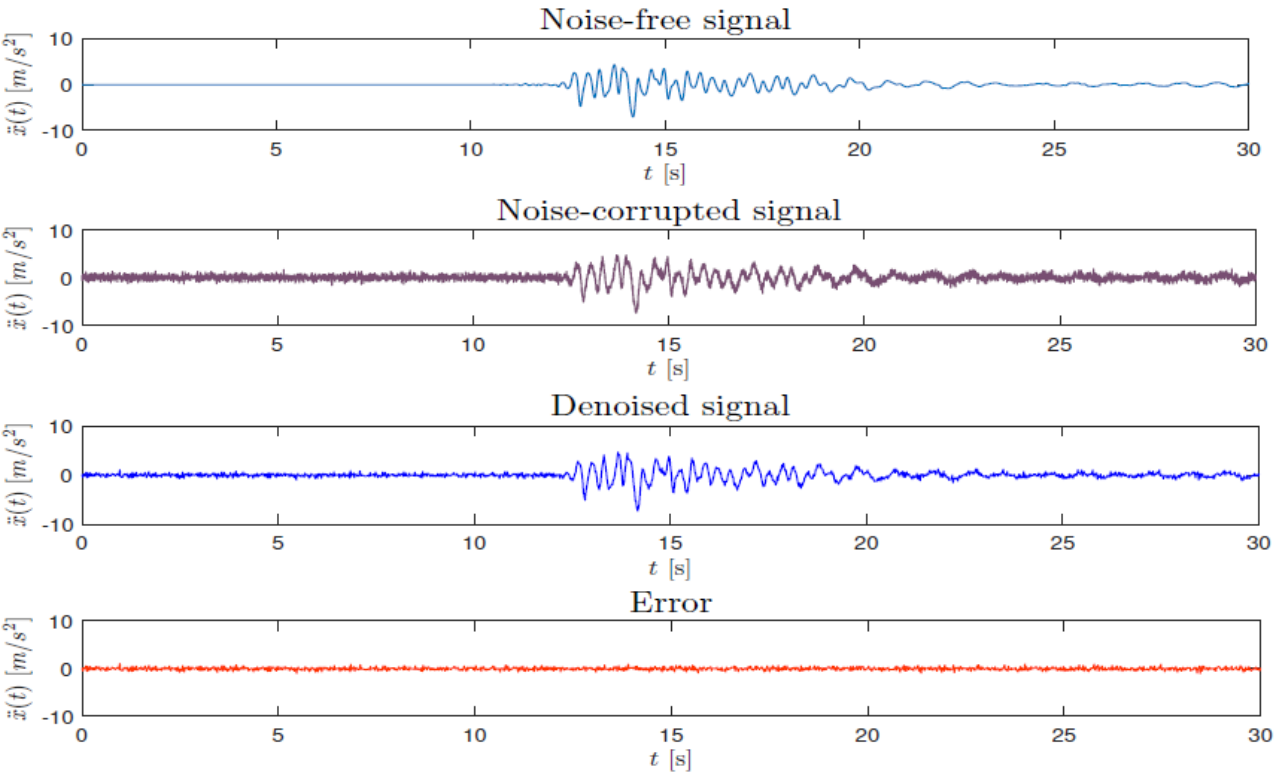

Figure 4.6: DWT-based denoising of noise-corrupted ẍ(t) under seismic input (25% N/S ratio).

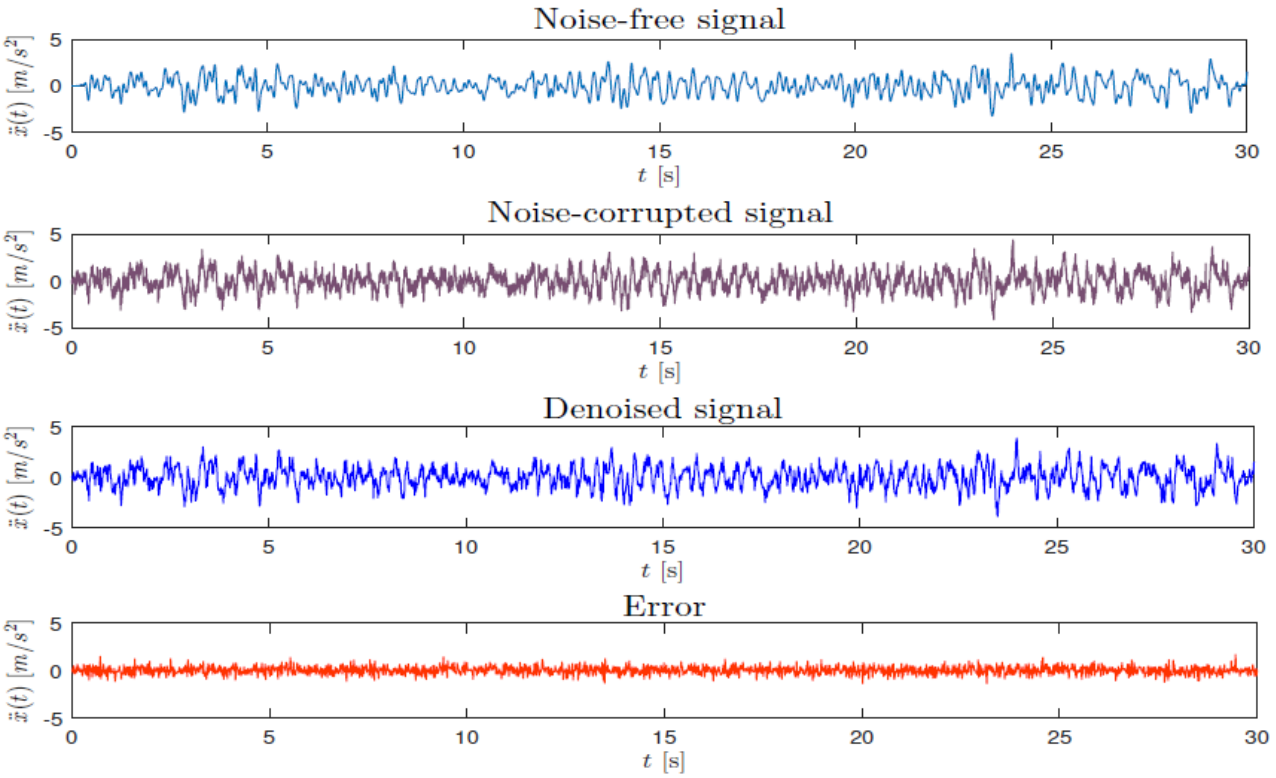

Figure 4.7: DWT-based denoising of noise-corrupted ẍ(t) under ambient vibration (25% N/S ratio).

4.3.3.2 SVD-based denoising application

The SVD application in the digital signal processing field for noise reduction is based on the calculation of the singular values of a characteristic matrix **A** representing noisy signal **y**. Since it has been shown that mainly the smaller singular values of **A** are related to the noisy part of the signal, removing those lower than a selected threshold ε, a new matrix $\hat{\mathbf{A}}$ (of a lower rank) containing the estimated filtered signal purified by noise $\hat{\mathbf{x}}$, may be obtained. As previously stated, it clearly emerges how, at this stage, the critical point is represented by the choice of an appropriate threshold ε. To this end, a similar criterion as used in the DWT-based denoising approach has been adopted, through which it has been proven that the lowest PrmsD index between noise-free and denoised signal may be obtained for $\varepsilon = 10^1$, in the present setting.

By applying the SVD-based denoising procedure to the seismic acceleration response signal affected by a 25% N/S ratio, it has been possible to remove most of the initially present noise, obtaining a very reliable purified signal, as represented in Fig. 4.8. Results seem to be in accordance with the previously treated DWT-based denoising and, in this sense, the SVD-based approach might constitute a valid alternative in clarification of noise-corrupted non-stationary signals.

Reliable outcomes derive even from the SVD-based denoising, performed on a stationary signal, namely the top-floor acceleration response of the studied benchmark building subjected to ambient vibration input, as it may be appreciated from Fig. 4.9. In fact, in this case, differently from what it has been obtained by applying the DWT approach (see Fig. 4.7), the error between the clean (noise-free) signal and the denoised one can be reduced to a value very close to zero, and an accurate estimate of the truthful response signal may be provided.

In conclusion, this SVD-based denosing technique appears to be more robust with respect to the previous treated DWT-based denoising approach, since its outcomes seem to be significantly less affected by the nature of the noise-corrupted signal to be processed, thus leading to a more reliable solution.

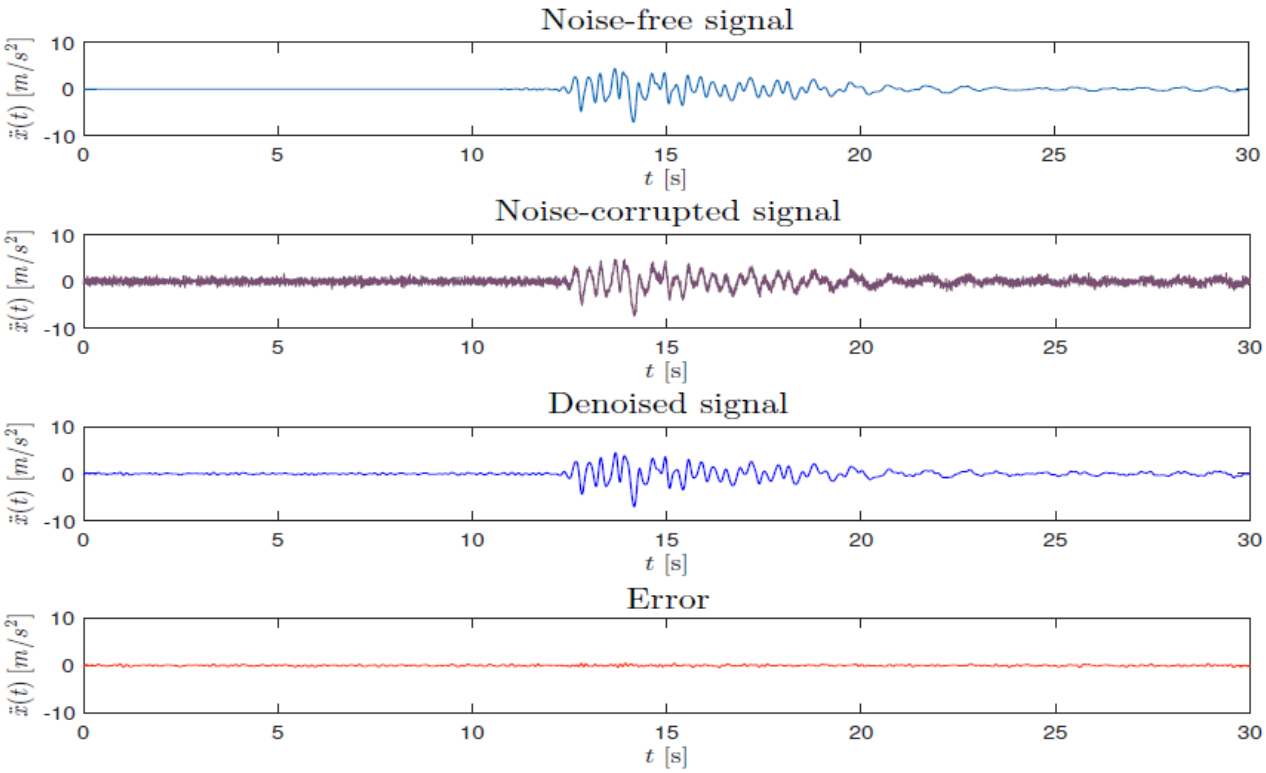

Figure 4.8: SVD-based denoising of noise-corrupted ẍ(t) under seismic input (25% N/S ratio).

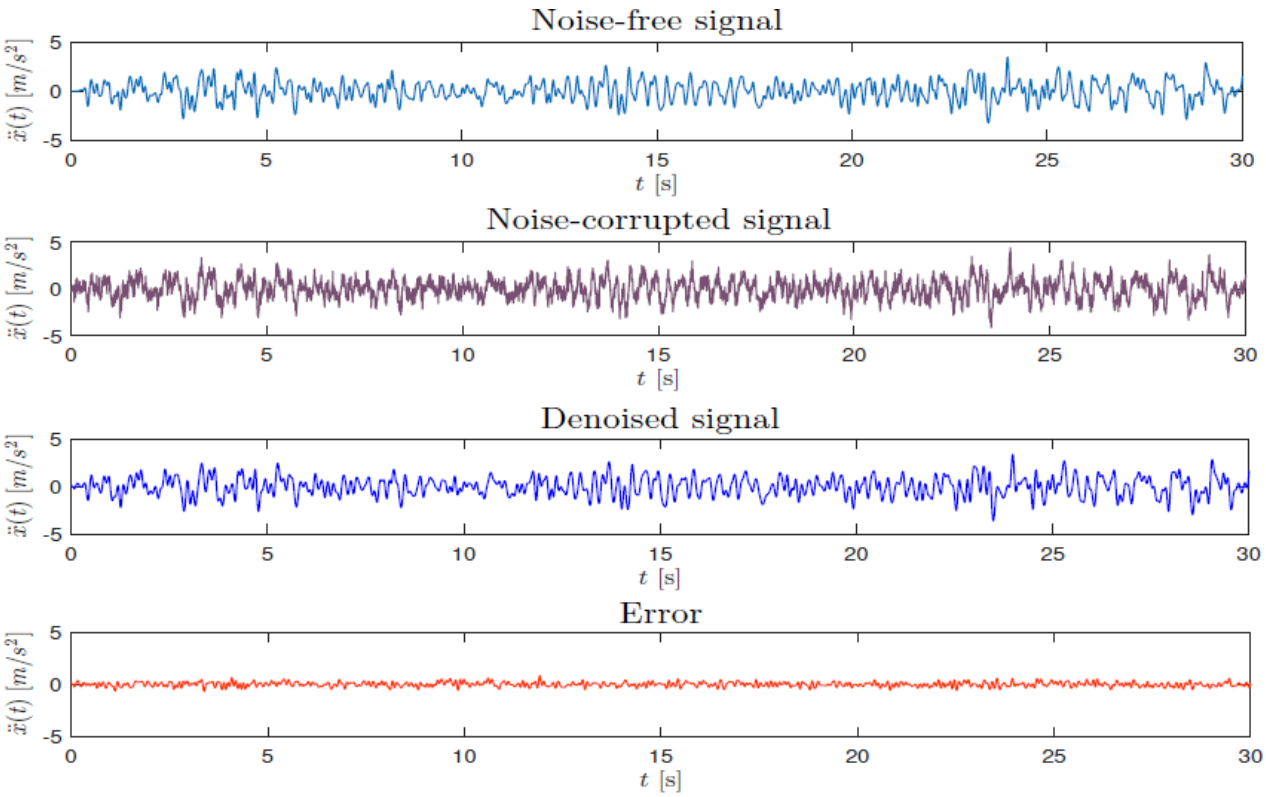

Figure 4.9: SVD-based denoising of noise-corrupted ẍ(t) under ambient vibration (25% N/S ratio).

4.3.4 Denoising technique comparison

In this section, a performance evaluation of the two inspected denoising approaches on synthetic signals is proposed. In particular, for a global understanding of the strengths and weaknesses of such inspected techniques, the evaluation of their performances is conducted in parallel, in both the Time Domain and the Frequency Domain.

4.3.4.1 Confrontation in the Time Domain

An analysis in the Time Domain is first presented. Here, the effectiveness of DWT- and SVD-based denoising techniques is assessed based on the PrmsD index between the denoised signal and the original (numerically determined) one, for increasing N/S ratios of added noise. Within the analysis, the two different acceleration response signals (seismic and ambient vibration) are assumed to be contaminated by N/S ratios up to 50%. Results are reported in both tabular (Table 4.3) and graphical form (Fig. 4.10).

N/S ratio [%]			**5**	**10**	**15**	**20**	**25**	**30**	**35**	**40**	**45**	**50**
PrmsD [%]	Seismic	DWT	0.06	0.13	0.18	0.20	0.88	1.18	1.23	1.39	2.11	2.69
		SVD	0.23	0.34	0.46	0.55	0.44	0.69	0.59	0.55	0.60	0.71
	Ambient	DWT	0.59	1.25	2.64	3.80	4.58	4.93	5.23	5.90	6.21	6.82
		SVD	0.15	0.07	0.21	0.39	0.57	0.53	0.66	1.19	2.33	2.88

Table 4.3: PrmsD [%] index between original and denoised signal, for different signal typologies and N/S ratios: DWT vs. SVD.

As it may be appreciated from Fig. 4.10a, in which the errors (in terms of PrmsD) of the two mentioned denoising techniques are compared, for the case of a seismic acceleration response signal, the DWT-based approach seems to be more performing, dealing with N/S ratios approximately lower than 20%, i.e. for typical values that may be encountered in real applications. However, for higher N/S ratios, the denoising based on SVD appears to be more robust, since it is not so affected by the level of noise considered on the data, and the PrmsD index remains at around 0.6%. Anyway, especially for limited N/S ratios, both the examined approaches may be considered as rather competitive in clarifying signals displaying a nonstationary nature.

The same cannot be affirmed for the case of ambient vibration response signals, as represented in Fig. 4.10b. In fact, only the SVD-based approach seems to be able to effectively reduce the amount of noise on stationary signals, in particular for N/S ratios between 5% and 15%. This makes this technique very useful in practical cases, as it may lead to a very accurate reconstruction of the truthful

signal, differently from the DWT-based approach, whose estimates present sensible errors and, consequently, they cannot be considered as reliable enough.

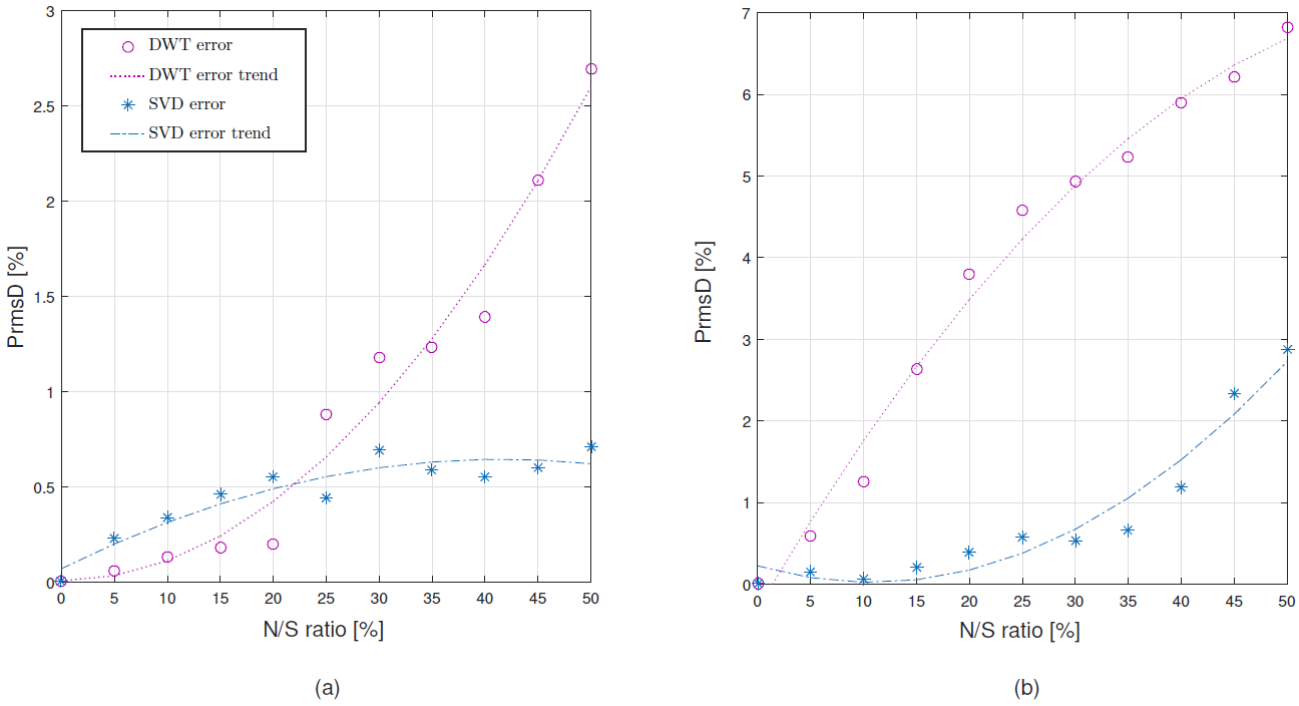

Figure 4.10: Effectiveness evaluation of DWT- and SVD-based denoising techniques for increasing N/S ratios and different signal typologies: (a) earthquake excitation; (b) ambient vibration. Notice that scales on the PrmsD axes are different, almost twice for (b). Indicated trends come from a polynomial fit of a degree 2.

Concerning the results and the benefits that the two investigated denoising techniques have brought about on the signal clarification, it is appropriate to investigate this cleaning effect even in terms of an alteration of the signal main peak value. This might be relevant, especially for the non-stationary response signals, where the acceleration peak may play a key role in the design or assessment phases. The acceleration peak values according to the two explored denoising techniques, as well as their percentage alteration, with respect to the noise-affected peak (Δ_{na}) and with respect to the clean numerically determined peak value (Δ_{nd}), are computed for each denoising approach, and summarized in Table 4.4. Both the analyzed signal typologies, i.e. non-stationary signal and stationary signal, are considered to be affected by increasing levels of Gaussian white-noise.

NON-STATIONARY (SEISMIC) SIGNAL							
		DWT denoising			SVD denoising		
N/S Ratio [%]	Signal peak $[m/s^2]$	peak $[m/s^2]$	Δ_{na} [%]	Δ_{nd} [%]	peak $[m/s^2]$	Δ_{na} [%]	Δ_{nd} [%]
0	*7.05*	*7.05*	*0.00*	*0.00*	*7.07*	*+0.28*	*0.28*
5	7.18	7.09	−1.30	0.57	7.13	−0.69	1.13
10	7.41	7.15	−3.51	1.42	7.20	−2.83	2.13
15	7.76	7.17	−7.60	1.70	7.19	−7.34	1.99
20	8.01	7.22	−9.86	2.41	7.30	−8.86	3.55
25	8.22	7.26	−11.68	2.97	7.37	−10.30	4.53
30	8.37	7.30	−12.78	3.55	7.45	−10.99	5.67
35	8.61	7.39	−14.17	4.82	7.60	−11.73	7.80
40	8.90	7.44	−16.40	5.53	7.67	−13.82	8.79
45	9.06	7.58	−16.33	7.52	7.80	−13.91	10.64
50	9.20	7.64	−16.95	8.37	7.88	−14.35	11.77
STATIONARY (white-noise) SIGNAL							
		DWT denoising			SVD denoising		
N/S Ratio [%]	Signal peak $[m/s^2]$	peak $[m/s^2]$	Δ_{na} [%]	Δ_{nd} [%]	peak $[m/s^2]$	Δ_{na} [%]	Δ_{nd} [%]
0	*3.48*	*3.46*	*−0.57*	*0.57*	*3.45*	*−0.86*	*0.86*
5	3.58	3.53	−1.40	1.43	3.50	−2.23	0.57
10	3.80	3.66	−3.68	5.17	3.57	−6.05	2.59
15	3.99	3.68	−7.77	5.75	3.71	−7.01	6.61
20	4.36	3.85	−10.49	10.63	3.80	−12.84	9.20
25	4.75	3.91	−17.68	12.36	3.77	−20.63	8.34
30	4.90	4.00	−18.37	14.94	3.85	−21.42	10.63
35	5.16	4.12	−20.16	18.39	3.95	−23.45	13.51
40	5.31	4.25	−19.96	22.13	4.08	−23.16	17.24
45	5.59	4.31	−22.90	23.85	4.13	−26.12	18.68
50	5.83	4.47	−23.33	28.45	4.27	−26.76	22.70

Table 4.4: Peak acceleration values of the DWT and SVD denoised signals, and their variation with respect to the noise-affected signal peak (Δ_{na}) and to the numerically determined signal peak (Δ_{nd}), for different typologies of signals (i.e. non-stationary (seismic) signal and stationary (white-noise) signal) and N/S ratios.

From the obtained results, concerning the effect that the denoising application displays on the main peak acceleration value of the processed signals, the following considerations may be drawn:

- The denoising process always leads to a peak reduction; this evident feature, may be interpreted by the fact that the artificial noise, applied onto the signals, acts in an additive sense. Thus, the resulting peak reduction, once the signal is cleaned.
- Considering the non-stationary (seismic) response signals, in particular, it may be stated that the application of the SVD-based denoising seems to be leading to a flattening effect on the main signal peak, which results to be slightly less evident than that obtained by applying the DWT-based denoising, as it may be appreciated by comparing the values of Δ_{na} obtained for the two analyzed signal typologies (Table 4.4).
- About the ambient vibration signal, it is generally associated to greater percentage variation values Δ_{nd}; however, this main peak analysis is more pertinent to non-stationary signals, for which Δ_{nd} presents low values, at least for common N/S ratios. In fact, in addition to having a greater practical relevance for vibration assessment purposes, the analysis conducted on non-stationary response signals turns out to be more significant than that performed on stationary signals, since the main acceleration peak clearly emerges and it is immediate to be detected, configuring itself as a characteristic feature describing this kind of signal.

4.3.4.2 Confrontation in the Frequency Domain

In order to inspect whether through the application of the studied denoising techniques it would be possible to even preserve the frequency content of the original (noise-free) response signal, a further analysis is performed in the Frequency Domain. Welch's method (Otis [146]) has been implemented, and the signal response spectrum has been obtained by decomposing the original time series data into possibly overlapping segments (weighted sinusoids), computing a modified periodogram of each segment, and averaging the Power Spectral Density (PSD) estimates.

The so-obtained response spectra of the processed response signals are depicted in Figs. 4.11–4.14. In particular, for both the analyzed denoising approaches, a comparison between the PSD of the original (noise-free) signal and the PSD of the denoised one, is shown. Two specific and significant noise levels are assumed on the clean signal, namely a 10% N/S ratio, since it may be considered as well representative of the amount of noise that may generally affect low-cost sensor instrumentations, and a 25% N/S ratio, i.e. the same noise level to which the previous Time Domain plots referred to.

Figs. 4.11 and 4.13 concern the earthquake response signal. The frequency spectrum of the original signal results well approximated by the spectrum of the purified signal, obtained through the SVD approach application (Figs. 4.11b and 4.13b). Even in the Frequency Domain, the SVD denoising

approach provides better results with respect to the DWT approach, especially within the frequency band after 10 Hz, referring to the 10% N/S ratio case (see Fig. 4.11a), or within the frequency band between 10 and 20 Hz, considering the 25% N/S ratio case (see Fig. 4.13a). However, the first peaks, corresponding to the natural frequencies of the first modes of vibration of the benchmark structural system, may clearly be identified in both cases.

The outcomes of a similar analysis procedure performed on ambient vibration response signals are instead represented in Figs. 4.12 and 4.14. In this case, the response spectrum of the original (noise-free) signal already does not appear to be as pure as the previous one. Moreover, the denoising procedure does not allow to satisfactorily recover it, especially referring to the DWT-based approach, which may also lead to the appearance of relevant peaks in the sub-band frequency region (see in particular Fig. 4.14a), i.e. the frequency band where the noise most affects the signal, which do not exist in the clean signal, and that can be ascribed to the effect of noise. In fact, within such a range of frequencies, the reconstructed spectrum results much more consistent with the spectrum of the noise-corrupted signal than with the clean one. Again, better results derive from the SVD-based approach (see Figs. 4.12b and 4.14b); however, also concerning this denoising technique, at least in this preliminary recognition phase, it is advisable not to consider as reliable the signal frequency content approximately between 10 and 15 Hz; curiously, a similar frequency band where it has been shown also the inefficiency of DWT-based denoising, concerning non-stationary signals affected by a 25% N/S ratio.

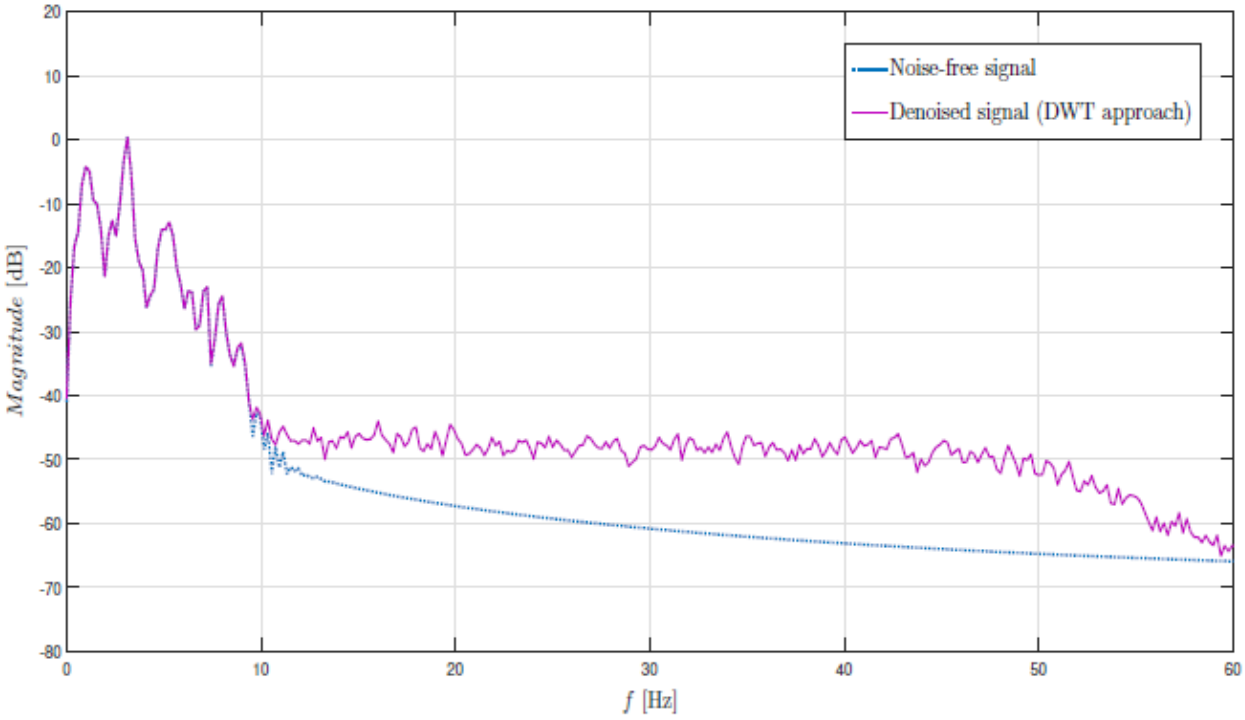

(a)

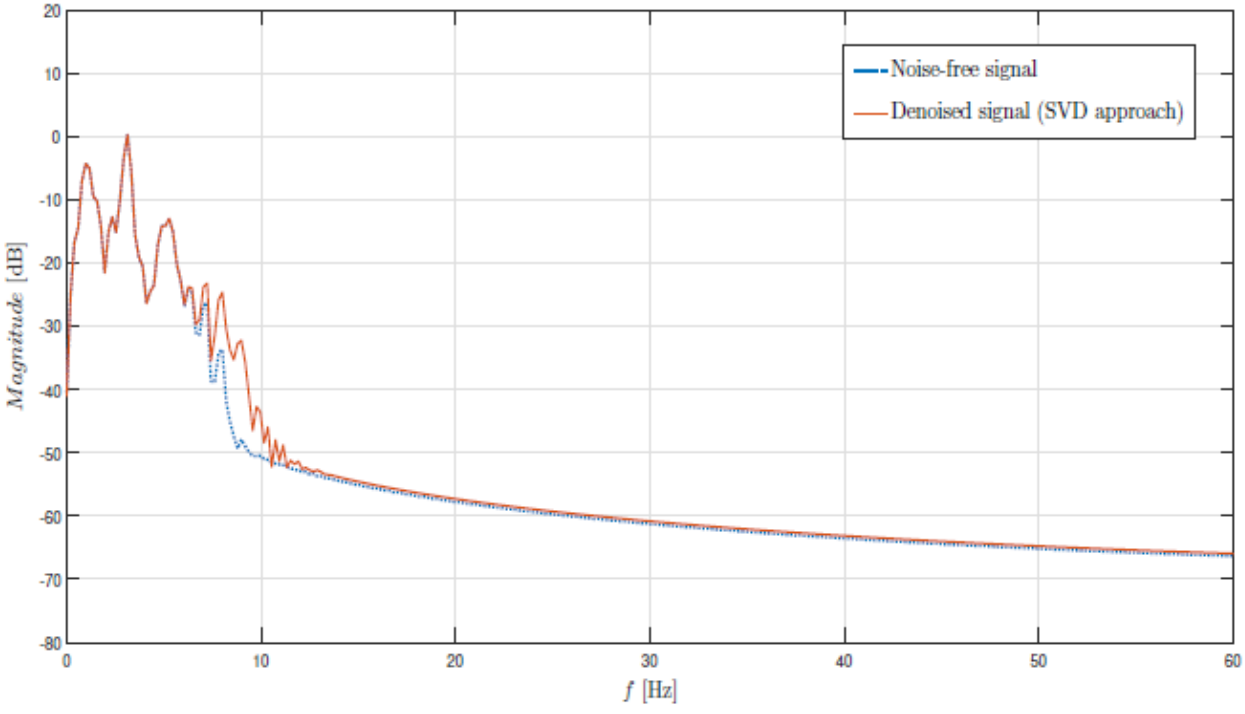

(b)

Figure 4.11: Seismic response signal in the frequency domain (10% N/S ratio). PSD of the noise-free signal vs. PSD of the denoised signal, for the two analyzed denoising techniques: (a) DWT-based denoising; (b) SVD-based denoising.

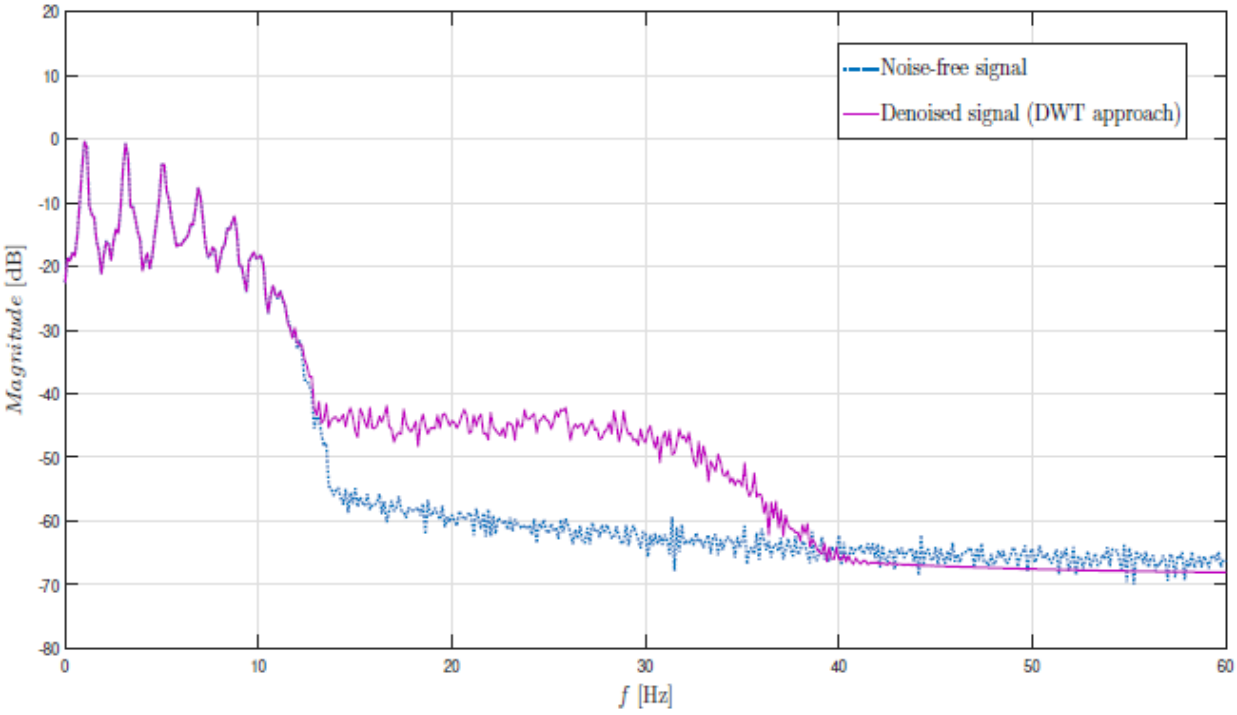

(a)

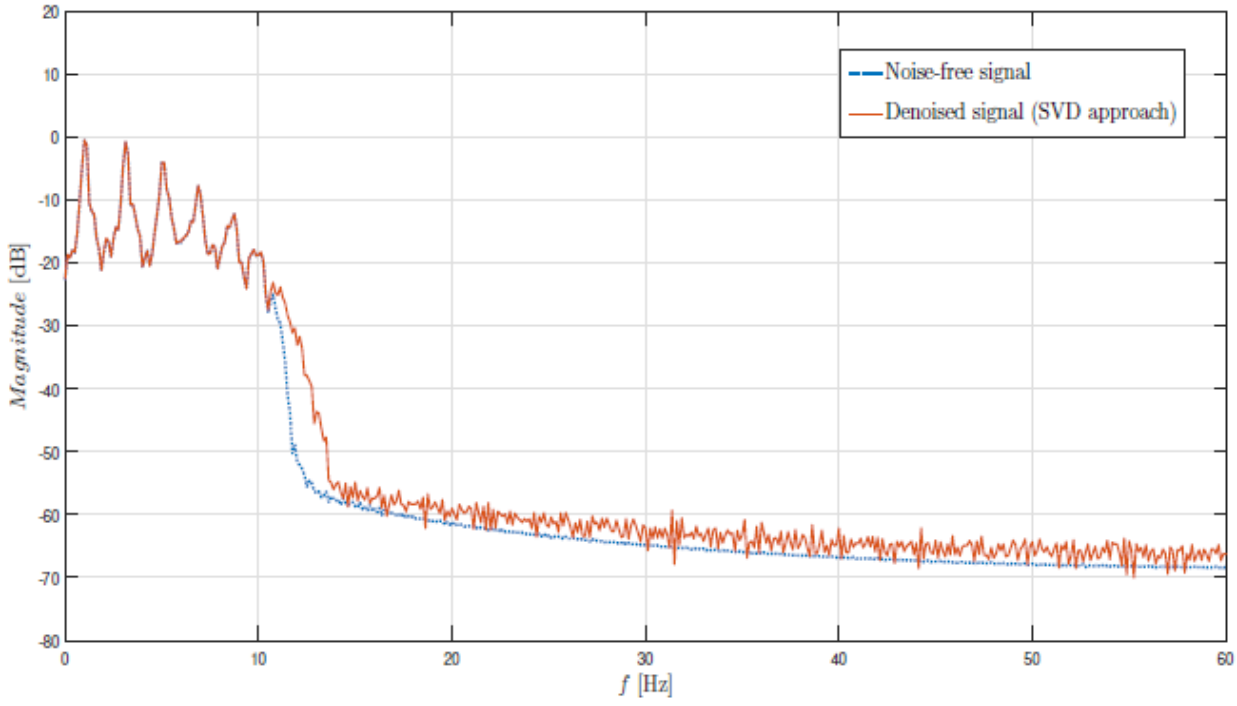

(b)

Figure 4.12: Ambient vibration response signal in the frequency domain (10% N/S ratio). PSD of the noise-free signal vs. PSD of the denoised signal, for the two analyzed denoising techniques: (a) DWT-based denoising; (b) SVD-based denoising.

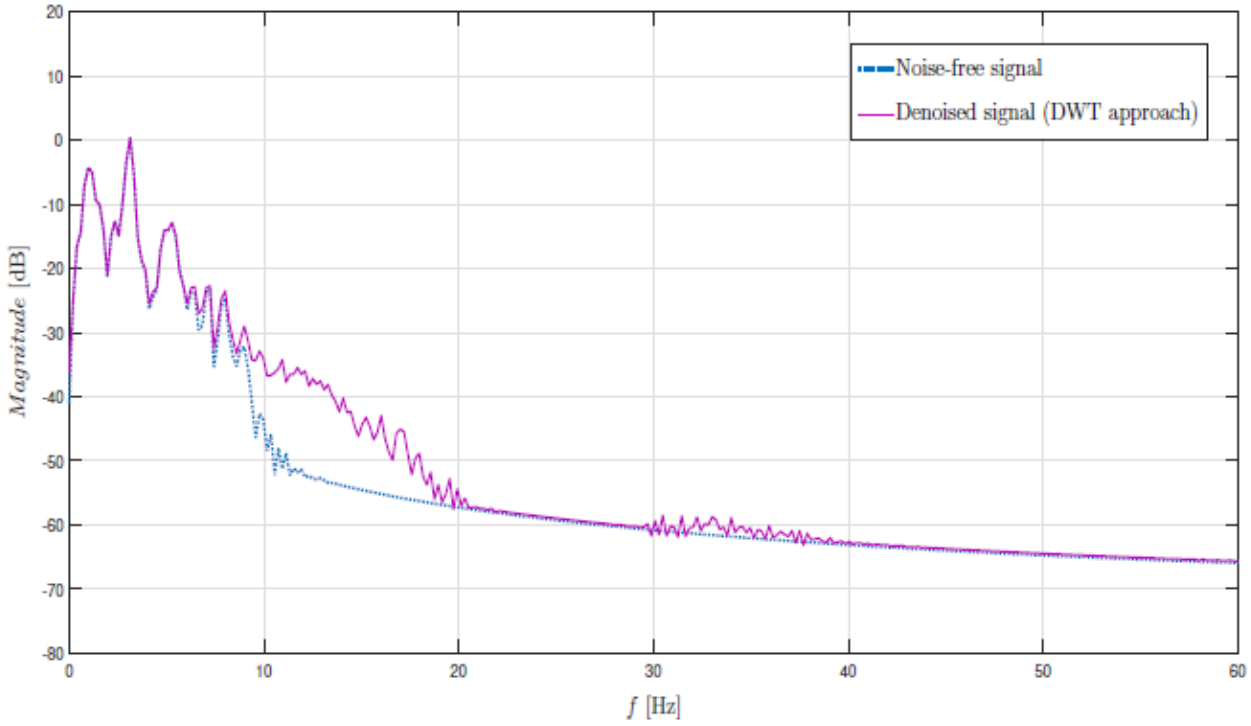

(a)

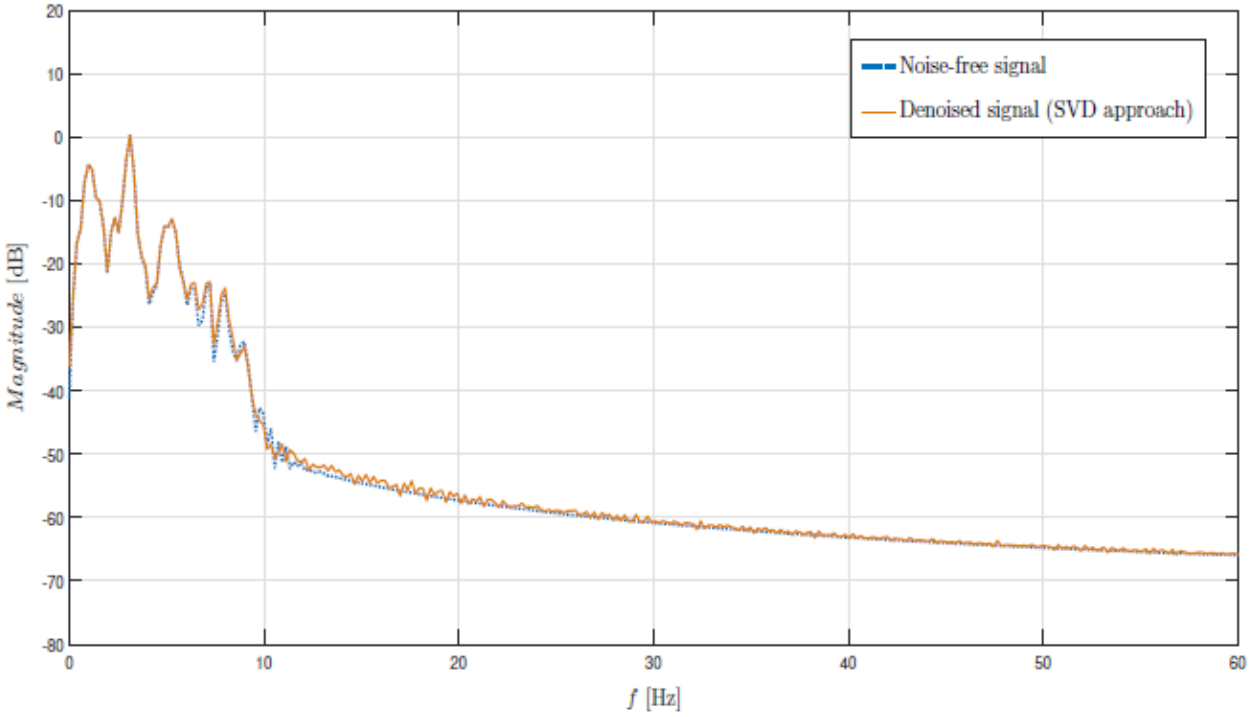

(b)

Figure 4.13: Seismic response signal in the frequency domain (25% N/S ratio). PSD of the noise-free signal vs. PSD of the denoised signal, for the two analyzed denoising techniques: (a) DWT-based denoising; (b) SVD-based denoising.

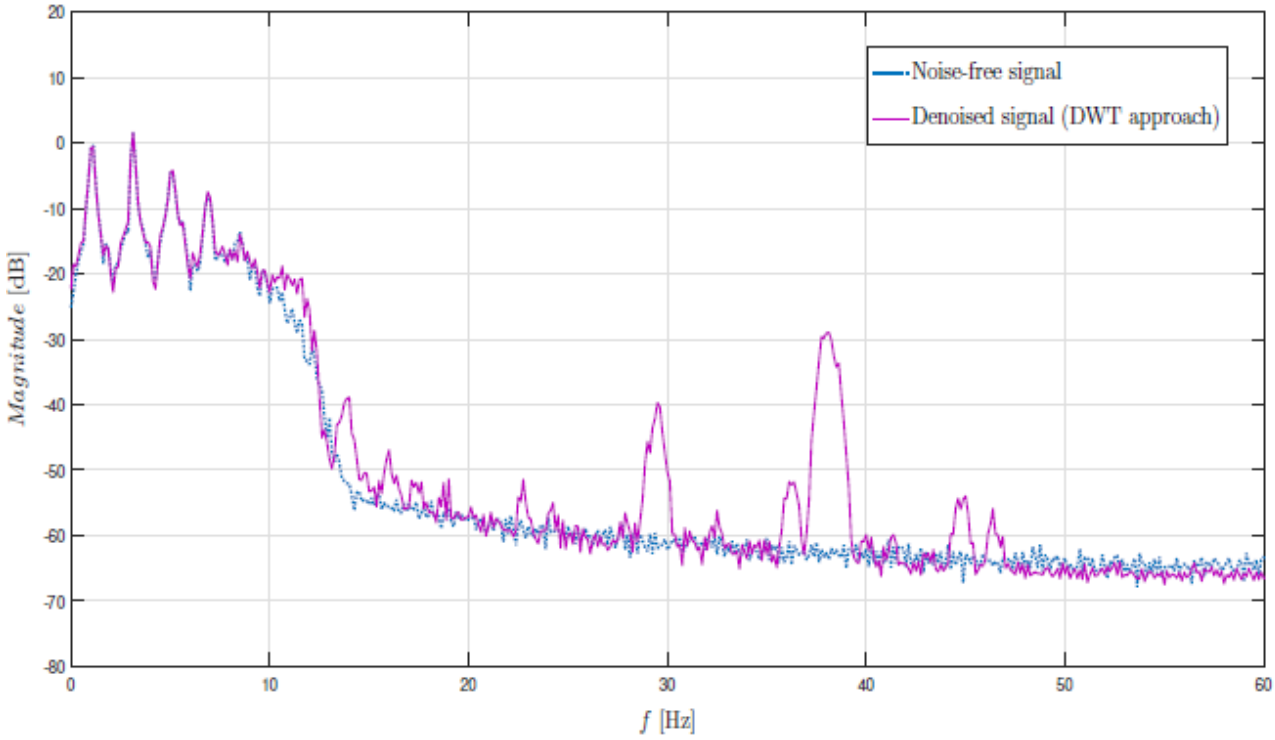

(a)

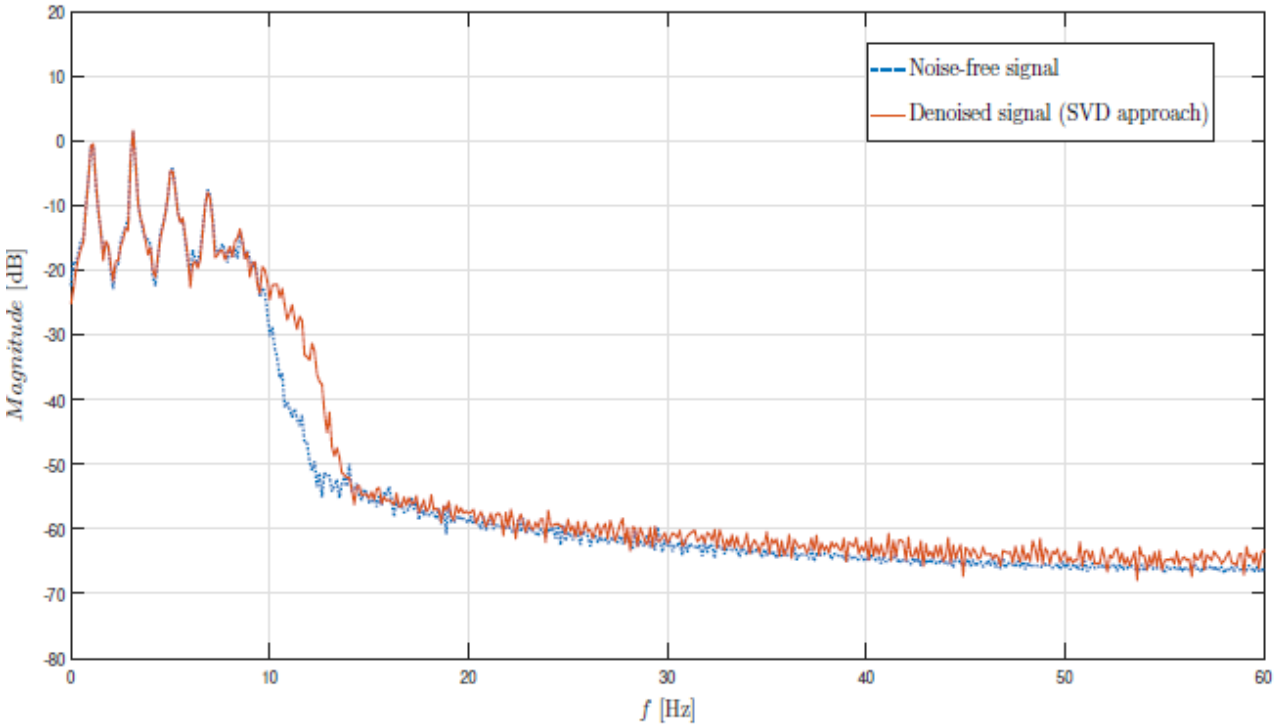

(b)

Figure 4.14: Ambient vibration response signal in the frequency domain (25% N/S ratio). PSD of the noise-free signal vs. PSD of the denoised signal, for the two analyzed denoising techniques: (a) DWT-based denoising; (b) SVD-based denoising.

As a further evaluation strategy of the performance of the two treated denoising techniques in the Frequency Domain, numerically determined undamped natural frequencies $f_{n,i}$ of the benchmark structure have been computed for each *i-th* mode, as well as associated damped modal frequencies $f_{d,i}$, inherent to the analyzed damped case of z_i=5%. Analysis results are summarized in Table 4.5, for both the aforementioned levels of noise applied on the measurements (i.e. 10% and 25% N/S ratios), and such frequencies are compared with identified damped natural frequencies $f_{id,DWT}$ and $f_{id,SVD}$, obtained from the clarified seismic and ambient vibration acceleration response signals, through a standard peak-picking procedure performed on Welch's diagram itself (Figs 4.11–4.14). Here, only the most evident frequency peaks have been considered as reliable estimates, in order to reconstruct the natural frequencies of the reference structure, since the focus of the present investigation is not specifically on the modal identification techniques. However, more refined results may alternatively be obtained by either Time Domain or Frequency Domain algorithms, such as those developed in Pioldi and Rizzi [157,158], and references quoted therein.

Mode			I	II	III	IV	V	VI	VII	VIII	IX	X
		$f_{n,i}$ [Hz]	1.055	3.131	5.107	6.930	8.567	10.019	11.285	12.336	13.127	13.617
		$f_{d,i}$ [Hz]	1.053	3.127	5.101	6.921	8.556	10.006	11.271	12.321	13.111	13.600
10% N/S	Seis.	$f_{id,DWT}$ [Hz]	0.976	3.127	5.170	7.031	8.208	-	-	-	-	-
		$f_{id,SVD}$ [Hz]	0.985	3.127	5.267	7.120	8.008	-	-	-	-	-
	Amb.	$f_{id,DWT}$ [Hz]	1.000	3.127	5.121	6.899	8.750	10.090	-	-	-	-
		$f_{id,SVD}$ [Hz]	1.000	3.127	5.125	6.901	8.756	10.130	-	-	-	-
25% N/S	Seis.	$f_{id,DWT}$ [Hz]	0.977	3.125	5.273	-	-	-	-	-	-	-
		$f_{id,SVD}$ [Hz]	0.982	3.125	5.270	-	-	-	-	-	-	-
	Amb.	$f_{id,DWT}$ [Hz]	1.116	3.125	5.012	6.874	-	-	-	-	-	-
		$f_{id,SVD}$ [Hz]	1.125	3.125	5.126	6.875	-	-	-	-	-	-

Table 4.5: Original (zi=5%) and identified natural frequencies from the denoised signal by a standard peak-picking on Welch's diagram: comparison involving different response signal typologies (seismic excitation vs. ambient vibration) and denoising techniques (DWT vs. SVD). The cases with 10% and 25% N/S ratios are reported.

Concerning the 10% N/S ratio case, through an inverse analysis procedure performed on the purified seismic response signal, it has been possible to clearly identify the first five natural frequencies of the benchmark structure; whereas, for the ambient vibration signal typology, even the sixth natural frequency can reliably be reconstructed. Consequently, it may be affirmed that, for modal identification purposes, in terms of number of identifiable frequencies, the results show that the

choice of the implemented denoising technique does not appear to be as crucial as the nature of the processed signal (non stationary vs. stationary), which instead seems to significantly condition the number of modal frequencies that may distinctly be identified.

With regard to the 25% N/S ratio initially present on the measurements, and considering the purified seismic response signal, instead, it may be observed that the identified frequencies result clearly and correctly determined only until the third mode, regardless for the implemented denoising technique. Similarly to the previous case, also here better results may be achieved for the ambient vibration response signal, where also the fourth peak, corresponding to the natural dumped frequency related to the fourth vibrational mode of the benchmark structure, appears as clearly identifiable. Also in this case, the denoising method does not seem to significantly affect the estimates, contrary to the signal typology. In particular, from what it has been observed, it may be stated that, as generally expected despite for the noise character, a stationary signal allows for a slightly better reconstruction of the structural modal properties (natural frequencies) in the Frequency Domain, with respect to a non-stationary one.

4.3.4.3 Further SVD identification analysis

To complete the numerical analysis based on synthetic response signals, a possible further research development, which involves both the two denoised signals (i.e. seismic excitation and ambient vibration), here solely obtained through the SVD-based denoising approach (for self-coherence), is now investigated.

In particular, the attempt concerns a further application of a standard SVD implementation in the Frequency Domain, on the already denoised signals in the Time Domain, by further applying a SVD on a previous Welch periodogram, directly on the PSD matrix (thus nearing what is normally performed in FDD methods, see e.g. Pioldi et al. [152–154] and Pioldi and Rizzi [155–158], and therein cited references, for the pertinent literature).

Then, through an automatic peak-picking procedure performed on the obtained SVD response spectra of the singular values, the natural frequencies of the 10th-floor benchmark structure may be identified. Such a proposed implementation, which might constitute a new interesting approach toward modal identification problems based on denoising signals, as a way to couple denoising and identification techniques, is schematically described in the conceptual flowchart depicted in Fig. 4.15.

It is worth mentioning that, as it may be appreciated within the upper Time-Domain box, although in this circumstance solely an SVD-based denoising is considered for clarifying the Time Domain noise-affected response signals (seismic and ambient vibration), the denoising of such row acceleration signals may also be performed by applying the DWT-based approach.

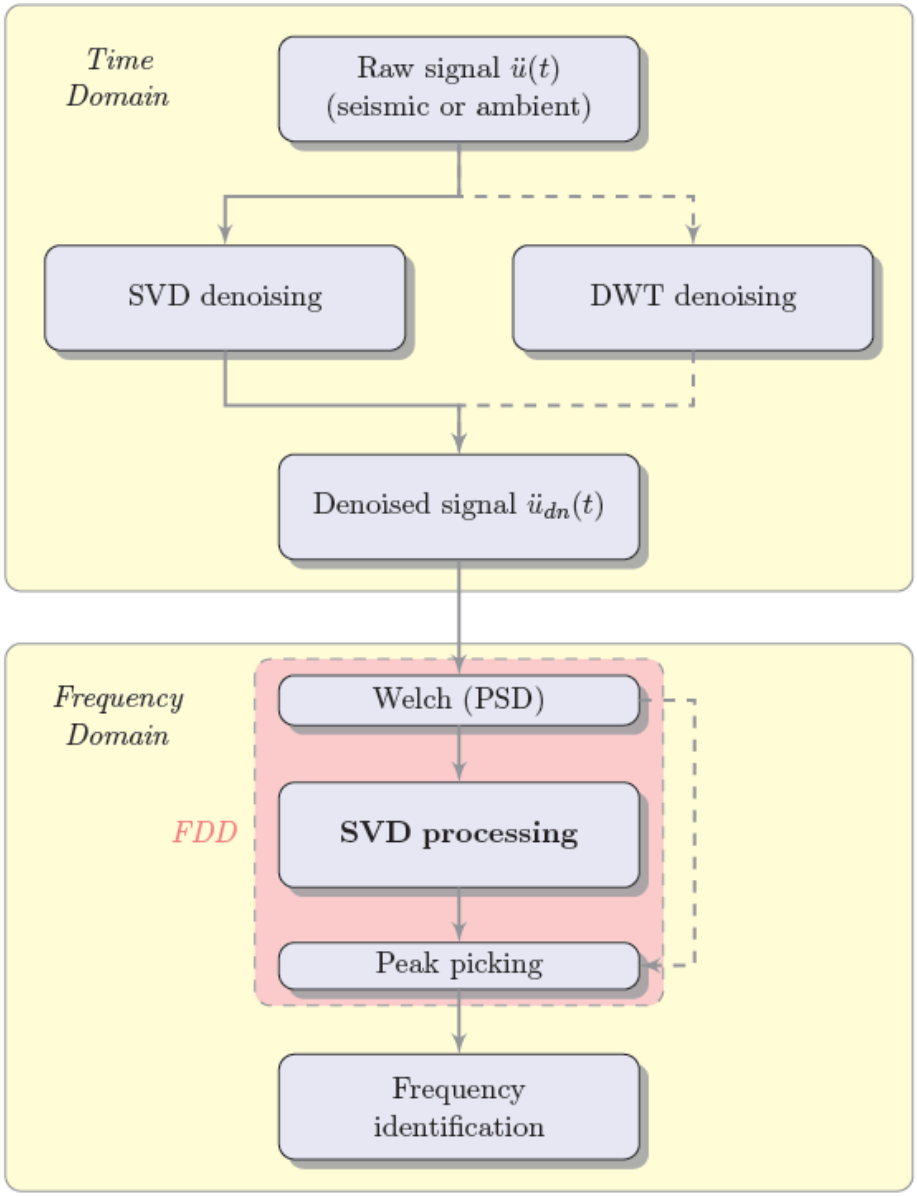

Figure 4.15: SVD-based implementation conceptual flowchart: an additional SVD is over applied on the Welch periodogram for modal frequency identification purposes.

The core of the Frequency Domain implementation lies instead in the reconstruction of a similar FDD approach, by performing the SVD on the PSD matrix, obtained through a Welch periodogram application. Finally, damped modal frequencies fid of the 10-DOF shear-type benchmark structure are thus extracted, by a standard peak-picking procedure on the first singular value for each processed signal.

The results of this procedure are illustrated in Fig. 4.16, for a very high artificial N/S ratio of 50%, to challenge the procedure, applied on both numerically determined seismic response signal (Fig. 4.16a) and ambient vibration response signal (Fig. 4.16b). Moreover, the frequencies thus identified are also

summarized in Table 4.6, and compared to the source numerically computed damped modal frequencies.

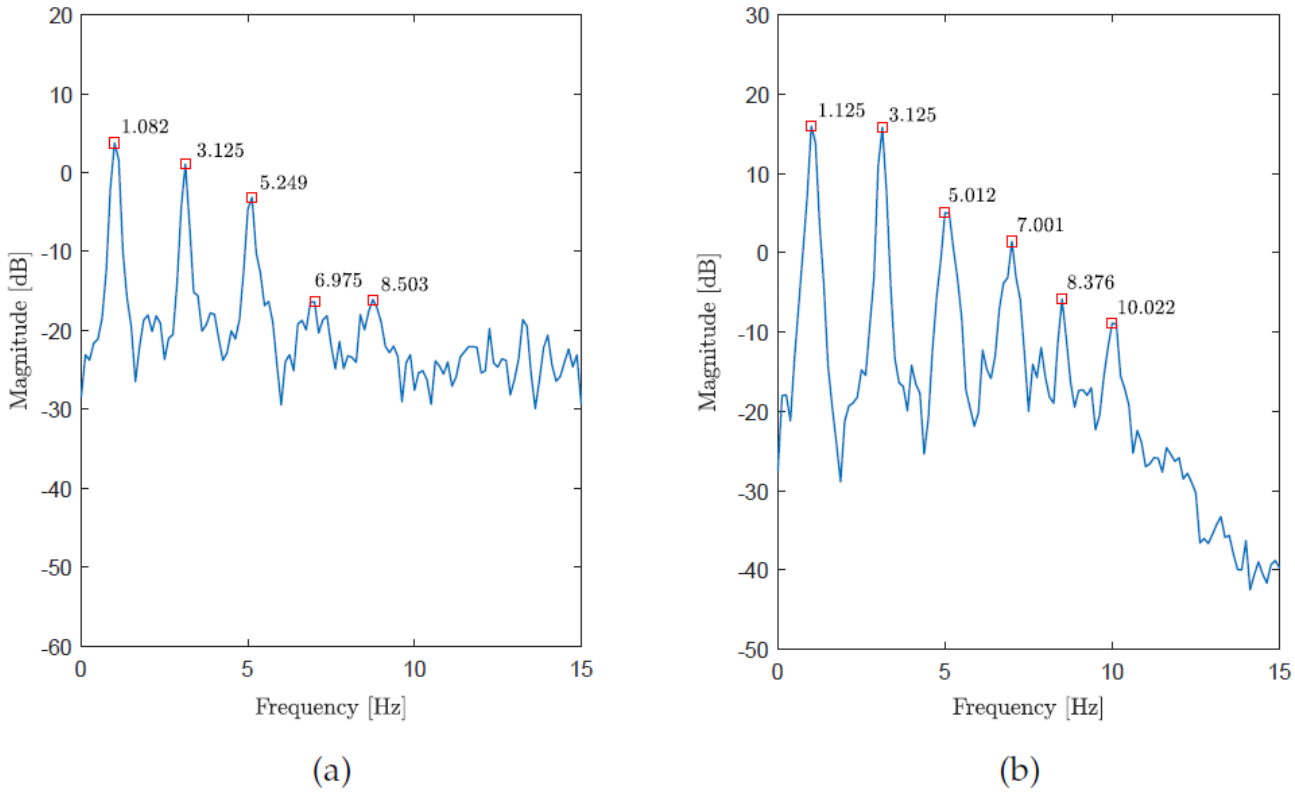

Figure 4.16: Modal identification based on SVD denoising and post-processing (first singular value). Natural frequencies identified through a peak-picking application on the first singular value of each analyzed denoised response signal typology: (a) seismic excitation; (b) ambient vibration. A 50% N/S ratio is assumed to be affecting both the original signals.

		Vibration mode									
SVD denoising		I	II	III	IV	V	VI	VII	VIII	IX	X
	$f_{d,i}$ [Hz]	1.053	3.127	5.101	6.921	8.556	10.006	11.271	12.321	13.111	13.600
Seismic	f_{id} [Hz]	1.082	3.125	5.249	6.975	8.503	-	-	-	-	-
Ambient	f_{id} [Hz]	1.125	3.125	5.012	7.001	8.376	10.022	-	-	-	-

Table 4.6: Identified natural frequencies from SVD denoised acceleration response signals and post-processing: seismic excitation vs. ambient vibration (50% N/S ratio).

As it may be appreciated from the reported results, a good agreement emerges, with numerically determined damped modal frequencies $f_{n,i}$ (see Table 4.6). Also, the fact that the seismic response signal proves to be more challenging to be processed is confirmed and, consequently, a lower number of frequencies may be extracted. Specifically, from the seismic acceleration response signal, five frequency peaks may doubtlessly be identified, with respect to the six frequencies obtained from the

ambient vibration response signal, which also presents even more pronounced peaks. However, despite the higher noise level assumed on the source signals (50% N/S ratio), with respect to the previous scenarios (10% and 25% N/S ratios), the procedure leads to even better estimates, to the point of stating that this new proposal of a further SVD processing, toward identification purposes draws promise about representing a viable option in coupling denoising and refining the modal dynamic identification process.

4.4 Final remarks

In this chapter, an original implementation and application of a DWT-based technique and a SVD-based approach toward signal denoising purposes has been presented, and inspected within the civil engineering range. Reference has been made to acceleration response signals artificially derived from a one-bay ten-story shear-type frame building, subjected to input loads of a different nature. In particular, within the analysis, a nonstationary input (i.e. Kalamata seismic excitation) and a stationary input (i.e. white-noise ambient vibration) have been considered as singularly acting on the structure, leading to different denoising outcomes on numerically generated synthetic response signals.

In particular, the salient contributions which the present investigation has brought to light may be summarized in four main items, as detailed below:

- Concerning the preliminary and necessary phase of calibration of the DWT-based denoising technique, the optimal configuration for dealing with non-stationary and stationary signals has been established. In particular, considering seismic response signals, the combination of *Smylet* having two oscillations in its mother wavelet and *Heursure* hard thresholding type at decomposition level 2, renders the smallest error (in terms of PrmsD index) between the original (noise-free) signal and the denoised one. The same analysis has been performed on ambient vibration response signals and, in this case, the optimal setting has been obtained by the combination of *Coiflet* having four oscillations in its mother wavelet and Minimax hard thresholding type at decomposition level 3.
- A critical comparison between DWT- and SVD-based denoising methods based on their performance evaluation as a function of the increasing level of Gaussian noise affecting the signals has been proposed. Most of the noise has been suppressed and the effectiveness in denoising earthquake response signals has been satisfactorily proven, for both the treated methods, as well as some limitations have been found in dealing with ambient vibration response signals, especially with reference to the implementation of the DWT-based approach. A further advantage in the use of a SVD-based denoising is that it does not require

any preliminary calibration, except for the threshold selection, and it is well suited for different N/S ratios, even if the signal to be processed may strongly be affected by noise. In general, it may be stated that the denoising based on SVD provides a better approximation of the original response signal; however, in some cases, the combined use of both techniques might represent an even more valid strategy.

- A further investigation approach for evaluating the denoising effectiveness has been based on the alteration of the main signal peak value. It emerged that non-stationary signals lead to better results than stationary signals, in term of percentage peak variation Δ_{nd} with respect to the numerically determined value, confirming the general trend. Also, another emerged feature is that SVD-based denoising seems to less flatten out the peaks than the DWT-based approach.
- Moreover, in order to compare the response spectrum of the denoised signal with the original one, a subsequent analysis within the Frequency Domain has also been performed, through the implementation of Welch's method. Quite satisfactory results have been obtained, considering seismic response signals, in particular those deriving from the SVD-based approach, whereas, concerning ambient vibration, the clarified response spectrum does not seem to be so coherent with the truthful spectrum, especially for the sub-band frequency region, where the noise more affects the signal. This may constitute a strong motivation for further research on this latter specific class of structural vibration response. In terms of peak-picking, the first three natural frequencies are anyway well identified, with an expected better representation for stationary ambient vibration input.

Finally, after this first necessary phase of effectiveness assessment of the two exposed denoising methods, where only numerically simulated synthetic signals have been involved, the next developments concern the employment and denoising of real response signals. To this specific further research topic, next Chapter 5 is dedicated.

Chapter 5. Denoising technique assessment for purifying real structural vibration response signals

Within the present research work, exclusively synthetic signals have been considered so far, namely pseudo-experimental signals numerically generated prior to the HDF-based analysis or to the denoising-based analysis. In fact, their employment within a numerical environment has been preliminarily considered as a crucial and necessary-condition validation for the presented research developments. Here, as well as in the next chapter, the focus is instead placed on real response signals, namely signals directly acquired “in situ", by means of appropriate sensors located on an existing monitored structure.

In particular, non-stationary acceleration response signals detected on a short-span railway RC bridge, are considered, within the denoising-based analysis. In the presented real scenario, both DWT and SVD-based denoising techniques are reinterpreted, aiming at exploring their effectiveness in clarifying these real experimentally recorded vibration response signals.

This chapter is organized as follows. Section 5.1 introduces the real case study object of the present analysis, i.e. a short-span railway RC bridge (monitored by ETH Zürich), and the typologies of the signals to be processed are also outlined. Section 5.2 describes the response signals in detail, through their presentation in both Time and Frequency Domains, and the previously treated denoising techniques, i.e. the DWT- and the SVD-based denoising approaches, are reconsidered. Results of the denoising analysis performed on real signals are then reported in Section 5.3, distinguishing between outcomes within the Time Domain and results within the Frequency Domain, and the similarities as well as the differences with the previous analysis involving synthetic signals are also discussed. Final comments are eventually provided in last Section 5.4.

5.1 Case study with real response signals

After a necessary condition validation by the numerical study discussed in previous Chapter 4, which has assessed the effectiveness of the two considered denoising techniques on numerically generated synthetic response signals, a case study with real signals is now developed and presented. In particular, real noisy acceleration signals are considered from the recordings on a modern railway RC bridge and, aiming at relieving the amount of noise affecting the signal, both DWT- and SVD-based denoising approaches are employed. They are first adjusted to the needs of treatment of real signals and then adopted for a complete assessment and comparison investigation.

Similarly to the previous numerical analysis, in order to strengthen the validity of the obtained results, even in this real application, the analysis is in parallel conducted, both in the Time Domain and in the Frequency Domain. In fact, in the absence of a numerically determined acceleration response value, assumed as a touchstone during the synthetic analysis, a more comprehensive description of the signal characteristics may be provided, in view of assessing whether the signal has been effectively cleaned from spurious noise, while preserving the useful information incorporated within it. In the next section, the structure selected as a benchmark specimen for the current monitoring analysis is first presented, and a brief description is provided.

5.1.1 SU Unterwalden railway bridge generalities

The structure considered for the case study in assessing the denoising effectiveness on real structural response signals is the SU Unterwalden railway bridge, located between the Unterwalden-Sempach railway stations, within the district of Sursee (canton of Lucerne, Switzerland). It is owned by Swiss Federal Railways (SBB), and inspected by monitoring campaigns at ETH Zürich. The bridge, which can be appreciated in the photographic representation in Fig. 5.1, as well as in the sectional drawing in Fig. 5.2 (Swiss railway database), is a typical short-span structure, having the main feature of being built with Ultra-High Performance Fiber Reinforced Concrete (UHPFRC). The use of this rather novel material already identifies the structure itself as an interesting object to be monitored, through the investigation of its structural safety and integrity, along time.

Figure 5.1: View of SU Unterwalden railway bridge (district of Sursee, canton of Lucerne, Switzerland).

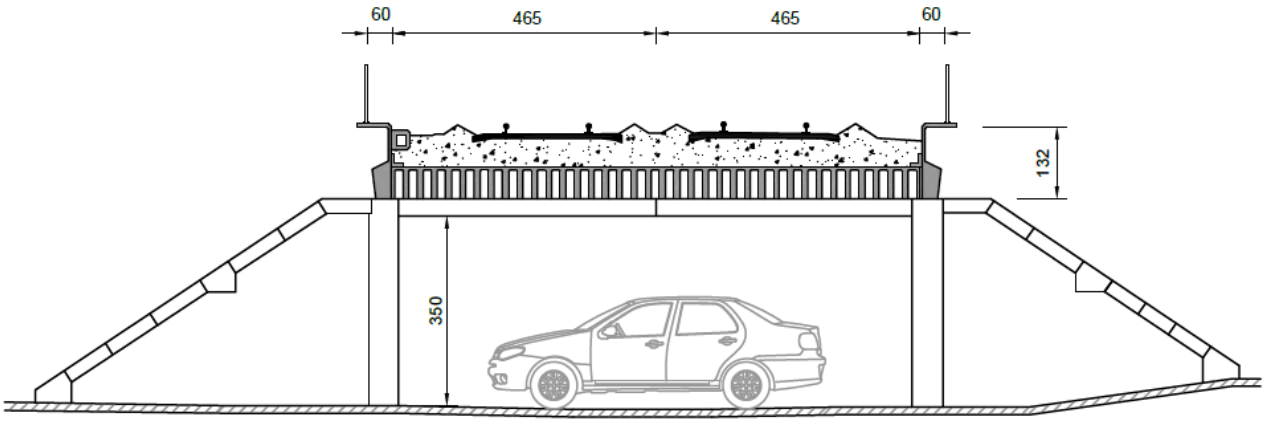

Figure 5.2: Transverse section of SU Unterwalden railway bridge (adapted from Swiss railway database; quotes in cm).

Toward this purpose, a sensor network instrumentation including easy-to-handle and low-cost sensors, such as accelerometers, a laser distance meter, tiltmeters, strain gauges and a temperature and humidity sensor, has been installed on the structure since 2018. This shall allow to acquire a deep insight on the structural behavior of the bridge within the two subsequent years, as well as information on the performance of UHPFRC as a pertinent structural material, within the civil engineering field. In the present research context, solely acceleration data are going to be treated, since they represent the most common physical quantity involved in usual monitoring activities typical of civil engineering applications, in view, here, of the target of denoising post-processing.

5.2 Denoising technique application

Two real (noise-affected) acceleration signals $\ddot{x}_1(t)$ and $\ddot{x}_2(t)$, recorded on the SU Unterwalden railway bridge at a train passage, on different times, will be made the subject of the following denoising analysis. Their main features are summarized in Table 5.1 and a representation of the two real signals in both Time and Frequency Domains is also provided in Figs. 5.3 and 5.4.

Signal	Recording day	Recording time	Samples	Duration $[s]$	RMS $[m/s^2]$	Peak $[m/s^2]$
$\ddot{x}_1(t)$	16.10.2018	22:53:10	2048	20	0.0068	0.2006
$\ddot{x}_2(t)$	19.10.2018	22:40:08	2048	20	0.0031	0.0581

Table 5.1: Global information on noisy real acceleration response signals $\ddot{x}_1(t)$ and $\ddot{x}_2(t)$ recorded on the SU Unterwalden railway bridge at a train passage on different times.

Such vibration response acceleration signals have been recorded by the passage of two different five-wagon trains on the short-span RC bridge, for a total recording time of 20 s each and, given their characteristics in Time and Frequency Domains, they clearly display a non-stationary nature. In

particular, real acceleration signal $\ddot{x}_1(t)$ (Fig. 6.3a) is characterized by a RMS equal to 0.0068 m/s^2 and a peak acceleration value of 0.2006 m/s^2, whereas real acceleration signal $\ddot{x}_2(t)$ (Fig. 5.4a), which displays lower amplitudes (notice the different scales of the y-axes), presents a RMS equal to 0.0031 m/s^2 and a peak acceleration value of 0.0581 m/s^2. Such values are then adopted for describing the signal within the Time Domain and, based on these, considerations about the amount of noise affecting the signal are going to be provided. Also note that a restricted time window of 0–3.5 s is considered for both the response signals, since the useful signal information is thereby embedded.

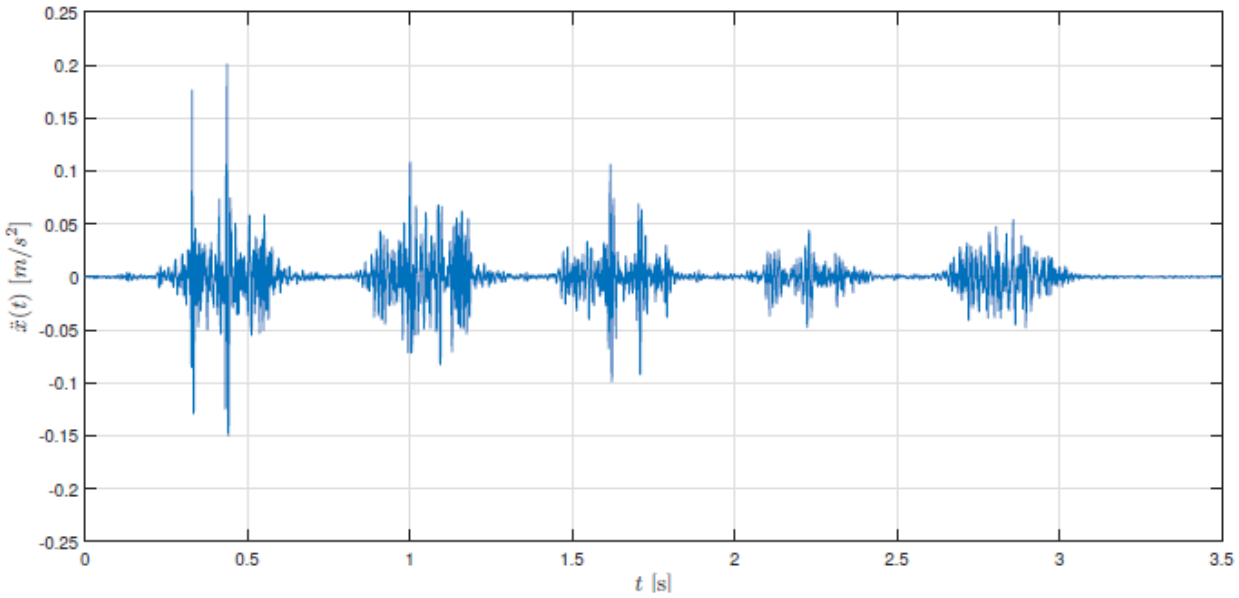

(a)

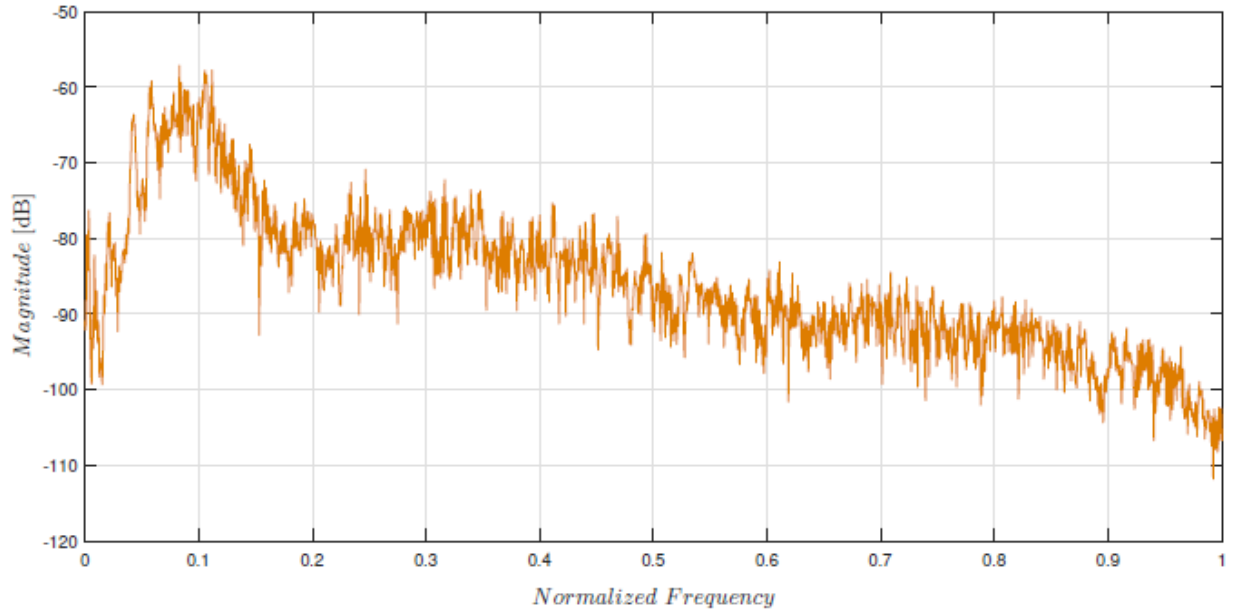

(b)

Figure 5.3: SU Unterwalden railway bridge acceleration signal $\ddot{x}_1(t)$ under a five-wagon train passage excitation: (a) Time Domain recording (time window 0–3.5 s); (b) Frequency Domain spectrum (Welch's PSD estimate) with frequency normalized to sampling frequency (200 Hz).

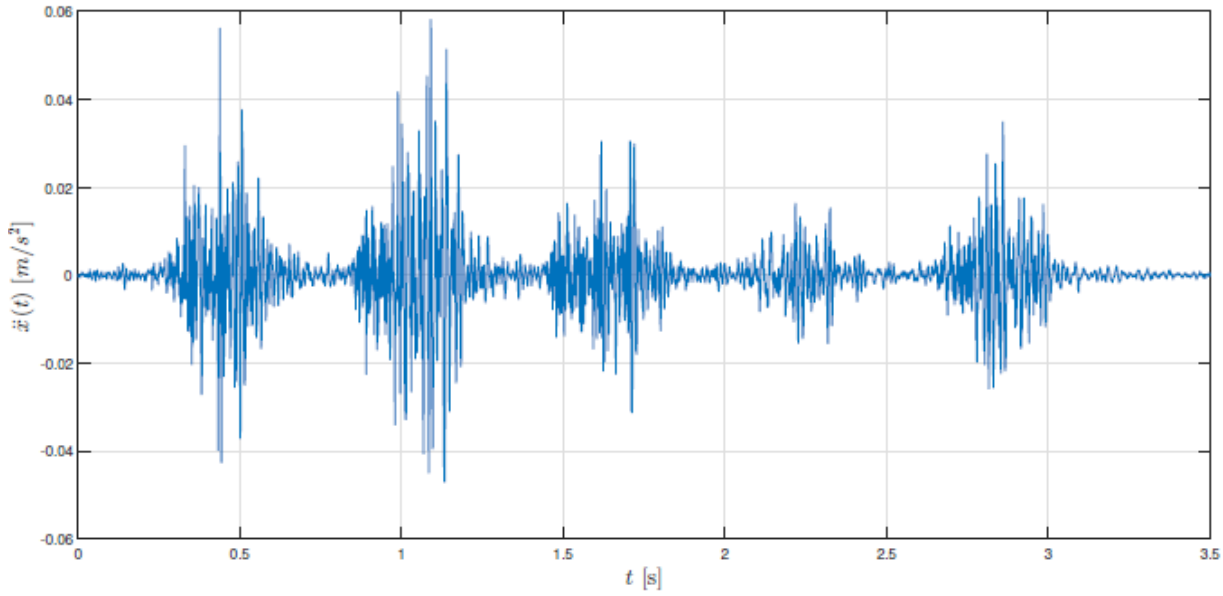

(a)

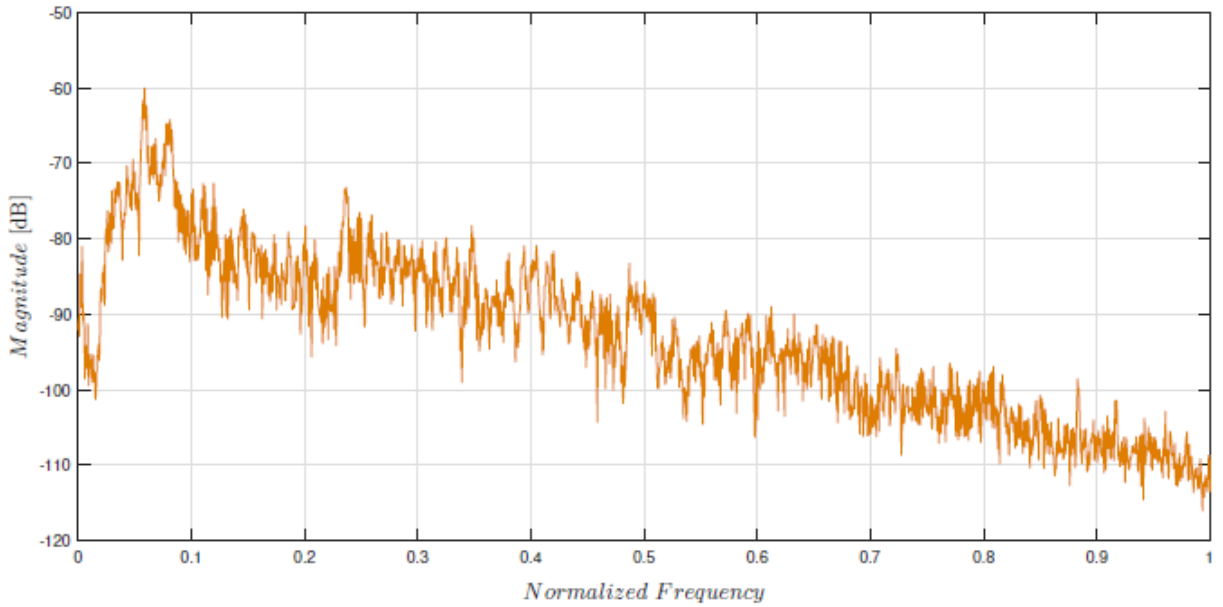

(b)

Figure 5.4: SU Unterwalden railway bridge acceleration signal $\ddot{x}_2(t)$ under a five-wagon train passage excitation: (a) Time Domain recording (time window 0–3.5 s); (b) Frequency Domain spectrum (Welch's PSD) with frequency normalized to sampling frequency (200 Hz). Notice that in (a) a different amplitude scale is adopted with respect to that in Fig. 5.3a.

About the representation within the Frequency Domain (Figs. 5.3b and 5.4b), the Welch's Power Spectral Density (PSD) estimate is expressed in normalized frequency, defined as the frequency (Hz) divided by the sampling frequency (Hz) of the considered signal, so that a normalized frequency equal to 1 represents the sampling frequency and a normalized frequency equal to 0.5 means the Nyquist frequency. In the considered signal, the recording sampling frequency is 200 Hz.

An important issue that shall be considered, in dealing with real response signals, concerns the modality of assessment of the denoising technique effectiveness. In this current phase of the analysis, in fact, the comparison term represented by the numerically determined response signal is no longer available and, consequently, the PrmsD index between the noise-corrupted signal and the denoised one cannot be computed. Thus, the effectiveness of the implemented denoising techniques has to be necessarily proven in alternative ways. A dual approach, aiming at evaluating the greater clarity acquired by the denoised signal with respect to the real one, is proposed. Two main points are considered, as follows:

- firstly, both DWT- and SVD-based denoising approaches are performed on the real acceleration signals and a comparison among the Time Domain results is sought, in terms of RMS and acceleration peak value, between the processed signal and the original (noise-affected) one;
- in addition, a critical comparison between the denoised signal response spectrum and the response spectrum of the real (noise-affected) signal is also considered. In this current phase of the analysis, in fact, without a reliable numerical reference, the analysis in the Frequency Domain becomes needful for evaluating if the signal, after the denoising procedure, shall preserve its useful information, specifically in terms of the underlying modal properties of the bridge.

Specific notions concerning the application of the two examined denoising techniques within a real scenario, as well as the similarities and differences with respect to the previously treated synthetic scenario, are presented in the next section.

5.3 Analysis results

5.3.1 Results in the Time Domain

The two denoising techniques are first independently implemented on two recorded real acceleration response signals $\ddot{x}_1(t)$ and $\ddot{x}_2(t)$ and, secondly, their results are compared. The DWT-based denoising approach is first investigated and processed denoised signal $\ddot{x}_1(t)$ is shown in Fig. 5.5a, together with the real (noise-affected) acceleration signal. For a better reading of the results, the plot just refers to the passage of the first wagon on the bridge (time window 0.2–0.7 s). This representative choice is motivated by the fact that, in such a region, the signal shows its most peculiar characteristics, since the two main peak values are there attained. In particular, the primary acceleration peak lies between 0.40 and 0.45 s, whereas the secondary one is located in the time interval between 0.30 and 0.35 s. The importance of the acceleration peak value is well known in practice, for vibration assessment purposes, since it constitutes a fundamental design parameter and, in this sense, it shall need to be

carefully determined and monitored. Acceleration response signal $\ddot{x}_2(t)$ is then processed within the same DWT-based denoising technique, and the obtained denoised signal is compared with the source (noisy) signal in Fig. 5.6a. In this case, the plot refers to the passage of the second wagon on the SU Unterwalden railway bridge (time window 0.9–1.3 s), since it is in this time region that the most characteristic signal features may be appreciated.

About the DWT-based denoising technique performed on real signals, the salient points and novelties emerged with respect to the previous analysis with synthetic signals, are mentioned below:

- The numerical analysis on synthetic data proves to be a necessary and useful starting point on which to base the analysis with real signals. In fact, in the phase of signal decomposition into the frequency domain, the mother wavelet typology (i.e. *Smylet* mother wavelet), as well as the thresholding rule (i.e. *Heursure* thresholding) and the decomposition level (i.e. a decomposition level 2), have been kept unchanged. However, this is not sufficient to guarantee good results with real signals.
- Consequently, the ideal setting of a DWT-based approach has to be slightly corrected, with respect to the previously performed numerical analysis with synthetic signals. Specifically, in the present scenario, the number of oscillations in the mother wavelet has been increased from 2 to 20, in order to achieve a better clarification of the real acceleration signal in the Time Domain and, at the same time, for obtaining a response spectrum coherent with the frequency content of the original signal.
- Thus, *Smylet* mother wavelet having 20 oscillations, combined with *Heursure* thresholding rule at decomposition level equal to 2, is assumed as a basic configuration for the current denoising method on real signals.

The benefits of the DWT denoising application in purifying the real signals result clear and tangible, as it may be appreciated from Figs. 5.5a and 5.6a, in which both denoised signals appear to be much smoother, if compared to the real, noise-affected, ones. An important effect of the DWT-based denoising application is a relevant alleviation of the peak values, in particular concerning the secondary acceleration peak of response signal $\ddot{x}_1(t)$, which is drastically reduced. A similar trend may even be observed for acceleration denoised signal $\ddot{x}_2(t)$, albeit to a lesser extent. Based on these assumptions, and comparing the real response signals with the denoised signals, it may be stated that the noise effect within the Time Domain mainly alters the peak values. Recall that such a feature was also revealed by the earlier analysis on synthetic signals, thus showing a general characteristics of the considered denoising process.

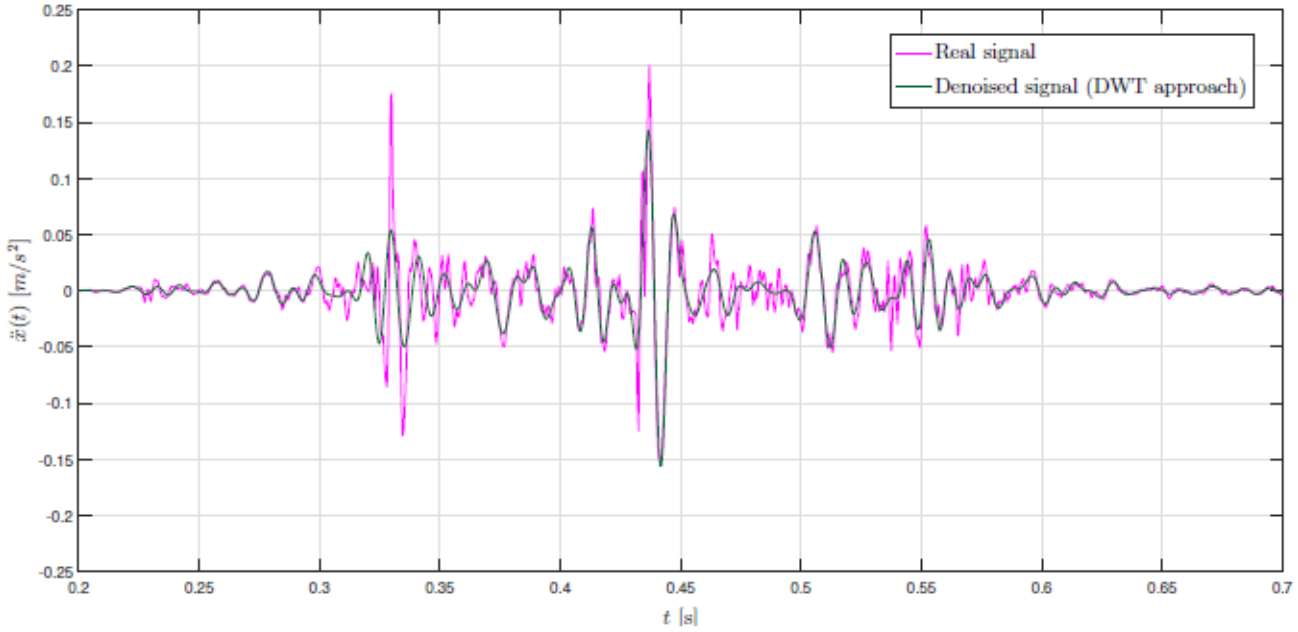

(a)

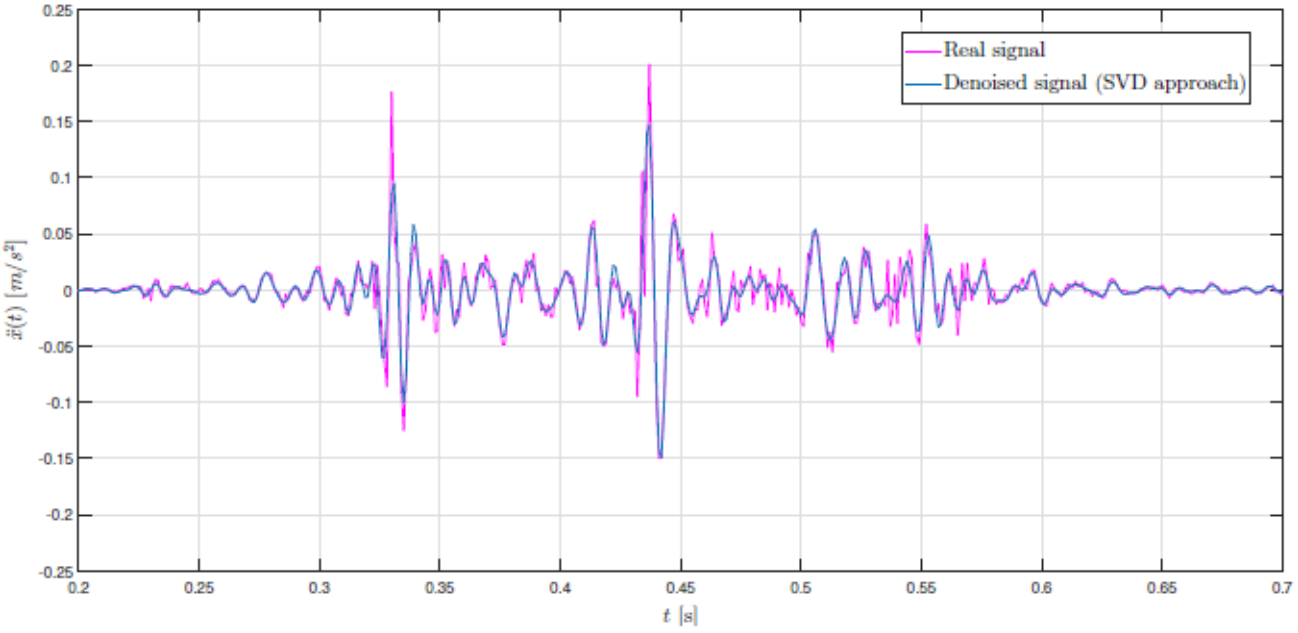

(b)

Figure 5.5: Denoising application on SU Unterwalden railway bridge real acceleration signal $\ddot{x}_1(t)$ under a five-wagon train passage (first wagon representation, time domain window 0.2–0.7 s): (a) DWT-based denoising; (b) SVD-based denoising.

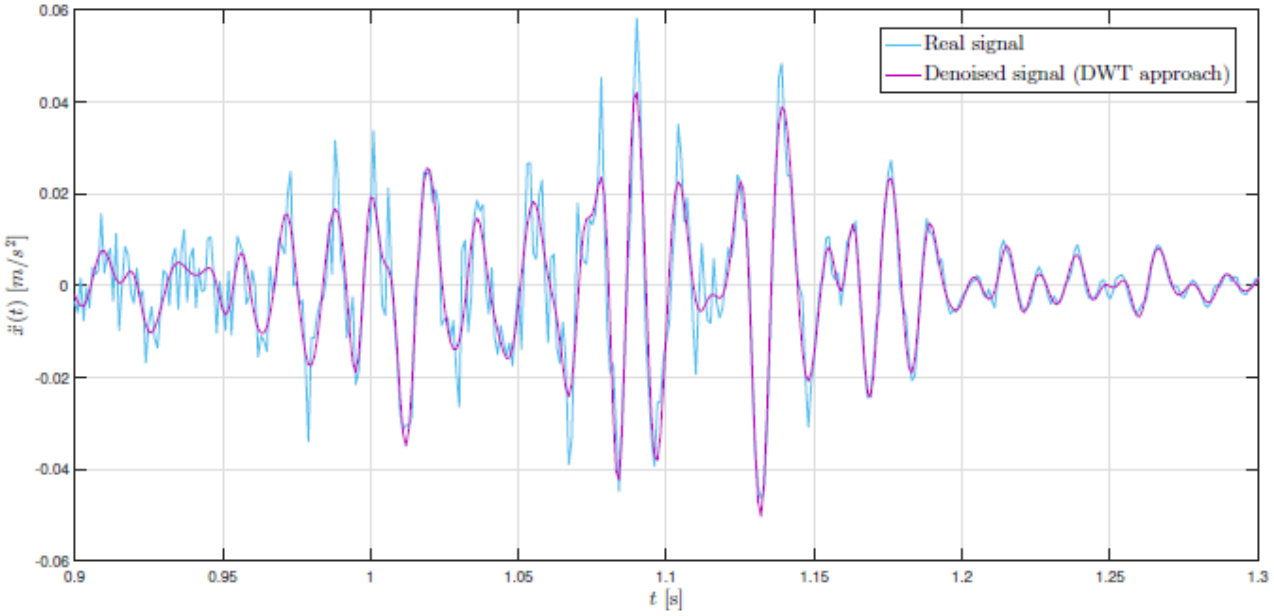

(a)

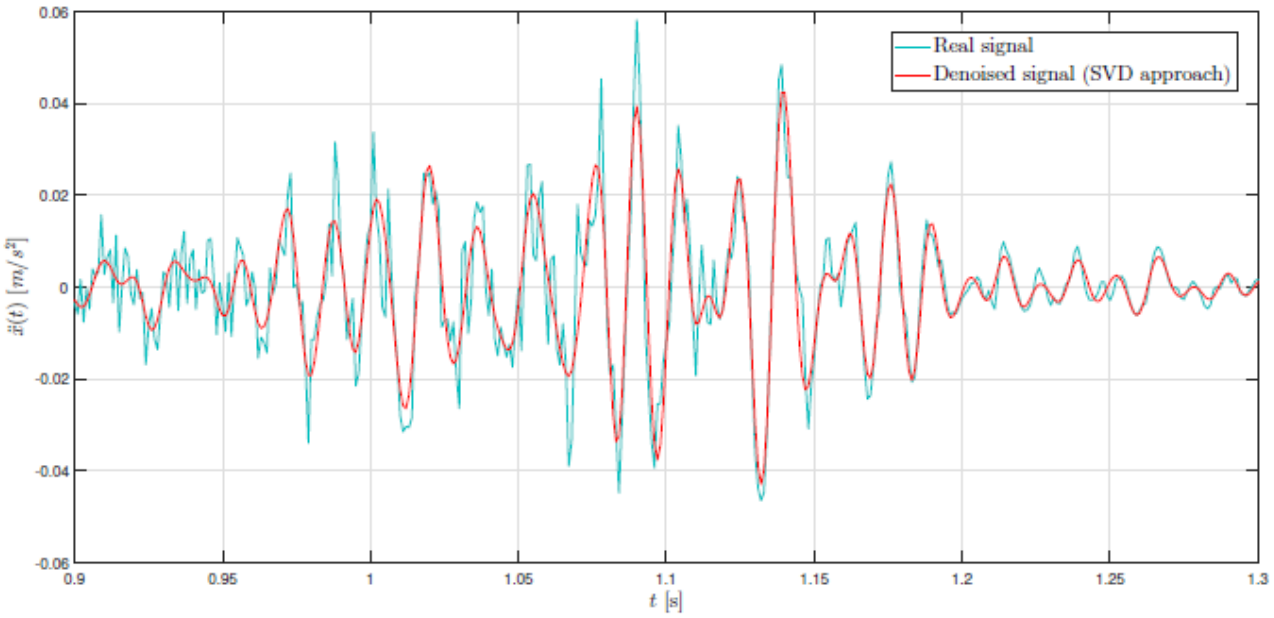

(b)

Figure 5.6: Denoising application on SU Unterwalden railway bridge real acceleration signal $\ddot{x}_2(t)$ under a five-wagon train passage (first wagon representation, time domain window 0.9–1.3 s): (a) DWT-based denoising; (b) SVD-based denoising.

The SVD-based denoising approach is then performed, and results are shown in Figs. 5.5b and 5.6b. With regard to this specific technique applied to real signals, the following considerations are worth mentioning:

- Again, the numerical analysis performed on synthetic signals proves to be needful for establishing an appropriate order of magnitude for the threshold value to be adopted in dealing

with real signals but, in this scenario, it is not enough for implementing an optimal denoising effect.

- As a consequence, in the calibration of the denoising technique based on SVD, greater threshold values have been explored with respect to those used for treating the synthetic analysis, for adapting the SVD-based denoising to real application contexts, aiming at achieving a denoised signal with a much coherent frequency content.
- Thus, in the calibration of the denoising based on SVD, to be performed on real acceleration signals, a threshold value equal to 30 is set (with respect to 10 for synthetic signals).

Concerning the results and the benefits that this second denoising approach has brought about, in terms of signal clarification, similar considerations to those outlined for the previously treated DWT-based denoising approach, may be drawn. In particular, also in this case, a significant reduction of the peaks, although not so pronounced as before (especially regarding the secondary acceleration peak of response signal $\ddot{x}_1(t)$), is clearly visible. Thus, SVD-based denoising seems to flatten out the peaks slightly less than DWT-based denoising. A similar relative effect among SVD- and DWT-denoising peak flattening was recorded for synthetic signals (see Table 4.4, non-stationary response signal case), likely pointing out to a general feature among the two considered techniques.

Comparing the results reported in Figs. 5.5a and 5.5b, as well as those shown in Figs. 5.6a and 5.6b, a good agreement emerges between the two treated techniques, in denoising the examined real acceleration signals. This is even more evident by the graphical comparisons further shown in following Figs. 5.7 and 5.8, which focus on the main acceleration peak of denoised signal $\ddot{x}_1(t)$ (time window 0.35–0.6 s) and denoised signal $\ddot{x}_2(t)$ (time window 1–1.25 s), respectively.

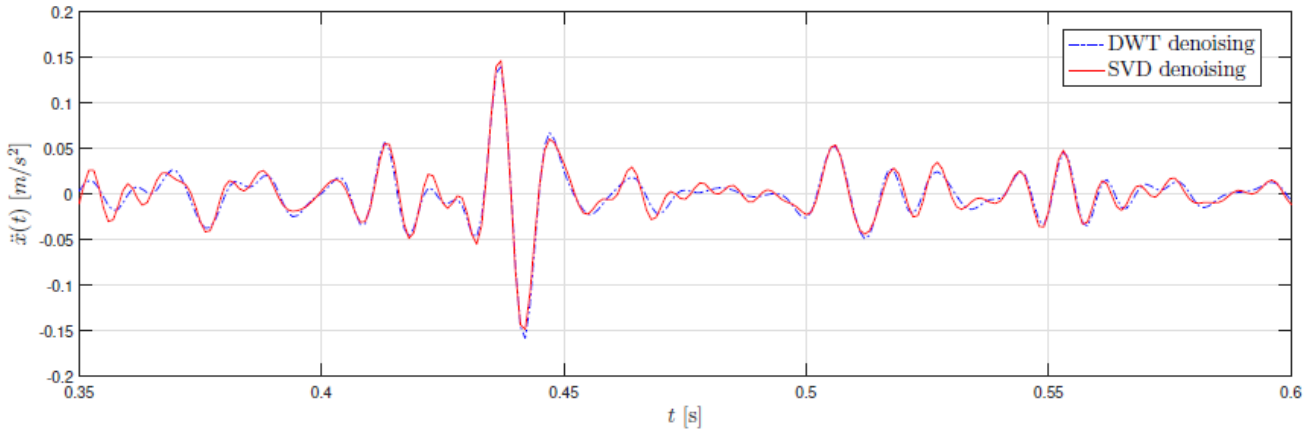

Figure 5.7: DWT vs. SVD-based denoising performed on SU Unterwalden railway bridge real acceleration signal $\ddot{x}_1(t)$ (zoomed time window 0.35–0.6 s).

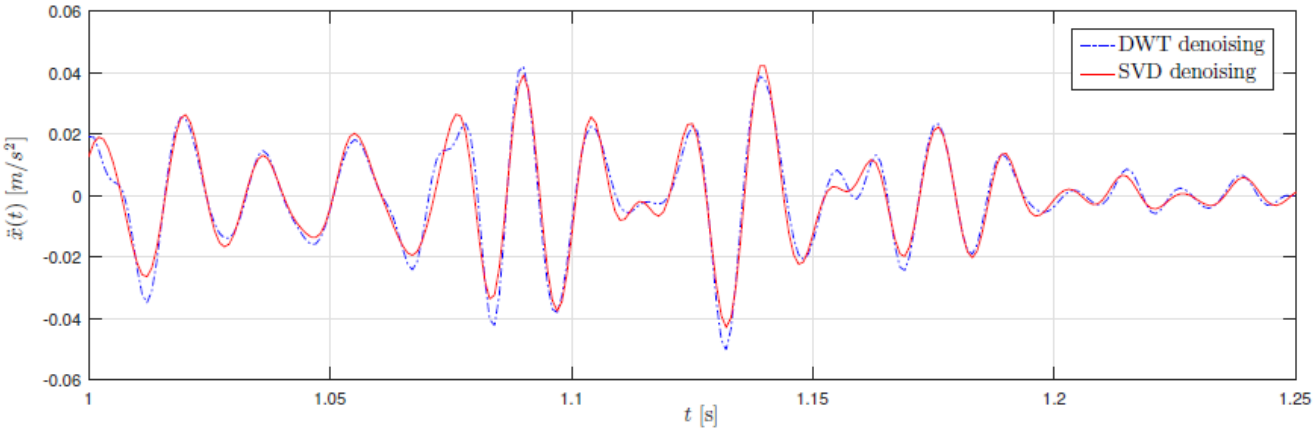

Figure 5.8: DWT vs. SVD-based denoising performed on SU Unterwalden railway bridge real acceleration signal $\ddot{x}_2(t)$ (zoomed time window 1–1.25 s). Notice that a different amplitude scale is adopted with respect to that in Fig. 5.7.

Such denoised peak values, as well as the RMS computed on the entire denoised signals (time window 0–3.5 s), namely the most characteristic signal values in the Time Domain analysis, are then reported in Table 6.2.

Signal	**RMS** $[m/s^2]$	Δ_{na} [%]	**Peak** $[m/s^2]$	Δ_{na} [%]
Real (noisy) signal $\ddot{x}_1(t)$	0.0068		0.2006	
DWT denoised signal	0.0062	−8.82	0.1402	−30.11
SVD denoised signal	0.0063	−7.35	0.1465	−26.97
Real (noisy) signal $\ddot{x}_2(t)$	0.0031		0.0581	
DWT denoised signal	0.0028	−9.68	0.0420	−27.71
SVD denoised signal	0.0029	−6.45	0.0425	−26.85

Table 5.2: Characteristic values of the entire denoised signals in the Time Domain and their variation Δ_{na} with respect to the real (noise-affected) signals: RMS and peak acceleration values.

Their variations Δ_{na} with respect to the same parameters computed on the real (noise-affected) signals (refer also to earlier Table 4.4), are also indicated. In particular, the noise reduction in terms of RMS provides information about the amount of noise affecting the original real signal which, concerning acceleration signal $\ddot{x}_1(t)$, may be estimated in a N/S ratio equal to 8.82% according to the DWT-based approach, and a N/S ratio of 7.35% concerning the SVD-based approach. Considering then acceleration signal $\ddot{x}_2(t)$, a similar trend may be outlined, with the DWT-based approach leading to a relevant RMS reduction of 9.68%, against a lower value of 6.45% for the SVD-based technique. About the main acceleration peak, the noise influence appears to be even more deleterious, since in

the case of source signal $\ddot{x}_1(t)$, a percentage reduction of 30.11% and 26.97% is measured for the DWT- and SVD-based denoising techniques, respectively, while concerning source signal $\ddot{x}_2(t)$, the application of the same denoising approaches leads to a similar peak reduction of 27.71% and 26.85%.

5.3.2 Results in the Frequency Domain

The very similar results provided by the two implemented approaches in the Time-Domain analysis might be considered as an encouraging sign for the success of the denoising process, on the inspected type of nonstationary railway vibration response signals. However, the evaluation of the denoising techniques, conducted within the Time Domain, may not be sufficient to fully prove their effectiveness, if not accompanied as well by an accurate analysis within the Frequency Domain, which aims at exploring the signal frequency content after the denoising application. So, through an output-only inverse analysis based on Welch's method, the PSD of the signal is computed, before and after the denoising application, and the response spectrum is obtained, for both the real (noise-affected) signal and the denoised signal.

Real acceleration signal $\ddot{x}_1(t)$ is first investigated, and a comparison between the two response spectra is shown in Fig. 5.9, for the DWT-based denoising technique, in both linear scale (Fig. 5.9a) and logarithmic scale (Fig. 5.9b). A clear reduction of the noise is visible, especially in the medium to high frequency bands, where the cleaning effect of the denoising application becomes more tangible, and the response spectrum turns out very smooth. However, an unjustified frequency peak (though at lower magnitude) appears in the medium frequency band (within a normalized frequency between 0.3 and 0.4), probably due to a deleterious effect produced by the remaining amount of noise, which could not be removed. Within the low frequency region, instead, the useful information has been successfully preserved, since the peaks corresponding to the significant modal frequencies of the structural system have been kept unchanged.

An analogous inverse analysis within the Frequency Domain is then performed on the denoised signal obtained through the SVD-based denoising approach, and the resulting response spectrum is shown in Fig. 5.10, together with the noisy response spectrum. The denoising technique based on SVD proves to be even more performing than the previous DWT one, leading to a denoised response spectrum that is totally smooth in the sub-band frequency region. Again, the useful information embedded into the signal has been preserved, and it may be stated that the denoising was rather successful.

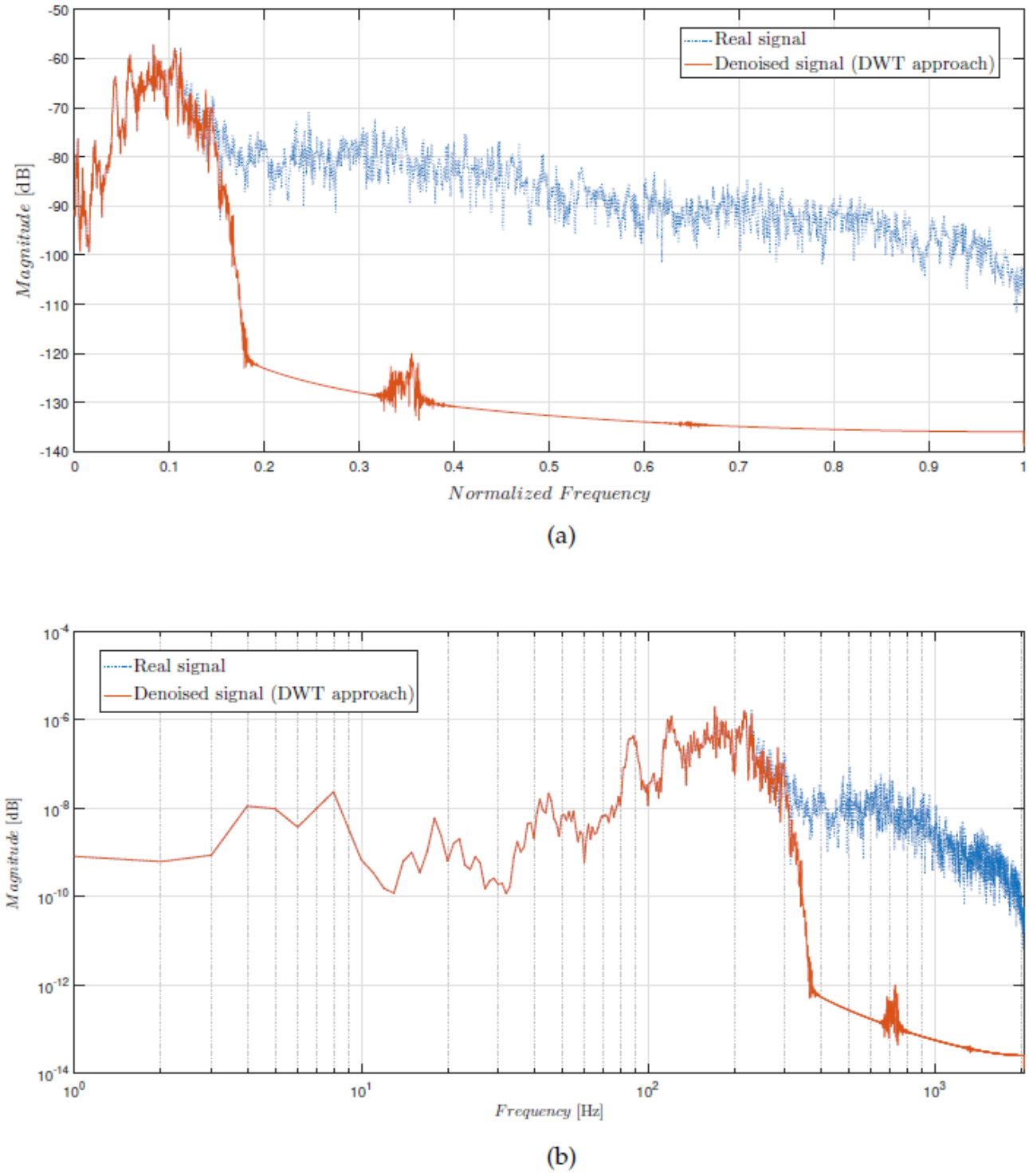

Figure 5.9: SU Unterwalden railway bridge real acceleration signal $\ddot{x}_1(t)$ in the Frequency Domain. DWT-based denoising technique. PSD of the real (noise-affected) signal vs. PSD of the denoised signal: (a) linear scale in frequency normalized to sampling rate (200 Hz); (b) logarithmic scale.

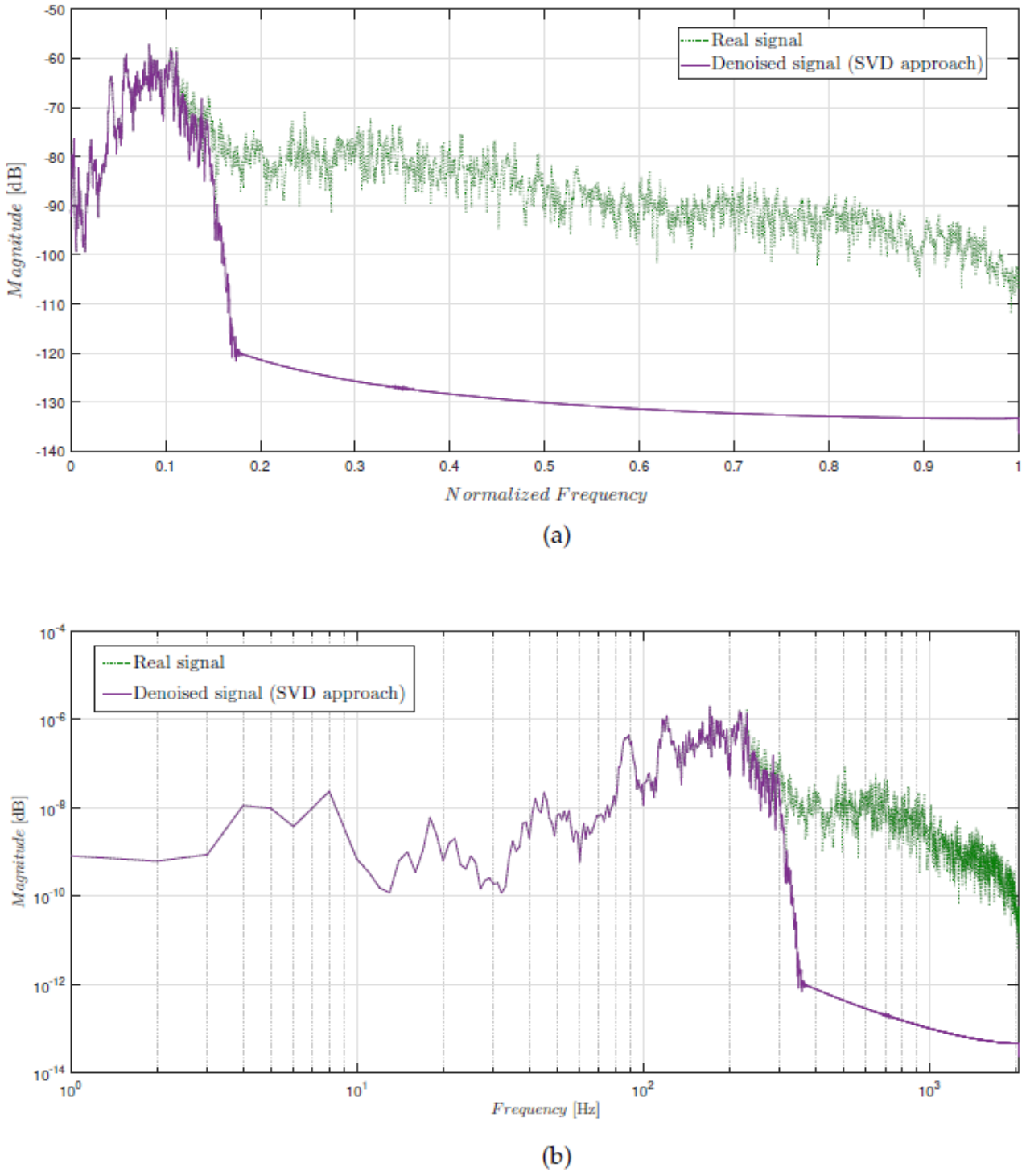

Figure 5.10: SU Unterwalden railway bridge real acceleration signal $\ddot{x}_1(t)$ in the Frequency Domain. SVD-based denoising technique. PSD of the real (noise-affected) signal vs. PSD of the denoised signal: (a) linear scale in frequency normalized to sampling rate (200 Hz); (b) logarithmic scale.

The same analysis within the Frequency Domain is then performed on SU Unterwalden railway bridge real acceleration signal $\ddot{x}_2(t)$, aiming at strengthening the results obtained about the denoising of real signals and generalizing some interesting aspects that have emerged. So, a further output-only inverse analysis based on Welch's method is performed, the response spectrum of denoised signal $\ddot{x}_2(t)$ is obtained and then compared with that of the source (noisy) signal. Results are shown in Figs. 5.11 and 5.12 for the case of DWT-based denoising and SVD-based denoising, respectively. Analogous considerations may be drawn even concerning this second analyzed real signal $\ddot{x}_2(t)$, since the noise effect seems to be largely relieved in both the studied denoising scenarios, even slightly more effectively than for the previously treated wider acceleration signal $\ddot{x}_1(t)$, in particular considering the denoising technique based on DWT (compare Figs. 5.9 and 5.11).

In light of what it has been shown, the effectiveness of DWT- and SVD-based denoising techniques may be considered to be proven, even for the examined real non-stationary railway vibration response acceleration signals. However, if in the Time Domain the benefits of the denoising application clearly emerge, some little inconsistencies remain about the analysis in the Frequency Domain. In fact, although sufficient for a validation of the Time-Domain results, it did not allow to identify a larger number of modal frequencies, with respect to the unprocessed signal, reinforcing the need for possible further research in such a direction.

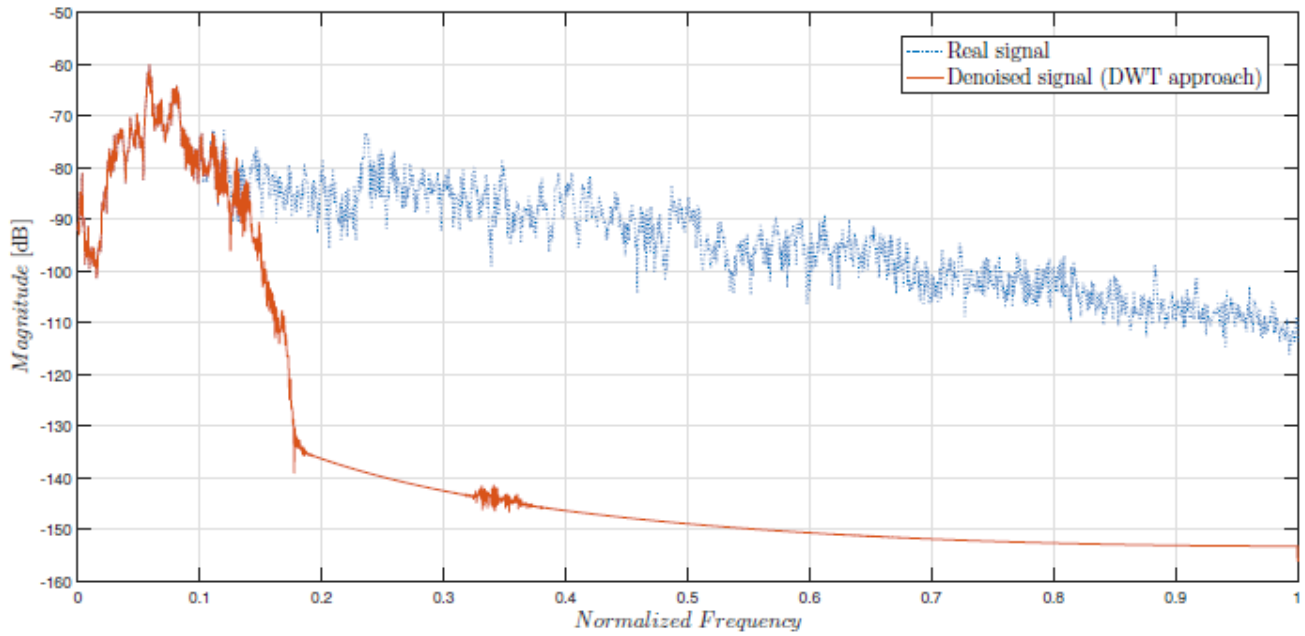

(a)

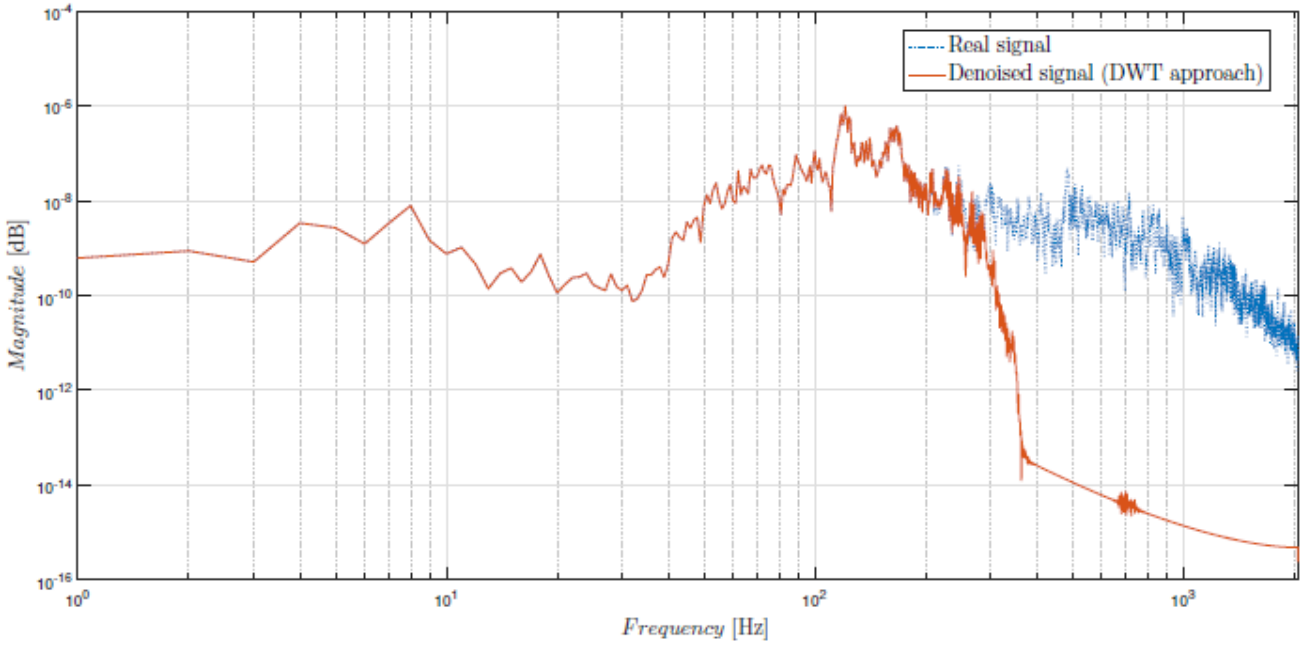

(b)

Figure 5.11: SU Unterwalden railway bridge real acceleration signal $\ddot{x}_2(t)$ in the Frequency Domain. DWT-based denoising technique. PSD of the real (noise-affected) signal vs. PSD of the denoised signal: (a) linear scale in frequency normalized to sampling rate (200 Hz); (b) logarithmic scale.

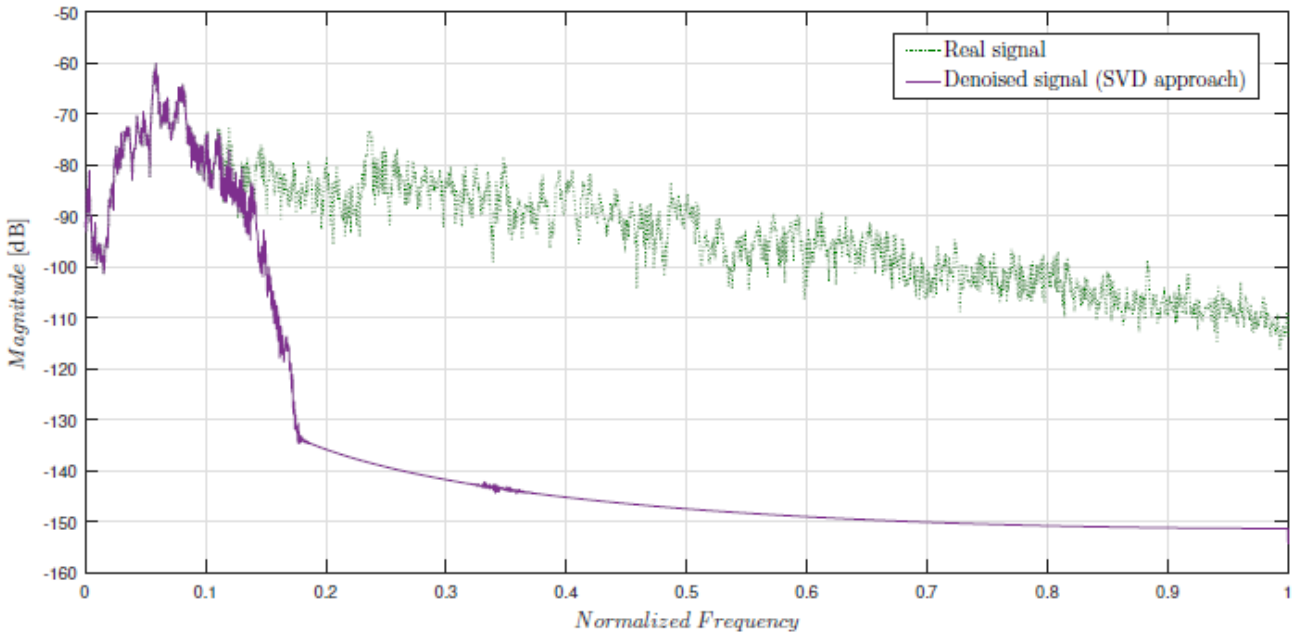

(a)

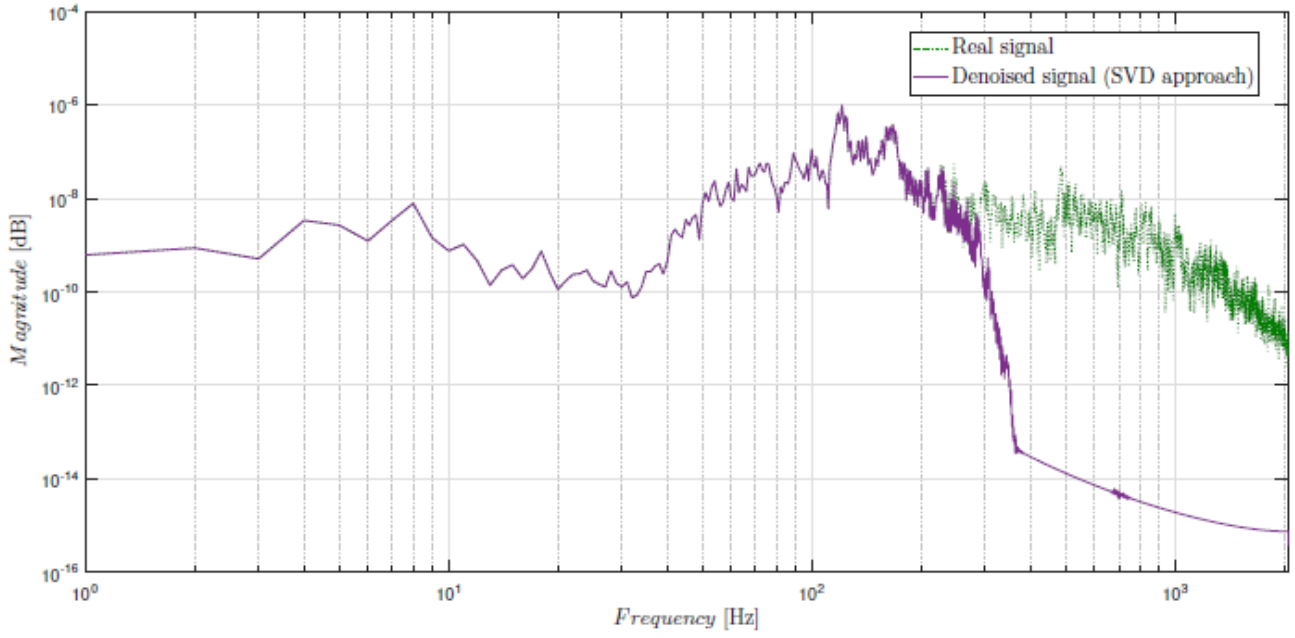

(b)

Figure 5.12: SU Unterwalden railway bridge real acceleration signal $\ddot{x}_2(t)$ in the Frequency Domain. SVD-based denoising technique. PSD of the real (noise-affected) signal vs. PSD of the denoised signal: (a) linear scale in frequency normalized to sampling rate (200 Hz); (b) logarithmic scale.

5.4 Final remarks

In this chapter, real acceleration response signals have been successfully processed from experimental recordings on a railway RC bridge, as nonstationary vibration response acceleration signals at train passage. In fact, after the numerical validation of DWT- and SVD-based denoising techniques, performed on synthetic signals in previous Chapter 4, here, a subsequent development has concerned the denoising of real signals, directly acquired in situ on a specific structure, by predisposing appropriate accelerometer sensors at a certain number of locations. In particular, two real non-stationary acceleration signals detected on the SU Unterwalden railway RC bridge (Switzerland) by ETH Zürich have been analyzed.

Both DWT and SVD-based denoising techniques have been independently adapted and employed, leading to the following outcomes:

- The benefits of the denoising application in purifying the considered real (noise-affected) acceleration response signals clearly appear within the Time-Domain analysis. In fact, results from the DWT and SVD-based denoising approaches seem to be in excellent agreement with each other, leading to similar values in terms of noise reduction, on the main acceleration peak and on the RMS value, with respect to the original real signals. This might also be considered as a proof of the fact that the effect of noise acts in an additive sense on the amplitude of the signal itself.
- As regard to the reduction of peak predictions by the denoising methods on synthetic signals, discussed in the previous chapter, here, the main trends are confirmed since, even with real signals, the denoised peak appears to be flatter than the real (noise-affected) one, according to both the applied denoising techniques. Moreover, the SVD-based approach confirmed to less flatten out the peaks than the DWT-based technique, configuring this to appear as a general trend of such denoising techniques.
- In order to inspect the frequency content of the signal after the denoising application, a further analysis within the Frequency Domain has been as well performed. The useful information embedded into the signals appears to be preserved even within the Frequency Domain, since the main modal frequencies turn out to be unchanged, despite for a visible cleaning of the noise in the medium and high frequency regions. However, there does not seem to appear any significant improvement in terms of the number of identifiable modal frequencies, at least for the available embedded content as a structural response trace within the recorded signals.
- Although the relevance of the denoising process mainly lies within the Time Domain, where its cleaning effect looks more evident, a further validation within the Frequency Domain looks needed, to check if the response spectrum of the signal after the denoising application may

still be coherent with its source inherited modal properties, and the useful information of the signal has effectively been preserved.

- In conclusion, the effectiveness of DWT- and SVD-based denoising techniques may be considered to be proven, even for real signals, at least for what it concerns a non-stationary acceleration signal typology, as that considered for the recorded railway bridge response at train passage (recall that the denoising analysis with synthetic ambient vibration signals has revealed to be more challenging, than for non-stationary signals).

After this validation phase of the two studied denoising approaches with real non-stationary response signals, possible subsequent developments of the present research scenario might concern the denoising of other typologies of real response signals that may be found in civil engineering contexts. In addition, not only accelerations but also displacement response signals might also be considered within the denoising analysis, even possibly through HDF approaches, as presented in previous Chapters 2–3. In fact, displacement data are typically associated with higher N/S ratios, with respect to acceleration data, mainly due to greater intrinsic errors, which shall characterize displacement sensor technologies. Consequently, the employment of DWT- and SVD-based denoising techniques for improving the quality of such signals could represent a very useful resource, leading to important practical implications in real applications.

Finally, a further possible research scenario may concern the deepening of the employment of such denoised signals toward modal identification purposes, aiming at significantly improving the structural identification phase within the Frequency Domain (see e.g. Pioldi et al. [152–154] and Pioldi and Rizzi [155–158]). This might result of a crucial interest for real applications related to the SHM context, within the civil engineering field. To these research developments, which aim at integrating HDF procedures with denoising-based approaches toward modal identification purposes, the next chapter is devoted.

Chapter 6. An integrated monitoring strategy fur current condition assessment of historic bridges

In this chapter, the two post-processing approaches covered in the present research work, namely HDF procedures (Chapter 2–3) and denoising-based techniques (Chapter 4–5), are reconsidered and rejoined, toward developing an innovative signal processing methodology for current condition assessment of (historic) bridges. In particular, such signal postprocessing approaches are combined within an integrated and innovative monitoring strategy, in an effort to enhance the reliability of the monitoring process. The effectiveness of the proposed platform is tested on data from a real structure, namely a historic bridge. Both dynamic acceleration and displacement response signals are processed within the proposed methodology, and then employed toward modal dynamic identification purposes. The chapter is organized as follows. Section 6.1 aims at contextualizing the present research scenario, through a statement on the motivations as well as on the research goals that are targeted to be achieved. In Section 6.2, a brief description of the structure of interest is outlined, whereas the proposed monitoring strategy is formulated and presented in Section 6.3. Then, the obtained results are reported and discussed in Section 6.4. Finally, last remarks and summary comments are provided within the conclusions reported in Section 6.5.

6.1 Introduction and contextualization

The analysis presented in this chapter is motivated by the awareness quest on the critical health condition that may characterize existing and historical infrastructures, especially those nearing the end of their life cycle. Despite their age, these structures often continue to play a crucial role in everyday life, constituting essential connections within the transportation network of several territories and communities. Consequently, a prompt and effective adoption of appropriate and modern strategies and action models toward their conservation and protection shall be set in place. In this scenario, the development of monitoring-based strategies toward structural condition assessment of such important infrastructures, shall constitute a fundamental tool toward the competent analysis. Accordingly, within the civil engineering context, the SHM research field is becoming increasingly important, since the goal of achieving structural safety is only possible through the possibility to extract more abundant and precise information about the health condition of a structure to be monitored, for instance by analyzing its current structural dynamic response. As a consequence, within SHM applications, after the signal acquisition stage, to be directly acquired on the structure by predisposing appropriate sensor networks, the subsequent phase of signal processing displays a determinant role, toward the success of the whole monitoring procedure.

Here, two complementary and possibly interacting approaches for the post-processing of structural response signals are reconsidered, i.e. a HDF procedure (see Chapter 2–3), as well as a denoising approach (see Chapter 4–5), aiming at achieving a better screening of real structural response signals, which may be corrupted by some amount of noise, especially in case of the use of a low-cost instrumentation.

In particular, recall that denoising techniques aim at clarifying the signal content, by directly acting on the contaminating noise, reducing its amount, while preserving the useful information embedded within the signal itself. Several denosing-based techniques may be employed for this purpose, including those exploiting SVD or DWT, as recently investigated in Ravizza et al. [167,168] and reported in previous chapters, where the effectiveness of these approaches has been inspected for both stationary (ambient vibration) and non stationary (seismic excitation) synthetic response signals (Chapter 4), and for instances of real vibration signals (Chapter 5).

Instead, recall that HDF-based approaches are procedures through which heterogeneous measurements may be combined all together, with the analogous purpose to enhance their quality, by alleviating the amount of noise on the signals and, consequently, reducing the induced uncertainties affecting the monitoring results. As already mentioned in the literary review in Chapter 1, several virtuous examples of HDF applications within the civil engineering field may be found in the literature, as for instance in Chatzi and Fuggini [26,27], Ferrari et al. [65–67] and in Ravizza et al. [166], where a KF has been involved within a HDF scheme between artificially generated acceleration and displacement response signals, aiming at obtaining enhanced displacement response measurements, for a 3-DOFs numerical dynamic system (see Chapter 2).

Here, a denoising-based approach, and a HDF procedure are considered all together and possibly coupled within an integrated monitoring methodology for the purification of real response signals, specifically displacement signals, which usually appear to be affected by higher levels of noise, if compared to accelerations. The obtained post-processed enhanced displacement measurements may then be employed toward modal dynamic identification purposes (see e.g. Pioldi et al. [152–154] and Pioldi and Rizzi [155–158]), and this might result of a crucial interest for real applications related to the SHM context.

Although the proposed methodology aims at a general formulation, as to be suitable for the monitoring of different structural systems, here, a specific real test structure is assumed as a case study for the analysis, in order to highlight the feasibility of the proposed monitoring strategy and show its effectiveness. For this purpose, the historic reinforced concrete (RC) bridge at Brivio (1917), i.e. a strategic infrastructure for some local connections within the northern Italy automotive road notwork, has been considered (Santarella and Miozzi [181], Ferrari et al. [68]).

6.1.1 Research goals

The multiple goals that this research scenario aims at achieving are:

- to pursue an effective denoising of real acceleration response data, detected on the monitored structure, through appropriate (wireless) acceleration sensors. In fact, although accelerations usually display a good resolution, when the sensor instrumentation employed during the signal acquisition stage is somehow of a low cost/quality, this may become necessary;
- to successfully perform a denoising-based approach on the original (raw) displacement signals, aiming at clarifying their content in the Time Domain, then resulting in a better representation and reading of the Time Domain signal features;
- to perform a successful HDF, by involving a KF within the fusion procedure between denoised acceleration and denoised displacement response signals, in order to obtain a further enhancement of the displacement data in the Time Domain;
- to employ the enhanced displacements, downstream from the HDF processing, toward possible modal dynamic identification purposes within the Frequency Domain, aiming at estimating the modal characteristics of the considered infrastructure.

To prove that the proposed monitoring methodology becomes competitive, leading to visible benefits to the structural identification process, the modal natural frequencies identified from post-processed displacements are then compared with the frequencies identified from raw data. The effectiveness of the method is proven, as well as its possible generalizations to different typologies of structures.

6.2 Presentation of the monitored structure

The peculiar class of structural systems to which this research development is addressed to, aims at covering civil engineering structures characterized by a significant and strategic importance, possibly combined with a historical-architectural value. In particular, the monitored structure considered as a case study in the current analysis, is the RC Brivio bridge (1917) (Santarella and Miozzi [181], Ferrari et al. [67]), represented in Fig. 6.1.

The bridge, located in northern Italy (Lombardia region), constitutes an important automotive connection between the provinces of Lecco and Bergamo, linking the banks of the Adda river (Brivio (LC) and Cisano Bergamasco (BG)), at an approximate height of 8 m from water.

Figure 6.1: RC three-span arched Brivio bridge (1917) over the Adda river.

About its description, the Brivio bridge consists of three spans, each characterized by a couple of parabolic arches, symmetrically located to the mid-longitudinal plane. The two spans aside the river banks are 43.4 m long; the central span is 44 m long, for a total length of 130.8 m. The deck is 9.2mwide and hosts two roadway lanes and two cantilever sidewalks, of a 0.8 m width each. The deck structural frame of each span is constituted by a grid supporting a RC slab of a thickness of 0.15 m. The peculiar parabolic arches of the bridge display a span of 42.80 m and a rise of 8.00 m. The symmetric arches show a cross section that is 0.60 m wide, with a height varying from 1.25 m (at the middle) to 1.37 m (at the ends). Sixteen vertical RC hangers, characterized by a rectangular cross section of sides of 0.32 m and 0.60 m, connect the deck to each arch. The bridge is supported on the river bed through two tapered concrete piers, each one presenting maximum dimensions at the basis equal to 12.8 m (transverse direction) and 3.8 m (longitudinal direction). The piers rest on foundation RC piles driven into the riverbed for a depth of 13mto 16m (Froio and Zanchi [72]).

The choice of Brivio bridge being taken as a benchmark structure for this study is motivated by the fact that, despite its age of more than one hundred years, the bridge is still subjected to continuous traffic loading, likely much heavier than that for which it was originally designed way back to 1917. Present use includes daily transit of heavy-duty and various vehicles in both rush hours and all day long. Indeed, similarly to other bridges located in the nearby territories (see e.g. the Paderno d'Adda bridge, Ferrari et al. [69], placed south downstream for just a few kilometers), the Brivio bridge still plays a crucial role in the local transportation network and, for this reason, it may largely benefit from a condition monitoring under operational conditions.

It is worth noting that all signals processed in the present analysis have been acquired during a three-day measurement campaign, performed directly on the Brivio bridge, in June 2014. Further details about such a measurement campaign, as for instance information about the employed measurement instrumentation, as well as on the sensor location, may be found in Ferrari et al. [65–68].

6.3 Monitoring methodology description

In this section, a comprehensive monitoring strategy for the health condition assessment of historic bridges is presented, by specifically assuming for illustration the case study of the RC Brivio bridge under operational loading conditions. Both acceleration and displacement response signals, directly detected on the structure as an integrated sensor network are involved within the proposed scheme. In fact, acceleration-based and displacement-based recordings are commonly exploited towards vibration-based monitoring purposes, and the choice of which approach should be preferred, usually depends on the specific monitoring goals to be pursued, as well as on the physical configuration of the analyzed structure.

In particular, acceleration-based monitoring allows to detect changes in the structural health conditions, which may be revealed by identifying variations in the structural modal properties, such as natural frequencies, mode shapes or modal damping ratios, since these quantities may then be employed within damage detection strategies for the current condition assessment of the monitored structure. Displacement-based monitoring, on the other hand, is often exploited both for evaluating the presence of excessive loads under standard service conditions, and for quantifying regular operational loads (e.g. traffic), to serve as reference in bridge design practice.

In this sense, acceleration- and displacement-based monitoring approaches may be considered as complementary, in providing useful tools toward an effective global assessment of historic and strategic infrastructural systems. However, especially due to the increasing demand for the adoption of low-cost monitoring instrumentation during the signal acquisition stage, these measurements may typically be accompanied by a significant amount of noise, which contaminates the structural response itself, by increasing the induced uncertainties and rendering more difficult their employment for SHM purposes. Such a deleterious noise effect is generally more evident on displacement data rather than on acceleration data, due to the intrinsic limits characterizing the present displacement sensor technology

To address this issue, in the proposed monitoring methodology, a denoising-based approach is possibly integrated with a HDF-based procedure, aiming at exploiting the (more reliable) acceleration measurements for clarifying the dynamic displacement response signal of the bridge, acquired by means of a non-contact QDaedalus system (Bürki et al. [18]). The so-obtained purified displacement

data may then be employed toward modal identification purposes, e.g. for extracting the natural frequencies and the mode shapes of the monitored structure, and assessing its current structural conditions.

The present methodology combines a Time-Domain analysis and a Frequency-Domain analysis, as illustrated in the flowchart of Fig. 6.2, representing a global conceptual view of the considered monitoring scheme.

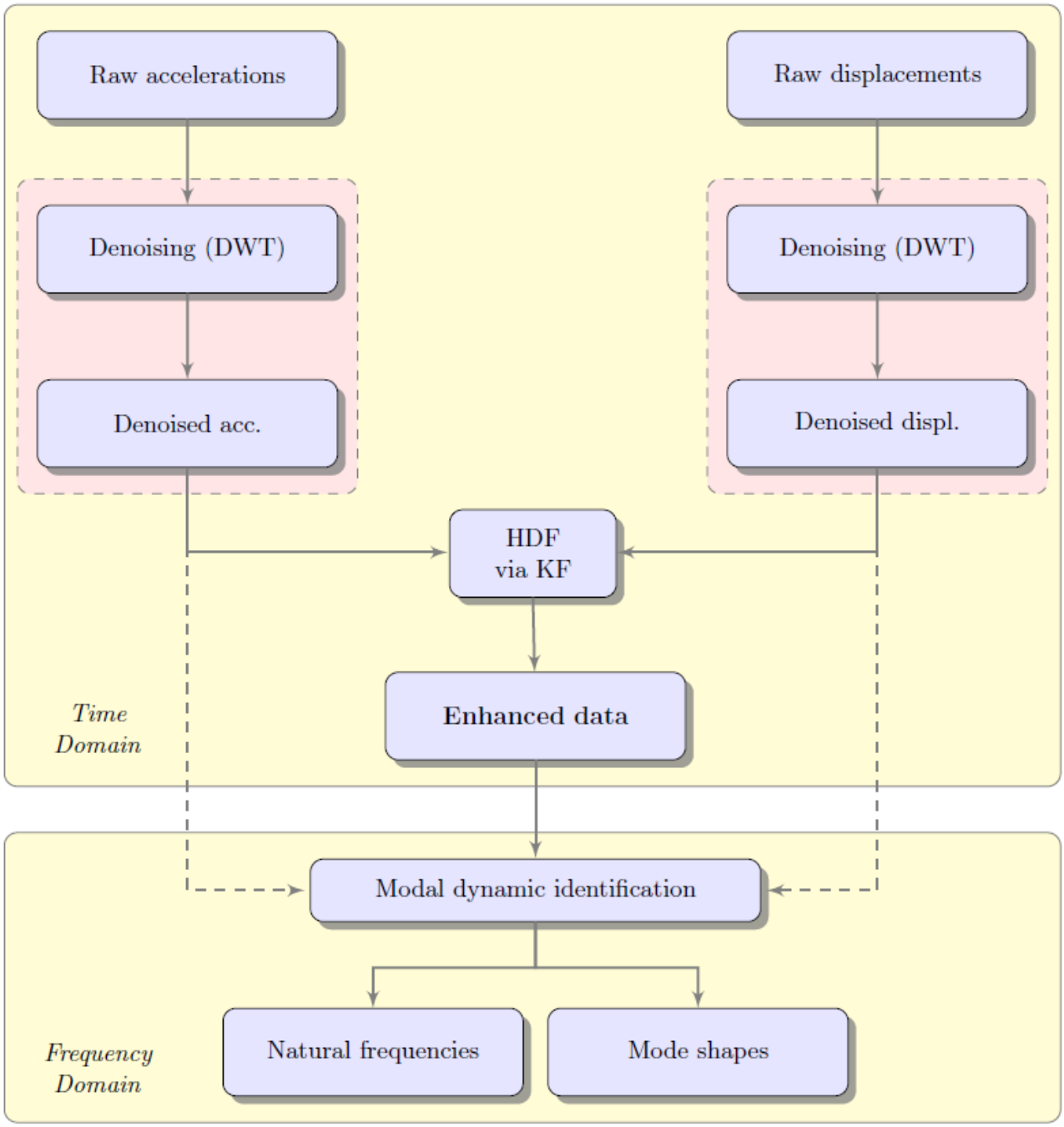

Figure 6.2: Flowchart of the proposed monitoring methodology, integrating a denoising-based and a HDF-based approach for the enhancement of response data collected on the structure, and a subsequent structural dynamic identification.

The Time-Domain analysis aims at a better appreciation of the raw displacement recordings, to be later exploited for modal identification purposes. In doing so, the additional availability of acceleration response data, collected by means of wireless MEMS accelerometers, can be taken at a disposal. Differently from data acquired through wired piezoelectric accelerometers, which may be considered as a rather reliable recording devices, even such raw acceleration data may first need to be purified, by applying appropriate denosing techniques, for reducing the noise level affecting the signal, while preserving the useful information within the recorded signal. To this purpose, a DWT-based denoising technique is implemented within the monitoring platform, resulting in the clarification of the detected acceleration response signal. Details about the calibration of the DWT-based denoising settings, adopted within this study, are provided in the next section. It is worth mentioning that also a SVD-based approach might be employed for the denoising of dynamic response signals; however, dealing with non stationary signals, such as those involved in this analysis, the DWT-based denoising approach should be preferred, as deeply shown and discussed in Ravizza et al. [167, 168].

In parallel to the (optional) acceleration denoising, a more frequently needed denoising of QDaedalus displacements is also foreseen. The same DWT-based technique is adopted, for the aforementioned reasons, and a preliminary cleaning effect on the signal is made achievable.

The core of the current implementation is now represented by the involvement of a KF (Chatzi and Fuggini [26]), see Chapter 2 (Section 2.2.3), within the HDF process, resulting in the merge of denoised QDaedalus displacements with acquired denoised accelerations, and an enhanced displacement response signal can be obtained.

A subsequent analysis within the Frequency Domain is then performed, in which the ambitious goal of successfully performing the modal dynamic identification on displacement data is inspected. In particular, the enhanced displacement response signal is employed for pursuing this purpose and, through an automatic peak-picking procedure performed on the Welch's periodogram, the modal natural frequencies of the Brivio bridge may be identified.

It is worth noting that, as it can be appreciated from the flowchart in Fig. 6.2, the monitoring platform also contemplates the possibility to perform the modal dynamic identification of the structure by solely using either the denoised accelerations or the denoised displacements (dashed arrows in Fig. 6.2), but the results may be less reliable, especially considering just the displacements. However, they can be exploited for comparative purposes, aiming at highlighting the benefits deriving from a HDF-based methodology in assessing the current health condition of the specific analyzed bridge, although such a monitoring platform also aims at assuming a more general connotation, being useful for the structural monitoring of any characteristic infrastructure.

6.4 Analysis results

In this section, some first outcomes obtained by applying the proposed monitoring methodology to the real case of the RC Brivio bridge, are shown. Time-Domain analysis results are firstly presented, followed by outcomes derived from a subsequent analysis within the Frequency Domain. Signals are taken from a measurement campaign as acquired and reported in Ferrari et al. [67].

6.4.1 Time-Domain analysis

The present analysis (upper box in Fig. 6.2) aims at purifying a raw displacement signal, making its features to emerge more clearly in the Time Domain, through an effective HDF with recorded accelerations, supposed to be more reliable. However, in some cases, a preliminary denoising of such acceleration data, may also become necessary, e.g. when the sensor instrumentation employed in the signal acquisition phase is not so performing. In fact, as opposed to a previous analysis by Ferrari et al. [67], in which wired acceleration signals have been processed, it is worthwhile to remark that, here, wireless data are newly employed within the postprocessing analysis, taken benefit from both denoising and HDF application. Therefore, a DWT-based denoising technique is implemented on the detected (original) accelerations (from wireless sensors), and the obtained denoised signal is reported in Fig. 6.3, as compared with the original one.

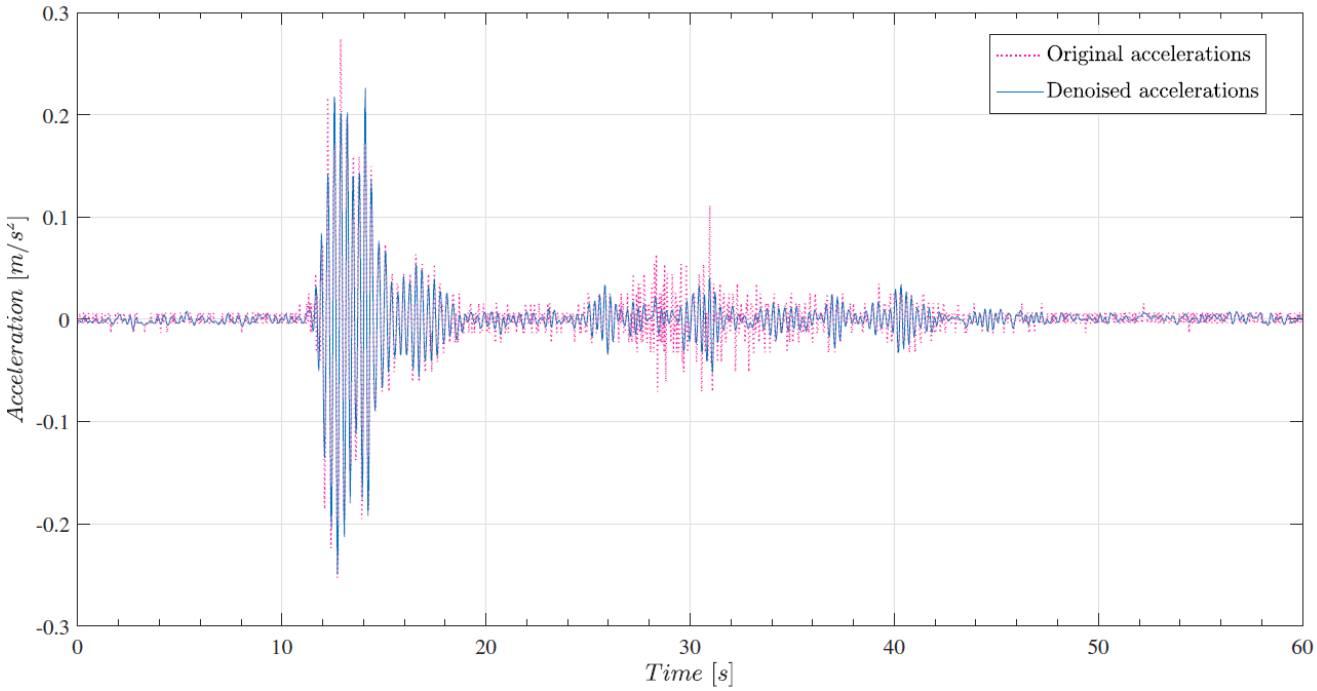

Figure 6.3: Brivio bridge (wireless) acceleration response signal, pre and post DWT-based denoising.

Given the non-stationary nature of the response data, a 60 seconds length acceleration response signal from a wireless sensor is denoised, by applying a DWT-based denoising technique, which shall best

fit with this signal typology, as shown in Ravizza et al. [167, 168]. In previous Chapter 4, the optimal calibration of the parameters involved within this technique to deal with non-stationary signals has been inspected, resulting in the adoption of a Smylet2 mother wavelet, combined with a Heursure hard thresholding rule, at decomposition level 2. Thus, the same setting is here assumed.

The effect of the denoising application is visible, especially in the time window between 25 s and 40 s, as it may be appreciated in Fig. 6.3, leading to a signal reduction of 6.58%, in terms of Root Mean Square (RMS). The acceleration peak value is also considered, as it represents one most peculiar Time-Domain signal feature, and a reduction of 9.11% is recorded. Such values are reported in following Table 6.1, for both the original and the denoised acceleration response signals.

Acceleration signal	**RMS** $[m/s^2]$	Δ [%]	**Peak** $[m/s^2]$	Δ [%]
Original (raw) signal	0.0319		0.2742	
DWT denoised signal	0.0298	−6.58	0.2492	−9.11

Table 6.1: Characteristic values of the analyzed acceleration response signals in the time domain and their variation with respect to the original (noise-affected) signal: RMS and peak acceleration values.

An analogous DWT-based denoising approach is now implemented, for the preliminary clarification of a 60 seconds length QDaedalus displacement response signal, acquired on the Brivio bridge. Despite the very small amplitude of such recordings, which might affect the success of the denoising technique, the denoised estimates appear to be considerably clearer, if compared to the original (raw) data, as represented in Fig. 6.4.

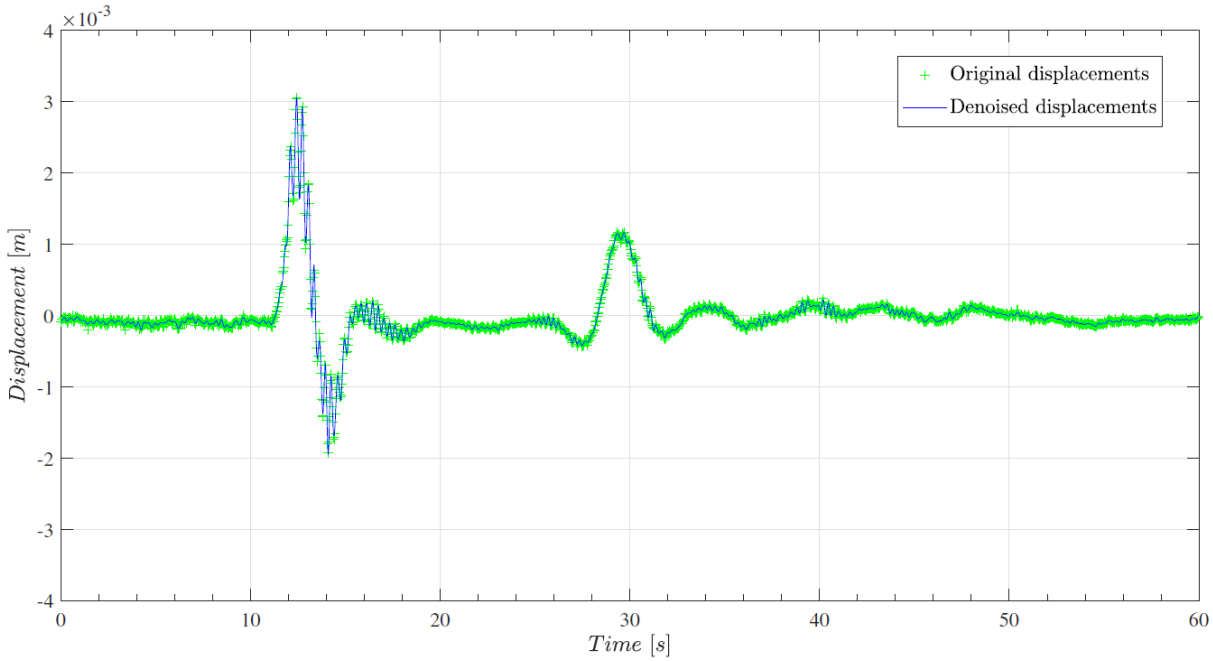

Figure 6.4: Brivio bridge (total station) displacement response signal, pre and post DWT-based denoising.

After this preliminary phase, devoted to the pre-treatment of the acquired data, the obtained denoised acceleration and displacement response signals are then processed within a HDF-based implementation, aiming at further enhancing the measured displacements, by enriching them through the information embedded within the denoised accelerations. To this end, a KF algorithm is exploited (see Chapter 2), allowing for the effective merge of the two heterogeneous source signals (Chatzi and Fuggini [26], Ferrari et al. [67], Ravizza et al. [166]). The result is represented by a new enhanced displacement signal, as shown in Fig. 6.5, which more reliably reflects the response of the monitored bridge.

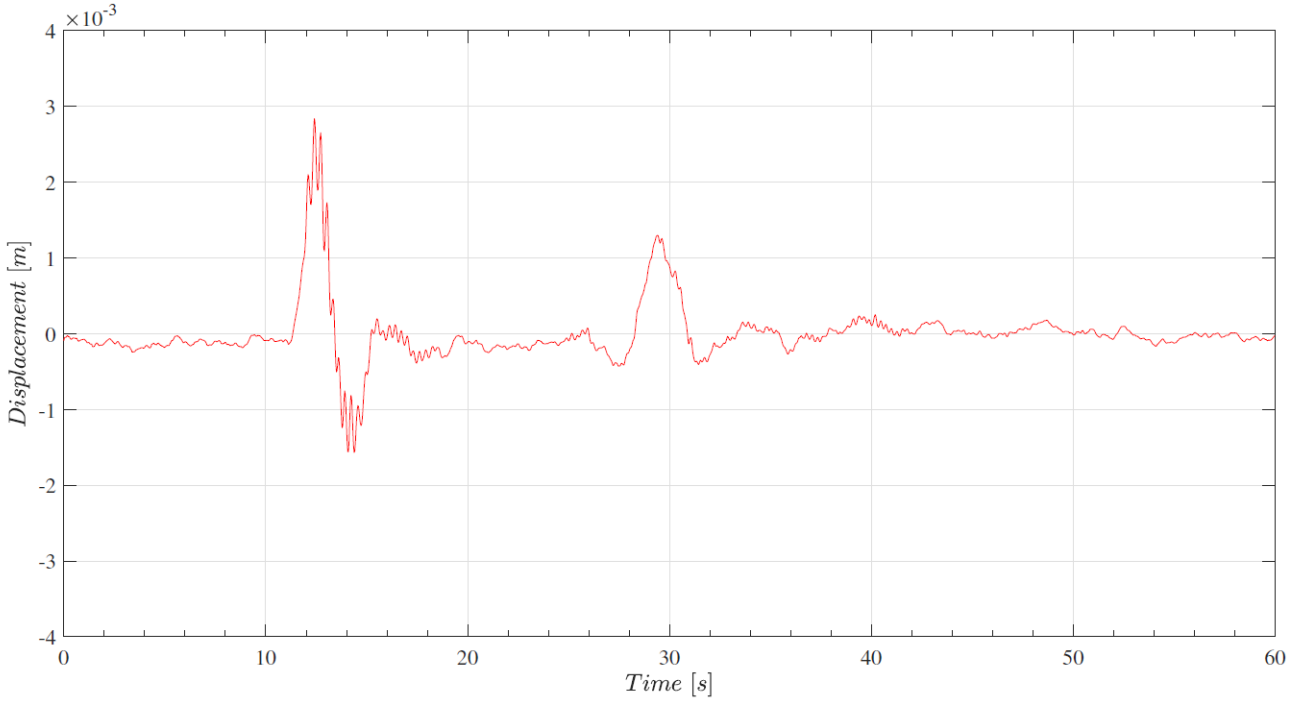

Figure 6.5: Enhanced Brivio bridge displacement response signal, obtained by HDF via KF with the denoised acceleration response signal.

To complete the Time Domain analysis, RMS and peak deflection values of the displacement signals are also computed, and summarized in Table 6.2.

Displacement signal	**RMS** $[mm]$	Δ [%]	**Peak** $[mm]$	Δ [%]
Original (raw) signal	0.4039		3.056	
DWT denoised signal	0.4001	−0.94	3.015	−1.34
HDF enhanced signal	0.3972	−1.66	2.833	−7.30

Table 6.2: Characteristic values of the analyzed displacement response signals in the Time Domain and their variation with respect to the original (noise-affected) signal: RMS and peak deflection values.

A reduction of both values, although lighter than that recorded in the previous acceleration case, is still observable, configuring itself as a peculiar feature of such techniques, as previously shown for synthetic signals in Chapter 4, as well as for real signals in Chapter 5.

6.4.2 Frequency-Domain analysis

The enhanced displacement data, downstream obtained from the HDF procedure with the denoised accelerations, are now employed for performing a modal dynamic identification analysis within the frequency domain. In particular, by applying a Welch's method on such displacements, the PSD function of the signal may be obtained. In following Fig. 6.6, the response spectrum derived from the HDF displacement signal and from the original (raw) displacement signal are represented and compared.

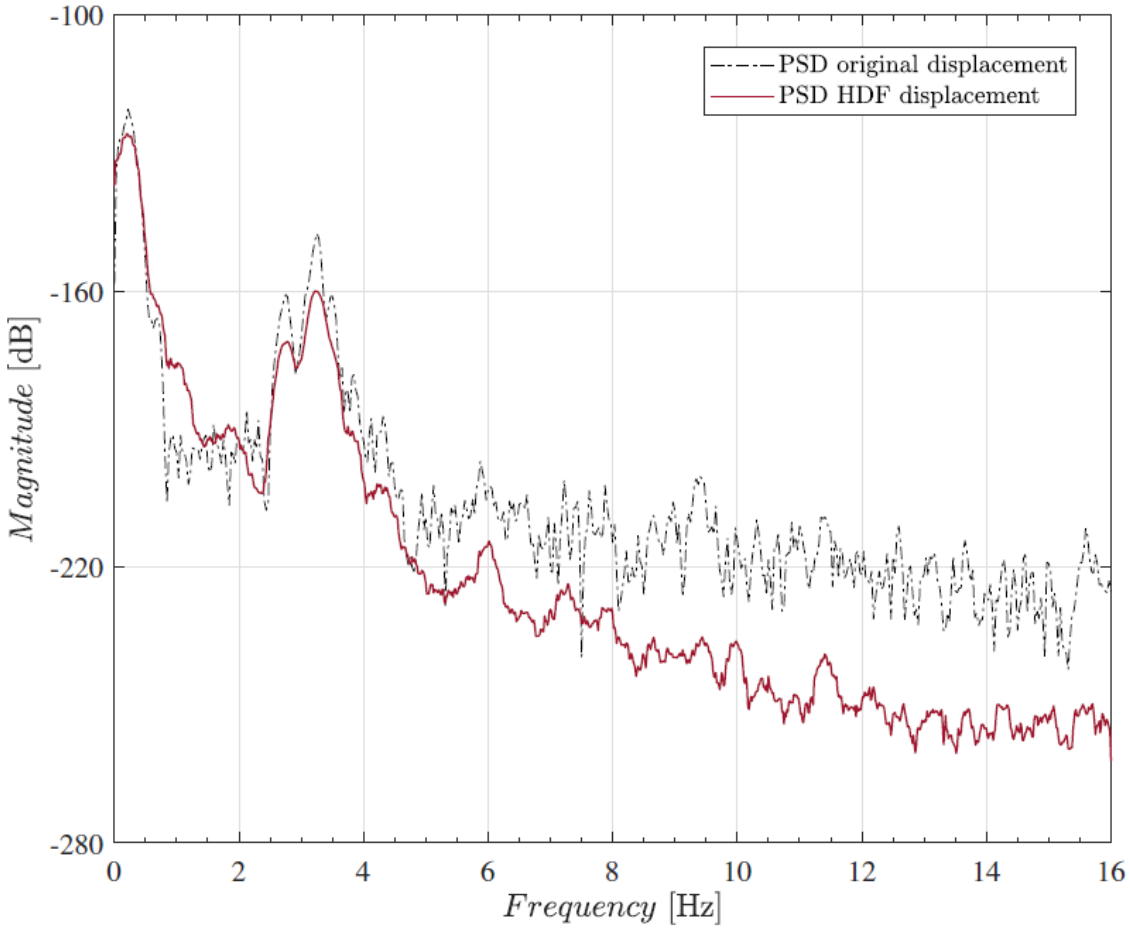

Figure 6.6: Brivio Bridge displacement (PSD) response spectrum: original (raw) displacement signal vs. HDF (enhanced) displacement signal.

The effect of the previously applied Time-Domain filtering techniques (i.e. DWT-based denoising and KF application) is evident, resulting in smoother curves, as well as in the reduction of the signal

magnitude, especially within the medium-high frequency region (approximately greater than 6 Hz), where the embedded noise mainly affects the data.

The benefits that the proposed methodology has brought to the identification process emerge by the comparison between the frequency content of the two signals. In fact, whether the original signal allows for the detection of just one frequency peak, corresponding to the first natural frequency of the bridge, the post-processed displacement signal reveals a greater number of frequency response peaks, which were previously indistinguishable, due to the deleterious effect of spurious noise. Consequently, a greater number of natural frequencies may be extracted.

However, due to the limited length of the time window, even the peaks associated to the external loading acting on the bridge (i.e. traffic load) might appear in the response spectrum, making harder the identification process. Thus, to distinguish such peaks from structural modes, an automatic peak-picking procedure is performed on the Welch's periodogram, and the first eight natural frequencies of the monitored structure may be identified. To emphasize the benefits that the proposed methodology may bring to the identification process, the same peak-picking technique is performed on the PSD of the original (raw) displacement signal, leading to the identification of the first natural frequency only. Such a comparison is represented in Fig. 6.7, where the modal natural frequencies are marked by vertical red lines, and further reported in Table 6.3, which coherently compare to analogous results provided in Ferrari et al. [67], namely frequencies identified through a classical FDD method on acceleration signals acquired out of standard wired accelerometer sensors.

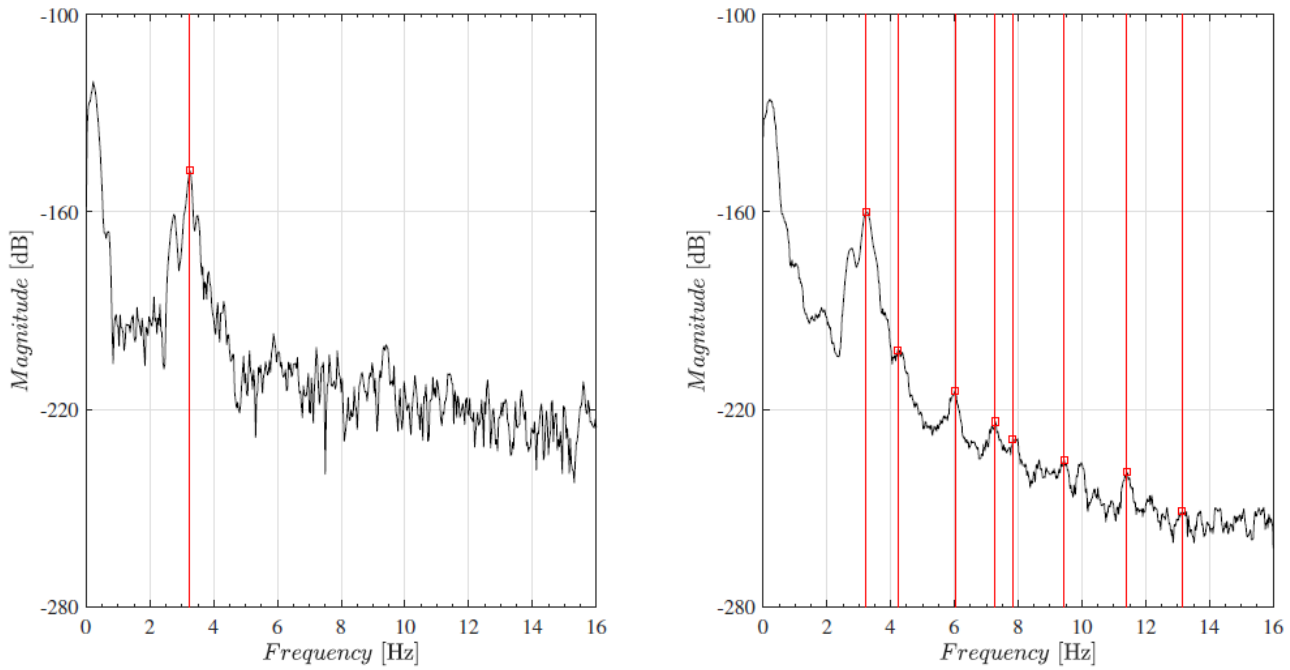

Figure 6.7: Brivio bridge identified natural frequencies from displacements. Peak-picking procedure on Welch's periodogram: original (raw) displacement signal vs. HDF (enhanced) displacement signal.

Modes	I	II	III	IV	V	VI	VII	VIII
$f_{id,WD}$ [Hz]	3.247	4.211	6.016	7.280	7.815	9.378	11.406	13.140
$f_{id,AC}$ [Hz]	3.564	3.857	6.018	7.178	7.690	9.009	11.377	13.086
Δ [%]	−8.89	9.18	−0.03	1.42	1.63	4.10	0.25	0.41

Table 6.3: Brivio bridge natural frequencies $f_{id,WD}$ identified from a HDF displacement response signal (wireless sensor), compared to frequencies $f_{id,AC}$ (Ferrari et al. [67]) identified from an acceleration response signal (wired sensor), and their variation.

Except for the first two and the sixth natural frequencies, which display a not negligible discrepancy with the respective outcomes deriving from a FDD-based inverse analysis on wired accelerations, assumed here as reference, the results show a good agreement, as the percentage variation is in any case below 2%. Finally, from a FDD analysis (Pioldi et al. [152–154]) on displacement signals (corroborated as above by acceleration data), the bridge first span mode shapes, corresponding to the previously identified frequencies, are obtained and represented in following Fig. 6.8.

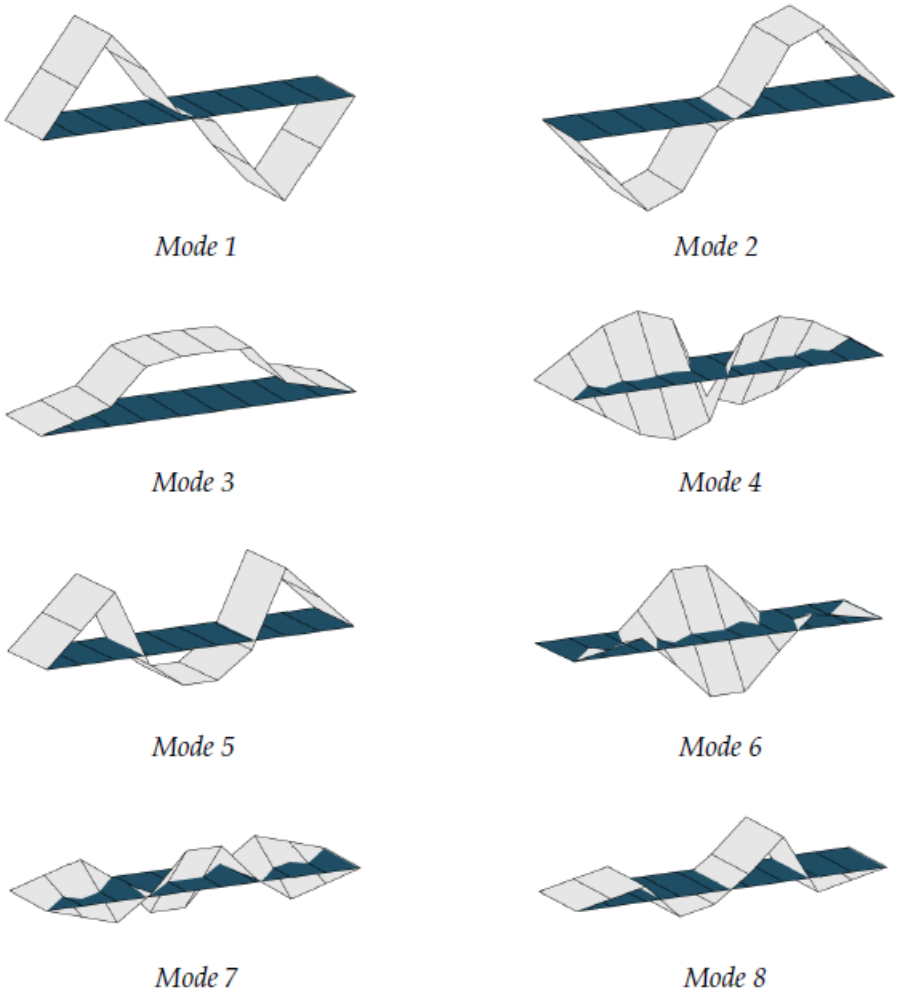

Figure 6.8: FDD vibration mode shapes of Brivio bridge first span.

In particular, the QDaedalus displacement data, enriched by reliable accelerations, as those acquired through a wireless detection system, represent the selected 8-channel input considered within the current analysis, for the representation of the mode shapes of the monitored structure.
Even concerning the vibration mode shapes, many analogies with the respective results reported in Ferrari et al. [67] may be observed. In particular, mode 1 and mode 2 show a very similar behaviour, although they are related to different natural frequencies. Moreover, most of the modes seem to be regular, characterized by bending or torsion, except for mode 7, in which bending and torsion appear to be coupled.
These similarities between the results may be considered as a further proof of the reliability of the proposed monitoring strategy, which provides an alternative approach aiming at evaluating the structural health condition of a generic civil structural system.

6.5 Final remarks

In this chapter, an innovative monitoring methodology that integrates a denoising-based approach with a HDF-based strategy is proposed, for the structural health condition assessment of historic and strategic bridges. In particular, the main achievements that the present research scenario has highlighted may be summarized as follows:

- the beneficial effect of the analyzed denoising technique is more pronounced within the Time Domain, where, after the DWT-based denoising application, the main signal features (i.e. peak value and RMS) may more clearly emerge;
- the acquired Brivio bridge acceleration and displacement response signals have been successfully denoised and, subsequently, involved within a HDF-based implementation, and an enhanced displacement response signal has been obtained;
- the output-only modal identification analysis performed on the enhanced displacement signal reveals the natural frequencies of the investigated structure, proving the effectiveness of the proposed methodology;
- by comparing the obtained results, by effective post-processing of response signals detected through wireless sensors, with those derived from signals acquired through standard wired sensors, no substantial differences emerge: this reinforces the belief that modern wireless sensor technology may become competitive at the signal acquisition stage, if adequately treated as here described, leading to reliable estimates.

In conclusion, the possibility of setting a monitoring platform that integrates a denoising-based approach with a HDF-based strategy may allow the user to achieve a more complete and reliable description of specific response signals, bringing to light their more peculiar characteristics, in both

Time and Frequency Domains. In this sense, the proposed post-processing methodology may constitute a useful tool within Structural Health Monitoring applications.

Conclusions

This research has concerned the implementation of multiple postprocessing approaches for the treatment of spurious noise affecting structural response signals of a different nature (non-stationary vs. stationary), and for their subsequent analysis, toward Structural Health Monitoring (SHM) purposes.

It is specifically aimed at improving the reliability of the monitoring process, in order to determine, with an adequate degree of precision, the current health condition of a certain examined structure. In particular, Heterogeneous Data Fusion (HDF)-based approaches between acceleration and displacement measurements, Denoising-based techniques, as well as integrated hybrid post-processing approaches, have been inspected, and addressed toward modal identification purposes, through the adoption of appropriate inverse analysis algorithms. To achieve an adequately exhaustive understanding of the research topics covered in the present work, firstly synthetic signals, i.e. pseudo-experimental signals artificially generated by numerical computation prior to the analysis, and subsequently real signals, namely signals truly recorded in situ through appropriate sensors, have been considered within the analysis.

Here, some of the main achievements that this research shall have brought to light are summarized and reported, chapter by chapter. Finally, possible future research developments, relevant to the covered topics, are also outlined.

Chapter 1 has been devoted to provide a main literature review on HDF procedures within SHM applications. With a chief reference to the civil engineering field, such a literature review has been conceived as a *trait d'union* between the practical finality of evaluating the health conditions of a monitored structure, and the need to develop post-processing approaches, which aim at improving the quality of response signals acquired by sensors of a different nature, by fusing them together. A Kalman Filter (KF) has been employed toward this purpose, as it represents a powerful and consolidated tool to deal with heterogeneous data, as it has further been revealed by the present research work.

In the literature review of the chapter, the following salient points have been disclosed.

- *Role of accelerations and displacements for SHM purposes* (through a comparison between strengths and weaknesses of the instrumentation employed for acquiring such types of data). From the literature, it has emerged that, for "on field" measurements, accelerometers have proven to be more reliable than displacement sensors, and this consideration has constituted a milestone for the whole analysis conducted in the present research.

- *Main issues of inherent data treatment that may occur within DF procedures.* In particular, a classification according to the typology of error that may affect the data (i.e. imperfection, correlation, inconsistency, disparateness) has been proposed. Sub-categories of such errors have also been mentioned.
- *Existing theories dealing with data affected by errors.* Great importance has been given to Probability Theory, that has allowed to introduce KF as an important tool for implementing DF-based procedures. In this instance, the linear-Gaussian assumption has also been disclosed, as well as its importance for the success of DF-based processes. Hybrid approaches (Fuzzy DSET Theory and Random Finite Set Theory) have also been presented, as valid alternatives to more classical ones, for treating imperfect data. However, a global theory able to deal with all the different kind of errors affecting the data has not been developed yet.
- *Emerging trends and future perspectives in DF procedures* (stressing on the necessity of common criteria for evaluating the effectiveness of a fusion system). From this, the need of a standardization of the measures of performance has emerged, as applicable to the practical evaluation of DF-based procedures.
- *Need of filtering procedures to reduce uncertainty* (in data that have to be fused). The main characteristics of a basic filter, such as operation in discrete time, linearity, optimality and finite dimensionality, have been inspected, as well as the probabilistic origin of KF, helpful to understand its operating conditions.
- *KF applications for SHM purposes within the structural engineering field*. Based on the fact that information about the dynamic response of a structure may allow to identify changes in its mechanical properties, KF may be employed for estimating such a dynamic response. This approach may also be extended to the identification of the structural modal parameters from the observation of the dynamic behaviour of an examined system.

Finally, recent examples in which a KF has been employed to merge data from heterogeneous sensors (i.e. accelerometers and GPS transducers), aiming at deriving more accurate displacement estimates, have also been provided.

Chapter 2 proposed several numerical analyses involving KF into the fusion of acceleration and displacement response signals, aiming at enhancing this specific latter class of data. As previously mentioned, the choice of these types of response data is reflected in practical applications. In fact, within the civil and mechanical engineering fields, accelerometers are most often used, although displacement sensors are becoming more and more common and useful for SHM purposes. This suggests, wherever possible, to combine acceleration and displacement measurements, in order to obtain estimates of an improved accuracy. Moreover, this may circumvent the issue of the time

integration of the acceleration data, which may lead to the so-called drift, as well as other issues involved in the differentiation of displacement data, which may amplify the high-frequency noise. In addition, the high-frequency resolution of displacement sensors is limited, and usually low sampling rates are used. In contrast, accelerometers are often more accurate within the high-frequency region, and higher sampling rates are often available. Thus, the merging of these measurements should combine data sampled at different frequencies. Accordingly, a multi-rate KF approach has been proposed, to tackle this issue. In order to simulate the errors that may occur during the measurement acquisition stage, different N/S ratios have been added to synthetic response data obtained from a 3-DOF shear-type dynamic system subjected to stationary ambient vibration top-floor loading.

Two main scenarios have been inspected, according to the level of noise affecting the acceleration measurements, namely **(i)** noise-free acceleration case and **(ii)** noise-affected acceleration case. Main conclusions about the proposed numerical analyses are listed in the following, for each of the above-mentioned scenarios.

i. *Noise-free acceleration case.* This represents the most explored scenario within the DF literature (Smyth andWu [192]). From the analysis performed in this research, it has been proven that KF turns out to be able to provide reliable estimates of the structural dynamic response, for N/S ratios on displacements up to 50%. Indeed, in such cases, RMS errors below 1% between the estimated displacements after KF application and the original (noise-free, numerically determined) displacements, have been observed. Results of this scenario seem to be in accordance with those reported within the reference literature.

ii. *Noise-affected acceleration case.* This scenario does not seem to have been deeply inspected in the literature yet. Results have shown that only N/S ratios on acceleration below 1% may lead to reliable estimates of the dynamic response after KF adoption. Consequently, in practice, the accelerometer placement shall play a key role for achieving reliable KF estimates. In fact, if the intrinsic error characterizing accelerometers appears to be greater than 1%, RMS errors greater than 8% between the estimated displacements after KF application and the original (noise-free, numerically determined) displacements, turn out to be observed.

Chapter 3 has concerned a subsequent research development of what it has been covered in the previous chapter, namely the extension of a HDF-based approach to the more challenging case of seismic-excited structural systems. In particular, a set of ten different seismic input signals, each one assumed to be singularly applied at the basis of the same 3-DOF benchmark structure, has been considered. A multi-rate KF is employed within a HDF procedure between acceleration and displacement response signals of such a structure and, through the proposed implementation, it has been possible to enhance the considered non-stationary displacement response signals, by integrating

it with a few standard acceleration measurements (considered as noise-free). Based on the obtained results, it may be stated that the procedure turned out to be rather effective, leading to a much better understanding of the structural modal properties within the Frequency Domain, specifically in terms of natural frequencies of the analyzed system. Furthermore, it has been shown that the resulting estimates obtained through the modal identification procedure carried out on the enhanced displacement signals, proved to be competitive with those deriving from accelerations. This might open up new interesting perspectives within SHM applications, since displacement signals may easily be acquired also through indirect instrumentation techniques, without directly acting on the monitored structure, for instance by means of a total station. As a result, this could ease the signal acquisition phase, making it faster and more efficient.

Chapter 4 introduced a new research topic, deeply treated in this research work, namely the issue of signal denoising, with reference to both non-stationary and stationary synthetic acceleration response signals. The main goal of such a procedure has concerned the purification of such noise-corrupted response signals, by removing the deleterious noise but maintaining the useful information contained within the signals. In particular, two denoising-based approaches have been studied, i.e. DWT- and SVD-based denoising techniques, assuming as a benchmark application structure a 10-DOF shear-type building. Through a numerical analysis within both the Time and the Frequency Domains, it has been possible to provide a comprehensive comparative framework on the effectiveness of the two implemented denoising approaches, leading to the following salient considerations:

- in general terms, both the denoising techniques revealed that stationary signals proved to be more problematic to be purified than for non-stationary ones, due to their almost constant distribution in time and frequency;
- the effectiveness of the SVD-based denoising method may be considered as being fully proven. It has been stated that it constitutes a rather robust technique, which is able to return reliable estimates of the original (noise-free) signal, despite for the significant amount of additive noise assumed on the source data. Moreover, this technique seems to be suitable for both non-stationary and stationary response signals;
- the DWT-based approach may be considered as useful for the denoising of non-stationary signals, such as seismic response signals, especially for N/S ratios lower than 20%, where it may provide even better results than those for the SVD-based approach. However, the performed analysis has proven also its limitations, especially in the processing of stationary signals, for which the application of the denoising method based on SVD should instead be suggested;

- about a further analysis aiming at evaluating the alteration of the main signal peak value, after the denoising application, it emerged that non-stationary signals lead to a more evident percentage peak reduction with respect to the numerically determined value, than for stationary response signals.
- interesting results have been obtained even within the Frequency Domain, where, through a comparison between the signal response spectra, pre- and post-denoising application, it has been possible to better appreciate the denoising effect, in particular within the medium-high frequency region.

Chapter 5 introduced the analysis of real response signals, detected on a short-span RC railway bridge (monitored at ETH Zürich), and their processing within a denoising-based implementation, aiming at clarifying their content in both Time and Frequency Domains. In particular, the previously presented DWT- and SVD-based denoising approaches have there been reconsidered, for dealing with such real acceleration response signals, and the considerations to which the obtained results led, may briefly be summarized as follows:

- the outcomes proved to be coherent with those deriving from the numerical analysis with synthetic signals, reinforcing the usefulness of such a denoising-based approach during the signal post-processing phase;
- the beneficial effect of the denoising application in alleviating the noise affecting the examined real response signals has mainly emerged within the Time-Domain analysis, where the processed signal appeared to be smoother, with respect to the noisy source signal and, consequently, its features might more clearly emerge;
- about the Frequency-Domain analysis, the useful information which the signals contain appeared to be preserved, as the most significant modal frequencies turned out to be unchanged, although there did not seem to be a marked gain in the number of identifiable modal frequencies, justifying the need for further possible research on this aspect;
- the reduction of the acceleration peak, visible on synthetic signals after the denoising application, has been confirmed even on real signals, according to both the applied denoising techniques, to such an extent that it may reasonably be considered as a general trend of such denoising techniques.
- From the analysis presented in Chapters 4 and 5, it can be concluded that the effectiveness of DWT- and SVD-based denoising techniques in clarifying both synthetic and real structural response signals may be considered to have been proven. Consequently, such a denoising-based approach should be taken into account within SHM applications, since it may provide

a decisive contribution to the monitoring process, especially within the Time Domain, as regards the post-processing phase of the acquired response signals.

Chapter 6 has finally concerned the development of an integrated monitoring strategy, which involves a HDF-based procedure via KF, and a denoising-based approach, aiming at enhancing real dynamic response signals detected on historic infrastructures. In particular, the historic RC Brivio bridge (1917) under operational conditions has been monitored, through the HDF between its accelerations and displacements, previously properly denoised by means of the DWT-based denoising technique. The presented strategy was specifically addressed to clarify the acquired wireless displacements, which have been subsequently employed for extracting the modal properties of the bridge, namely its natural frequencies and associated mode shapes. Satisfactory results have been achieved, as briefly summarized as follows:

- the DWT-based denoising confirmed to be effective for clarifying both real acceleration and displacement response signals, and the main Time-Domain signal features (i.e. the signal peak, as well as its RMS) could appear more clearly;
- the HDF-based approach, instead, revealed to be more useful within the Frequency Domain, allowing for the modal identification of the first eight natural frequencies of the monitored bridge, as well as of the associated vibration modes;
- the modal identification procedure performed on the post-processed displacements has proven to be effective, configuring itself as a competitive alternative to the most common modal identification performed on accelerations.

Concluding, it may be stated that an integrated procedure which exploits both the potential of a HDF-based approach and of a denoising-based approach, revealed to be an important tool which may allow the user to better understand the peculiar characteristics of real response signals, and, consequently, to perform a more effective monitoring of the examined structure.

Finally, some possible future research developments which are worth mentioning, are also outlined. A first scenario could represent the exclusive employment of (possibly cleaned) displacement response signals for modal identification purposes, without the support of any acceleration data, in order to avoid directly acting on the structure, by predisposing accelerometers at a certain number of locations. This would speed up the phase of signal acquisition during in situ measurement campaigns. A further scenario might eventually concern the extension of the presented methodologies to other classes of dynamic signals, also not necessarily strictly belonging to the mechanical response within the civil engineering field, such as, for instance, temperature and humidity signals, since their variation may display some implications also on the structural behaviour and, consequently, they are worth being monitored, for a complete success of SHM applications.

Appendices

Appendix A

In present Appendix A, the data of the seismic ground motions employed within the HDF-based analysis developed in Chapter 3 are reported. The associated seismic input signals have been supposed as singularly acting at the base of a 3-DOF shear-type building (see Fig. 3.1), taken as a benchmark structure for the related investigation. In particular, a set of ten earthquake excitations, which differ for location of the epicenter, magnitude, duration and Peak Ground Acceleration (PGA), are considered, as summarized in Table A.1.

	Earthquake	Station	Comp.	M	Dur. [s]	PGA [g]
(A.1)	Imperial Valley 1940	El Centro	S00E	6.9	40	0.359
(A.2)	Tabas 1978	70, Boshrooyeh	WE	7.3	43	0.929
(A.3)	Imperial Valley 1979	01260	NS	6.4	58	0.331
(A.4)	Loma Prieta 1989	Corralitos	0	7.0	25	0.801
(A.5)	Northridge 1994	24436	WE	6.7	60	1.778
(A.6)	L'Aquila 2009	Valle Aterno	WE	5.8	50	0.676
(A.7)	Chile 2010	Angle	WE	8.8	180	0.697
(A.8)	New Zealand 2010	163541	NS	7.1	82	0.752
(A.9)	Tohoku 2011	Sendai	NS	9.0	180	1.402
(A.10)	Katmandu 2015	Kanti Path	NS	7.8	100	0.164

Table A.1: Seismic input data-set generalities and reference labels adopted in the subsequent plots.

The acceleration records describing the considered earthquake motions are instead depicted in following Figs. A.1–A.10, which refer to previous Table A.1. Further information on time-frequency spectra may be found in Pioldi and Rizzi [157, 158], as well as in Pioldi et al. [152–154].

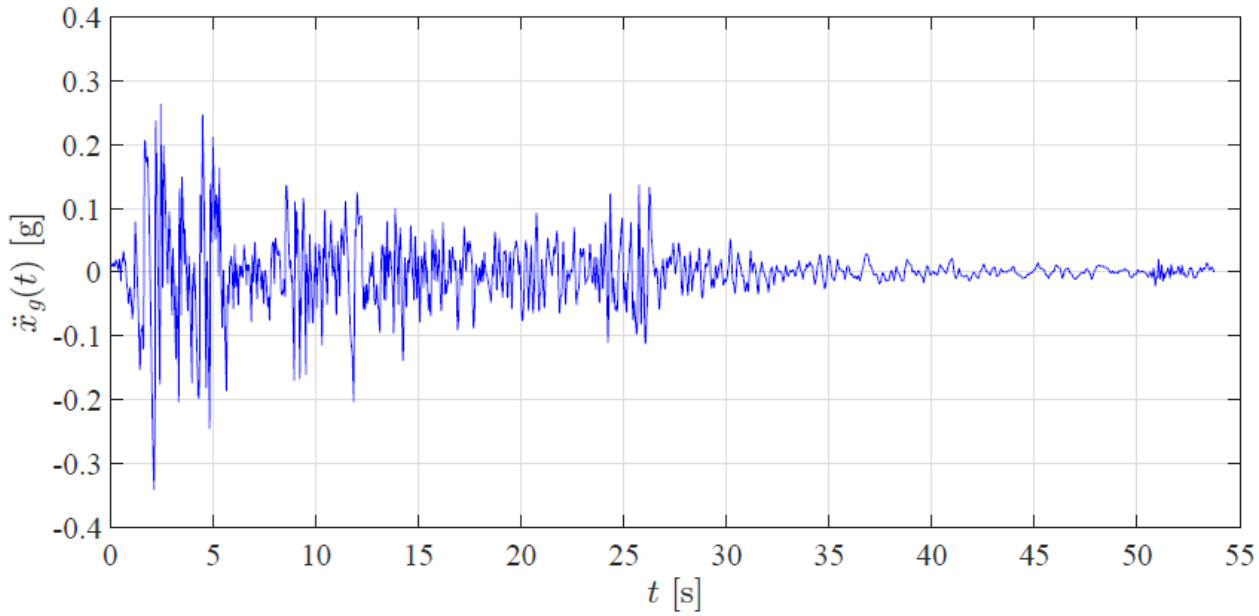

Figure A.1: Imperial Valley (1940) seismic accelerogram.

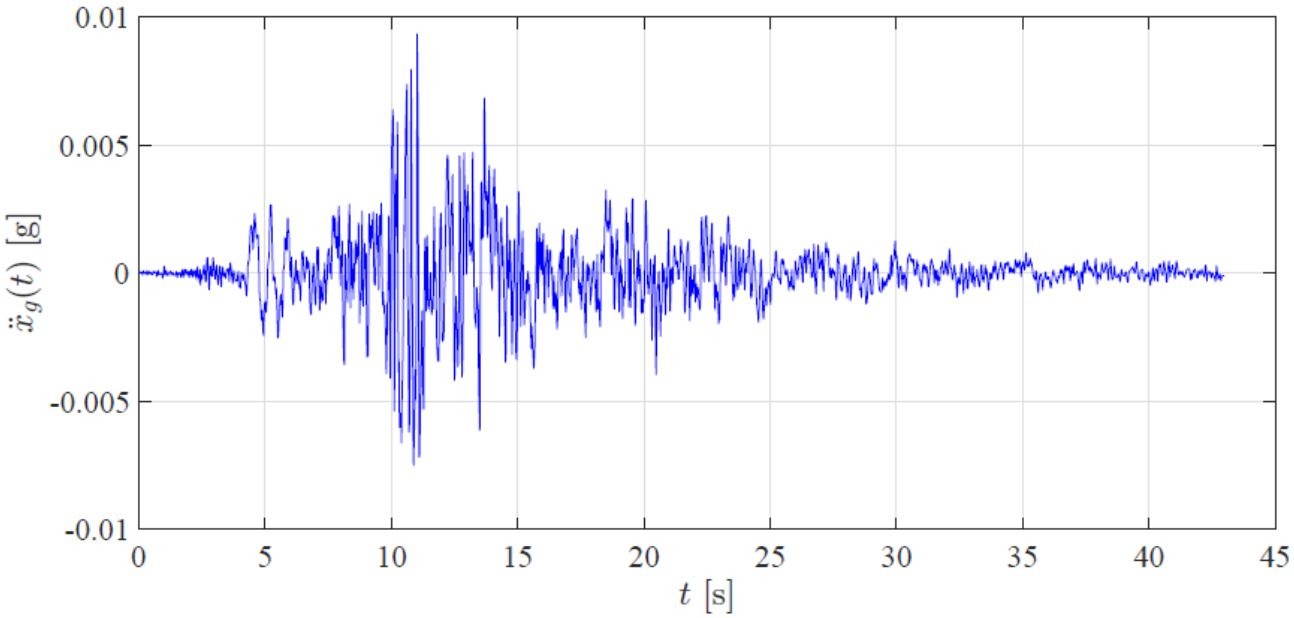

Figure A.2: Tabas (1978) seismic accelerogram.

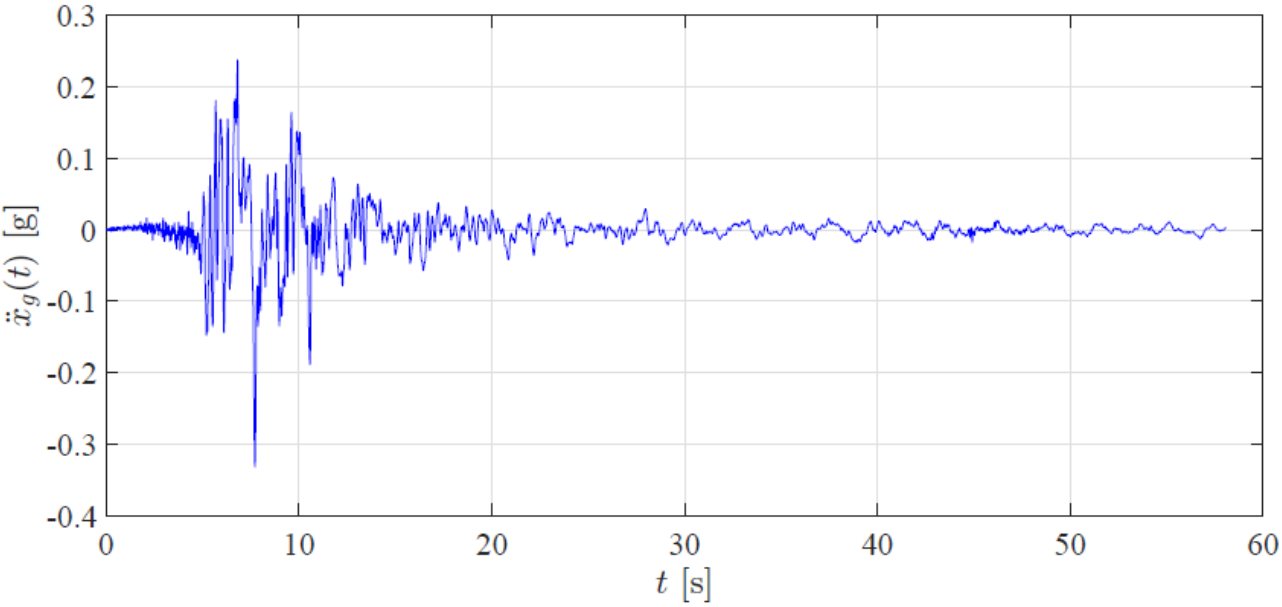

Figure A.3: Imperial Valley (1979) seismic accelerogram.

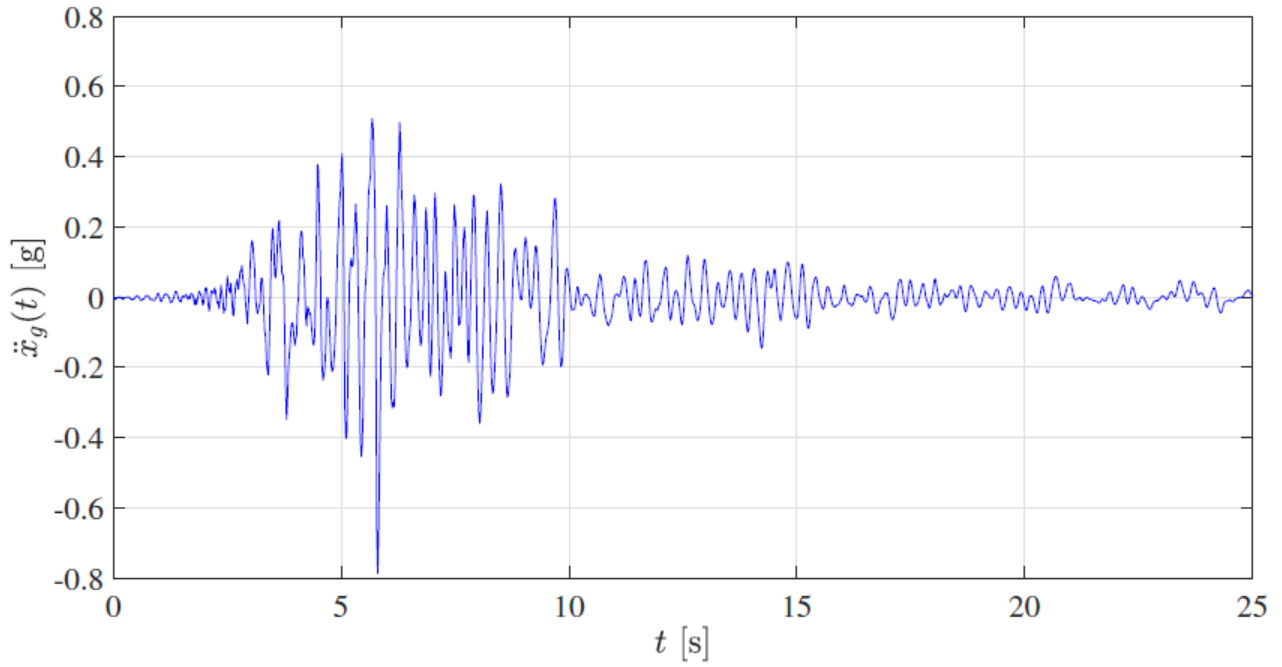

Figure A.4: Loma Prieta (1989) seismic accelerogram.

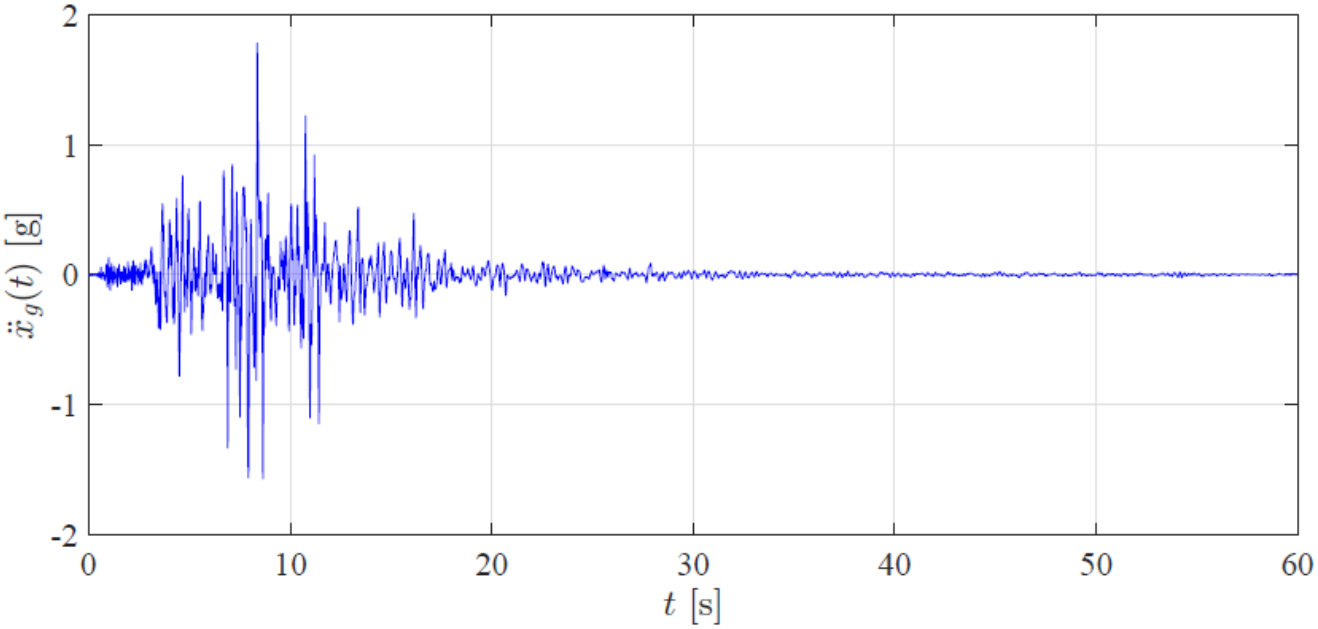

Figure A.5: Northridge (1994) seismic accelerogram.

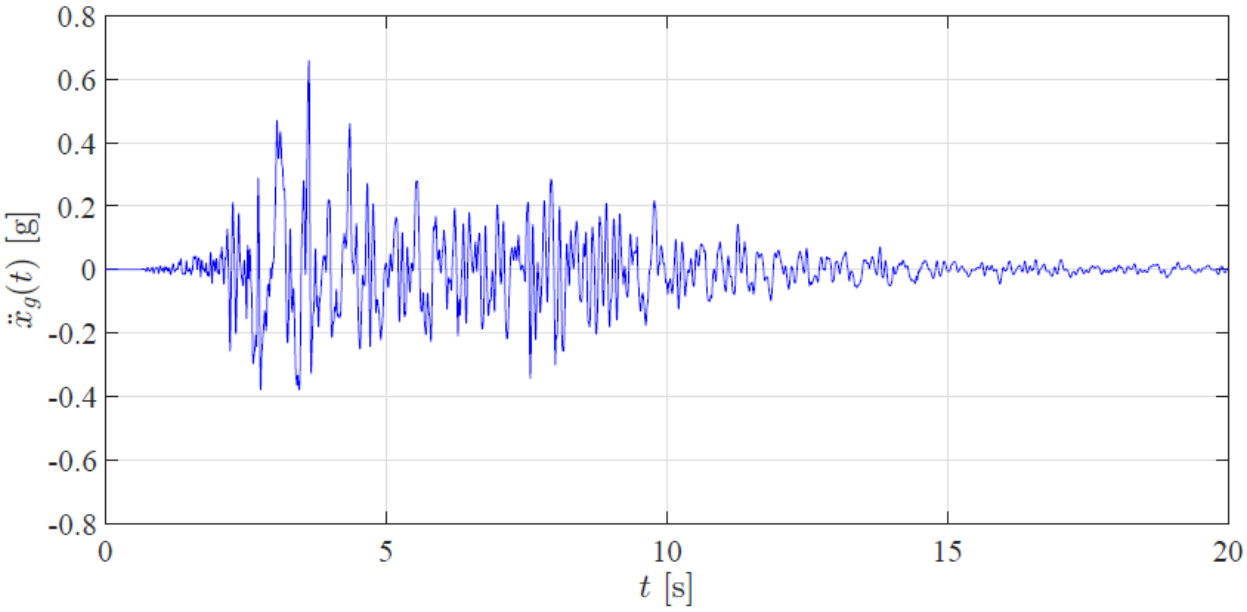

Figure A.6: L'Aquila (2009) seismic accelerogram.

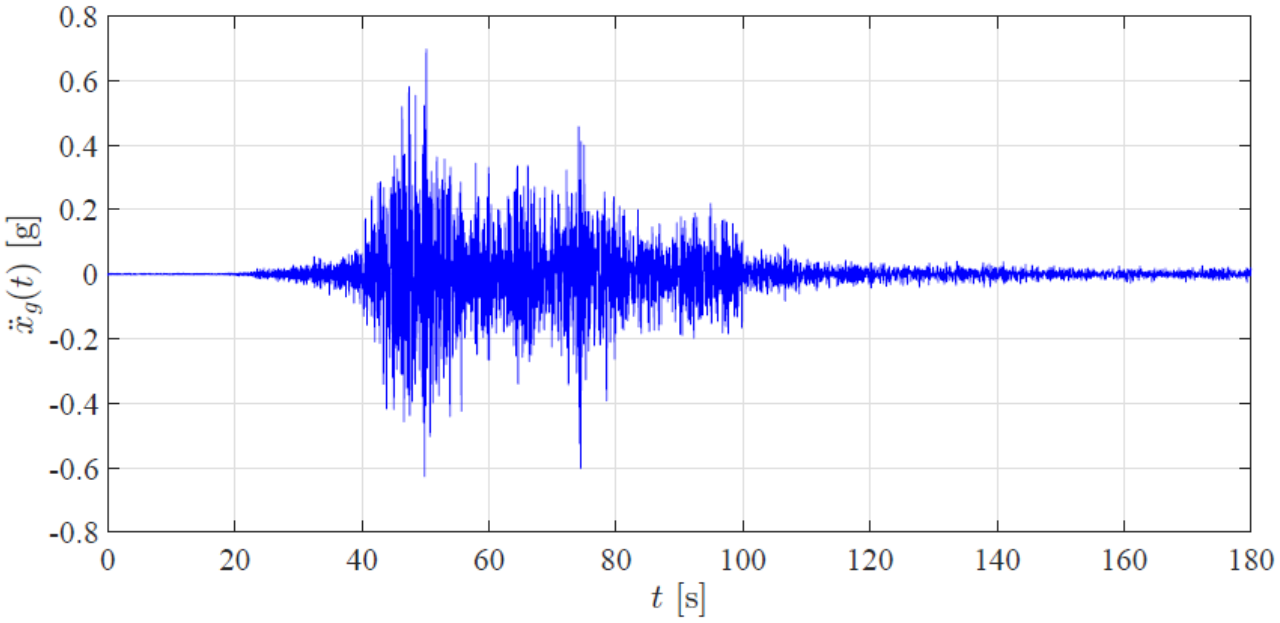

Figure A.7: Chile (2010) seismic accelerogram.

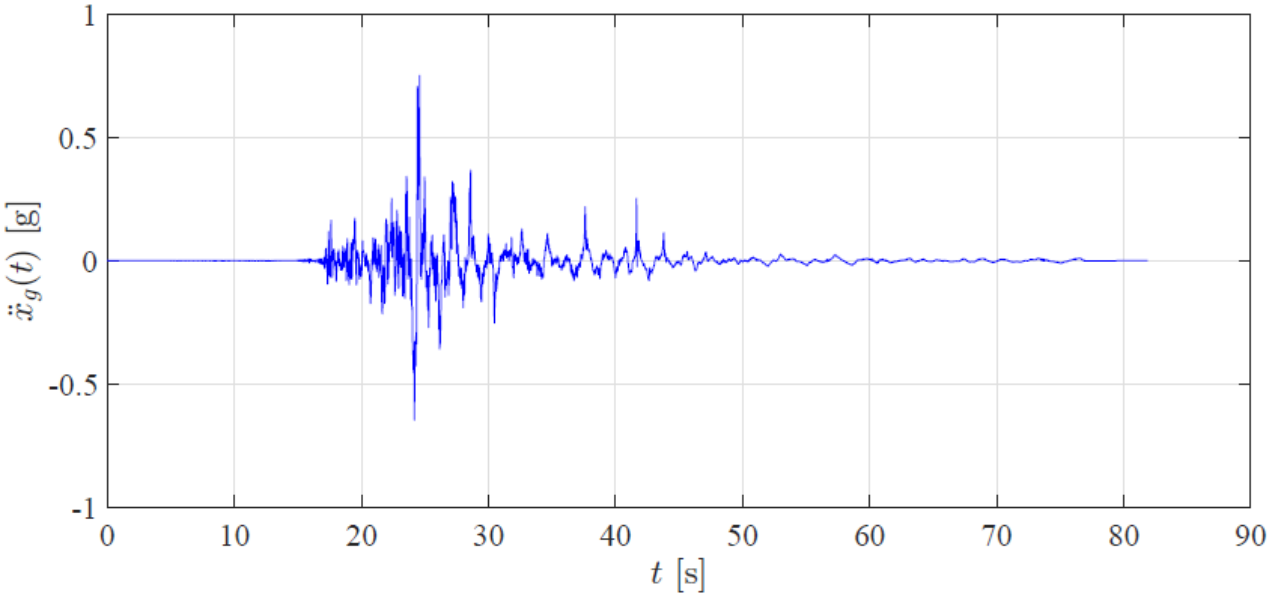

Figure A.8: New Zealand (2010) seismic accelerogram.

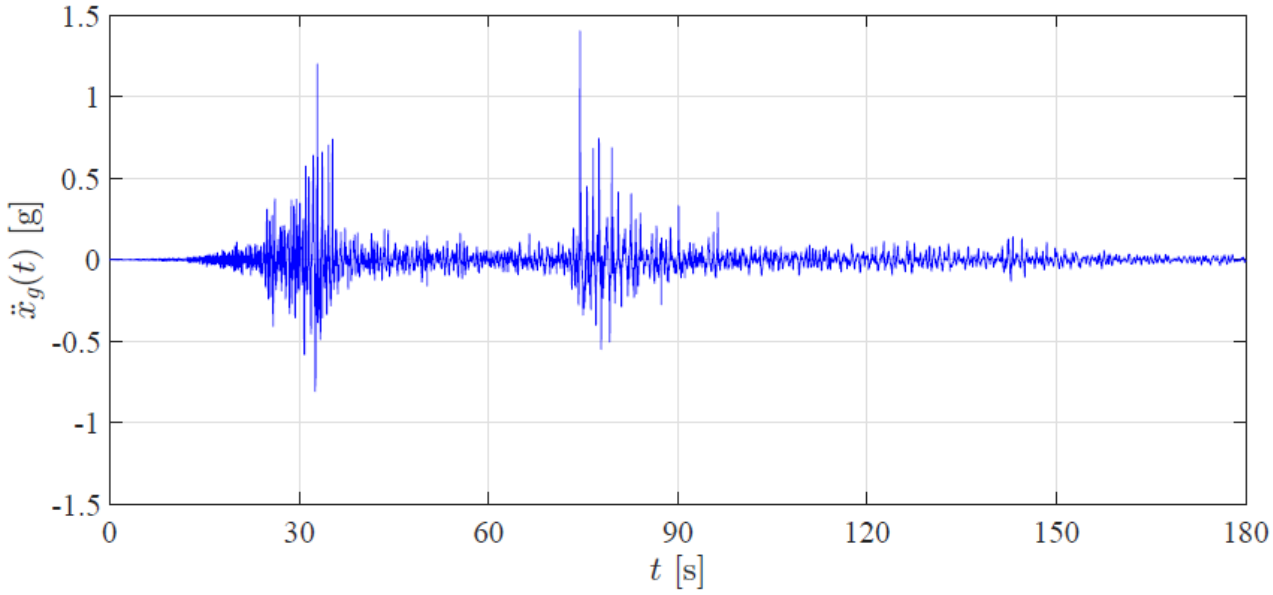

Figure A.9: New Zealand (2010) seismic accelerogram.

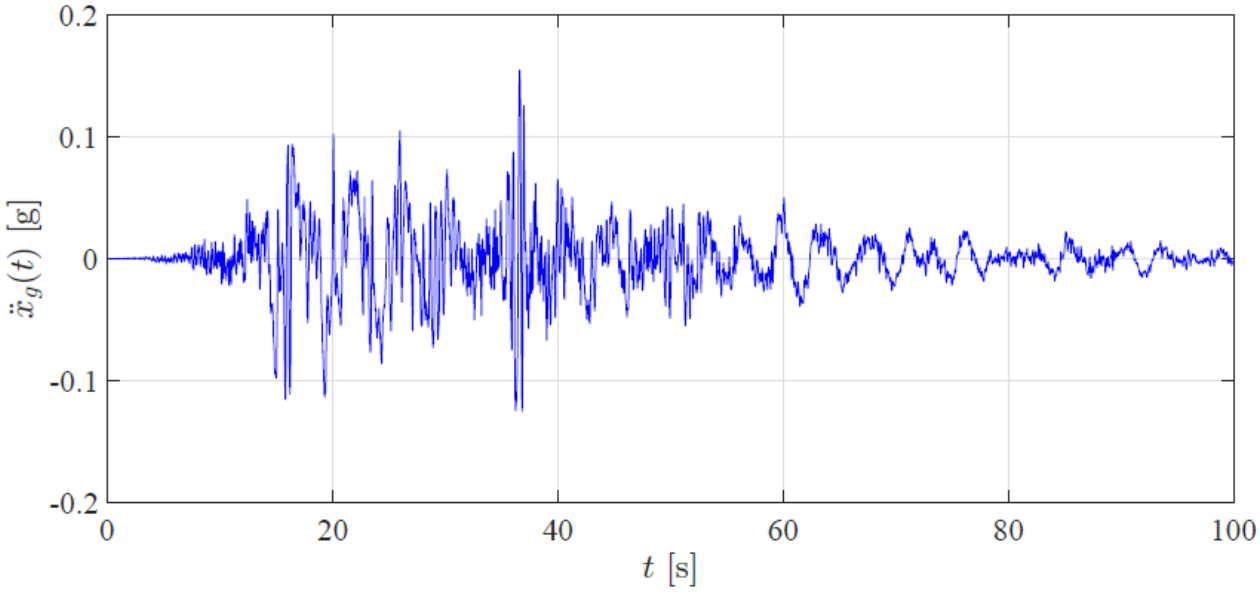

Figure A.10: Katmandu (2015) seismic accelerogram.

Appendix B

A KF application on a displacement response signal of a 3-DOF shear-type building (see Fig. 3.1) subjected to L'Aquila earthquake input (see Fig. A.6), leads to the following results. In particular, in Table B.1, the top-floor displacement response estimates (pre- and post-KF application), in terms of signal peak, are reported. Percentage variation Δ_{u3} between the filtered KF estimates and the numerically determined displacements is also reported, for increasing N/S ratios.

N/S ratio [%]	$u_{3,noisy}$ [cm]	$u_{3,KF}$ [cm]	Δ_{u_3} [%]
0	*9.38*	*9.38*	*0*
5	10.13	9.41	0.32
10	11.25	9.32	0.64
15	10.60	9.50	1.28
20	12.71	9.12	2.77
25	14.60	9.85	5.01

Table B.1: L'Aquila (2009) earthquake: maximum values of numerically determined top-floor displacements u_3 and KF estimates $u_{3,KF}$, and their percentage variation Δ_{u3} , for different N/S ratios.

Furthermore, the outcomes are also presented in graphical form, in following Figs. B.1–B.6, which refer to previous Table B.1.

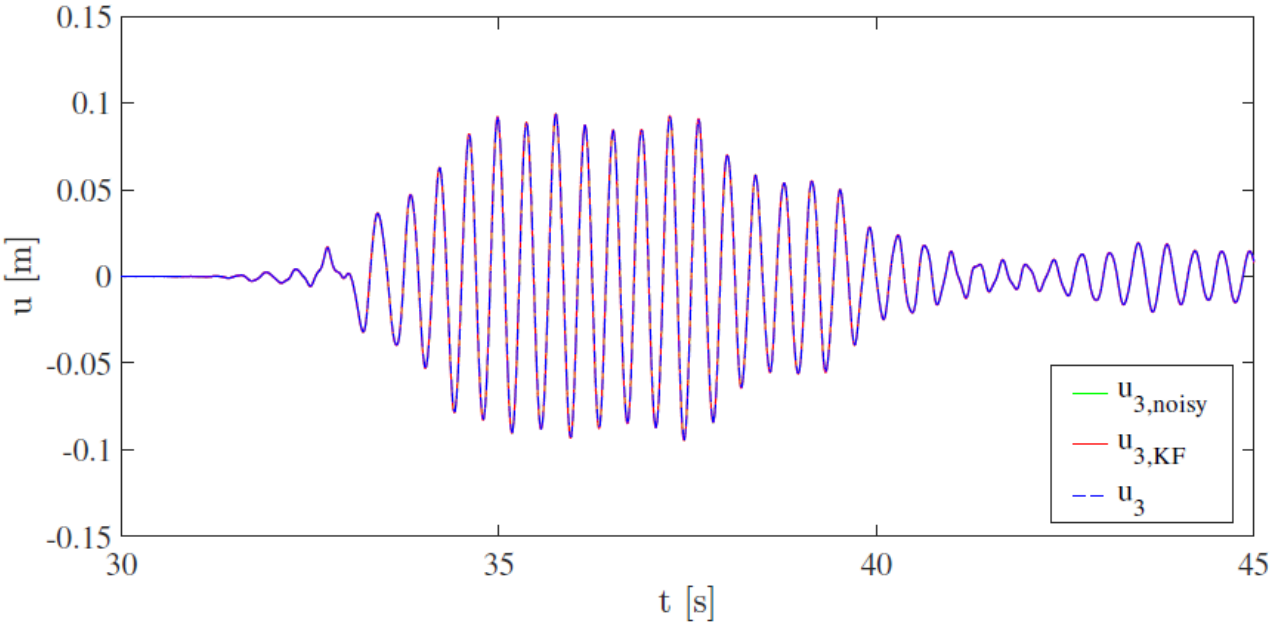

Figure B.1: KF application on top-floor displacement signal (0% N/S ratio).

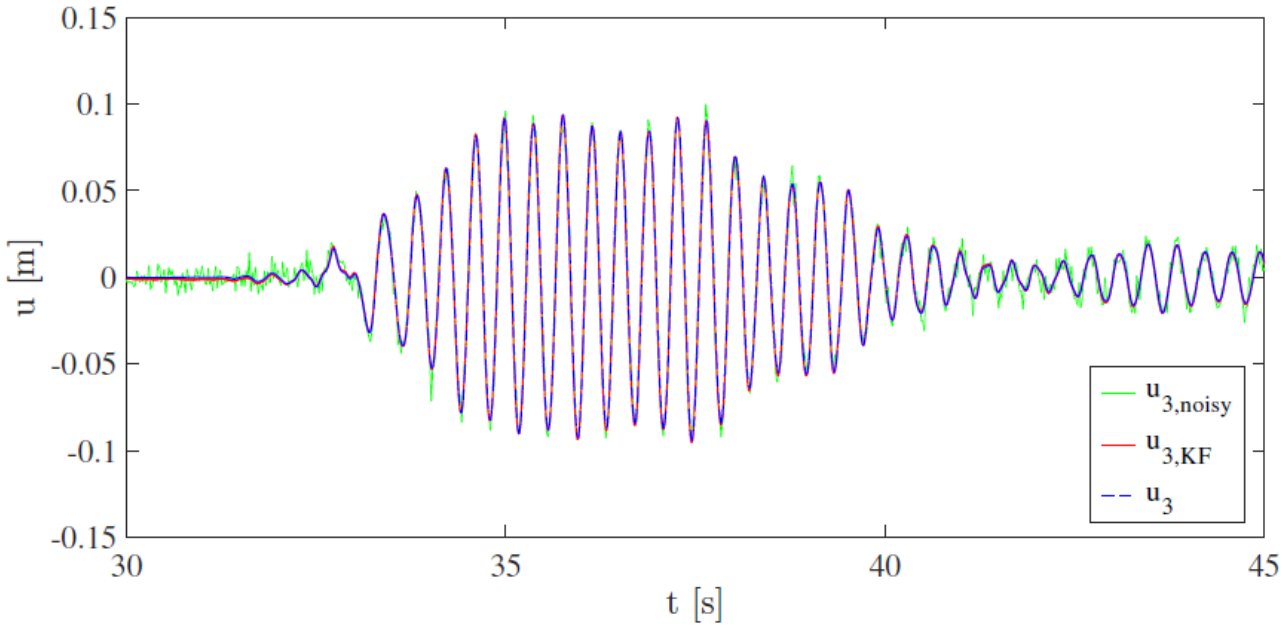

Figure B.2: KF application on top-floor displacement signal (5% N/S ratio).

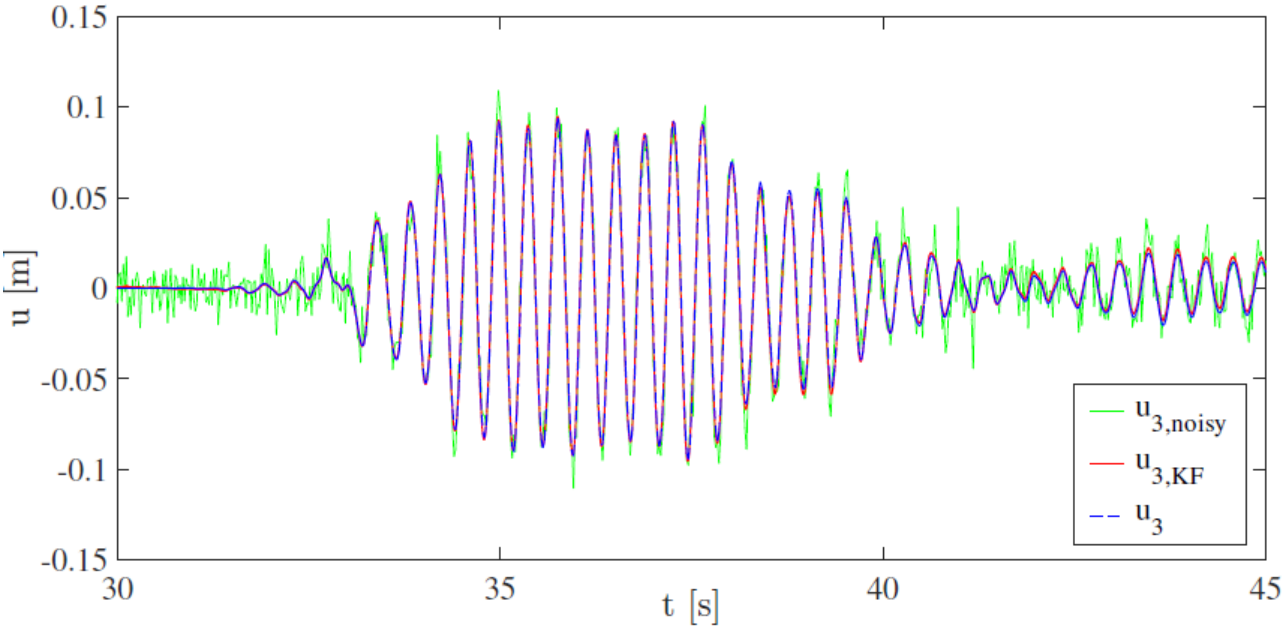

Figure B.3: KF application on top-floor displacement signal (10% N/S ratio).

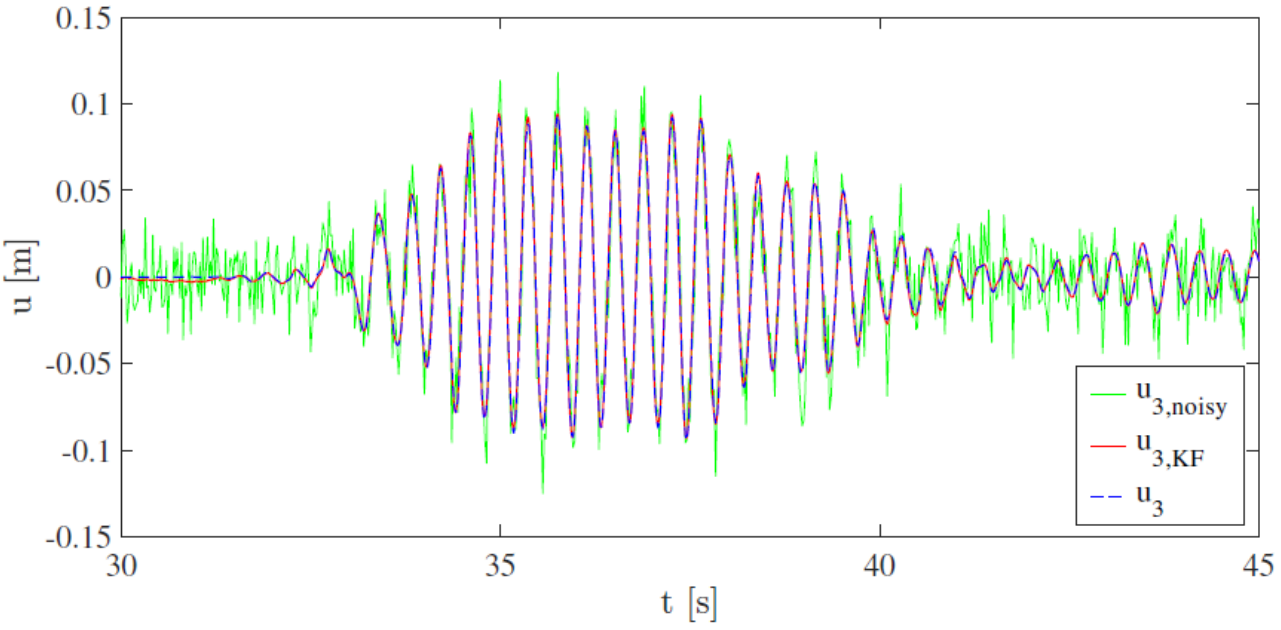

Figure B.4: KF application on top-floor displacement signal (15% N/S ratio).

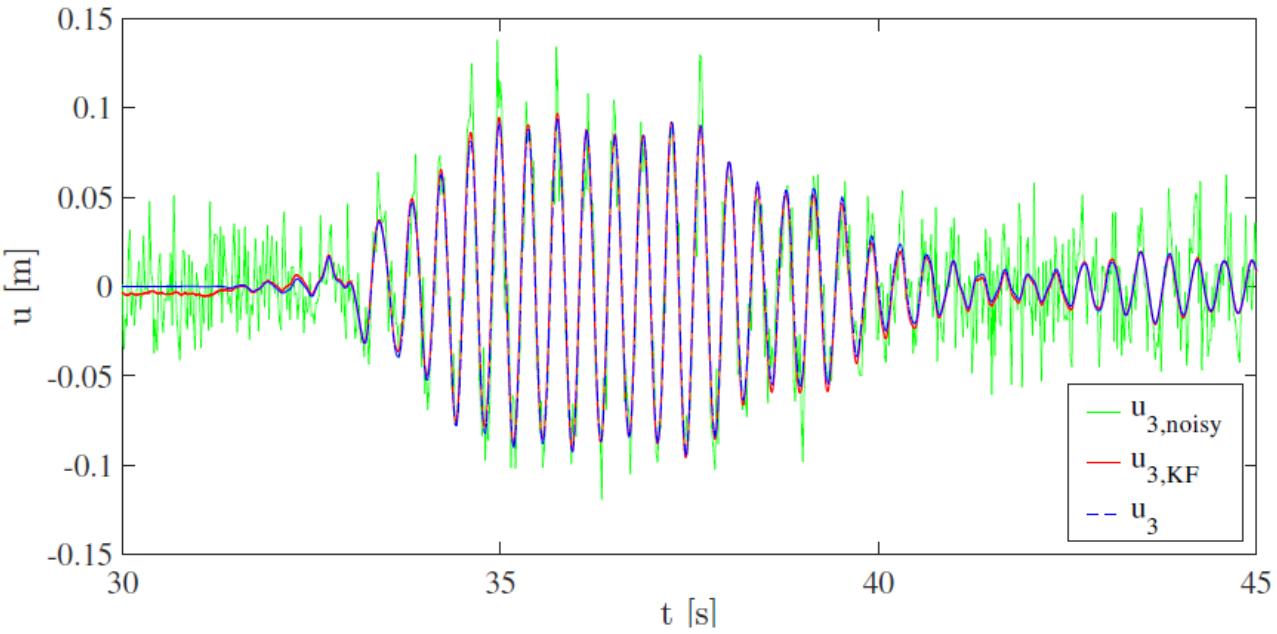

Figure B.5: KF application on top-floor displacement signal (20% N/S ratio).

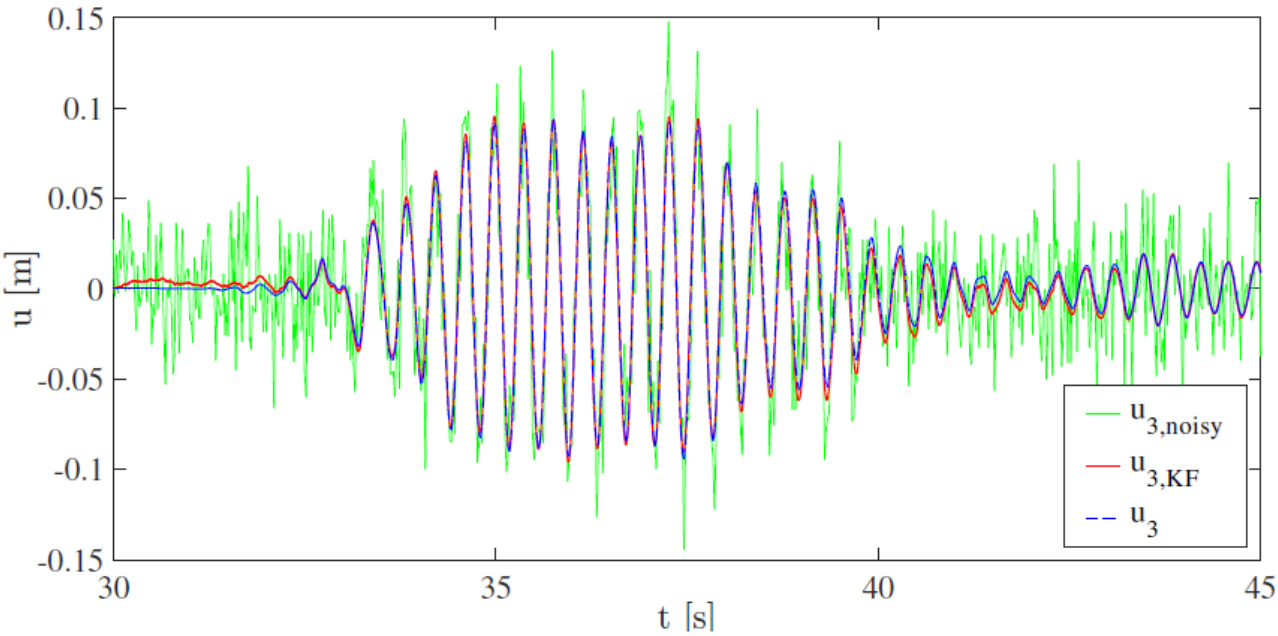

Figure B.6: KF application on top-floor displacement signal (25% N/S ratio).

Appendix C

Maximum values of displacement response signals of an examined 3-DOF shear-type building (see Fig. 3.1) subjected to single instances from a set of ten seismic ground motions listed in Table A.1 are reported in following Tables C.1–C.10, for increasing N/S ratios. Percentage variation Δ_{ui} between the displacement response signal post-KF application and the numerically determined value is also reported, for each of the three analyzed dofs.

N/S ratio [%]	$u_{1,noisy}$ [cm]	$u_{1,KF}$ [cm]	Δ_{u_1} [%]	$u_{2,noisy}$ [cm]	$u_{2,KF}$ [cm]	Δ_{u_2} [%]	$u_{3,noisy}$ [cm]	$u_{3,KF}$ [cm]	Δ_{u_3} [%]
0	*2.28*	*2.28*	*0*	*3.45*	*3.45*	*0*	*4.43*	*4.43*	*0*
5	2.34	2.27	0.44	3.51	3.48	0.87	4.58	4.50	0.08
10	2.48	2.34	2.63	3.69	3.51	1.74	4.78	4.54	0.16
15	2.88	2.35	3.07	3.80	3.63	5.22	5.22	4.80	0.08
20	3.31	2.18	4.39	4.04	3.72	7.83	5.47	4.91	3.27
25	3.62	2.41	5.70	4.29	3.81	10.43	5.83	5.03	0.82

Table C.1: Imperial Valley (1940) earthquake: maximum values of numerically determined displacements u_1, u_2, u_3 and KF estimates $u_{1,KF}$, $u_{2,KF}$, $u_{3,KF}$, and their percentage variation Δ_{ui}, for different N/S ratios.

N/S ratio [%]	$u_{1,noisy}$ [cm]	$u_{1,KF}$ [cm]	Δ_{u_1} [%]	$u_{2,noisy}$ [cm]	$u_{2,KF}$ [cm]	Δ_{u_2} [%]	$u_{3,noisy}$ [cm]	$u_{3,KF}$ [cm]	Δ_{u_3} [%]
0	*5.46*	*5.46*	*0*	*9.62*	*9.62*	*0*	*12.35*	*12.35*	*0*
5	6.08	5.58	2.19	10.14	9.65	0.31	12.10	12.39	0.32
10	6.45	5.32	2.56	10.53	9.78	1.66	12.89	12.47	0.97
15	6.79	5.40	1.10	10.92	9.95	3.43	13.13	12.61	2.11
20	7.66	5.66	3.66	11.22	10.05	4.47	14.06	12.69	2.75
25	8.49	5.87	7.51	12.25	10.36	7.69	14.87	12.04	2.51

Table C.2: Tabas (1978) earthquake: maximum values of numerically determined displacements u_1, u_2, u_3 and KF estimates $u_{1,KF}$, $u_{2,KF}$, $u_{3,KF}$, and their percentage variation Δ_{ui}, for different N/S ratios.

N/S ratio [%]	$u_{1,noisy}$ [cm]	$u_{1,KF}$ [cm]	Δ_{u_1} [%]	$u_{2,noisy}$ [cm]	$u_{2,KF}$ [cm]	Δ_{u_2} [%]	$u_{3,noisy}$ [cm]	$u_{3,KF}$ [cm]	Δ_{u_3} [%]
0	*1.86*	*1.86*	*0*	*3.25*	*3.25*	*0*	*3.97*	*3.97*	*0*
5	1.93	1.90	2.15	3.16	3.24	0.31	4.10	3.92	1.26
10	1.81	1.84	1.08	3.68	3.33	2.46	4.56	4.02	1.26
15	2.49	1.99	6.99	3.95	3.16	2.77	4.59	3.91	1.51
20	2.45	1.82	2.15	3.99	3.40	4.62	4.71	4.07	2.52
25	3.32	1.79	3.77	4.07	3.41	4.92	4.62	4.06	2.27

Table C.3: Imperial Valley (1979) earthquake: maximum values of numerically determined displacements u_1, u_2, u_3 and KF estimates $u_{1,KF}$, $u_{2,KF}$, $u_{3,KF}$, and their percentage variation Δ_{ui}, for different N/S ratios.

N/S ratio [%]	$u_{1,noisy}$ [cm]	$u_{1,KF}$ [cm]	Δ_{u_1} [%]	$u_{2,noisy}$ [cm]	$u_{2,KF}$ [cm]	Δ_{u_2} [%]	$u_{3,noisy}$ [cm]	$u_{3,KF}$ [cm]	Δ_{u_3} [%]
0	*5.29*	*5.29*	*0*	*9.59*	*9.59*	*0*	*12.22*	*12.22*	*0*
5	5.53	5.36	1.32	10.01	9.66	0.73	13.16	12.23	0.08
10	6.85	5.19	1.89	12.09	9.36	2.40	13.33	12.24	0.16
15	7.43	5.21	1.51	12.77	10.13	5.63	14.48	12.23	0.08
20	8.03	5.56	5.10	14.19	10.21	6.46	14.94	11.82	3.27
25	10.06	4.88	7.75	14.56	9.90	3.23	16.78	12.32	0.82

Table C.4: Loma Prieta (1989) earthquake: maximum values of numerically determined displacements u_1, u_2, u_3 and KF estimates $u_{1,KF}$, $u_{2,KF}$, $u_{3,KF}$, and their percentage variation Δ_{ui}, for different N/S ratios.

N/S ratio [%]	$u_{1,noisy}$ [cm]	$u_{1,KF}$ [cm]	Δ_{u_1} [%]	$u_{2,noisy}$ [cm]	$u_{2,KF}$ [cm]	Δ_{u_2} [%]	$u_{3,noisy}$ [cm]	$u_{3,KF}$ [cm]	Δ_{u_3} [%]
0	*8.60*	*8.60*	*0*	*15.26*	*15.26*	*0*	*18.75*	*18.75*	*0*
5	9.20	8.56	0.47	16.71	15.27	0.07	18.04	18.63	0.64
10	9.71	8.83	2.67	18.04	15.21	0.33	19.69	18.59	0.85
15	10.68	7.89	8.26	18.99	15.08	1.18	20.50	19.08	1.76
20	11.50	9.62	10.60	19.50	15.67	2.69	21.22	19.01	1.39
25	12.23	7.80	9.30	20.78	14.80	3.01	22.47	18.93	0.96

Table C.5: Northridge (1994) earthquake: maximum values of numerically determined displacements u_1, u_2, u_3 and KF estimates $u_{1,KF}$, $u_{2,KF}$, $u_{3,KF}$, and their percentage variation Δ_{ui}, for different N/S ratios.

N/S ratio [%]	$u_{1,noisy}$ [cm]	$u_{1,KF}$ [cm]	Δ_{u_1} [%]	$u_{2,noisy}$ [cm]	$u_{2,KF}$ [cm]	Δ_{u_2} [%]	$u_{3,noisy}$ [cm]	$u_{3,KF}$ [cm]	Δ_{u_3} [%]
0	*4.15*	*4.15*	*0*	*7.48*	*7.48*	*0*	*9.38*	*9.38*	*0*
5	4.58	4.18	0.72	8.29	7.50	0.27	10.13	9.41	0.32
10	4.48	4.20	1.20	8.87	7.53	0.67	11.25	9.32	0.64
15	5.48	4.22	1.69	10.82	7.68	2.67	10.60	9.50	1.28
20	5.65	4.34	4.57	12.15	7.76	3.74	12.71	9.12	2.77
25	6.59	4.41	6.27	12.46	8.08	8.02	14.60	9.85	5.01

Table C.6: L'Aquila (2009) earthquake: maximum values of numerically determined displacements u_1, u_2, u_3 and KF estimates $u_{1,KF}$, $u_{2,KF}$, $u_{3,KF}$, and their percentage variation Δ_{ui}, for different N/S ratios.

N/S ratio [%]	$u_{1,noisy}$ [cm]	$u_{1,KF}$ [cm]	Δ_{u_1} [%]	$u_{2,noisy}$ [cm]	$u_{2,KF}$ [cm]	Δ_{u_2} [%]	$u_{3,noisy}$ [cm]	$u_{3,KF}$ [cm]	Δ_{u_3} [%]
0	*4.42*	*4.42*	*0*	*7.78*	*7.78*	*0*	*10.04*	*10.04*	*0*
5	4.76	4.45	0.68	8.15	7.99	2.27	10.42	10.07	0.30
10	5.37	4.41	0.23	8.79	8.05	3.47	10.79	10.38	3.39
15	6.64	4.24	4.07	8.20	7.83	0.65	11.81	10.24	1.99
20	7.52	4.38	0.90	10.66	8.17	5.01	12.94	10.22	1.79
25	10.32	4.94	11.76	10.68	8.38	7.71	14.41	9.74	2.99

Table C.7: Chile (2010) earthquake: maximum values of numerically determined displacements u_1, u_2, u_3 and KF estimates $u_{1,KF}$, $u_{2,KF}$, $u_{3,KF}$, and their percentage variation Δ_{ui}, for different N/S ratios.

N/S ratio [%]	$u_{1,noisy}$ [cm]	$u_{1,KF}$ [cm]	Δ_{u_1} [%]	$u_{2,noisy}$ [cm]	$u_{2,KF}$ [cm]	Δ_{u_2} [%]	$u_{3,noisy}$ [cm]	$u_{3,KF}$ [cm]	Δ_{u_3} [%]
0	*5.13*	*5.13*	*0*	*9.02*	*9.02*	*0*	*11.20*	*11.20*	*0*
5	5.48	5.04	1.75	9.58	9.03	0.11	11.71	11.24	0.36
10	5.31	5.16	0.58	10.31	9.20	1.96	12.32	11.27	0.63
15	6.72	5.38	4.87	11.01	9.27	2.77	12.98	11.44	2.14
20	7.40	5.37	4.67	12.12	9.57	6.10	13.61	11.56	3.21
25	8.02	5.58	8.77	13.41	9.89	9.65	14.27	11.70	4.46

Table C.8: New Zealand (2010) earthquake: maximum values of numerically determined displacements u_1, u_2, u_3 and KF estimates $u_{1,KF}$, $u_{2,KF}$, $u_{3,KF}$, and their percentage variation Δ_{ui}, for different N/S ratios.

N/S ratio [%]	$u_{1,noisy}$ [cm]	$u_{1,KF}$ [cm]	Δ_{u_1} [%]	$u_{2,noisy}$ [cm]	$u_{2,KF}$ [cm]	Δ_{u_2} [%]	$u_{3,noisy}$ [cm]	$u_{3,KF}$ [cm]	Δ_{u_3} [%]
0	*7.68*	*7.68*	*0*	*13.63*	*13.63*	*0*	*16.74*	*16.74*	*0*
5	7.39	7.54	1.82	14.00	13.67	0.29	17.31	16.86	0.72
10	8.51	7.39	3.78	14.81	13.88	1.83	18.04	16.66	0.48
15	9.39	7.17	6.64	15.51	13.17	3.37	18.74	16.20	3.23
20	9.81	8.18	6.51	15.87	13.09	3.96	19.12	16.25	2.93
25	10.44	8.23	7.16	16.42	13.02	4.48	19.79	16.12	3.70

Table C.9: Tohoku (2011) earthquake: maximum values of numerically determined displacements u_1, u_2, u_3 and KF estimates $u_{1,KF}$, $u_{2,KF}$, $u_{3,KF}$, and their percentage variation Δ_{ui}, for different N/S ratios.

N/S ratio [%]	$u_{1,noisy}$ [cm]	$u_{1,KF}$ [cm]	Δ_{u_1} [%]	$u_{2,noisy}$ [cm]	$u_{2,KF}$ [cm]	Δ_{u_2} [%]	$u_{3,noisy}$ [cm]	$u_{3,KF}$ [cm]	Δ_{u_3} [%]
0	*1.10*	*1.10*	*0*	*1.92*	*1.92*	*0*	*2.36*	*2.36*	*0*
5	1.17	1.09	0.91	1.87	1.92	0	2.49	2.37	0.42
10	1.70	1.14	3.64	1.97	1.90	1.04	2.68	2.33	1.27
15	1.75	1.16	5.45	2.46	1.95	1.56	2.71	2.41	2.12
20	2.31	1.07	2.73	2.67	2.00	4.16	3.15	2.37	0.42
25	2.37	1.09	0.91	3.20	1.86	3.13	3.21	2.39	1.27

Table C.10: Katmandu (2015) earthquake: maximum values of numerically determined displacements u_1, u_2, u_3 and KF estimates $u_{1,KF}$, $u_{2,KF}$, $u_{3,KF}$, and their percentage variation Δ_{ui}, for different N/S ratios.

Appendix D

Additional results concerning the Frequency-Domain analysis presented in Section 3.3.2 are here reported. In particular, the natural frequencies identified from a benchmark structure (a 3-DOF shear-type building depicted in Fig. 3.1), subjected to single instances from a set of ten different seismic ground motions (see list in Table A.1) are summarized in following Tables D.1–D.10. Specifically, natural frequencies $f_{dspl,Welch}$, identified from the top-floor displacement response signal after KF application, are compared to frequencies $f_{acc,Welch}$ and $f_{acc,FDD}$, identified from the top-floor acceleration response signals, through the application of Welch's method and of the FDD method, respectively. For each case, the variation between the identified frequencies and the numerically determined frequencies, is also shown. A N/S ratio equal to 10% is considered on the source displacement response signals.

Modes	**I**	**II**	**III**
$f_{d,i}$ [Hz]	*2.658*	*7.448*	*10.762*
$f_{dspl,Welch}$ [Hz]	2.661	7.300	10.376
Δ [%]	+0.11	−1.99	−3.59
$f_{acc,Welch}$ [Hz]	2.661	7.251	10.400
Δ [%]	+0.11	−2.65	−3.36
$f_{acc,FDD}$ [Hz]	2.656	7.344	10.385
Δ [%]	−0.08	−1.40	−3.50

Table D.1: Imperial Valley (1940) earthquake: natural frequencies identified from top-floor displacements $f_{dspl,Welch}$ vs. natural frequencies identified from accelerations $f_{acc,Welch}$ and $f_{acc,FDD}$: comparison and their variation with respect to numerically determined damped frequencies $f_{d,i}$.

Modes	**I**	**II**	**III**
$f_{d,i}$ [Hz]	*2.658*	*7.448*	*10.762*
$f_{dspl,Welch}$ [Hz]	2.686	7.340	10.524
Δ [%]	+1.05	−1.45	−2.21
$f_{acc,Welch}$ [Hz]	2.602	7.381	10.540
Δ [%]	−2.11	−0.90	−2.06
$f_{acc,FDD}$ [Hz]	2.646	7.365	10.480
Δ [%]	−0.45	−1.11	−2.62

Table D.2: Tabas (1978) earthquake: natural frequencies identified from top-floor displacements $f_{dspl,Welch}$ vs. natural frequencies identified from accelerations $f_{acc,Welch}$ and $f_{acc,FDD}$: comparison and their variation with respect to numerically determined damped frequencies $f_{d,i}$.

Modes	I	II	III
$f_{d,i}$ [Hz]	*2.658*	*7.448*	*10.762*
$f_{dspl,Welch}$ [Hz]	2.686	7.324	10.498
Δ [%]	+1.05	−1.66	−2.45
$f_{acc,Welch}$ [Hz]	2.661	7.300	10.400
Δ [%]	+0.11	−1.99	−3.36
$f_{acc,FDD}$ [Hz]	2.690	7.345	10.402
Δ [%]	+1.20	−1.38	−3.35

Table D.3: Imperial Valley (1979) earthquake: natural frequencies identified from top-floor displacements $f_{dspl,Welch}$ vs. natural frequencies identified from accelerations $f_{acc,Welch}$ and $f_{acc,FDD}$: comparison and their variation with respect to numerically determined damped frequencies $f_{d,i}$.

Modes	I	II	III
$f_{d,i}$ [Hz]	*2.658*	*7.448*	*10.762*
$f_{dspl,Welch}$ [Hz]	2.702	7.381	10.660
Δ [%]	+1.66	−0.90	−0.95
$f_{acc,Welch}$ [Hz]	2.688	7.375	10.590
Δ [%]	+1.13	−0.98	−1.60
$f_{acc,FDD}$ [Hz]	2.631	7.400	10.607
Δ [%]	−1.02	−0.64	−1.44

Table D.4: Loma Prieda (1989) earthquake: natural frequencies identified from top-floor displacements $f_{dspl,Welch}$ vs. natural frequencies identified from accelerations $f_{acc,Welch}$ and $f_{acc,FDD}$: comparison and their variation with respect to numerically determined damped frequencies $f_{d,i}$.

Modes	I	II	III
$f_{d,i}$ [Hz]	*2.658*	*7.448*	*10.762*
$f_{dspl,Welch}$ [Hz]	2.630	7.361	10.590
Δ [%]	−1.05	−1.17	−1.60
$f_{acc,Welch}$ [Hz]	2.628	7.400	10.547
Δ [%]	−1.13	−0.64	−2.00
$f_{acc,FDD}$ [Hz]	2.611	7.377	10.470
Δ [%]	−1.77	−0.95	−2.71

Table D.5: Northridge (1994) earthquake: natural frequencies identified from top-floor displacements $f_{dspl,Welch}$ vs. natural frequencies identified from accelerations $f_{acc,Welch}$ and $f_{acc,FDD}$: comparison and their variation with respect to numerically determined damped frequencies $f_{d,i}$.

Modes	I	II	III
$f_{d,i}$ [Hz]	*2.658*	*7.448*	*10.762*
$f_{dspl,Welch}$ [Hz]	2.612	7.373	10.669
Δ [%]	−1.73	−1.01	−0.86
$f_{acc,Welch}$ [Hz]	2.637	7.373	10.645
Δ [%]	−0.79	−1.01	−1.09
$f_{acc,FDD}$ [Hz]	2.630	7.360	10.650
Δ [%]	−1.05	−1.18	−1.05

Table D.6: L'Aquila (2009) earthquake: natural frequencies identified from top-floor displacements $f_{dspl,Welch}$ vs. natural frequencies identified from accelerations $f_{acc,Welch}$ and $f_{acc,FDD}$: comparison and their variation with respect to numerically determined damped frequencies $f_{d,i}$.

Modes	I	II	III
$f_{d,i}$ [Hz]	*2.658*	*7.448*	*10.762*
$f_{dspl,Welch}$ [Hz]	2.661	7.251	10.376
Δ [%]	+0.11	−2.64	−3.59
$f_{acc,Welch}$ [Hz]	2.661	7.249	10.400
Δ [%]	+0.11	−2.67	−3.36
$f_{acc,FDD}$ [Hz]	2.656	7.344	10.391
Δ [%]	+0.08	−1.40	−3.45

Table D.7: Chile (2010) earthquake: natural frequencies identified from top-floor displacements $f_{dspl,Welch}$ vs. natural frequencies identified from accelerations $f_{acc,Welch}$ and $f_{acc,FDD}$: comparison and their variation with respect to numerically determined damped frequencies $f_{d,i}$.

Modes	I	II	III
$f_{d,i}$ [Hz]	*2.658*	*7.448*	*10.762*
$f_{dspl,Welch}$ [Hz]	2.601	7.402	10.350
Δ [%]	−2.14	−0.62	−3.83
$f_{acc,Welch}$ [Hz]	2.612	7.365	10.401
Δ [%]	−1.73	−1.11	−3.35
$f_{acc,FDD}$ [Hz]	2.620	7.380	10.478
Δ [%]	−1.43	−0.91	−2.64

Table D.8: New Zealand (2010) earthquake: natural frequencies identified from top-floor displacements $f_{dspl,Welch}$ vs. natural frequencies identified from accelerations $f_{acc,Welch}$ and $f_{acc,FDD}$: comparison and their variation with respect to numerically determined damped frequencies $f_{d,i}$.

Modes	I	II	III
$f_{d,i}$ [Hz]	*2.658*	*7.448*	*10.762*
$f_{dspl,Welch}$ [Hz]	2.637	7.422	10.655
Δ [%]	−0.79	−0.35	−0.99
$f_{acc,Welch}$ [Hz]	2.637	7.422	10.693
Δ [%]	−0.79	−0.35	−0.64
$f_{acc,FDD}$ [Hz]	2.655	7.433	10.671
Δ [%]	−0.11	−0.20	−0.85

Table D.9: Tohoku (2011) earthquake: natural frequencies identified from top-floor displacements $f_{dspl,Welch}$ vs. natural frequencies identified from accelerations $f_{acc,Welch}$ and $f_{acc,FDD}$: comparison and their variation with respect to numerically determined damped frequencies $f_{d,i}$.

Modes	I	II	III
$f_{d,i}$ [Hz]	*2.658*	*7.448*	*10.762*
$f_{dspl,Welch}$ [Hz]	2.661	7.324	10.889
Δ [%]	+0.11	−1.66	+1.18
$f_{acc,Welch}$ [Hz]	2.686	7.324	10.690
Δ [%]	+1.05	−1.66	−0.67
$f_{acc,FDD}$ [Hz]	2.658	7.420	10.662
Δ [%]	+0.00	−0.38	−0.93

Table D.10: Katmandu (2015) earthquake: natural frequencies identified from top-floor displacements $f_{dspl,Welch}$ vs. natural frequencies identified from accelerations $f_{acc,Welch}$ and $f_{acc,FDD}$: comparison and their variation with respect to numerically determined damped frequencies $f_{d,i}$.

List of figures

Figure 1.1: Taxonomy of the main challenging issues of input data (adapted from Khaleghi et al. [111]).....14

Figure 1.2: Main mathematical theories available to deal with data imperfection (adapted from Khaleghi et al. [111]). 17

Figure 1.3: Finite-dimensional linear system serving as a signal-model (adapted from Anderson and Moore [6])......35

Figure 1.4: Founding concepts in Kalman filtering theory (adapted from Mohinder and Angus [139])......40

Figure 1.5: Venn diagram detailing the role of KF in the interdisciplinary approach of stability and operational safety of structures (adapted from Gulal [85]). 43

Figure 2.1: Schematic view of the analyzed 3-DOF shear-type building under top-floor input force......51

Figure 2.2: Multi-rate KF flowchart (adapted from Ferrari et al. [67]). 54

Figure 2.3: Schematic conception of the treated HDF cases: noise-free acceleration case (excluding the part in blue colour) and noise-affected acceleration case (considering the whole scheme). Determination of filtered displacements and possible subsequent phase of modal identification, based on displacements. 56

Figure 2.4: KF displacement response estimation (25% N/S ratio, z_i = 1%).....57

Figure 2.5: RMS error trend of KF estimation at increasing displacement noise levels (noise-free acceleration case). A visible kink is recorded at 50% noise level. 58

Figure 2.6: Welch-based modal frequency identification on displacement signal for a 25% N/S ratio (z_i=1%)......59

Figure 2.7: KF displacement response estimation for 25% N/S ratio on displacements and 1% N/S ratio on accelerations. 60

Figure 2.8: RMS error of KF displacement response estimation at increasing N/S ratios on displacements (for 1%, 2% and 3% N/S ratios on accelerations). 62

Figure 2.9: Welch-based modal frequency identification on displacements for a 25% N/S ratio on displacements and a 1% N/S ratio on accelerations. 63

Figure 3.1: Schematic view of the monitored 3-DOF shear-type building under seismic ground excitation $\ddot{u}_g(t)$. 69

Figure 3.2: Schematic conception of the illustrated HDF procedure via KF between noise-affected displacements and noise-free accelerations at seismic excitation. Determination of filtered displacements and subsequent phase of modal identification, based on displacements. ……..……71

Figure 3.3: KF application on top-floor displacement response signal of a 3-DOF shear-type frame subjected to L'Aquila 2009 earthquake input, for different N/S ratios on displacements (top-floor displacements are depicted). ……..……73

Figure 3.4: Identified natural frequencies by an automatic peak-picking procedure on displacements (Welch's method): (a) pre-KF application; (b) post-KF application.……..……75

Figure 3.5: Identified natural frequencies by an automatic peak-picking procedure on accelerations: (a) Welch's method; (b) standard FDD method. ……..……...…76

Figure 4.1: Schematic view of the analyzed one-bay 10-DOF shear-type frame building. ……..……95

Figure 4.2: Kalamata (1986) seismic input acting at the base on the benchmark structure: (a) Time Domain; (b) Frequency Domain. ……..……..……..……97

Figure 4.3: Dynamic acceleration response signals of the benchmark structure under Kalamata earthquake input and noise addition process (25% N/S ratio); (a) 1st floor; (b) 10th floor. ……...……97

Figure 4.4: Ambient vibration input acting on the last floor of the benchmark structure: (a) Time Domain; (b) Frequency Domain. ……..……..……..……..……98

Figure 4.5: Dynamic acceleration response signals of the benchmark structure under ambient vibration input and noise addition process (25% N/S ratio); (a) 1st floor; (b) 10th floor. ……..……..……..…99

Figure 4.6: DWT-based denoising of noise-corrupted ẍ(t) under seismic input (25% N/S ratio). ……103

Figure 4.7: DWT-based denoising of noise-corrupted ẍ(t) under ambient vibration (25% N/S ratio)...103

Figure 4.8: SVD-based denoising of noise-corrupted ẍ(t) under seismic input (25% N/S ratio). ...…..105

Figure 4.9: SVD-based denoising of noise-corrupted ẍ(t) under ambient vibration (25% N/S ratio). .. 105

Figure 4.10: Effectiveness evaluation of DWT- and SVD-based denoising techniques for increasing N/S ratios and different signal typologies: (a) earthquake excitation; (b) ambient vibration. Notice that scales on the PrmsD axes are different, almost twice for (b). Indicated trends come from a polynomial fit of a degree 2. …..……..……..……..……..……..……..……..……107

Figure 4.11: Seismic response signal in the frequency domain (10% N/S ratio). PSD of the noise-free signal vs. PSD of the denoised signal, for the two analyzed denoising techniques: (a) DWT-based denoising; (b) SVD-based denoising. …..……..……..……..……..……..……111

Figure 4.12: Ambient vibration response signal in the frequency domain (10% N/S ratio). PSD of the noise-free signal vs. PSD of the denoised signal, for the two analyzed denoising techniques: (a) DWT-based denoising; (b) SVD-based denoising. …..……..……..……..……..……..……..112

Figure 4.13: Seismic response signal in the frequency domain (25% N/S ratio). PSD of the noise-free signal vs. PSD of the denoised signal, for the two analyzed denoising techniques: (a) DWT-based denoising; (b) SVD-based denoising. …..……..……..……..……..……..……..113

Figure 4.14: Ambient vibration response signal in the frequency domain (25% N/S ratio). PSD of the noise-free signal vs. PSD of the denoised signal, for the two analyzed denoising techniques: (a) DWT-based denoising; (b) SVD-based denoising. ……114
Figure 4.15: SVD-based implementation conceptual flowchart: an additional SVD is over applied on the Welch periodogram for modal frequency identification purposes. ……117
Figure 4.16: Modal identification based on SVD denoising and post-processing (first singular value). Natural frequencies identified through a peak-picking application on the first singular value of each analyzed denoised response signal typology: (a) seismic excitation; (b) ambient vibration. A 50% N/S ratio is assumed to be affecting both the original signals. ……118
Figure 5.1: View of SU Unterwalden railway bridge (located in the district of Sursee, canton of Lucerne, Switzerland). ……122
Figure 5.2: Transverse section of SU Unterwalden railway bridge (adapted from Swiss railway database; quotes in cm). ……123
Figure 5.3: SU Unterwalden railway bridge acceleration signal $\ddot{x}_1(t)$ under a five-wagon train passage excitation: (a) Time Domain recording (time window 0–3.5 s); (b) Frequency Domain spectrum (Welch's PSD estimate) with frequency normalized to sampling frequency (200 Hz). ……124
Figure 5.4: SU Unterwalden railway bridge acceleration signal $\ddot{x}_2(t)$ under a five-wagon train passage excitation: (a) Time Domain recording (time window 0–3.5 s); (b) Frequency Domain spectrum (Welch's PSD) with frequency normalized to sampling frequency (200 Hz). Notice that in (a) a different amplitude scale is adopted with respect to that in Fig. 5.3a. ……125
Figure 5.5: Denoising application on SU Unterwalden railway bridge real acceleration signal $\ddot{x}_1(t)$ under a five-wagon train passage (first wagon representation, time domain window 0.2–0.7 s): (a) DWT-based denoising; (b) SVD-based denoising. ……128
Figure 5.6: Denoising application on SU Unterwalden railway bridge real acceleration signal $\ddot{x}_2(t)$ under a five-wagon train passage (first wagon representation, time domain window 0.9–1.3 s): (a) DWT-based denoising; (b) SVD-based denoising. ……129
Figure 5.7: DWT vs. SVD-based denoising performed on SU Unterwalden railway bridge real acceleration signal $\ddot{x}_1(t)$ (zoomed time window 0.35–0.6 s). ……130
Figure 5.8: DWT vs. SVD-based denoising performed on SU Unterwalden railway bridge real acceleration signal $\ddot{x}_2(t)$ (zoomed time window 1–1.25 s). Notice that a different amplitude scale is adopted with respect to that in Fig. 5.7. ……131
Figure 5.9: SU Unterwalden railway bridge real acceleration signal $\ddot{x}_1(t)$ in the Frequency Domain. DWT-based denoising technique. PSD of the real (noise-affected) signal vs. PSD of the denoised signal: (a) linear scale in frequency normalized to sampling rate (200 Hz); (b) logarithmic scale. ……133

Figure 5.10: SU Unterwalden railway bridge real acceleration signal $\ddot{x}_1(t)$ in the Frequency Domain. SVD-based denoising technique. PSD of the real (noise-affected) signal vs. PSD of the denoised signal: (a) linear scale in frequency normalized to sampling rate (200 Hz); (b) logarithmic scale. ……134
Figure 5.11: SU Unterwalden railway bridge real acceleration signal $\ddot{x}_2(t)$ in the Frequency Domain. DWT-based denoising technique. PSD of the real (noise-affected) signal vs. PSD of the denoised signal: (a) linear scale in frequency normalized to sampling rate (200 Hz); (b) logarithmic scale. ……136
Figure 5.12: SU Unterwalden railway bridge real acceleration signal $\ddot{x}_2(t)$ in the Frequency Domain. SVD-based denoising technique. PSD of the real (noise-affected) signal vs. PSD of the denoised signal: (a) linear scale in frequency normalized to sampling rate (200 Hz); (b) logarithmic scale. ……137
Figure 6.1: RC three-span arched Brivio bridge (1917) over the Adda river. ……144
Figure 6.2: Flowchart of the proposed monitoring methodology, integrating a denoising-based and a HDF-based approach for the enhancement of response data collected on the structure, and a subsequent structural dynamic identification. ……146
Figure 6.3: Brivio bridge (wireless) acceleration response signal, pre and post DWT-based denoising application. ……148
Figure 6.4: Brivio bridge (total station) displacement response signal, pre and post DWT-based denoising. ……149
Figure 6.5: Enhanced Brivio bridge displacement response signal, obtained by HDF via KF with the denoised acceleration response signal. ……150
Figure 6.6: Brivio Bridge displacement (PSD) response spectrum: original (raw) displacement signal vs. HDF (enhanced) displacement signal. ……151
Figure 6.7: Brivio bridge identified natural frequencies from displacements. Peak-picking procedure on Welch's periodogram: original (raw) displacement signal vs. HDF (enhanced) displacement signal. 152
Figure 6.8: FDD vibration mode shapes of Brivio bridge first span. ……153
Figure A.1: Imperial Valley (1940) seismic accelerogram. ……166
Figure A.2: Tabas (1978) seismic accelerogram. ……166
Figure A.3: Imperial Valley (1979) seismic accelerogram. ……167
Figure A.4: Loma Prieta (1989) seismic accelerogram. ……167
Figure A.5: Northridge (1994) seismic accelerogram. ……168
Figure A.6: L'Aquila (2009) seismic accelerogram. ……168
Figure A.7: Chile (2010) seismic accelerogram. ……169
Figure A.8: New Zealand (2010) seismic accelerogram. ……169
Figure A.9: New Zealand (2010) seismic accelerogram. ……170
Figure A.10: Katmandu (2015) seismic accelerogram. ……170
Figure B.1: KF application on top-floor displacement signal (0% N/S ratio). ……172

Figure B.2: KF application on top-floor displacement signal (5% N/S ratio). 172
Figure B.3: KF application on top-floor displacement signal (10% N/S ratio). 173
Figure B.4: KF application on top-floor displacement signal (15% N/S ratio). 173
Figure B.5: KF application on top-floor displacement signal (20% N/S ratio). 174
Figure B.6: KF application on top-floor displacement signal (25% N/S ratio). 174

List of tables

Table 1.1: Examples of estimation problems (adapted from Mohinder and Angus [139])......41

Table 2.1: Frequencies $f_{d,i}$ of the damped system (z_i=1%, 3% and 5%).……..…..……52

Table 2.2: RMS error of KF displacement response estimation for increasing imposed N/S ratios and damping ratios z_i (noise-free acceleration case). ……..……..……57

Table 2.3: RMS error of KF response estimation (z_i = 1%) at increasing displacement noise level (noise-affected acceleration case). ……..……..……61

Table 3.1: Seismic input data-set generalities (see also Appendix A). ……...……70

Table 3.2: L'Aquila 2009 earthquake: maximum values of numerically determined displacements u_1, u_2, u_3 and KF estimates $u_{1,KF}$, $u_{2,KF}$, $u_{3,KF}$, and their percentage variation Δu_i , for different N/S ratios. …….74

Table 3.3: L'Aquila 2009 earthquake: natural frequencies identified from top-floor displacements $f_{dspl,Welch}$ vs. natural frequencies identified from accelerations $f_{acc,Welch}$ and $f_{acc,FDD}$: comparison and their variation with respect to target numerically determined damped frequencies $f_{d,i}$. ……..77

Table 4.1: PrmsD index [%] between original (noise-free) signal and denoised signal for different mother wavelets and thresholding rules (10% N/S ratio, decomposition level 3). ……..…..101

Table 4.2: PrmsD index [%] between original (noise-free) signal and denoised signal for different decomposition levels and thresholding types (10% N/S ratio). ……..……..…..102

Table 4.3: PrmsD [%] index between original and denoised signal, for different signal typologies and N/S ratios: DWT vs. SVD. ……..……..…..106

Table 4.4: Peak acceleration values of the DWT and SVD denoised signals, and their variation with respect to the noise-affected signal peak (Δ_{na}) and to the numerically determined signal peak (Δ_{nd}), for different typologies of signals (i.e. non-stationary (seismic) signal and stationary (white-noise) signal) and N/S ratios. ……..……..……..…..108

Table 4.5: Original (zi=5%) and identified natural frequencies from the denoised signal by a standard peak-picking on Welch's diagram: comparison involving different response signal typologies (seismic excitation vs. ambient vibration) and denoising techniques (DWT vs. SVD). The cases with 10% and 25% N/S ratios are reported. ……..……..……115

Table 4.6: Identified natural frequencies from SVD denoised acceleration response signals and post-processing: seismic excitation vs. ambient vibration (50% N/S ratio). ……..……118

Table 5.1: Global information on noisy real acceleration response signals $\ddot{x}_1(t)$ and $\ddot{x}_2(t)$ recorded on the SU Unterwalden railway bridge at a train passage on different times. ……..……123

Table 5.2: Characteristic values of the entire denoised signals in the Time Domain and their variation Δ_{na} with respect to the real (noise-affected) signals: RMS and peak acceleration values. ……..……131

Table 6.1: Characteristic values of the analyzed acceleration response signals in the time domain and their variation with respect to the original (noise-affected) signal: RMS and peak acceleration values………149

Table 6.2: Characteristic values of the analyzed displacement response signals in the Time Domain and their variation with respect to the original (noise-affected) signal: RMS and peak deflection values…150

Table 6.3: Brivio bridge natural frequencies $f_{id,WD}$ identified from a HDF displacement response signal (wireless sensor), compared to frequencies $f_{id,AC}$ (Ferrari et al. [67]) identified from an acceleration response signal (wired sensor), and their variation. ……..……..…153

Table A.1: Seismic input data-set generalities and reference labels adopted in the subsequent plots.…165

Table B.1: L'Aquila (2009) earthquake: maximum values of numerically determined top-floor displacements u_3 and KF estimates $u_{3,KF}$, and their percentage variation Δ_{u3} , for different N/S ratios..171

Table C.1: Imperial Valley (1940) earthquake: maximum values of numerically determined displacements u_1, u_2, u_3 and KF estimates $u_{1,KF}$, $u_{2,KF}$, $u_{3,KF}$, and their percentage variation Δ_{ui}, for different N/S ratios. ……...….175

Table C.2: Tabas (1978) earthquake: maximum values of numerically determined displacements u_1, u_2, u_3 and KF estimates $u_{1,KF}$, $u_{2,KF}$, $u_{3,KF}$, and their percentage variation Δ_{ui}, for different N/S ratios. ...…175

Table C.3: Imperial Valley (1979) earthquake: maximum values of numerically determined displacements u_1, u_2, u_3 and KF estimates $u_{1,KF}$, $u_{2,KF}$, $u_{3,KF}$, and their percentage variation Δ_{ui}, for different N/S ratios. ……..…..…176

Table C.4: Loma Prieta (1989) earthquake: maximum values of numerically determined displacements u_1, u_2, u_3 and KF estimates $u_{1,KF}$, $u_{2,KF}$, $u_{3,KF}$, and their percentage variation Δ_{ui}, for different N/S ratio……..……...176

Table C.5: Northridge (1994) earthquake: maximum values of numerically determined displacements u_1, u_2, u_3 and KF estimates $u_{1,KF}$, $u_{2,KF}$, $u_{3,KF}$, and their percentage variation Δ_{ui}, for different N/S ratios……..176

Table C.6: L'Aquila (2009) earthquake: maximum values of numerically determined displacements u_1, u_2, u_3 and KF estimates $u_{1,KF}$, $u_{2,KF}$, $u_{3,KF}$, and their percentage variation Δ_{ui}, for different N/S ratios…177

Table C.7: Chile (2010) earthquake: maximum values of numerically determined displacements u_1, u_2, u_3 and KF estimates $u_{1,KF}$, $u_{2,KF}$, $u_{3,KF}$, and their percentage variation Δ_{ui}, for different N/S ratios. …..177

Table C.8: New Zealand (2010) earthquake: maximum values of numerically determined displacements u_1, u_2, u_3 and KF estimates $u_{1,KF}$, $u_{2,KF}$, $u_{3,KF}$, and their percentage variation Δ_{ui}, for different N/S ratios………..177

Table C.9: Tohoku (2011) earthquake: maximum values of numerically determined displacements u_1, u_2, u_3 and KF estimates $u_{1,KF}$, $u_{2,KF}$, $u_{3,KF}$, and their percentage variation Δ_{ui}, for different N/S ratios…178

Table C.10: Katmandu (2015) earthquake: maximum values of numerically determined displacements u_1, u_2, u_3 and KF estimates $u_{1,KF}$, $u_{2,KF}$, $u_{3,KF}$, and their percentage variation Δ_{ui}, for different N/S ratios……...……...178

Table D.1: Imperial Valley (1940) earthquake: natural frequencies identified from top-floor displacements $f_{dspl,Welch}$ vs. natural frequencies identified from accelerations $f_{acc,Welch}$ and $f_{acc,FDD}$: comparison and their variation with respect to numerically determined damped frequencies $f_{d,i}$......179

Table D.2: Tabas (1978) earthquake: natural frequencies identified from top-floor displacements $f_{dspl,Welch}$ vs. natural frequencies identified from accelerations $f_{acc,Welch}$ and $f_{acc,FDD}$: comparison and their variation with respect to numerically determined damped frequencies $f_{d,i}$......179

Table D.3: Imperial Valley (1979) earthquake: natural frequencies identified from top-floor displacements $f_{dspl,Welch}$ vs. natural frequencies identified from accelerations $f_{acc,Welch}$ and $f_{acc,FDD}$: comparison and their variation with respect to numerically determined damped frequencies $f_{d,i}$. 180

Table D.4: Loma Prieda (1989) earthquake: natural frequencies identified from top-floor displacements $f_{dspl,Welch}$ vs. natural frequencies identified from accelerations $f_{acc,Welch}$ and $f_{acc,FDD}$: comparison and their variation with respect to numerically determined damped frequencies $f_{d,i}$......180

Table D.5: Northridge (1994) earthquake: natural frequencies identified from top-floor displacements $f_{dspl,Welch}$ vs. natural frequencies identified from accelerations $f_{acc,Welch}$ and $f_{acc,FDD}$: comparison and their variation with respect to numerically determined damped frequencies $f_{d,i}$......180

Table D.6: L'Aquila (2009) earthquake: natural frequencies identified from top-floor displacements $f_{dspl,Welch}$ vs. natural frequencies identified from accelerations $f_{acc,Welch}$ and $f_{acc,FDD}$: comparison and their variation with respect to numerically determined damped frequencies $f_{d,i}$......181

Table D.7: Chile (2010) earthquake: natural frequencies identified from top-floor displacements $f_{dspl,Welch}$ vs. natural frequencies identified from accelerations $f_{acc,Welch}$ and $f_{acc,FDD}$: comparison and their variation with respect to numerically determined damped frequencies $f_{d,i}$......181

Table D.8: New Zealand (2010) earthquake: natural frequencies identified from top-floor displacements $f_{dspl,Welch}$ vs. natural frequencies identified from accelerations $f_{acc,Welch}$ and $f_{acc,FDD}$: comparison and their variation with respect to numerically determined damped frequencies $f_{d,i}$......181

Table D.9: Tohoku (2011) earthquake: natural frequencies identified from top-floor displacements $f_{dspl,Welch}$ vs. natural frequencies identified from accelerations $f_{acc,Welch}$ and $f_{acc,FDD}$: comparison and their variation with respect to numerically determined damped frequencies $f_{d,i}$. 182

Table D.10: Katmandu (2015) earthquake: natural frequencies identified from top-floor displacements $f_{dspl,Welch}$ vs. natural frequencies identified from accelerations $f_{acc,Welch}$ and $f_{acc,FDD}$: comparison and their variation with respect to numerically determined damped frequencies $f_{d,i}$. 182

Bibliography

[1] Akselrod, D., Tharmarasa, R., Kirubarajan, T., Ding, Z. and Ponsford, T. (2009), *Multisensor-multitarget tracking testbed*. In: Proceedings of the IEEE Symposium on Computational Intelligence for Security and Defense Applications, pp. 1–6.

[2] Alfaouri, M. and Daqrouq, K. (2008), *ECG signal denoising by wavelet transform thresholding*. American Journal of Applied Sciences, 5(3): 276–281.

[3] Al-Qazzaz, N.K., Ali, S., Ahmad, S.A., Islam, M.S. and Arif M.I. (2015), *Selection of mother wavelets thresholding methods in denoising multi-channel EEG signals during working memory task.* Sensors, 15(11): 15–35.

[4] Alyasseri, Z.A.A., Khader, A.T. and Al-Betar, M.A. (2017), *Electroencephalogram signals denoising using various mother wavelet functions: a comparative analysis*. In: Proceedings of the International Conference on Imaging, Signal Processing and Communication, Penang, Malaysia, July 26-28, 2017, pp. 100–105.

[5] Al-Hmouz, R. and Challa, S. (2005), *Optimal placement for opportunistic cameras using genetic algorithm*. In: Proceedings of the International Conference on Intelligent Sensors, Sensor Networks and Information Processing, December 5-8, 2005, Sydney, Australia, pp. 337–341.

[6] Anderson, B.D.O. and Moore, J.B. (1979), *Optimal Filtering*. New Jersey (USA), Prentice-Hall Publisher, 1979.

[7] Antoni, J. and Randall, R.B. (2006), *The spectral kurtosis: application to the vibratory surveillance and diagnostics of rotating machines*. Mechanical Systems and Signal Processing, 20(2006): 308–331.

[8] Arezki, M. and Berkani, D. (2009), *Fast algorithms with low complexity for adaptive filtering*. In: WSEAS Transactions on Signal Processing, 5(2009): 23–31.

[9] Aqil, M., Jbari, A. and Bourouhou, A. (2017), *ECG signal denoising by Discrete Wavelet Transform.* International Journal of Online Engineering, 13(9): 51–68.

[10] Azam, S.E, Chatzi, E.N. and Papadimitriou, C. (2015), *A dual Kalman filter approach for state estimation via output-only acceleration measurements*. Mechanical Systems and Signal Processing, 60-61: 866–885.

[11] Baravdish, G., Evangelista, G., Svensson, O. and Sofya, F. (2012), *Effective heterogeneous data fusion procedure via Kalman filtering.* In: 5th International Symposium on Communications, Control and Signal Processing, May 2-4, 2012, Rome, Italy, pp. 1–4.

[12] Barnett, J.A. (1981), *Computational methods for a mathematical theory of evidence*. In: Proceedings of the International Joint Conference on Artificial Intelligence, pp. 868–875.

[13] Basir, O., Karray, F. and Hongwei, Z. (2005), *Connectionist-based Dempster-Shafer evidential reasoning for data fusion.* IEEE Transactions on Neural Networks, 6(6): 1513–1530.

[14] Blu, T. (1998), *A new design algorithm for two-band orthonormal rational filter banks and orthonormal rational wavelets*. In: IEEE Transactions on Signal Processing, 46(6): 1494–1504.

[15] Boström, H., Andler, S., Brohede, M., Johansson, R., Karlsson, A., van Laere, J., Niklasson, L., Nilsson, M., Persson, A. and Ziemke, T. (2007), *On the Definition of Information Fusion as a Field of Research. Informatics Research Centre*, Skövde, Sweden, HS-IKI-TR-07-006.

[16] Brunner, F.K. (2007), On the methodology of Engineering Geodesy. Journal of Applied Geodesy, 1(2): 57–62.

[17] Buades, A. and Coll, B. (2006), *A review of image denoising algorithms, with a new one*. Multiscale Modelling and Simulations, 4(2): 490–530.

[18] Bürki, B., Guillaume, S., Sorber, P. and Oesch, H. (2010), *DAEDALUS: a versatile usable digital clip-on measuring system for total stations.* In: International Conference on Indoor Positioning and Indoor Navigation, Zürich, Switzerland, September 15–17, 2010.

[19] Capellari, G., Chatzi, E.N., Mariani, S. and Azam, S.E. (2017), *Optimal design of sensor networks for damage detection.* In: EURODYN 2017, 10th International Conference on Structural Dynamics, Faculty of Civil and Industrial Engineering, Rome, Italy, September 10-13, 2017, Proceedia Engineering, 199: 1864–1869.

[20] Capellari, G., Chatzi, E.N. and Mariani, S. (2018), *Structural Health Monitoring Sensor Network Optimization through Bayesian Experimental Design*. Journal of Risk and Uncertainty in Engineering Systems, 4(2): 401–427.

[21] Challa, S., Gulrez, T., Chaczko, Z. and Paranesha, T.N. (2005), *Opportunistic information fusion: a new paradigm for next generation networked sensing systems*. In: Proceedings of the 8th International Conference on Information Fusion, Sydney, Australia, July 25-28, 2005, pp. 720–727.

[22] Chang, C.C. and Ji, Y.F. (2007), *Flexible videogrammetric technique for threedimensional structural vibration measurement*. Journal of Engineering Mechanics, 133(6): 511–520.

[23] Chang, C.C. and Xiao, X. (2010), *Three-dimensional structural translation and rotation measurement using monocular videogrammetry*. Journal of Engineering Mechanics, 136(7): 840–848.

[24] Chang, S.G., Bin, Y. and Vetterli, M. (2000), *Adaptive wavelet thresholding for image denoising and compression.* In: IEEE Transactions on Image Processing, 9(2000): 1532–1546.

[25] Chatzi, E.N. and Smyth, A.W. (2009), *The unscented Kalman filter and particle filter methods for non-linear structural system identification with non-collocated heterogeneous sensing*. Structural Control and Health Monitoring, 16(1): 99–123.

[26] Chatzi, E.N. and Fuggini, C. (2012), *Structural identification of a super-tall tower by GPS and accelerometer data fusion using a multi-rate Kalman filter*. In: Proceedings of the 3rd International Symposium on Life-Cycle Civil Engineering, Delft, Netherlands, October 3-6, 2012, 10: 144–151.

[27] Chatzi, E.N. and Fuggini, C. (2015), *Online correction of drift in Structural Identification using artificial white-noise observations and an Unscented Kalman filter*. Smart Structures and Systems, 16(2): 296–328.

[28] Chatzi, E.N. and Smyth, A.W. (2016), *Particle filter scheme with mutation for the estimation of time-invariant parameters in structural health monitoring applications*. Structural Control and Health Monitoring, 20(7): 1081–1095.

[29] Chatzis, M.N., Chatzi, E.N. and Triantafyllou, S.P. (2017), *A Discontinuous Extended Kalman Filter for non-smooth dynamic problems.* Mechanical Systems and Signal Processing, 92: 13–29.

[30] Chen, G. and Bui, T. (2003), Multiwavelets denoising using neighboring coefficients. IEEE Signal Processing Letters, 10(7): 211–214.

[31] Chen, H., Chen, G., Blasch, E.P., Douville, P. and Pham, K. (2009), *Information theoretic measures for performance evaluation and comparison*. In: Proceedings of the 12th International Conference on Information Fusion, New Orleans, LA, USA, July 6-9, 2009, pp. 874–881.

[32] Chen, T., Morris, J. and Martin, E. (2005), *Particle filters for state and parameter estimation in batch processes*. Journal of Process Control, 15(6): 665–673.

[33] Chen, Y. and Zhang, P. (2012), *Bearing fault detection based on SVD and EMD*. Applied Mechanics and Materials, 184–185(2012): 70–74.

[34] Ching, J., Beck, J.L., Porter, K.A. and Shaikhutdinov, R. (2005), *Bayesian state estimation method for non-linear systems and its application to recorded seismic response*. Journal of Engineering Mechanics, 132(4): 396–410.

[35] Cho, S., Yun, C.B. and Sim, S.H (2015), *Displacement estimation of bridge structures using data fusion of acceleration and strain measurement incorporating finite element model*. Smart Structures and Systems, 15(3): 645–663.

[36] Cholvy, L. (2004), *Information evaluation in fusion: a case study*. In: Proceedings of the International Conference on Information Processing and Management of Uncertainty in Knowledge-Based Systems, pp. 993–1000.

[37] Cholvy, L. (2007), *Modeling information evaluation in fusion*. In: Proceedings of the 10th International Conference on Information Fusion, Toulouse, France, July 9-12, 2007, pp. 1–6.

[38] Chong, C.Y. (2000), *Problem characterization in tracking/fusion algorithm evaluation*. IEEE Aerospace and Electronic Systems Magazine, 16(7): 12–17.

[39] Crawley, E.F. and O'Donnell, K.J. (1987), *Force-state mapping identification of non-linear joints.* AIAA Journal, 25(7): 1003–1010.

[40] Dasarathy, B.V. (1994), *Decision Fusion. Los Alamitos (CA),* IEEE Computer Society Press, 1994.

[41] Delmotte, F., Dubois, L., and Borne, P. (1996), *Context-dependent trust in data fusion within the possibility theory.* In: Proceedings of the International Conference on Information Fusion, Lille, France, October 14-17, 1996, pp. 538–543.

[42] Dempster, A.P. (1968), *A generalization of Bayesian inference*. Journal of the Royal Statistical Society, Series B, 30(2): 205–247.

[43] Di Monte, C.L. and Arun, K.S. (1990), *Tracking the frequencies of superimposed time-varying harmonics.* In: International Conference on Acoustics, Speech and Signal Processing, 2535(1990): 2539–2542.

[44] Ding, Y. and Guo, L. (2016), *Structural identification based on incomplete measurements with iterative Kalman filter.* Structural Engineering and Mechanics, 59(6): 1037–1054.

[45] Djurovic, Z. and Kovacevic, B. (1995), *QQ-plot approach to robust Kalman filtering*. International Journal of Control, 61(4): 837–857.

[46] Dohono, D.L. and Johnston, L.M. (1994), *Ideal spatial adaptation by wavelet shrinkage.* Biometrika, 81(3): 425–455.

[47] Dohono, D.L. and Johnston, L.M. (1995), *Adapting to unknown smoothness via wavelet shrinkage*. Journal of the American Statistical Association, 90(432): 1200–1224.

[48] Dohono D.L. (1995), *Denoising by soft thresholding*. IEEE Transaction on Information Theory, 41(3): 613–627.

[49] Dohono D.L. and Johnston, L.M. (1998), *Minimax estimation via wavelet shrinkage*. Annals of Statistics, pp. 879–921.

[50] Drummond, O.E. (1999), *Methodologies for performance evaluation of multi-target multisensor tracking*. In: Proceedings of the SPIE Conference on Signal and Data Processing of Small Targets, San Diego, CA, USA, October 4, 1999, pp. 355–369.

[51] Dubois, D. and Prade, H. (1988), *Possibility Theory: An Approach to Computerized Processing of Uncertainty*. Plenum Publisher, 1988.

[52] Dubois, D. and Prade, H. (1990), *Rough fuzzy sets and fuzzy rough sets*. International Journal of General Systems, 17(2-3): 191–209.

[53] Dubois, D. and Prade, H. (1994), *Possibility theory and data fusion in poorly informed environments.* Journal of Control Engineering Practice, 2(5): 811–823.

[54] Dubois, D. and Prade, H. (2000), *Possibility theory in information fusion*. In: Proceedings of the 3rd International Conference on Information Fusion, Toulouse, France, July 10-13, 2000, pp. 6–19.

[55] Durrant-Whyte, H.F. and Henderson, T.C. (2008), *Multi-sensor data fusion. Handbook of Robotics*, Springer Publishers, 2008.

[56] Eichhorn, A. (2006), *Analysis of Dynamic Deformation Processes with Adaptive Kalman Filtering.* In: 12th FIG Symposium on Deformation Measurement and Analysis, Hong Kong, China, November 2-4, 2011.

[57] Eichstadt, S., Makarava, N. and Elster, C. (2016), *On the evaluation of uncertainties for state estimation with the Kalman filter*. Measurement Science and Technology, 27(12).

[58] Elouedi, Z., Mellouli, K. and Smets, P. (2004), *Assessing sensor reliability for multi-sensor data fusion within the transferable belief model*. IEEE Transactions on SMC – Part B, 34(1): 782–787.

[59] Ergen, B. (2012), *Signal and image denoising using Wavelet Transform*. Extract from: Advances in Wavelet Theory and Their Applications in Engineering, Physics and Technology, Dumitru Baleanu editor, Fırat University, Turkey, 634 pages.

[60] Escamilla-Ambrosio, P.J. and Mort, N. (2003), *Hybrid Kalman filter-fuzzy logic adaptive multisensor data fusion architectures.* In: Proceedings of the 42nd IEEE Conference on Decision and Control, Miami, Florida, USA, December 9-12, 2003, pp. 5215–5220.

[61] Ewins, D.J. (2000), *Modal testing: Theory, procedures and applications*. Beadlock (UK), Research Studies Press Publisher, 2000.

[62] Farrar, C.R. and James III, G.H. (1997), *System identification from ambient vibration measurements on a bridge.* Journal of Sound and Vibration, 205(1): 1–18.

[63] Fedi, M., Lenarduzzi, R., Primiceri, R. and Quarta, T. (2000), *Localized denoising filtering using theWavelet Transform.* Pure and Applied Geophysics, 157(9): 1463–1491.

[64] Feng, Y., Thanagasundram, S. and Schlindwein, F.S. (2006), *Discrete wavelet-based thresholding study on acoustic emission signals to detect bearing defect on a rotating machine*. In: Proceedings of the 13th International Congress on Sound and Vibration.

[65] Ferrari, R., Froio, D., Chatzi, E.N., Gentile, C., Pioldi, F. and Rizzi, E. (2015), *Experimental and numerical investigation for the structural characterization of a historic RC arch bridge.* In: COMPDYN 2015, 5th ECCOMAS Thematic Conference on Computational Methods in Structural Dynamics and Earthquake Engineering, Crete Island, Greece, May 25-27, 2015, 1: 2337–2353, available online in Eccomas Proceedia, www.eccomasproceedia.org/conferences/thematic-conferences/compdyn-2015/3542.

[66] Ferrari, R., Pioldi, F., Rizzi, E., Gentile, C., Chatzi, E.N., Klis, R., Serantoni, E. and Wieser, A. (2015), *Heterogeneous sensor fusion for reducing uncertainty in Structural Health Monitoring.* In: UNCECOMP 2015, 1st ECCOMAS Thematic Conference on International Conference on Uncertainty Quantification in Computational Sciences and Engineering, Crete Island, Greece, May 25-27, 2015, pp. 511–528, available online in Eccomas Proceedia, www.eccomasproceedia.org/conferences/thematicconferences/uncecomp-2015/4289.

[67] Ferrari, R., Pioldi, F., Rizzi, E., Gentile, C., Chatzi, E.N., Serantoni, E. and Wieser, A. (2016), *Fusion of wireless and non-contact technologies for the dynamic testing of a historic RC bridge.* Measurement Science and Technology, 27(12): 1–19.

[68] Ferrari, R., Froio, D., Rizzi, E., Gentile, C. and Chatzi, E.N. (2018), *Model updating of a historic concrete bridge by sensitivity- and global optimization-based Latin Hypercube Sampling*. Engineering Structures, 179(January 2019): 139–160.

[69] Ferrari, R., Cocchetti, G. and Rizzi, E. (2019), *Reference structural investigation on a 19th-century arch iron bridge loyal to design-stage conditions*. International Journal of Architectural Heritage, Conservation, Analysis, and Restoration. Published online on 05 July 2019: 1-31.

[70] Ferrin, G., Snidaro, L., Canazza, S. and Foresti, G.L. (2008), *Soft data issues in fusion of video surveillance*. In: Proceedings of the 11th International Conference on Information Fusion, New York, NY, USA, 30 June-3 July, 2008, pp. 1–8.

[71] Fisher, R.A. (1912), *On an Absolute Criterion for Fitting Frequency Curves.* Messenger of Math, 41(1): 55.

[72] Froio, D. and Zanchi, R. (2014), *Finite element modelization and modal dynamic analyses of an historical reinforced concrete bridge with parabolic arches*. MSc Thesis in Building Engineering, Advisor Rizzi E., Co-Advisor Ferrari R., University of Bergamo, School of Engineering, 232 pages.

[73] Gao, H.Y. and Andrew, G.B. (1997),*WaveShrink with firm shrinkage*. Statistica Sinica, 7(4): 855–874.

[74] Gao, H.Y. (1998), *Wavelet shrinkage denoising using non-negative garrote*. Journal of Computational and Graphical Statistics, 7(4): 469–488.

[75] Garvey, T.D., Lowrance, J.D. and Fischler, M.A. (1981), *An inference technique for integrating knowledge from disparate sources*. In: Proceedings of the International Joint Conference on Artificial Intelligence, Vancouver, Canada, August 24-28, 1981, pp. 319–325.

[76] Gelb, A., Kasper, J.F., Nash, R.A., Price, C.F. and Sutherland, A.A. (1974), *Applied Optimal Estimation. Cambridge (UK),* MIT Press Publisher, 1974.

[77] Gelfand, A.E., Smith, C., Colony, M. and Bowman, C. (2009), *Performance evaluation of decentralized estimation systems with uncertain communications.* In: Proceedings of the 12th International Conference on Information Fusion, Arlington, VA, USA, July 6-9, 2009, pp. 786–793.

[78] Gillijns, S. and DeMoor, B. (2007), *Unbiased minimum-variance linear state estimation for linear discrete-time systems.* Journal of Automatica, 43(1): 111–116.

[79] Gold, B. and Rader, C.M. (1969), *Digital Processing of Signals. New York (USA),* McGraw-Hill Book Company Publisher, 1969.

[80] Goodman, I.R., Mahler, R.P.S. and Nguyen, H.T. (1997), *Mathematics of Data Fusion*. Norwell (MA), Kluwer Academic Publishers, 1997.

[81] Gordon, J. and Shortliffe, E.H. (1985), *A method for managing evidential reasoning in a hierarchical hypothesis space.* Journal of Artificial Intelligence, 26(3): 323–357.

[82] Gordon, J., Salmond, D.J. and Smith, A.F.M. (1993), *Novel approach to nonlinear/non-Gaussian Bayesian state estimation.* In: Proceedings of Radar and Signal Processing, 140(2): 107–113.

[83] Gradolewski, D. and Redlarski, G. (2013), *The use of wavelet analysis to denoising of electrocardiography signal.* In: XV International PhD Workshop OWD, October 19-22, 2013, pp. 456–461.

[84] Gulal, E. (1997), *Geodaetische Uberwachung einer Talsperre*; eine Anwendung der Kalman Filtertechnik, Dissertationen, Wissenschaftliche Arbeiten der Fachrichtung Vermessungswesen der Universitaet Hannover.

[85] Gulal, E. (2013), *Structural Deformations Analysis by Means of Kalman Filtering*. Analise da deformação estrutural com filtros de Kalman, 19(1): 98–113.

[86] Guo, Q., Zhang, C., Zhang, Y. and Liu, H. (2016), *An efficient SVD-based method for image denoising.* In: IEEE Transactions on Circuits and Systems for Video Technology, 26(5): 868–880.

[87] Haenni, R. and Hartmann, S. (2006), *Modeling partially reliable information sources: a general approach based on Dempster-Shafer theory*. Journal of Information Fusion, 7(4): 361–379.

[88] Hall, D.L., McNeese, M., Llinas, J. and Mullen, T. (2008), *A framework for dynamic hard/soft fusion.* In: Proceedings of the 11th International Conference on Information Fusion, New York, NY, USA, 30 June-3 July, 2008, pp. 1–8.

[89] Hall, D.L., McNeese, M., Hellar, D.B., Panulla, B.J. and Shumaker, W. (2009), *A cyber infrastructure for evaluating the performance of human centered fusion.* In: Proceedings of the 11th International Conference on Information Fusion, New York, NY, USA, 30 June-3 July, 2008, pp. 1257–1264.

[90] Hamilton, F., Berry, T. and Sauer, T., (2016), *Ensemble Kalman filtering without a model*. Physical Review X, 6(011021): 1–12.

[91] Hesse, C. (2002), *Deformation analysis of a shell structure under varying loads with Kalman filter techniques.* In: 2nd Symposium for Geotechnical and Structural Engineering, Berlin, DK, 2002.

[92] Heunecke, O. and Welsch, W. (2000), *A Contribution to Terminology and Classification of Deformation Models in Engineering Surveys*. Journal of Geospatial Engineering, 2(1): 35–44.

[93] Hong, L. (1991), *Adaptive data fusion*. In: Proceedings of the IEEE International Conference on SMC, Hong Kong, China, October 9-12, 2015, pp. 767–772.

[94] Hoshiya, M. and Sato, E. (1984), *Structural identification by Extended Kalman filter*. Journal of Engineering Mechanics, 112(12): 102–123.

[95] Hsieh, C.S. (2000), *Robust two-stage Kalman filters for systems with unknown inputs*. IEEE Transactions on Automatic Control, 45(12): 2374–2378.

[96] Imai, H., Yun, C.B., Maruyama, O. and Shinozuka, M. (1989), *Fundamentals of system identification in structural dynamics.* Probabilistic Engineering Mechanics, 4(4): 162–173.

[97] Jackson, P. and Musiak, J.D. (2009), *Boeing fusion performance analysis (FPA) tool*. In: Proceedings of the International Conference on Information Fusion, Seattle, WA, USA, July 6-9, 2009, pp. 1444–1450.

[98] Jensen, S.H., Hansen, P.C., Hansen, S.D. and Sorensen, J.A. (1995), *Reduction of broad-band noise in speech by truncated QSVD*. In: IEEE Transaction on Speech and Audio Processing, 3(1995): 439–448.

[99] Jiang, S.F., Wang, L.S., Yin, X.Z. and Liu, M. (2005), *Data fusion technique in structural health monitoring.* Journal of Shenyang Jianzhu University (Natural Science), 21(1): 18–22.

[100] Jiang, S.F., Chan, G.K. and Zhang, C.M. (2006), *Data fusion technique and its application in structural health monitoring.* Structural Health Monitoring and Intelligent Infrastructure - Proceedings of the 2nd International Conference on Structural Health Monitoring of Intelligent Infrastructure, SHMII, 2005(2): 1125–1130.

[101] Jing, J., Hu, Y., Li, X. and Huang, Z. (2007), *Feature extraction of pulse signal based on Hilbert-Huang transformation and Singular Value Decomposition*. In: Proceedings of the 1st International Conference on Bioinformatics and Biomedical Engineering, Wuhan, China, July 6-8, 2007.

[102] Julier, S.J. and Uhlmann, J.K. (1997), *A new extension of the Kalman filter to non-linear systems.* In: Proceedings of SPIE 3068, Signal Processing, Sensor Fusion, and Target Recognition, Orlando, FL, USA, April 21, 1997, pp. 182–193.

[103] Julier, S.J. and Uhlmann, J.K. (1998), *A non-divergent algorithm in the presence of unknown correlation.* In: Proceedings of the American Control Conference, Albuquerque, New Mexico, USA, June 1997, vol.4, pp. 2369–2373.

[104] Julier, S.J. and Uhlmann, J.K. (2004), *Unscented filtering and non-linear estimation*. IEEE Signal Processing Magazine, 92(3): 401–422.

[105] Kalman, R.E. (1960), *A New Approach to Linear Filtering and Prediction Problems*. Journal of Basic Engineering, 82(1): 35–45.

[106] Kalman, R.E. and Bucy, R.S. (1961), *New Results in Linear Filtering and Prediction Theory.* Journal of Basic Engineering, Trans. ASME, Series D, 83(1): 95–108.

[107] Kalman, R.E. (1963), *New Methods in Wiener Filtering Theory*. In: Proceedings of the 1st Symposium of Engineering Applications of Random Function Theory and Probability, New York, NY, USA, September 16, 1963, pp. 270–388.

[108] Kam, H.S., Cheong, S.N. and Tan, W.H. (2005), *An adaptive fuzzy image smoothing filter for Gaussian noise.* In: WSEAS International Conference on Automation and Information, 2005, pp. 323–328.

[109] Karthikeyan, P., Murugappan, M. and Yaacob, S. (2012), *ECG signal denoising using wavelet thresholding technique in human stress assessment*. International Journal of Electrical Engineering and Information, 4(2): 306–319.

[110] Kendall, D.G. (1974), *Foundations of a theory of random sets*. Journal of Information and Control, 42(4): 322–376, doi:10.30-364X/94/4204-0750.

[111] Khaleghi, B., Khamis, A., Karray, F. and Razavi, S. (2011), *Multisensor data fusion: a review of the state of the art.* Journal of Information Fusion, 14(1): 28–44.

[112] Kim, K., Choi, J., Koo, G. and Sohn, H. (2016), *Dynamic displacement estimation by fusing biased high-sampling rate acceleration and low-sampling rate displacement measurements using two-stage Kalman estimator.* Smart Structures and Systems, 17(4): 647–667.

[113] Kim, K. and Sohn, H. (2017), *Dynamic displacement estimation by fusing LDV and LiDAR measurements via smoothing based Kalman filtering*. Mechanical Systems and Signal Processing, 82: 339–355.

[114] Kitanidis, P.K. (1987), *Unbiased minimum-variance linear state estimation*. Journal of Automatica, 23(1): 775–778.

[115] Klein, L. (1999), *Sensor and Data Fusion Concepts and Applications*, Second Ed., Society of Photo-optical Instrumentation Engineers (SPIE), Bellingham, WA, USA, 1999.

[116] Kokar, M.M., Tomasik, J.A. and Weyman, J. (2004), *Formalizing classes of information fusion systems. Journal of Information Fusion,* 5(3): 189–202.

[117] Kolmogorov, A.N. (1941), *Interpolation and Extrapolation. Bulletin de l'académie des sciences de U.S.S.R.,* 5(1): 3–14.

[118] Konstantinides, K., Natarajan, B. and Yovanof, G.S. (1997), *Noise estimation and filtering using Block-based Singular Value Decomposition.* In: IEEE Transactions on Image Processing, 6(3): 479–483.

[119] Konstantinides, K. and Yao, K. (1998*), Statistical analysis of effective singular values in matrix rank determination.* In: IEEE Transactions on Acoustics, Speech, and Signal Processing, 36(5): 757–763.

[120] Koo, K.Y., Brownjohn, J.M.V., List, D.I. and Cole, R. (2003), *Structural health monitoring of the Tamar suspension bridge.* Structural Control and Health Monitoring, 20(4): 609–625.

[121] Kreinovich, V. (1997), *Random sets unify, explain, and aid known uncertainty methods in expert systems.* Random Sets: Theory and Applications, Springer-Verlag Publisher, pp. 321–345.

[122] Kuhlmann, H., Schwieger, V., Wieser, A. and Niemeier, W. (2014), *Engineering Geodesy - Definition and Core Competencies.* Journal of Applied Geodesy, 8(4): 327–334.

[123] Lee, J.J., Fukuda, Y., Shinozuka, M., Cho, S. and Yun, C.B. (2007), *Development and application of a vision-based displacement measurement system for structural health monitoring of civil structures*. Smart Structures and Systems, 3(3): 373–384.

[124] Lee, J.L. and Shinozuka, M. (2006), *A vision-based system for remote sensing of bridge displacement.* NDT & E International, 39(5): 425–431.

[125] Lee, K.G. and Yun, C.B. (2008), *Parameter identification for non-linear behavior of RC bridge piers using sequential modified extended Kalman filter*. Smart Structures and Systems, 4(3): 319–342.

[126] Lee, K.C., Ou, J.S., and Fang, M.C. (2008), *Application of SVD noise-reduction technique to PCA based radar target recognition.* Progress In Electromagnetics Research, 81(January2008): 447–459.

[127] Lei, Y., Chen, F. and Zhou, H. (2015), *A two-stage and two-step algorithm for the identification of structural damage and unknown excitations: numerical and experimental studies*. Smart Structures and Systems, 15(1): 57–80.

[128] Lei, Y., Luo, S. and Su, Y. (2016), *Data fusion based improved Kalman filter with unknown inputs and without collocated acceleration measurements*. Smart Structures and Systems, 18(3): 375–387.

[129] Lin, X. and Luo, Z.C. (2016), *A new adaptive multi-rate Kalman filter for the data fusion of displacement and acceleration*. Chine Journal of Geophysics, 59(5): 1608–1615.

[130] Liu, L., Zhu, J., Su, Y. and Lei, Y. (2016), *Improved Kalman filter with unknown inputs based on data fusion of partial acceleration and displacement measurements*. Smart Structures and Systems, 17(6): 903–915.

[131] Ljung, L. (1997), *System identification: Theory for the user*. New Jersey (USA), Prentice-Hall Publisher, 1997.

[132] Llinas, J., Bowman, C.L., Rogova, G., Steinberg, A.N.,Waltz, E. and White, F.E. (2004), *Revisiting the JDL data fusion model II*. In: Proceedings of the International Conference on Information Fusion, San Diego, CA, USA, 2004, pp. 1218–1230.

[133] Loy, G., Fletcher, L., Apostoloff, N. and Zelinsky, A. (2002), *An adaptive fusion architecture for target tracking*. In: Proceedings of the 5th IEEE International Conference on Automatic Face and Gesture Recognition, Camberra, Australia, May 21, 2002, pp. 261–266.

[134] Lyon-Caen, H., Armijo, R., Drakopoulos, J., Baskoutass, J., Delibassis, N., Gaulon, R., Kouskouna, V., Latousakis, J., Makropoulos, K., Papadimitriou, P., Panastasiou, D. and Pedotti, G. (1988), *The 1986 Kalamata (South Peloponnesus) earthquake: detailed study of a normal fault, evidences for east-west extension in the Hellenic arc.* Journal of Geophysical Research Atmospheres, 93(1988): 14967–15000.

[135] Madisetti, V.K. and Williams, D.B. (1999), *Digital Signal Processing Handbook*, CRC Press LLC, 1999.

[136] Mahler, R.P.S. (2007), *Statistical Multisource-Multitarget Information Fusion*. Boston (MA), Artech House Publisher, 2007.

[137] Makarenko, A., Brooks, A., Kaupp, T., Durrant-Whyte, H.F. and Dellaert, F. (2009), *Decentralised data fusion: a graphical model approach*. In: Proceedings of the International Conference on Information Fusion, pp. 545–554.

[138] Mallat, S.G. (1999), *A wavelet tour of signal processing*, Academic Press, London, 1999.

[139] Mohinder, S.G. and Angus, P.A. (2001), *Kalman Filtering: Theory and Practice*. New York (USA), Wiley-Interscience Publisher, 2001.

[140] Mori, S. (1997), *Random sets in data fusion. Multi-object state-estimation as a foundation of data fusion theory*. Random Sets: Theory and Applications, Springer-Verlag Publisher, pp. 321–345.

[141] Moulin, P. and Liu, J. (1999), *Analysis of multiresolution image denoising schemes using generalized Gaussian and complexity priors*. IEEE Transactions on Information Theory, 45(3): 909–919.

[142] Nassif, H.H., Gindly M., and Davis J. (2005), *Comparison of Laser Doppler Vibrometer with contact sensors for monitoring bridge deflection and vibration.* NDT & E International, 38(3): 213–218.

[143] Nimier, V. (1994), *Introducing contextual information in multisensor tracking algorithms*. In: Proceedings of the 16th International Conference on Processing and Management of Uncertainty in Knowledge-Based Systems, Advances in Intelligent Computing, June 20, 1994, Chatillon, France, pp. 595–604.

[144] Nimier, V. (2004), *Information evaluation: a formalization of operational recommendations.* In: Proceedings of the 7th International Conference on Information Fusion, Heidelberg, Germany, July 5-8, 2004, pp. 1166–1171.

[145] Olaszek, P. (1999) *Investigation of the dynamic characteristic of bridge structures using a computer-vision method*. Measurement, 25(3): 227–236.

[146] Otis, M.S.Jr. (1991), *PSD computations using Welch's method*. Sandia National Laboratories Albuquerque, Printed in the USA, December 1991.

[147] Park, J.W., Sim, S.H. and Jung, H.J. (2013), *Displacement estimation using multimetric data fusion*. IEEE/ASME T. Mechatronics, 18(6):1675-1682.

[148] Papadimitriou, C. and Lombaert, G. (2012), *The effect of prediction error correlation on optimal sensor placement in structural dynamics.* Mechanical Systems and Signal Processing, 28(2012): 105–127.

[149] Patsias, S. and Staszewski,W. (2002), *Damage detection using optical measurements and wavelets.* Structural Health Monitoring, 1(1): 5–22.

[150] Pawlak, Z. (1992), *Rough Sets: Theoretical Aspects of Reasoning about Data*. Norwell (MA), Kluwer Academic Publishers, 1992.

[151] Pintelon, R. and Schoukens, J. (2001), *System identification: A frequency domain approach*. New York (USA), IEEE Press Publisher, 2001.

[152] Pioldi, F., Ferrari, R. and Rizzi, E. (2015), *Output-only modal dynamic identification of frames by a refined FDD algorithm at seismic input and high damping*. Mechanical Systems and Signal Processing, 68-69(February 2016):265–291.

[153] Pioldi, F., Ferrari, R. and Rizzi, E. (2015), *Earthquake structural modal estimates of multi-storey frames by a refined FDD algorithm*. Journal of Vibration and Control, 23(13):2037-2063.

[154] Pioldi, F., Ferrari, R. and Rizzi, E. (2017), *Seismic FDD modal identification and monitoring of building properties from real strong-motion structural response signals*. Structural Control and Health Monitoring, 24(11):1-20.

[155] Pioldi, F. and Rizzi, E. (2017), *Refined Frequency Domain Decomposition modal dynamic identification from earthquake-induced structural responses*. Meccanica, 52(13):3165-3179.

[156] Pioldi, F. and Rizzi, E. (2017), A refined Frequency Domain Decomposition tool for structural modal monitoring in earthquake engineering. Earthquake Engineering and Engineering Vibration, 16(3):627-648.

[157] Pioldi, F. and Rizzi, E. (2018), *Assessment of Frequency versus Time Domain enhanced technique for response-only modal dynamic identification under seismic excitation*. Bulletin of Earthquake Engineering, 16(3):1547-1570.

[158] Pioldi, F. and Rizzi, E. (2018), *Earthquake-induced structural response output-only identification by two different Operational Modal Analysis techniques*. Earthquake Engineering and Structural Dynamics, 47(1):257-264.

[159] Portilla, J. and Strela, V. (2003), *Image denoising using scale mixtures of Gaussians in the wavelet domain.* IEEE Transactions on Image Processing, 12(11): 1338–1351.

[160] Pravia, M.A., Prasanth, R.K., Arambel, P.O., Sidner, C. and Chong, C.Y. (2008), *Generation of a fundamental data set for hard/soft information fusion.* In: Proceedings of the 11th International Conference on Information Fusion, New York, NY, USA, 30 June-3 July, 2008, pp. 1–8.

[161] Pravia, M.A., Babko-Malaya, O., Schneider, M.K., White, J.V. and Chong, C.Y. (2009), *Lessons learned in the creation of a data set for hard/soft information fusion*. In: Proceedings of the 11th International Conference on Information Fusion, New York, NY, USA, 30 June-3 July, 2008, pp. 2114–2121.

[162] Premaratne, K., Murthi, M.N., Zhang, J., Scheutz, M. and Bauer, P.H. (2009), *A Dempster-Shafer theoretic conditional approach to evidence updating for fusion of hard and soft data*. In: Proceedings of the 11th International Conference on Information Fusion, New York, NY, USA, 30 June-3 July, 2008, pp. 2122–2129.

[163] Premchaiswadi, N., Yimgnagmand, S. and Premchaiswadi, W. (2010), *A scheme for salt and pepper noise reduction and its application for OCR system.* In: WSEAS Transactions on Computers, 9(2010): 351–360.

[164] Rabiner, L.R. and Gold, B. (1975), *Theory and Application of Digital Signal Processing*. New Jersey (USA), Prentice-Hall Publisher, 1975.

[165] Ravizza, G. (2017), *Dynamic response estimation by heterogeneous data fusion via Kalman filter adaptation.* Master Thesis in Building Engineering, Advisor: E. Rizzi, Co-advisor: R. Ferrari, School of Engineering, University of Bergamo, Italy, March 31, 2017, 186 pages.

[166] Ravizza, G., Ferrari, R., Rizzi, E. and Chatzi, E.N. (2018), *Effective heterogeneous data fusion procedure via Kalman filtering.* Smart Structures and Systems, 22(5): 631–641.

[167] Ravizza, G., Ferrari, R., Rizzi, E., Dertimanis, V. and Chatzi, E.N. (2019), *Denoising corrupted structural vibration response: critical comparison and assessment of related methods.* In: Proceedings of the 7th International Conference on Computational Methods in Structural Dynamics and Earthquake Engineering (COMPDYN 2019), An ECCOMAS Thematic Conference, An IACM Special Interest Conference, M. Papadrakakis, M. Fragiadakis (eds.), June 24-26, 2019, Hersonissos, Crete Island, Greece, Institute of Structural Analysis and Antiseismic Research, National Technical University of Athens (NTUA), Conference Proceeding ID: 19291, Category: RS02 - ALGORITHMS FOR STRUCTURAL HEALTH MONITORING, 12 pages.

[168] Ravizza, G., Ferrari, R., Rizzi, E., Dertimanis, V. and Chatzi, E.N. (2020), *Critical assessment of two denoising techniques for purifying structural vibration response signals*. To be submitted.

[169] Rioul, O. and Vetterli, M. (1991), *Wavelets and signal processing*. Signal Processing Magazine, 8(4): 14–38.

[170] Roberts, G.W. and Dodson, A.H. (2003), *A remote bridge health monitoring system using computational simulation and GPS sensor data.* In: Proceedings of the 11th FIG Symposium on Deformation Measurements, Santorini, Greece, 2003.

[171] Rogova, G.L. and Nimier, V. (2004), *Reliability in information fusion: literature survey*. In: Proceedings of the 7th International Conference on Information Fusion, October 27-31, 2004, CA, USA, pp. 1158–1165.

[172] Rothrock, R.L. and Drummond, O.E. (2000), *Performance metrics for multiple-sensor multiple-target tracking.* In: Proceedings of the SPIE Conference on Signal and Data Processing of Small Targets, Orlando, FL, USA, July 13, 2000, pp. 521–531.

[173] Ruotolo, R. and Surace, C. (1999), *Using SVD to detect damage in structures with different operational conditions*. Journal of Sound and Vibration, 226(3): 425–439.

[174] Sadooghi, S.S. and Khadem, E.K. (2016), *A new performance evaluation scheme for jet engine vibration signal denoising.* Mechanical Systems and Signal Processing, 76–77(2016): 201–212.

[175] Salvi, J. and Rizzi, E. (2014), *Optimum tuning of Tuned Mass Dampers for frame structures under earthquake excitation.* Structural Control and Health Monitoring, 22(4): 707–725.

[176] Salvi, J., Rizzi, E., Rustighi, E. and Ferguson, N.S. (2015), *On the optimization of a hybrid Tuned Mass Damper for impulse loading*. Smart Materials and Structures, 24(8): 85–100.

[177] Salvi, J. and Rizzi, E. (2016), Closed-form optimum tuning formulas for passive Tuned Mass Dampers under benchmark excitations. Smart Structures and Systems, 17(2): 231–256.

[178] Salvi, J. and Rizzi, E. (2017), Optimum earthquake-tuned TMDs: seismic performance and new design concept of balance of split effective modal masses. Soil Dynamics and Earthquake Engineering, 101(October 2017): 67–80.

[179] Sandri, S.A., Dubois, L. and Kalfsbeek, H.W. (1995), *Elicitation, assessment and pooling of expert judgments using possibility theory.* IEEE Transactions on Fuzzy Systems, 3(3): 131–335.

[180] Sanliturk, K.Y. and Cakar, O. (2005), *Noise elimination from measured frequency response functions*. Mechanical Systems and Signal Processing, 19(2005): 615–631.

[181] Santarella, L. and Miozzi, E. (1948), *Ponti Italiani in Cemento Armato*. Milano: Hoepli.

[182] Sasiadek, J.Z. and Hartana, P. (2000), *Sensor data fusion using Kalman filter*. In: Proceeding of the Third International Conference on Information Fusion, July 10-13, 2000, pp. 19–25.

[183] Schanze, T. (2017), *Removing noise in biomedical signal recordings by singular value decomposition.* Current Directions in Biomedical Engineering, 3(2): 253–256.

[184] Schumacher, D., Vo, B.T. and Vo, B.N. (2008), *A consistent metric for performance evaluation of multi-object filters.* IEEE Transactions on Signal Processing, 56(8): 3447–3457.

[185] Schumacher, D., Vo, B.T. and Vo, B.N. (2009), *On performance evaluation of multi-object filters*. In: Proceedings of the 11th International Conference on Information Fusion, Crawley, Australia, 30 June-3 July, 2009, pp. 1–8.

[186] Shafer, G. (1976), A Mathematical Theory of Evidence. Princeton University Press, 1976.

[187] Shanxue, Z. and Chao, G. (2010), *Wavelet transform threshold noise reduction methods in the oil pipeline leakage monitoring and positioning systems*. Journal of Electronics, 27(2010): 405–411.

[188] Sheridan, F.K.J. (1991), *A survey of techniques for inference under uncertainty*. Artificial Intelligence Review, 5(1): 89–119.

[189] Shinozuka, M. and Ghanem, R. (1995), *Structural system identification II: Experimental verification.* ASCE Journal of Engineering Mechanics, 121(2): 265–273.

[190] Skilling, H.H. (1957), *Electrical Engineering Circuits*. New York (USA), John Wiley & Sons Publisher, 1957.

[191] Sifuzzaman, M., Islam, M.R. and Ali, M.Z. (2009), *Application of Wavelet Transform and its advantages compared to Fourier Transform*. In: Journal of Physical Sciences, 13(2009): 121–134.

[192] Smyth, A. and Wu, M. (2007), *Multi-rate Kalman filtering for the data fusion of displacement and acceleration response measurements in dynamic system monitoring*. Mechanical Systems and Signal Processing, 21(2): 706–723.

[193] Soken, H.E. and Hajiyev, C. (2009), *Adaptive unscented Kalman filter with multiple fading factors for pico satellite attitude estimation*. In: Proceedings of the 4th International Conference on Recent Advances in Space Technologies, Istanbul, Turkey, June 11-13, 2009, pp. 541–546.

[194] Sorenson, H.W. (1970), *Least-squares Estimation: from Gauss to Kalman*. IEEE Spectrum, 7(7): 63–68.

[195] STANAG 2022 (1992), *Intelligence Reports*. North Atlantic Treaty Organization (NATO).

[196] Steinberg, A.N., Bowman, C.L. and White, F.E. (1999), *Revisions to the JDL data fusion model.* In: Proceedings of the SPIE Conference on Sensor Fusion: Architectures, Algorithms, and Applications III, Monterey, CA, USA, November 17-19, 1999, pp. 430–441.

[197] Stone, L.D., Corwin, T.L. and Barlow, C.A. (1999), *Bayesian Multiple Target Tracking*. Norwood (MA), Artech House Publisher, 1999.

[198] Storer, J.E. (1957), *Passive Network Synthesis*. New York (USA), McGraw-Hill Book Company Publisher, 1957.

[199] Su, Z., Wang, X., Cheng, L., Long, Y. and Chen, Z. (2009), *Erratum to On selection of data fusion schemes for structural damage evaluation.* Structural Health Monitoring, 8(6): 573.

[200] Swerling, P. (1959), *A Proposed Stagewise Differential Correction Procedure for Satellite Tracking and Prediction*. Journal of Astronautical Sciences, 6(1): 46–59.

[201] Tafti, A.D. and Sadati, N. (2008), *Novel adaptive Kalman filtering and fuzzy track fusion approach for real time applications*. In: Proceedings of the 3rd IEEE Conference on Industrial Electronics and Applications, Tehran, Iran, June 3-5, 2008, pp. 120–125.

[202] Terman, F.E. (1955), *Electronic and Radio Engineering*. New York (USA), McGraw- Hill Book Company Publisher, 1955.

[203] Teskey, W.F. (1988), *Integrierte Analyse von geodätischen, geotechnischen und physikalischen Modelldaten zur Beschreibung des Deformationsverhaltens großer Erddämme unter statischer Belastung,* DGK Reihe C, München.

[204] Tucker, M.G. (1967), *A Graduate Course in Probability*. New York (USA), Academic Press Publisher, 1967.

[205] Van Laere, J. (2009), *Challenges for IF performance evaluation in practice*. In: Proceedings of the 12th International Conference on Information Fusion, Skövde, Sweden, July 6-9, 2009, pp. 866–873.

[206] Vasilescu, G. (2006), *Electronic noise and interfering signals: principles and applications*. Springer Science and Business Media, 2006.

[207] Veerakumar, T., Esakkirajan, S. and Vennila, I. (2012), *Combine fuzzy logic and asymmetric trimmed median filter approach for the removal of high density impulse noise*. In: WSEAS Transactions on Signal Processing, 8(2012): 32–42.

[208] Verma, N. and Verma, A.K. (2012), *Performance analysis of wavelet thresholding methods in denoising of audio signals of some Indian musical instruments*. International Journal of Engineering Science and Technology, 4(5): 2047–2052.

[209] Vetterli, M. and Herley, C. (1992), *Wavelets and filter banks: theory and design*. IEEE Transactions on Signal Processing, 40(9): 2207–2232.

[210] Viterbi, A.J. (1966), *Principles of Coherent Communication*. New York (USA), McGraw-Hill Book Company Publisher, 1966.

[211] Xiao, C., Qu, W. and Tan, D. (2005), *An application of data fusion technology in structural health monitoring and damage identification*. Proceedings of SPIE – The International Society for Optical Engineering, 5758(55): 451–461.

[212] Yager, R.R. (1982), *Generalized probabilities of fuzzy events from fuzzy belief structures*. Journal of Information Sciences, 28(1): 45–62.

[213] Yen, J. (1990), *Generalizing the Dempster-Shafer theory to fuzzy sets*. IEEE Transactions on SMC, 20(3): 559–570.

[214] Yeung, D.S., Degang, C., Tsang, E.C.C., Lee, J.W.T. and Wang, X. (2005), *On the generalization of fuzzy rough sets.* IEEE Transactions on Fuzzy Systems, 13(3): 343–361.

[215] Yoshida, J., Abe, M., Kumano, S., and Fujino, Y. (2003), *Construction of a measurement system for the dynamic behaviors of membrane by using image processing*. In: Conference on Textile Composites and Inflatable Structures, New York, USA, 2013.

[216] Yu, B. and Sycara, K. (2006), *Learning the quality of sensor data in distributed decision fusion.* In: Proceedings of the 9th International Conference on Information Fusion, Pittsburgh, PA, USA, July 10-13, 2006, pp. 1–8.

[217] Yun, C.B. and Shinozuka, M. (1980), Identification of non-linear structural dynamic systems. Journal of Structural Mechanics, 8(2): 187–203.

[218] Yuqing, Z., Xinfang, L., Fengping, L., Bingtao, S. and Wei, X. (2015), *An online damage identification approach for numerical control machine tools based on data fusion using vibration signals*. Journal of Vibration and Control, 21(15): 2925–2936.

[219] Wainstein, L.A. and Zubakov, V.D. (1962), *Extraction of Signals form Noise*. New Jersey (USA), Prentice-Hall Publisher, 1962.

[220] Wang, J.F. and Lin, C.C. (2013), *Extracting parameters of TMD and primary structure from the combined system responses.* Smart Structures and Systems, 16(5): 937–960.

[221] White, F.E. (1991), Data Fusion Lexicon. Joint Directors of Laboratories, Technical Panel for C3, Data Fusion Sub-panel, Naval Ocean Systems Center, San Diego, CA, USA, 1991.

[222] Wiener, N. (1949), *Extrapolation, Interpolation and Smoothing of Stationary Time Series*. Cambridge (UK), MIT Press Publisher, 1949.

[223] Wright, E.J. and Laskey, K.P. (2006), *Credibility models for multi-source fusion.* In: Proceedings of the 9th International Conference on Information Fusion, Arlington, VA, USA, July 10-13, 2006, pp. 1–7.

[224] Wu, C. and Aghajan, H. (2007), *Model-based human posture estimation for gesture analysis in an opportunistic fusion smart camera network*. In: Proceedings of the IEEE Conference on Advanced Video and Signal Based Surveillance, Stanford, USA, September 5-7, 2007, pp. 453–458.

[225] Wu, B. and Wang, T. (2014), *Model updating with constrained unscented Kalman filter for hybrid testing.* Smart Structures and Systems, 14(6): 1105–1129.

[226] Zadeh, L.A. (1965), Fuzzy sets. *Journal of Information and Control*, 8(3): 338–353.

[227] Zadeh, L.A. (1978), *Fuzzy sets as a basis for a theory of possibility*. Fuzzy Sets and Systems, 1(1): 3–28.

[228] Zghal, M., Mevel, L. and Del Moral, P. (2014), *Modal parameter estimation using interacting Kalman filter*. Mechanical Systems and Signal Processing, 47(1-2): 139–150.

[229] Zajic, T., Hoffman, J.L. and Mahler, R.P.S. (2000), *Scientific performance metrics for data fusion: new results.* In: Proceedings of the SPIE Conference on Signal Processing, Sensor Fusion and Target Recognition, Orlando, FL, USA, August 4, 2000, pp. 172–182.

[230] Zhao, X. and Ye, B. (2009*), Similarity of signal processing effect between Hankel matrix-based SVD and wavelet transform and its mechanism analysis*. Mechanical Systems and Signal Processing, 23(2009): 1062–1075.

[231] Zhao, X., Li, M., Song, G. and Xu, J. (2010), *Hierarchical ensemble-based data fusion for structural health monitoring*. Smart Materials and Structures, 12(4).

[232] Zhao, X. and Ye, B. (2011), *Selection of effective singular values using difference spectrum and its application to fault diagnosis of headstock,* Mechanical Systems and Signal Processing, 25(2011): 1617–1631.

[233] Zhao, M. and Jia, X. (2017), *A novel strategy for signal denoising using reweighted SVD and its application to weak fault feature enhancement of rotating machinery*. Mechanical Systems and Signal Processing, 94(2017): 129–147.

[234] Zhu, H. and Basir, O. (2006), *A novel fuzzy evidential reasoning paradigm for data fusion with applications in image processing*. Journal of Soft Computing, 10(12): 1169–1180.

[235] Zijian, Q. and Zhengrong, P. (2015), *SVD principle analysis and fault diagnosis for bearings based on the correlation coefficient.* Measurement Science and Technology, 26(2015): 85–114.

[236] Zou, H. and Tewfik, A.H. (1993), *Parametrization of compactly supported orthonormal wavelets*. In: IEEE Transactions on Signal Processing, 41(3): 1428–1431.